

NBSIR 74-389

ELECTROMAGNETIC NOISE IN McELROY MINE

M. Kanda
J. W. Adams
W. D. Bensema

Electromagnetics Division
Institute for Basic Standards
National Bureau of Standards
Boulder, Colorado 80302

The views and conclusions contained in this document should not be interpreted as necessarily representing the official policies or recommendations of the Interior Department's Bureau of Mines of the U. S. Government.

June 1974

Prepared for
U. S. Bureau of Mines
United States Department of the Interior
Pittsburgh, Pennsylvania 15222
Working Fund Agreement HO 133005



U.S. DEPARTMENT OF COMMERCE, Frederick B. Dent, Secretary
NATIONAL BUREAU OF STANDARDS, Richard W. Roberts, Director

FOREWORD

This report was prepared by the National Bureau of Standards, Boulder, Colorado, under USBM Contract No. HO 133005. The contract was initiated under the Coal Mine Health and Safety Research Program. It was administered under the technical direction of the Pittsburgh Mining and Safety Research Center with Mr. Howard Parkinson and Mr. Harry Dobroski acting as the technical project officers.

This report is a summary of the work completed as part of this contract during the period January 1973 to June 1974. This report was submitted by the authors in October 1974.

CONTENTS

	<u>Page</u>
1. INTRODUCTION-----	1
1.1 Background-----	2
1.2 Mine Description-----	3
2. MEASUREMENT INSTRUMENTATION-----	5
3. SPECTRUM MEASUREMENT RESULTS-----	10
3.1 Introduction-----	10
3.2 Antenna Sites-----	10
3.3 Electromagnetic Noise Spectrum Results-----	10
3.3.1 Interpretation-----	10
3.3.2 Uncertainties-----	11
3.3.3 Section Measurements-----	11
3.3.4 Haulageway Measurements-----	14
3.3.5 Arc Welder Measurement-----	15
3.3.6 Surface Measurements-----	16
3.4 Miscellaneous Measurements-----	17
3.4.1 Measurement of Voltage Between Roof Bolts-----	17
3.4.2 Shuttle-Car Current Spectrum-----	17
3.5 Intercomparison of Magnetic-Field Noise in Different Mines-----	18
3.5.1 Summary of 1 kHz to 3 kHz Data-----	18
3.5.2 Summary of 3 kHz to 180 kHz Data-----	19

CONTENTS (continued)

	<u>Page</u>
4. AMPLITUDE PROBABILITY DISTRIBUTION MEASUREMENTS-----	67
4.1 Introduction and Uncertainties-----	67
4.2 Results-----	68
4.2.1 Introduction-----	68
4.2.2 Measurement Results-----	69
4.2.3 RMS and Average Values-----	70
4.2.4 Summary Curves-----	71
5. CONCLUSIONS-----	151
6. RECOMMENDATIONS-----	153
7. ACKNOWLEDGMENTS-----	153
8. REFERENCES-----	154
9. APPENDIX-----	155

LIST OF FIGURES

		<u>Page</u>
Figure 2-1.	Block diagram of portable instrumentation--	7
Figure 2-2.	System for field recording data to obtain amplitude probability distributions-----	8
Figure 2-3.	Block diagram of laboratory recording sys- tem modified for field use-----	9
Figure 3-1.	Map of portion of McElroy Coal Mine where first day measurements were made (April 10, 1973)-----	20
Figure 3-2.	Map of portion of McElroy Coal Mine where second day measurements were made (April 12, 1973)-----	21
Figure 3-3.	Spectrum at location C in power entry. Spectral resolution is 78.1 Hz-----	22
Figure 3-4.	Expanded spectrum at location C in power entry. Spectral resolution is 3.91 Hz-----	23
Figure 3-5.	Spectrum at location D near operating miner. Spectral resolution is 78.1 Hz-----	24
Figure 3-6.	Spectrum at location E in crosscut. Spectral resolution is 78.1 Hz-----	25
Figure 3-7.	Expanded spectrum at location E in cross- cut. Spectral resolution is 3.91 Hz-----	26
Figure 3-8.	Spectrum at location F in middle of angle cut. Spectral resolution is 78.1 Hz-----	27
Figure 3-9.	Spectrum at location B with no equipment operating. Spectral resolution is 78.1 Hz-	28
Figure 3-10.	Expanded spectrum at location B with no equipment operating. Spectral resolution is 3.91 Hz-----	29
Figure 3-11.	Spectrum at location B near operating miner and loader. Spectral resolution is 78.1 Hz	30

LIST OF FIGURES (continued)

	<u>Page</u>
Figure 3-12. Expanded spectrum at location B near operating miner and loader. Spectral resolution is 3.91 Hz-----	31
Figure 3-13. Spectrum at location F in return entry. Spectral resolution is 78.1 Hz-----	32
Figure 3-14. Expanded spectrum at location G in return entry. Spectral resolution is 3.91 Hz-----	33
Figure 3-15. Spectrum at location A near operating machinery. Spectral resolution is 156 Hz--	34
Figure 3-16. Spectrum at location A near operating machinery. Spectral resolution is 19.5 Hz-	35
Figure 3-17. Spectrum at location A near operating machinery. Spectral resolution is 156 Hz--	36
Figure 3-18. Spectrum at location A near operating machinery. Spectral resolution is 156 Hz--	37
Figure 3-19. Spectrum at location A near operating machinery. Spectral resolution is 19.5 Hz-	38
Figure 3-20. Spectrum at location A near operating machinery. Spectral resolution is 156 Hz--	39
Figure 3-21. Spectrum at location A near operating machinery. Spectral resolution is 156 Hz--	40
Figure 3-22. Spectrum at location A near operating machinery. Spectral resolution is 19.5 Hz-	41
Figure 3-23. Spectrum at location A of an impulse. Spectral resolution is 156 Hz-----	42
Figure 3-24. Spectrum in haulageway near bottom of elevator shaft. Spectral resolution is 78.1 Hz-----	43
Figure 3-25. Expanded spectrum in haulageway near bottom of elevator shaft. Spectral resolution is 3.91 Hz-----	44

LIST OF FIGURES (continued)

	<u>Page</u>
Figure 3-26.	Spectrum at location B near train passing by. Spectral resolution is 78.1 Hz----- 45
Figure 3-27.	Expanded spectrum at location B near train passing by. Spectral resolution is 3.91 Hz 46
Figure 3-28.	Expanded spectrum at location B near empty train going by. Spectral resolution is 3.91 Hz----- 47
Figure 3-29.	Spectrum at location C at head piece with conveyor and car-pull operating. Spectral resolution is 78.1 Hz----- 48
Figure 3-30.	Expanded spectrum at location C at head piece with conveyor and car-pull operating. Spectral resolution is 3.91 Hz----- 49
Figure 3-31.	Spectrum at location A of haulageway. Spectral resolution is 156 Hz----- 50
Figure 3-32.	Expanded spectrum at location A of haulageway. Spectral resolution is 19.5 Hz----- 51
Figure 3-33.	Spectrum at location A which was the highest measured on April 12, 1973. Spectral resolution is 78.1 Hz----- 52
Figure 3-34.	Spectrum of operating arc welder 15 meters away. Spectral resolution is 78.1 Hz----- 53
Figure 3-35.	Spectrum of noise near powerline on surface above McElroy Mine. Spectral resolution is 78.1 Hz----- 54
Figure 3-36.	Expanded spectrum of noise near powerline on surface above McElroy Mine. Spectral resolution is 3.91 Hz----- 55
Figure 3-37.	Spectrum of noise at surface above McElroy Mine. Spectral resolution is 156 Hz----- 56
Figure 3-38.	Spectrum of noise at surface above McElroy Mine. Spectral resolution is 156 Hz----- 57

LIST OF FIGURES (continued)

	<u>Page</u>
Figure 3-39. Expanded spectrum of noise at surface above McElroy Mine. Spectral resolution is 19.5 Hz-----	58
Figure 3-40. Voltage spectrum from roof bolts separated 21.7 meters. Spectral resolution is 78.1 Hz-----	59
Figure 3-41. Expanded voltage spectrum from roof bolts separated 21.7 meters. Spectral resolution is 3.91 Hz-----	60
Figure 3-42. Expanded voltage spectrum from roof bolts separated 11.2 meters. Spectral resolution is 3.91 Hz-----	61
Figure 3-43. Expanded spectrum of noise from current-carrying conductor. Spectral resolution is 3.91 Hz-----	62
Figure 3-44. Logarithmic average magnetic field strength in McElroy Coal Mine in the frequency range 1080 Hz to 2880 Hz, produced usually by power line harmonics 3 through 8 of 360 Hz. Antenna sensitive axis orientation is vertical (up-down)-----	63
Figure 3-45. Comparison of magnetic field strengths of Grace and Robena Mines as a function of distance from noise source-----	64
Figure 3-46. Comparison of E-M noise levels near operating machinery from four mines. Vertical magnetic-field components are shown. Broken sections of the curves represent system noise-----	65
Figure 3-47. Comparison of E-M noise levels along haulageways in four mines. Vertical magnetic-field components are shown. Broken sections of the curves represent measurement-system noise levels-----	66
Figure 4-1. APD, 10 kHz, vertical component, location B on figure 3-1-----	73

LIST OF FIGURES (continued)

		<u>Page</u>
Figure 4-2.	APD, 30 kHz, vertical component, location B on figure 3-1-----	74
Figure 4-3.	APD, 70 kHz, vertical component, location B on figure 3-1-----	75
Figure 4-4.	APD, 130 kHz, vertical component, location B on figure 3-1-----	76
Figure 4-5.	APD, 160 kHz, vertical component, location B on figure 3-1-----	77
Figure 4-6.	APD, 250 kHz, vertical component, location B on figure 3-1-----	78
Figure 4-7.	APD, 500 kHz, vertical component, location B on figure 3-1-----	79
Figure 4-8.	APD, 1 MHz, vertical component, location B on figure 3-1-----	80
Figure 4-9.	APD, 2 MHz, vertical component, location B on figure 3-1-----	81
Figure 4-10.	APD, 6 MHz, vertical component, location B on figure 3-1-----	82
Figure 4-11.	APD, 14 MHz, vertical component, location B on figure 3-1-----	83
Figure 4-12.	APD, 10 kHz, horizontal component, (NE-SW), location B on figure 3-1-----	84
Figure 4-13.	APD, 30 kHz, horizontal component, (NE-SW), location B on figure 3-1-----	85
Figure 4-14.	APD, 70 kHz, horizontal component, (NE-SW), location B on figure 3-1-----	86
Figure 4-15.	APD, 130 kHz, horizontal component, (NE-SW), location B on figure 3-1-----	87
Figure 4-16.	APD, 160 kHz, horizontal component, (NE-SW), location B on figure 3-1-----	88
Figure 4-17.	APD, 250 kHz, horizontal component, (NE-SW), location B on figure 3-1-----	89

LIST OF FIGURES (continued)

		<u>Page</u>
Figure 4-18.	APD, 500 kHz, horizontal component (NE-SW), location B on figure 3-1-----	90
Figure 4-19.	APD, 1 MHz, horizontal component, (NE-SW), location B on figure 3-1-----	91
Figure 4-20.	APD, 2 MHz, horizontal component, (NE-SW), location B on figure 3-1-----	92
Figure 4-21.	APD, 6 MHz, horizontal component, (NE-SW), location B on figure 3-1-----	93
Figure 4-22.	APD, 14 MHz, horizontal component, (NE-SW), location B on figure 3-1-----	94
Figure 4-23.	APD, 32 MHz, horizontal component, (NE-SW), location B on figure 3-1-----	95
Figure 4-24.	APD, 10 kHz, vertical component, quiet time, location B on figure 3-1-----	96
Figure 4-25.	APD, 30 kHz, vertical component, quiet time, location B on figure 3-1-----	97
Figure 4-26.	APD, 70 kHz, vertical component, quiet time, location B on figure 3-1-----	98
Figure 4-27.	APD, 130 kHz, vertical component, quiet time, location B on figure 3-1-----	99
Figure 4-28.	APD, 10 kHz, vertical component, location A on figure 3-1-----	100
Figure 4-29.	APD, 30 kHz, vertical component, location A on figure 3-1-----	101
Figure 4-30.	APD, 70 kHz, vertical component, location A on figure 3-1-----	102
Figure 4-31.	APD, 130 kHz, vertical component, location A on figure 3-1-----	103
Figure 4-32.	APD, 160 kHz, vertical component, location A on figure 3-1-----	104

LIST OF FIGURES (continued)

		<u>Page</u>
Figure 4-33.	APD, 250 kHz, vertical component, location A on figure 3-1-----	105
Figure 4-34.	APD, 500 kHz, vertical component, location A on figure 3-1-----	106
Figure 4-35.	APD, 1 MHz, vertical component, location A on figure 3-1-----	107
Figure 4-36.	APD, 2 MHz, vertical component, location A on figure 3-1-----	108
Figure 4-37.	APD, 10 kHz, horizontal component (N-S), location A on figure 3-1-----	109
Figure 4-38.	APD, 30 kHz, horizontal component (N-S), location A on figure 3-1-----	110
Figure 4-39.	APD, 70 kHz, horizontal component (N-S), location A on figure 3-1-----	111
Figure 4-40.	APD, 130 kHz, horizontal component (N-S), location A on figure 3-1-----	112
Figure 4-41.	APD, 160 kHz, horizontal component (N-S), location A on figure 3-1-----	113
Figure 4-42.	APD, 500 kHz, horizontal component (N-S), location A on figure 3-1-----	114
Figure 4-43.	APD, 1 MHz, horizontal component (N-S), location A on figure 3-1-----	115
Figure 4-44.	APD, 10 kHz, vertical component, quiet time, location A on figure 3-1-----	116
Figure 4-45.	APD, 30 kHz, vertical component, quiet time, location A on figure 3-1-----	117
Figure 4-46.	APD, 70 kHz, vertical component, quiet time, location A on figure 3-1-----	118
Figure 4-47.	APD, 130 kHz, vertical component, quiet time, location A on figure 3-1-----	119

LIST OF FIGURES (continued)

	<u>Page</u>
Figure 4-48. APD, 1 MHz, vertical component, quiet time, location A on figure 3-1-----	120
Figure 4-49. APD, 10 kHz, vertical component, location B on figure 3-2-----	121
Figure 4-50. APD, 30 kHz, vertical component, location B on figure 3-2-----	122
Figure 4-51. APD, 70 kHz, vertical component, location B on figure 3-2-----	123
Figure 4-52. APD, 130 kHz, vertical component, location B on figure 3-2-----	124
Figure 4-53. APD, 160 kHz, vertical component, location B on figure 3-2-----	125
Figure 4-54. APD, 500 kHz, vertical component, location B on figure 3-2-----	126
Figure 4-55. APD, 1 MHz, vertical component, location B on figure 3-2-----	127
Figure 4-56. APD, 2 MHz, vertical component, location B on figure 3-2-----	128
Figure 4-57. APD, 6 MHz, vertical component, location B on figure 3-2-----	129
Figure 4-58. APD, 14 MHz, vertical component, location B on figure 3-2-----	130
Figure 4-59. APD, 10 kHz, vertical component, location A on figure 3-2-----	131
Figure 4-60. APD, 30 kHz, vertical component, location A on figure 3-2-----	132
Figure 4-61. APD, 70 kHz, vertical component, location A on figure 3-2-----	133
Figure 4-62. APD, 130 kHz, vertical component, location A on figure 3-2-----	134

LIST OF FIGURES (continued)

	<u>Page</u>
Figure 4-63. APD, 160 kHz, vertical component, location A on figure 3-2-----	135
Figure 4-64. APD, 250 kHz, vertical component, location A on figure 3-2-----	136
Figure 4-65. APD, 500 kHz, vertical component, location A on figure 3-2-----	137
Figure 4-66. APD, 1 MHz, vertical component, location A on figure 3-2-----	138
Figure 4-67. APD, 2 MHz, vertical component, location A on figure 3-2-----	139
Figure 4-68. APD, 6 MHz, vertical component, location A on figure 3-2-----	140
Figure 4-69. APD, 10 kHz, roof bolt measurements-----	141
Figure 4-70. APD, 150 kHz, roof bolt measurements-----	142
Figure 4-71. Field strength excursions between 0.001 and 99% of the time as a function of frequency, vertical component, location B on figure 3-1-----	143
Figure 4-72. Field strength excursions between 0.001 and 99% of the time as a function of frequency, horizontal component, (NE-SW), location B on figure 3-1-----	144
Figure 4-73. Field strength excursions between 0.001 and 99% of the time as a function of frequency, vertical component, quiet time, location B on figure 3-1-----	145
Figure 4-74. Field strength excursions between 0.001 and 99% of the time as a function of frequency, vertical component, location A on figure 3-1-----	146

LIST OF FIGURES (continued)

	<u>Page</u>
Figure 4-75. Field strength excursions between 0.001 and 99% of the time as a function of frequency, horizontal component, location A on figure 3-1-----	147
Figure 4-76. Field strength excursions between 0.001 and 99% of the time as a function of frequency, vertical component, quiet time, location A on figure 3-1-----	148
Figure 4-77. Field strength excursions between 0.001 and 99% of the time as a function of frequency, vertical component, location B on figure 3-2-----	149
Figure 4-78. Field strength excursions between 0.001 and 99% of the time as a function of frequency, vertical component, location A on figure 3-2-----	150

ELECTROMAGNETIC NOISE IN MCELROY MINE

Two different techniques were used to make measurements of the absolute value of electromagnetic noise in and above an operating coal mine, McElroy Mine, located near Moundsville, West Virginia. The electromagnetic environment created by 300 volt dc and 480 volt ac machinery was measured. In one technique noise was measured over the entire electromagnetic spectrum of interest for brief time periods. The noise was recorded using broadband analog magnetic tape. The noise data was later transformed to give spectral plots. In the other technique, noise amplitudes were recorded at several discrete frequencies for a sufficient length of time to provide amplitude probability distributions.

The specific, measured results are given in a number of spectral plots and amplitude probability distribution plots.

Key words: Amplitude probability distribution; coal mine noise; digital data; electromagnetic communications; electromagnetic interference; electromagnetic noise; Fast Fourier Transform; Gaussian distribution; impulsive noise; magnetic field strength; measurement instrumentation; spectral density; time-dependent spectral density.

1. INTRODUCTION

This report gives data concerning electromagnetic noise in a coal mine that used dc shuttle-car and rail-haulage power; the remainder of the section machinery and belt haulage used ac power. In this section, background information and a brief mine description are covered. In Section 2, measurement instrumentation is discussed. In Section 3, spectral plots of data are presented. In Section 4, amplitude probability distributions (APD) of magnetic-field noise are given. The last two sections cover conclusions and recommendations.

Only representative samples of the total data measured are given in this report, and only a limited set of data-presentation formats have been used. Additional data, or data presentation in other formats may be obtained from the authors with the specific permission of the Bureau of Mines. A more complete description of the measurement systems used is given in previous publications [1,4].

1.1 Background

The need for reliable communication systems in mines is a long-standing problem. For emergency use, when all power in a mine is off, the residual electromagnetic noise is no problem. However, if a communication system were designed only for emergency use, it would have two serious drawbacks. First, it would not be ready for immediate use in an emergency; second, it would not be of any value during normal operations. Therefore, the Bureau of Mines decided to design a communication system that could be used for both emergency and normal operational conditions.

During operation, the electrical machinery used in mines creates a wide range of many types of intense electromagnetic interference (EMI). This EMI is a major limiting factor in the design of a communication system.

The work reported here gives the results of comprehensive measurements of this EMI in critical communication locations where miners extract coal, as well as along haulageways.

There are several EMI parameters that can be measured: magnetic field strength, H ; electric field strength, E ; conducted current, I ; and voltage, V , between two conductors. One parameter was emphasized, magnetic field strength. There are several reasons. First, electric field sensors are very

insensitive at lower frequencies, and hence probably will not be useful in any practical mine communication system. Second, at any air-earth interface, only the magnetic field is essentially undisturbed, while the electric field is severely reduced. Third, any currents will induce magnetic fields, and hence measurement of the magnetic field will directly sense currents. Fourth, power line voltages are propagated as transmission line phenomena, are directly related to transmission line currents, and hence to magnetic fields induced. Thus, measuring magnetic field strength gives a representative composite picture of noise from currents and voltages from most sources, as well as measuring the magnetic fields induced by arcing equipment.

Although magnetic field strength measurements are emphasized, this parameter is difficult to measure meaningfully. The IEEE definition [2] of magnetic field strength, H (magnitude of the magnetic field vector), is used in this report. Since there are a multitude of different sources that generate all known types of noise, the resultant magnetic field strength noise vector is a function of frequency, time, orientation, and location. Small variations in these parameters can cause several orders of magnitude difference in measured field strength.

1.2 Mine Description

The results and data presented in this report are based on measurements made on April 10 and 12, 1973, in the McElroy Coal Mine, near Moundsville, West Virginia. The mine belongs to the Consolidation Coal Company. Room-and-pillar mining techniques are used. The measurements were made primarily in section 1-left, 1-north. The overburden in this area is 200 to 275 meters.

Mining is accomplished using a continuous miner, head-loader, shuttle-cars (buggies), conveyor belt, and electric-trolley haulage. The electric trolley and the shuttle-cars were powered by 300 volts dc. All other equipments, including fans and rock dusting machines, were ac powered. The continuous miner had a telescoping feature to allow roof bolting simultaneous with mining. No one had to work under roofing that had not been bolted.

2. MEASUREMENT INSTRUMENTATION

Two measurement techniques were used. In the first technique used, a large portion of the spectrum is covered as a "snapshot" at one relatively short period of time. In three-dimensional form, several such "snapshots" can show how drastically a signal varies, not only with frequency, but also with time. In the second technique, variations over a 20-minute time interval are measured at a single frequency. Usually, a set of twelve different frequencies was used. Both techniques were used to measure two orthogonal components of magnetic field strength. This was done either by using two systems simultaneously or by varying the orientation of one system; both techniques were used in as many different locations as possible.

With the exception of the roof bolt APD plots, all measured noise is reported in absolute quantities (instead of relative) to allow others to make effective use of the data. For the magnetic field strength measurements, the NBS field calibration site was used with each complete measurement system to assure correct calibration [3].

A complication to making these measurements is the mine environment, which is generally humid, dusty, poorly lighted, and potentially explosive. Battery-operated, dust-protected, permissible gear was used for most of our portable measuring equipment.

There are two types of noise recorded in the spectral plots, and hence two different magnetic-field-strength parameters are required, H and H_d . Results are given as the rms value of one component of magnetic field strength, H , versus frequency for discrete frequencies, or as one component of magnetic-field-strength spectrum density level [2], H_d , versus frequency for broadband noise in the spectral plots. In the amplitude probability distributions, results are given as the rms value

of one component of the instantaneous magnetic field strength versus percent of time this value is exceeded. The APD gives the distribution of the actual instantaneous value only as far as the measurement-system detector bandwidth will allow the detector to follow the time variations of the actual magnetic field. (In this context, noise envelope is sometimes used.) Thus, the results are applicable for a communication receiver whose bandwidth is similar to the measurement-system detector bandwidth.

Three measurement systems were used to make measurements underground. The three systems are described in the block diagrams shown in figures 2-1, 2-2, and 2-3. Figures are located at the end of each section in this report. For a detailed description of these systems, see previous publications [1,4]. The systems used in McElroy are the same as those used in Grace.

In the first system, data is measured for spectral plots and is fully mine permissible and portable. In the second system, data is measured for statistical descriptions of time variations, most commonly amplitude probability distribution; it is also permissible. The third system is not permissible but is portable (with considerable effort); it records data for both spectral plots and statistical presentations.

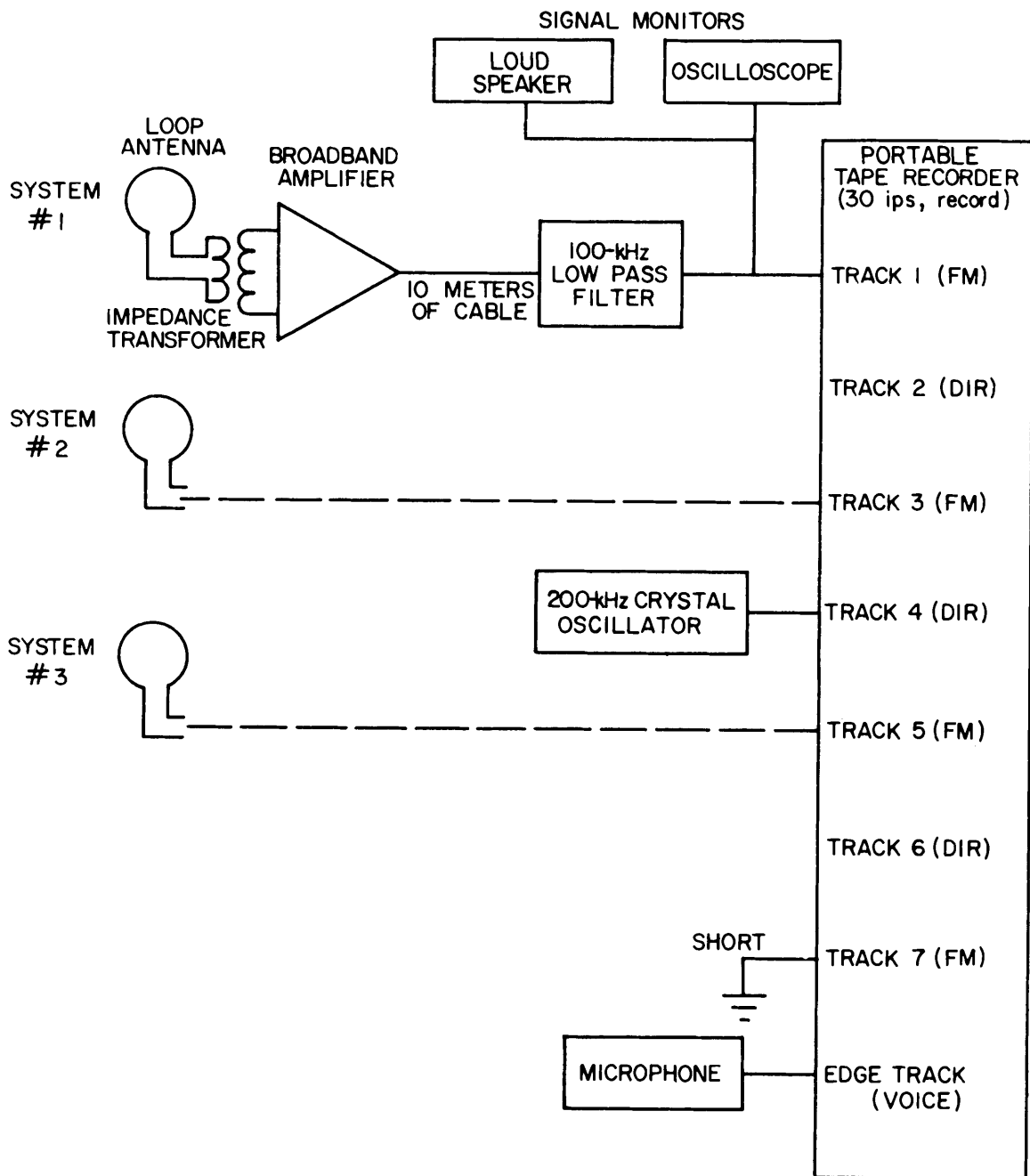


Figure 2-1 Block diagram of portable instrumentation. FM tracks are used to record from 100 Hz to 100 kHz; direct tracks are used from 3 kHz to 320 kHz. Systems 2 and 3 are identical to system 1. When the direct tracks are used, the 100-kHz low pass filters are eliminated, and the amplifier bandwidth is increased from 100 kHz to 300 kHz. The microphone is used for occasional vocal comments by the operator.

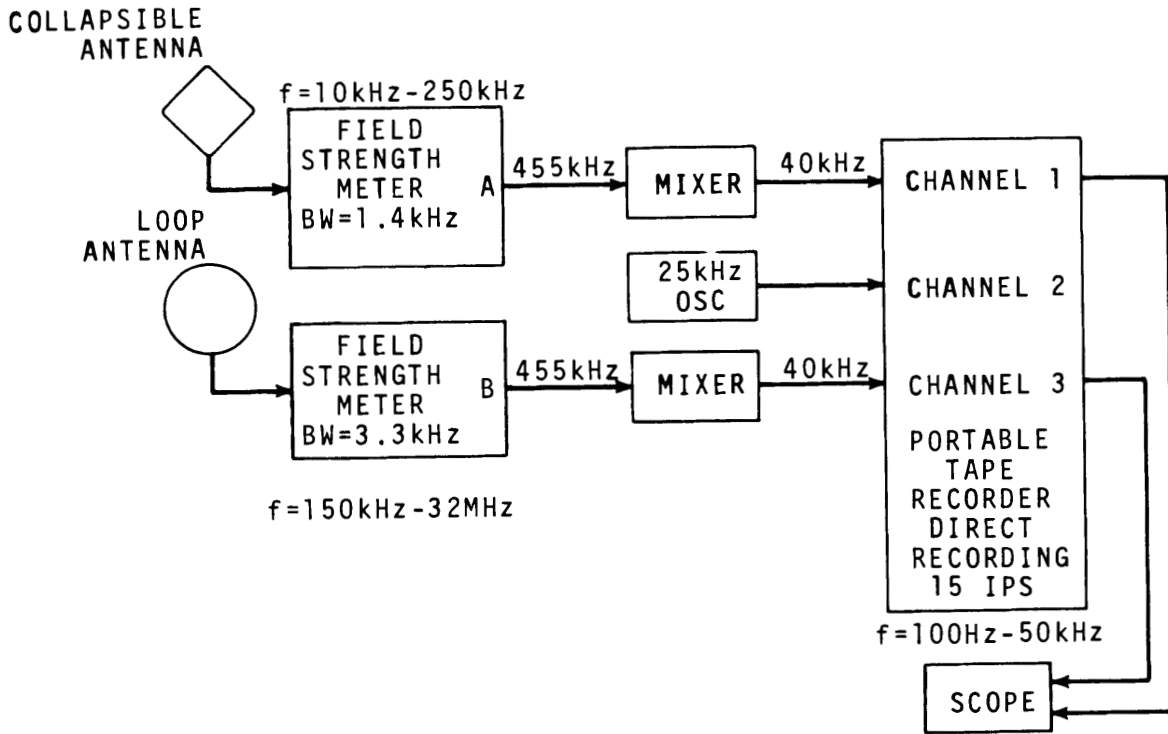


Figure 2-2 System for field recording data to obtain amplitude probability distributions.

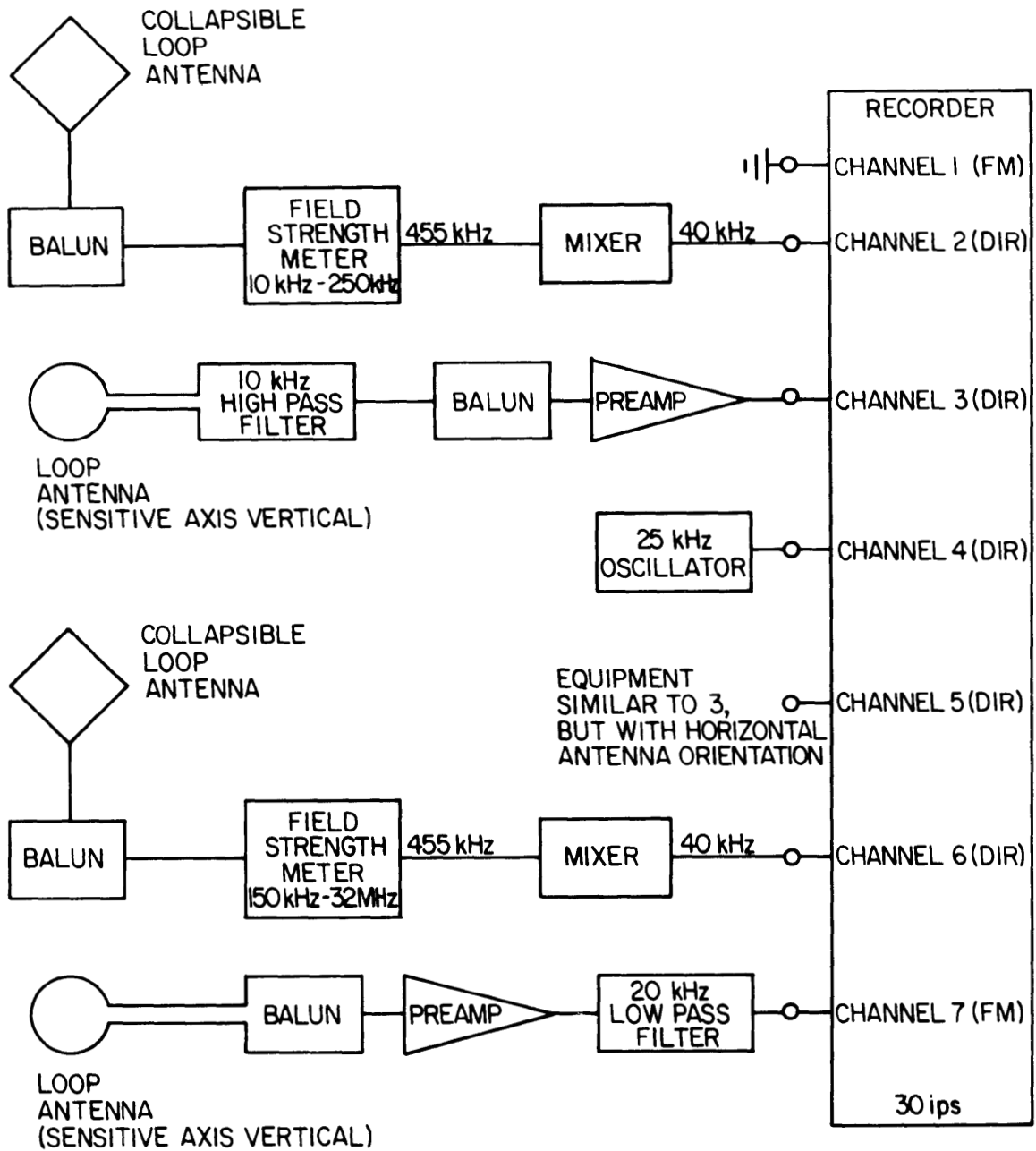


Figure 2-3 Block diagram of laboratory recording system modified for field use.

3. SPECTRUM MEASUREMENT RESULTS

3.1 Introduction

In this section of the report, spectrum plots are presented and discussed. Most of these plots present magnetic field strength up to 100 kHz. Measurements were made at many different locations and results can be used to characterize electromagnetic noise levels generated by most fixed and mobile equipment used in this mine.

3.2 Antenna Sites

Figure 3-1 is a map of section 1-left 1-north as it was on April 10, 1973 when the first day of measurements were made. In the mining operation, four entries are driven forward and are identified on figure 3-1, from right to left: power entry, rail entry (trolley tracks), belt entry, and return air entry. Noise spectrum measurements were taken in 7 locations the first day and are designated by letters A through G on figure 3-1. Results are reported from measurements taken at five locations on the second day, four of which are designated by letters A through D on figure 3-2.

3.3 Electromagnetic Noise Spectrum Results

3.3.1 Interpretation

When reading values from the spectra in this report, the following points should be kept in mind:

1. Field strength values above the upper roll-off frequency and below the lower roll-off frequency are not calibrated and are therefore not shown on most spectra.
2. The correct units for the spectral peaks are micro-amperes per meter ($\mu\text{A}/\text{m}$), as these are cw signals.

3. The broadband noise between spectral peaks is as seen by a receiver having the same bandwidth as the Fast Fourier Transform (FFT) spectral resolution bandwidth used to compute the spectrum. The correct units for the background noise between peaks are microamperes per meter per square root x hertz $[(\mu\text{A}/\text{m})/\sqrt{x \text{ Hz}}]$, where x is the spectral resolution of the FFT (x equals 78.1 Hz for the 1-to-100-kHz graphs).

An easy way to obtain the spectral density per (one) root hertz for broadband noise is to subtract the required number of dB, remembering that the units have now changed to $(\mu\text{A}/\text{m})/\sqrt{\text{Hz}}$. For spectra with a resolution bandwidth of 78.1 Hz, subtract $10 \log_{10} (78.1)$ or 18.93 dB.

The Appendix gives the code key used in determining the meaning of the numbers in the header block at the top of each spectrum. The resolution bandwidth is also given on the ordinate of the plots.

3.3.2 Uncertainties

The spectra to 100 kHz, to 3 kHz, and to 20 kHz have uncertainties of ± 1 dB over the following portions of the spectra. The 100 kHz spectra are valid either from 1 to 100 kHz or 10 kHz to 100 kHz as stated or shown. The 3 kHz spectra have a ± 1 dB uncertainty from 100 Hz to 3 kHz. The 20 kHz spectra have an uncertainty of ± 1 dB from 750 Hz to 20 kHz.

The spectra shown to 180 kHz have an uncertainty of ± 2 dB from 3 kHz to 180 kHz.

3.3.3 Section Measurements

Figure 3-3, upper curve, shows the magnetic field noise spectrum from 1 kHz to 100 kHz received at the antenna location identified as C (in figure 3-1). Location C is the section

power center and contains the step-down transformer and rectifier. C is one of the noisier locations in the mine (a small band of frequencies around 10 kHz measured at location B on the second day was 8 dB higher). This steady background noise is made up primarily of harmonics of 360 Hz, produced when three-phase, 60 Hz power is full-wave rectified. Figure 3-4 shows the expanded spectrum measured at location C. This spectrum is one of the strongest measured in the mine. Oddly, while multiples of 360 Hz (6th harmonic of 60 Hz) predominate elsewhere in the mine, in this case, harmonics 60 Hz on either side of multiples of 360 Hz predominate.

Figure 3-5 shows the noise spectrum measured two meters from the continuous miner (location D on figure 3-1). This location was also a relatively noisy location in the mine in the frequency range from 20 kHz to 60 kHz. With the head-loader operating, and the miner not operating, the noise spectrum is similar to figure 3-5. With both the miner and head-loader not operating, the noise above 10 kHz drops 6 to 10 dB.

Figures 3-6 and 3-7 show noise spectra measured at location E. A measurement made 30 minutes later showed a 10 dB increase from 8 to 12 kHz and a 3 to 5 dB decrease from 25 to 60 kHz. Figure 3-8 shows the noise spectrum measured at location F. This spectrum was taken when most equipment in the mine was not working. The noise spectrum has about the same shape as shown in the previous location, but at location F, the noise is 5 to 14 dB less from 5 to 60 kHz. This figure also shows the signal from the 100 kHz mine phone.

Figures 3-9 and 3-10 show the noise measured at location B on the first day, with no equipment running. Figures 3-11 and 3-12 show the noise measured at the same location later when all the mining equipment was working and about 15 meters distant. The latter two figures show a noise increase of 8 to 30 dB, depending on frequency, when the face machinery 15 meters distant was working.

The quietest location measured in McElroy mine was in the return air entry, during shift change. This area is designated by letter G on figure 3-1, and is located 55 meters from the power center. Figures 3-13 and 3-14 show one of the strongest of the three orthogonal components measured at location G. The antenna sensitive axis was horizontal and parallel with the return-air-entry. The spectrum taken with the antenna sensitive axis horizontal and perpendicular to the return-air-entry shows the harmonics to be within 6 to 10 dB of those shown in figure 3-14. The spectrum of the vertical noise shows about 13 dB higher noise levels at the low end and about 22 dB lower at the high end of the spectrum than the horizontal, parallel spectrum shown in figure 3-14. The crossover occurs near 500 Hz. Measurements made in the same location 2 days later (letter D, figure 3-2) during shift change, and also after the mine had closed for a strike, show that the noise was within a few dB of that shown on figure 3-13. This return-air-entry location is unusual in that the noise received with the antenna axis horizontal was stronger than for the antenna axis vertical.

The noise measured at the section power center with the mine running (noisy location), with the antenna axis vertical, is 40 to 60 dB stronger over the 1 to 100 kHz frequency range than the noise measured in the return-air-entry (quiet location), between shifts, with the antenna axis vertical.

Measurements were taken with the third measurement system in a crosscut shown as location A on figure 3-2 in the immediate (one to three meters) vicinity of a continuous miner and supporting shuttle buggies. Figures 3-15 through 3-22 show spectra of noise generated by this machinery. Figure 3-23 shows field levels generated by an impulse in this same location.

3.3.4 Haulageway Measurements

On April 12, 1973, the second day in the mine, measurements were made at three locations along the mine haulageway.

Figures 3-24 and 3-25 show the vertical-antenna-axis noise spectrum measured at the point in the haulageway where men board man-trips for transportation to the working sections. No trains were in the vicinity when the measurement was made. This point is near the bottom of an elevator shaft and is several kilometers from the locations measured in section 1-left, 1-north. Between 5 and 60 kHz the noise received with the antenna sensitive axis vertical was stronger by 10 to 20 dB than the noise received for horizontal antenna axis orientation. Here, as in most other locations, the noise is primarily powerline-related multiples of 360 Hz. The spectrum shape was slightly different. For example, the relative minimum was at 25 kHz instead of 22 kHz. Below 2 kHz, the noise received on the antenna with the sensitive axis horizontal was 8 to 15 dB stronger than the noise shown on figure 3-25. At this location, the 100 kHz unmodulated carrier signal strength from a mine phone on a portal-bus 210 meters away was measured as 47 dB μ A/m.

A second haulageway location where noise was measured was on the main-line haulage near section 1-left, 1-north. This location is lettered B on figure 3-2. Figures 3-26 and 3-27 show the noise recorded during the passing of a rapidly moving train that was drawing power. The noise at this location was found to vary more than in other locations. Other spectra taken here showed 10 to 20 dB lower noise than figure 3-26 for trains moving slowly, or for the absence of trains. As an illustration, figure 3-28 shows the spectrum from 100 Hz to 3 kHz for a train of empty cars

moving slowly. From this it can be seen that a transient has briefly raised the background level of the previous spectrum, figure 3-27. While at location B, second day, a 100 kHz trolley phone signal from a remote location was measured as 27 dB relative to 1 μ A/m.

The third location along a haulageway where noise was measured is lettered C on figure 3-2. This location is on the opposite side of the recirculating "run-around" from location B. The left side of the run-around is kept supplied with empty coal cars. An automatic car-pull located at C moves the empty cars forward as the coal coming off the conveyor belt "headpiece" fills the cars. Full cars are then periodically removed from the right hand side of the run-around. Figures 3-29 and 3-30 show the noise measured at location C. At this time, the conveyor belt and the car pull were running.

Data from measurements taken at the end of a rail haulage, location A in figure 3-1, are shown in figures 3-31 and 3-32. These data were taken with the third measurement system.

3.3.5 Arc Welder Measurement

On the second day in the mine, the face had advanced as shown in figure 3-2. Figure 3-33 shows the noise measured in location A in figure 3-2 (the arc welder was not operating). Later, a helium-gas-shielded arc welder began operation. The welder used ac input voltage, and delivered 250 amperes at 30 volts to the welding rod. Figure 3-34 shows the spectrum measured with the welder drawing full current. The antenna was about 15 meters away. The spectrum with the welder operating is lower than with the welder off by as much as 16 dB at some frequencies. A quiet crackling, sounding like grease frying, was heard on the audio monitor. This indicates

that this particular welder produced no strong spectral components. It did produce some impulses, but they were generally of a smaller amplitude than those associated with switching transients from section mining equipment.

3.3.6 Surface Measurements

Noise measurements were made on the surface of the ground, above the mine, at 5:25 p.m. on April 11, 1973. The location was a rural hilltop over 1 left, 1 north. The antenna site was 12 meters from a rural, single-phase distribution power line. The site was about one kilometer from a large, high tension line. Figures 3-35 and 3-36 show the spectrum measured on the surface with the antenna sensitive axis pointing N-S and parallel to the local power line. This figure shows many man-made transmitted signals, as well as what appears to be some atmospheric noise in the region below 30 kHz. The energy shown around 100 kHz is broadcast by a Loran-C navigation system. Note the signal from the National Bureau of Standards WWVB, frequency-and-time radio station transmission at 60 kHz. This transmitter is located near Fort Collins, Colorado. Surface noise measurements were made in all 3 orthogonal directions; however, only one direction (N-S) is shown. The other orthogonal directions showed lower signal strengths from man-made carriers and more momentary broadband sferics.

Other spectral plots taken with the third measurement system are shown in figures 3-37, 3-38, and 3-39.

3.4 Miscellaneous Measurements

3.4.1 Measurement of Voltage Between Roof Bolts

Two roof-support bolt measurements were performed at location F on the first day. The voltage was measured using non-shielded copper wire clipped to the bolts. For the first measurement, the separation between bolts was 21.7 meters. Figures 3-40 and 3-41 show the spectrum measured. For the second measurement, the separation between bolts was reduced to 11.2 meters. Figure 3-42 shows the spectrum measured. No receiver system noise curve is available for these spectra. With the exception of the sixth harmonic of 60 Hz, the shorter distance between roof bolts shows higher power line noise than the longer separation. The second spectrum (shorter separation) shows an impulse that has been picked up. It is not possible to say that the voltage measured between bolts was induced by any single mechanism. It may be any combination of electric and magnetic fields acting on the copper wires connected to the bolts, as well as by any potential produced by current flow between the bolts.

3.4.2 Shuttle-Car Current Spectrum

While no calibrated current measurements were made in McElroy mine, one measurement was made with the loop antenna placed directly adjacent to the shuttle-car power cable. This adjacent placement caused the loop to strongly couple to the current in the cable. Figure 3-43 shows the resulting spectrum. Note the strong 360 Hz fundamental and harmonics of this dc-driven machine. This spectrum gives the characteristic signature of dc-powered machinery supplied by three-phase, full-wave rectifiers. This figure shows the highest field strength values measured; this is due to the loop being unusually and artificially close to the current carrying cable.

3.5 Intercomparison of Magnetic-Field Noise in Different Mines

3.5.1 Summary of 1 kHz to 3 kHz Data

Figure 3-44 is a summary of magnetic field strength at power-line harmonic frequencies observed within McElroy. Plotted are the logarithmic averages (arithmetic average dB value) of the six highest powerline harmonics. The logarithmic average masks the highest single value. Average fields at nine locations in the mine and one on the surface are plotted as a function of distance from the nearest current-carrying cable or wire. The six frequencies chosen are between 1020 Hz and 2940 Hz and are either the third through eighth harmonic of 360 Hz, or the highest adjacent powerline harmonic.

Figure 3-45 is a summary of magnetic field strength over the same frequency region as measured in the Robena Coal Mine (all 600 V dc) and the Grace Iron Mine (diesel-powered haulage).

A comparison of the magnetic noise from 1 kHz to 3 kHz in the three mines shows:

1. McElroy is quieter than Robena.
 - a. The highest logarithmic average of section noise measured one meter from a cable in McElroy is 51 dB relative to 1 μ A/m (power center). The noise in Robena at an "air split" on a haulageway is 16 dB higher and at a car pull during operation is 21 dB higher than this 51 dB value.
 - b. The quietest location in McElroy is 26 dB quieter than the quietest location in Robena.
2. McElroy is noisier than Grace.
 - a. Most of the McElroy measurements in the section were noisier than the noisiest Grace measurement (the diesel-powered Load-Haul-Dump (LHD) vehicle) by as much as 10 dB.

b. The quietest location in McElroy is 12 dB noisier than the quietest location in Grace.

The magnetic noise from 1 kHz to 3 kHz in the three mines compared to the noise measured on the surface above McElroy shows:

1. All measurements in Robena were higher by 15 to 78 dB.
2. Most measurements in McElroy were higher by 14 to 33 dB.
3. The LHD measurement in Grace was higher by 22 dB.

3.5.2 Summary of 3 kHz to 180 kHz Data

Figures 3-46 and 3-47 are given to show how field-strength levels at McElroy compare with levels in some other mines (i.e., Grace, Robena, and Itmann Mines). Figure 3-46 shows levels near operating equipment while figure 3-47 shows levels in haulageways. The curves are shown to 200 kHz, but the ± 2 dB uncertainty is valid only from 3 to 180 kHz. The Robena curves are shown to 100 kHz.

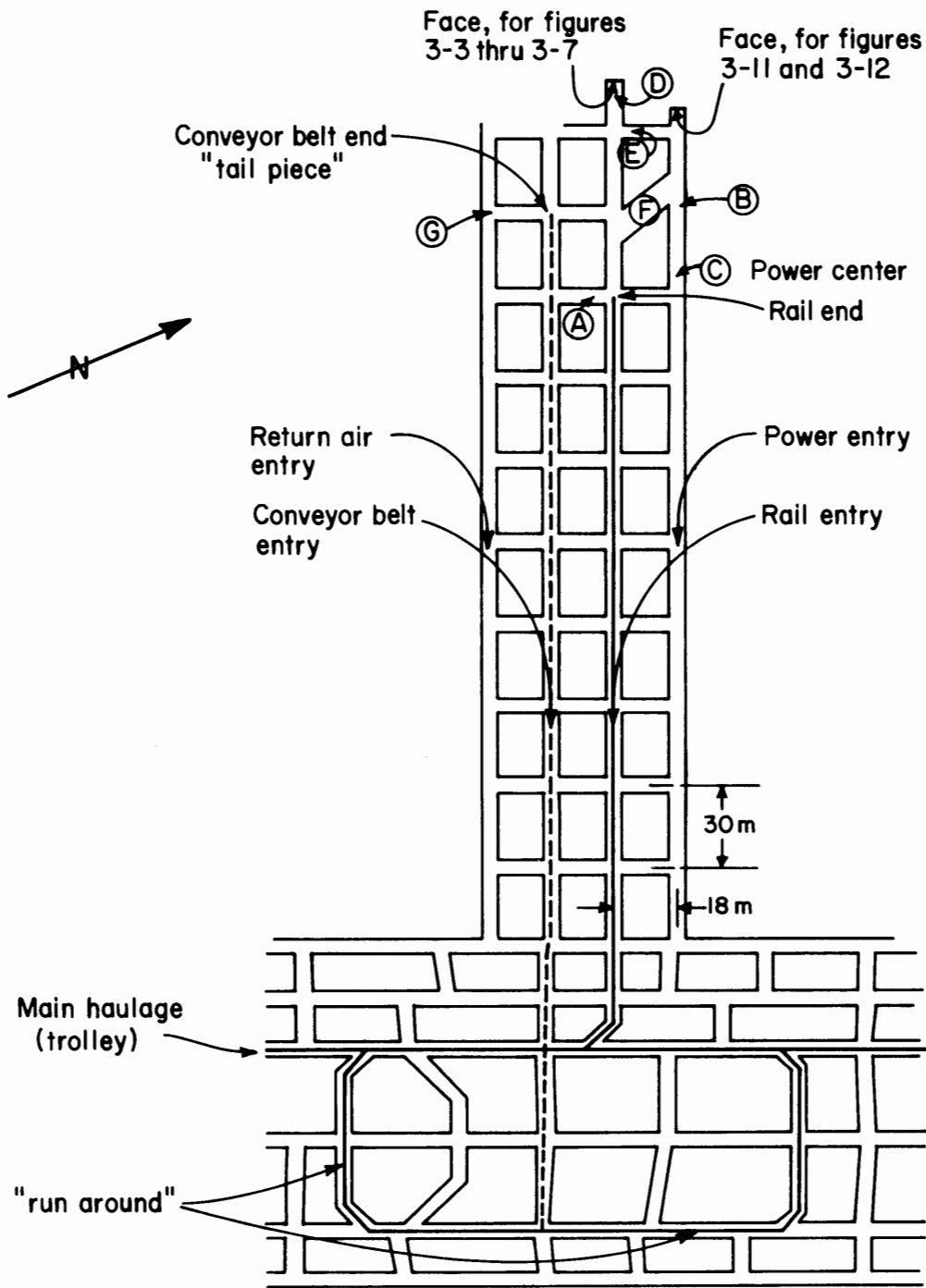


Figure 3-1 Map of McElroy Coal Mine, section 1-left, 1-north for April 10, 1973, the first day of measurements.

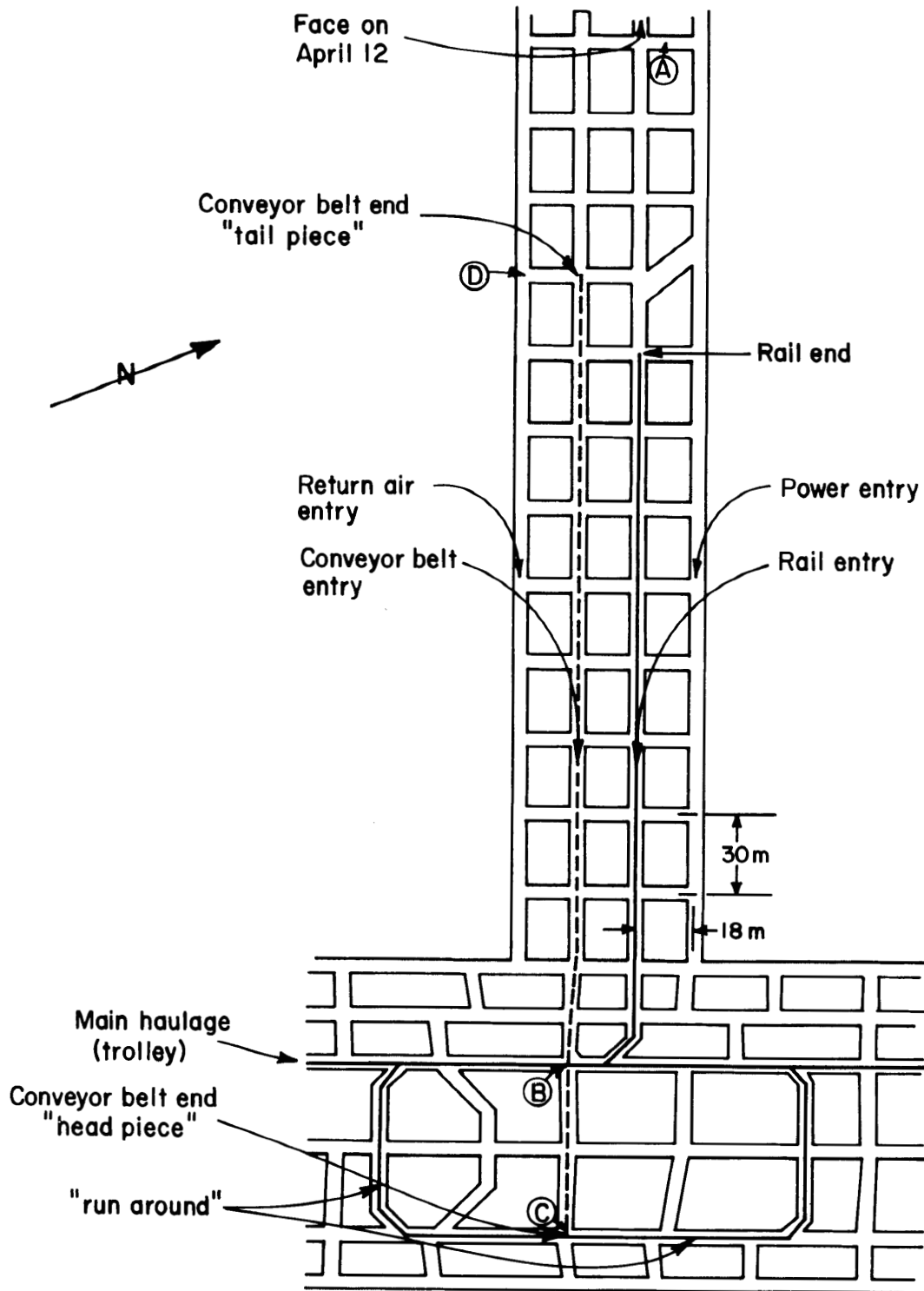


Figure 3-2 Map of McElroy Coal Mine, section 1-left, 1-north for April 12, 1973, the second day of measurements.

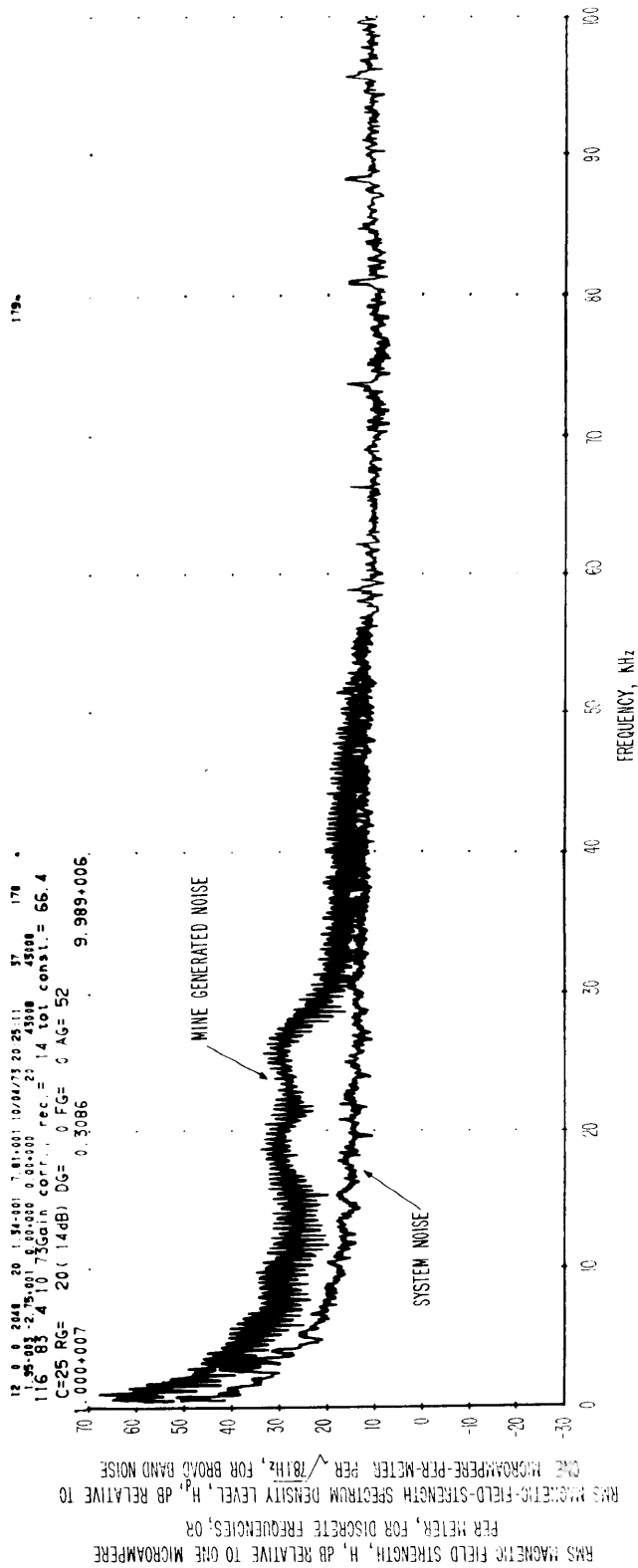


Figure 3-3 Spectrum of magnetic field strength obtained on a loop antenna 1 kHz to 100 kHz, McElroy Mine, location C, antenna in power entry between transformer and rectifier sled power center, antenna sensitive axis vertical, 2:25 p.m., April 10, 1973. Spectral resolution is 78.1 Hz.

12 0 0 2048 20 2.69+000 3.91+000 15/21/74 12:16:54 35 12 *
 1.95+003 -3.99+000 0.00+000 0.00+000 21 43:58 43:58
 34 112 4 10 73Gain corr., rec.= 14 tot const.= 66.4
 C=42 RG= 20 (14dB) DG= 0 FG= 0 AG= 52
 1.000+011 0.3086 3.054+010.

RMS MAGNETIC FIELD STRENGTH, H, dB RELATIVE TO ONE MICROAMPERE
 PER METER, FOR DISCRETE FREQUENCIES; OR
 RMS MAGNETIC-FIELD-STRENGTH SPECTRUM DENSITY LEVEL, H, dB RELATIVE TO
 ONE MICROAMPERE-PER-METER PER $\sqrt{391}$ Hz, FOR BROAD BAND NOISE

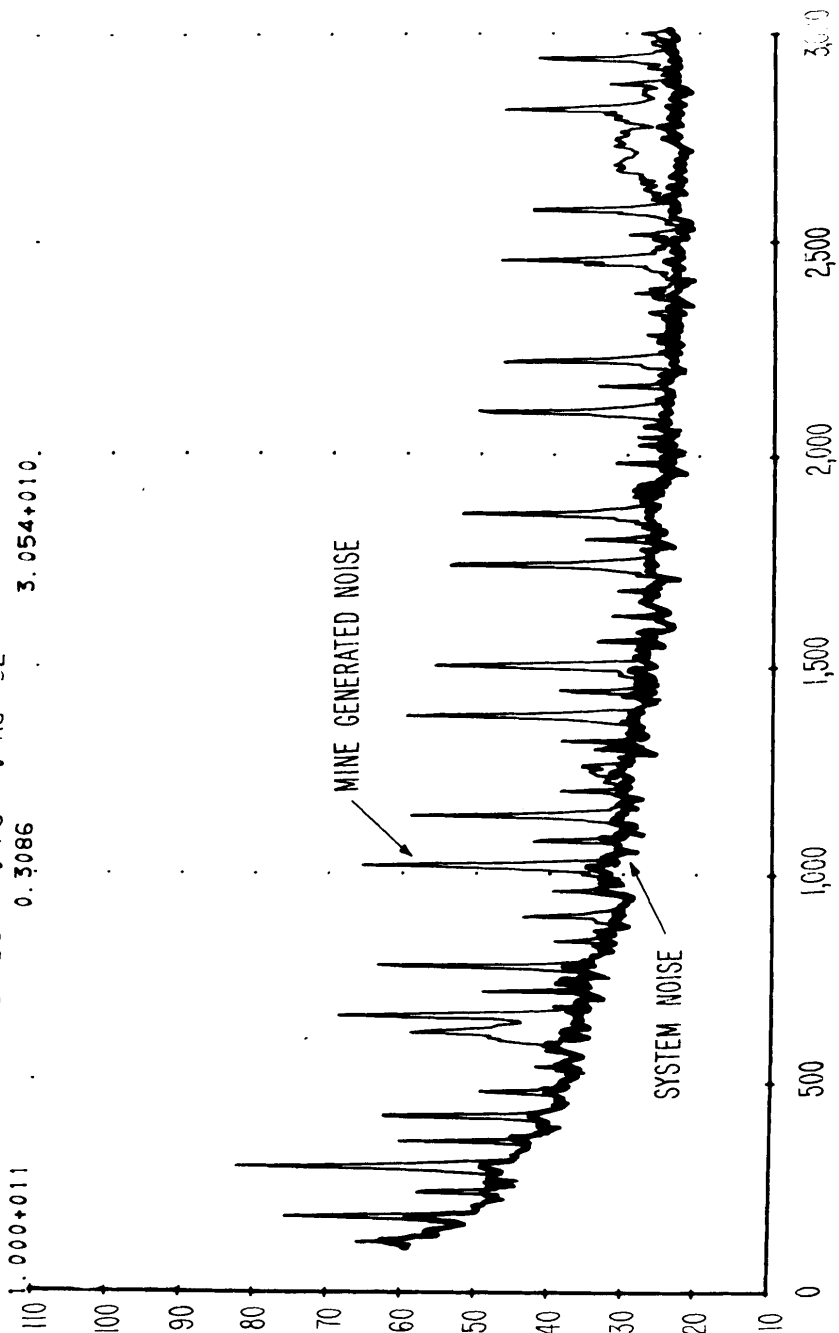


Figure 3-4 Spectrum of magnetic field strength obtained on a loop antenna
 100 Hz to 3 kHz, McElroy Mine, location C, antenna in power
 entry between power center transformer and rectifier sited, antenna
 sensitive axis vertical, 2:25 p.m., April 10, 1973. Spectral
 resolution is 3.91 Hz.

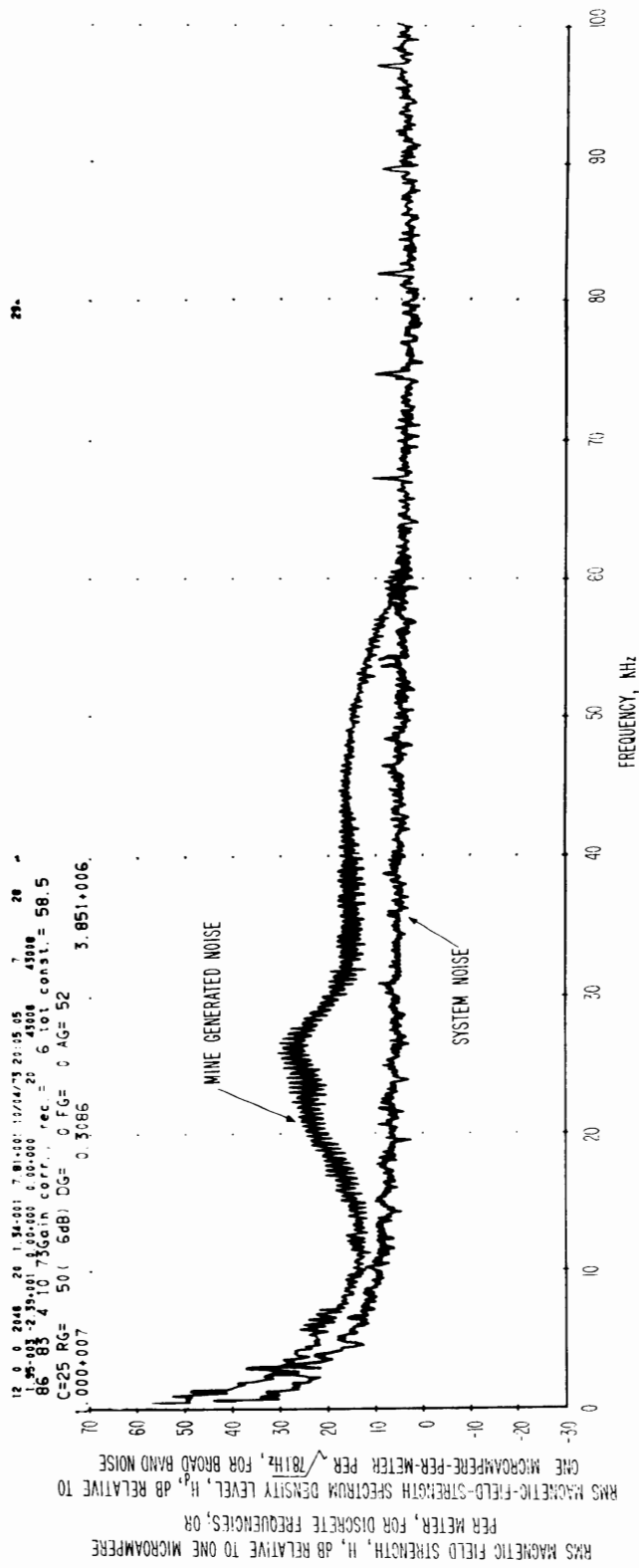


Figure 3-5 Spectrum of magnetic field strength obtained on a loop antenna 1 kHz to 100 kHz, McElroy Mine, two meters from miner, miner operating, location D, antenna sensitive axis vertical, 11:30 a.m., April 10, 1973. Spectral resolution is 78.1 Hz.

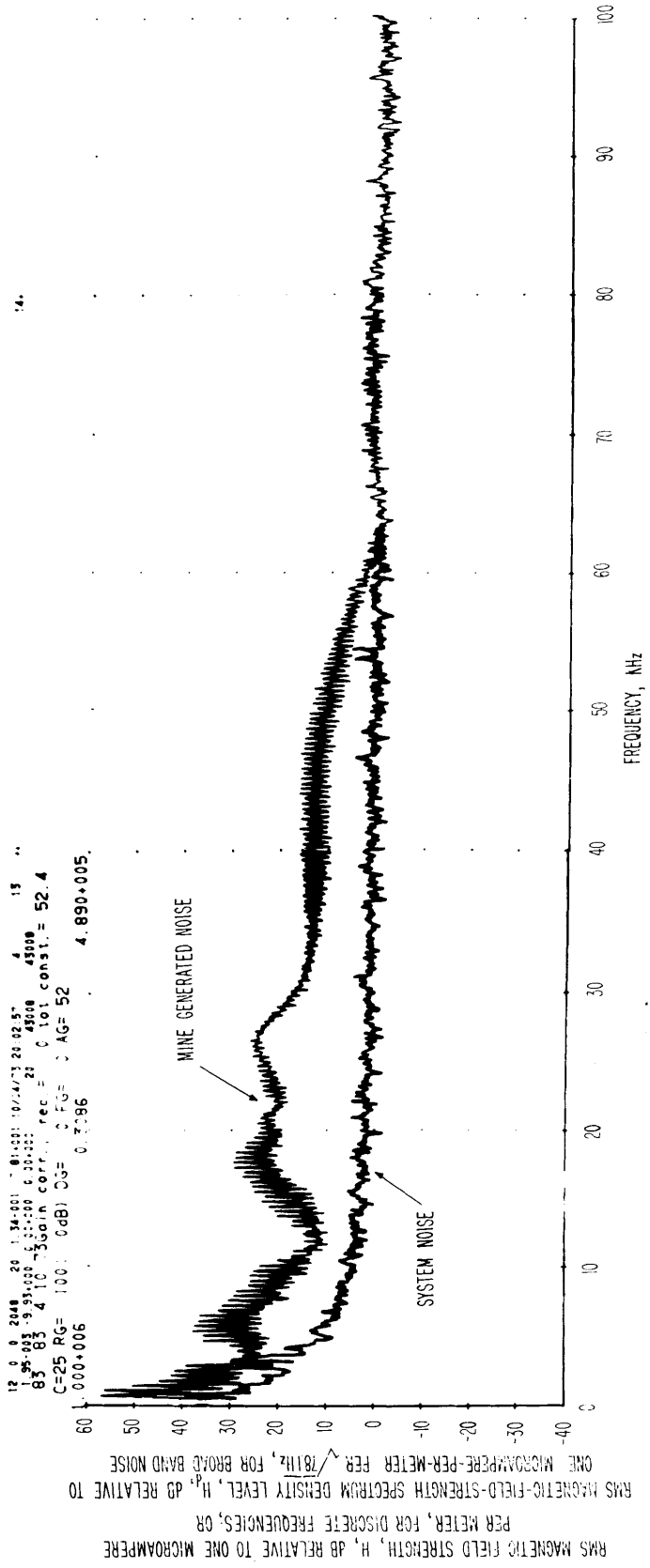


Figure 3-6 Spectrum of magnetic field strength obtained on a loop antenna 1 kHz to 100 kHz, McElroy Mine, location E, in crosscut, antenna sensitive axis vertical, 11:30 a.m., April 10, 1973. Spectral resolution is 78.1 Hz.

12 0 0 2048 20 2.69+000 3.91+000 04/23/74 2:11:27 52
 1.95-003 -3.00+001 0.00+000 0.00+000 2: 43:08 43:08
 15 112 4 10 73 Gain corr., rec. = 0 tot const. = 52.4
 C=42 RG= 100 (0dB) DG= 0 FG= 0 AG= 52
 1.000+009 0.3086 6.476+008.

RMS MAGNETIC FIELD STRENGTH, H, dB RELATIVE TO ONE MICROAMP/ERE
 PER METER, FOR DISCRETE FREQUENCIES; OR
 RMS MAGNETIC FIELD-STRENGTH SPECTRUM DENSITY LEVEL, H_p, dB RELATIVE TO
 ONE MICROAMP/ERE-PER-METER PER $\sqrt{3.91 \text{ Hz}}$, FOR BROAD BAND NOISE

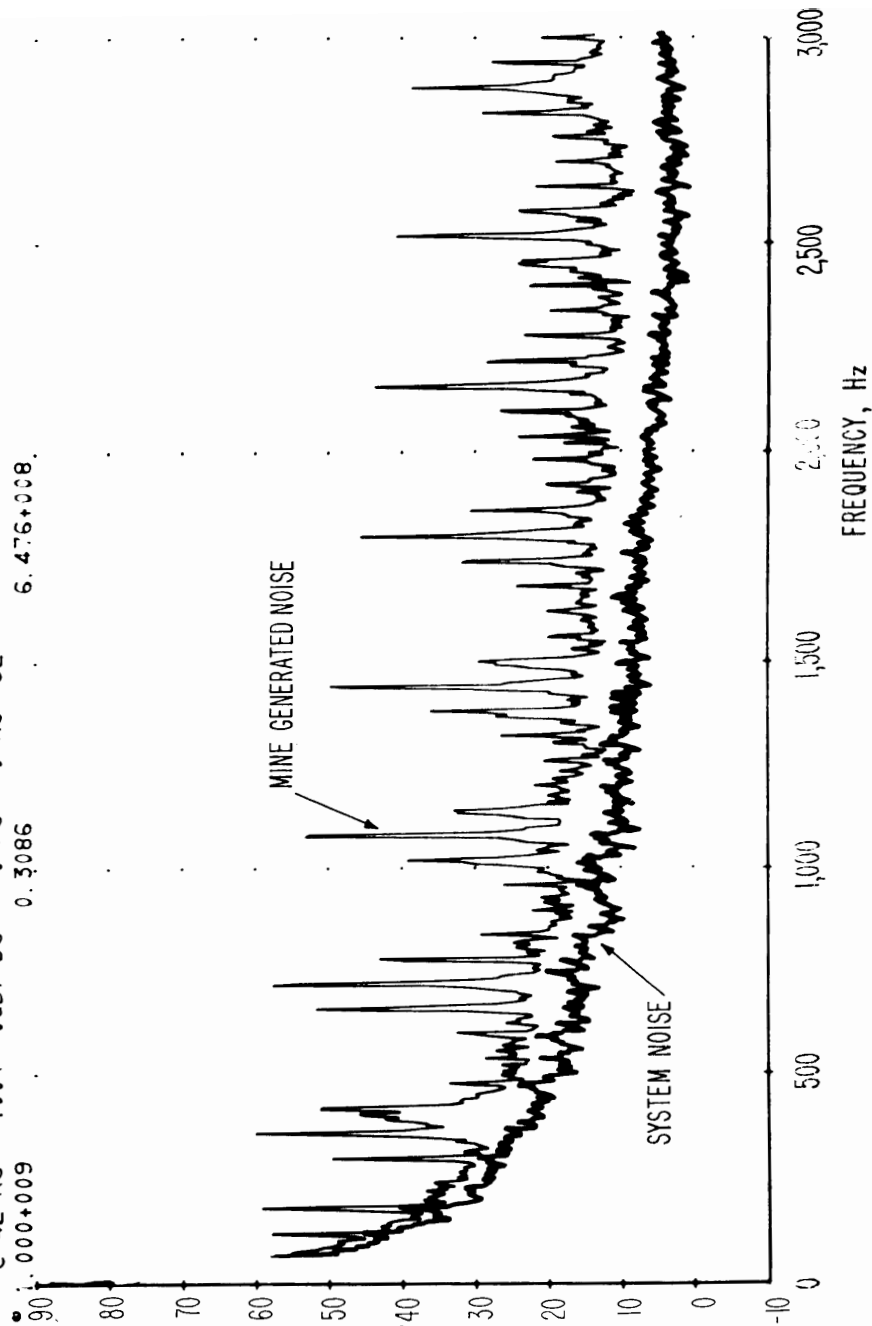


Figure 3-7 Spectrum of magnetic field strength obtained on a loop antenna
 100 Hz to 3 kHz, McElroy Mine, location E, in crosscut,
 antenna sensitive axis vertical, 11:30 a.m., April 10, 1973.
 Spectral resolution is 3.91 Hz.

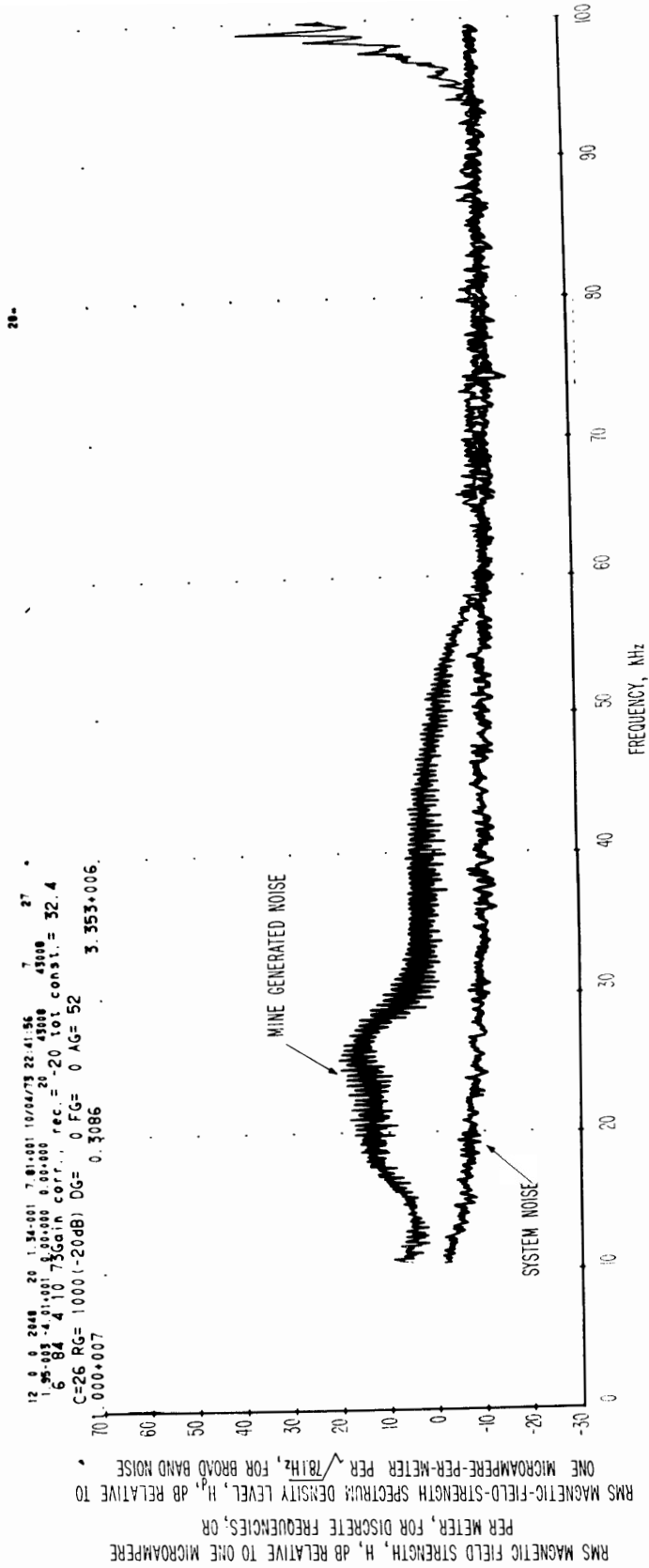


Figure 3-8 Spectrum of magnetic field strength obtained on a loop antenna 1 kHz to 100 kHz, McElroy Mine, location F, middle of angle cut, antenna sensitive axis vertical, 6:30 p.m., April 10, 1973. Spectral resolution is 78.1 Hz.

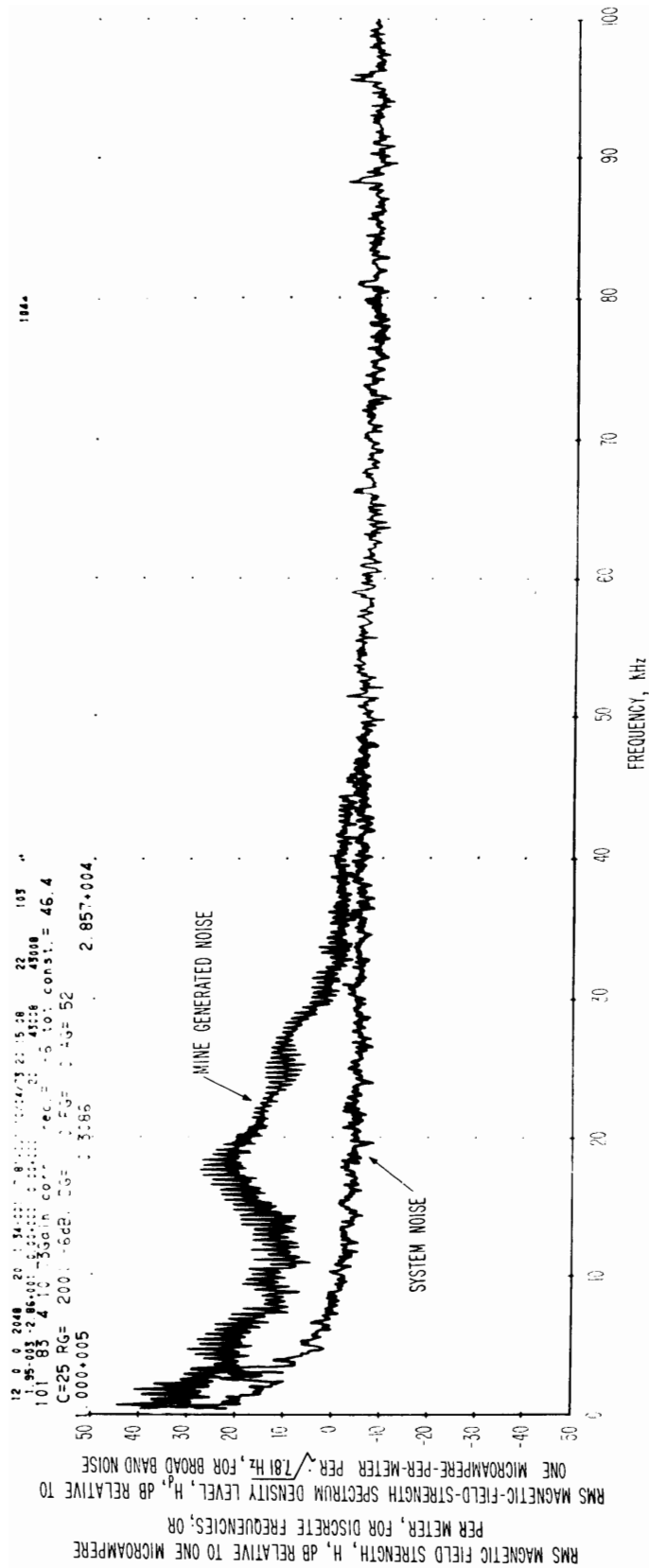


Figure 3-9 Spectrum of magnetic field strength obtained on a loop antenna 1 kHz to 100 kHz, McElroy Mine, location B, no equipment operating, antenna sensitive axis vertical, 1:00 p.m., April 10, 1973. Spectral resolution is 78.1 Hz.

12 0 0 2048 20 2.69+000 3.91+000 04/03/74 08127.34 25 117
 1.95+003 4.23+000 0.00+000 0.00+000 20 43.08 43.08
 24 112 4 10 75Gain corr. req. = -6 tot const. = 46.4
 C=42 RG= 200 (-6dB) DG= 0 FG= 0 AG= 52
 1.000+009 0.3086 3.311+008

RMS MAGNETIC FIELD STRENGTH, H, dB RELATIVE TO ONE MICROAMPERE PER METER, FOR DISCRETE FREQUENCIES; OR
 RMS MAGNETIC-FIELD-STRENGTH SPECTRUM DENSITY LEVEL, H, dB RELATIVE TO ONE MICROAMPERE-PER-METER PER $\sqrt{391}$ Hz, FOR BROAD BAND NOISE

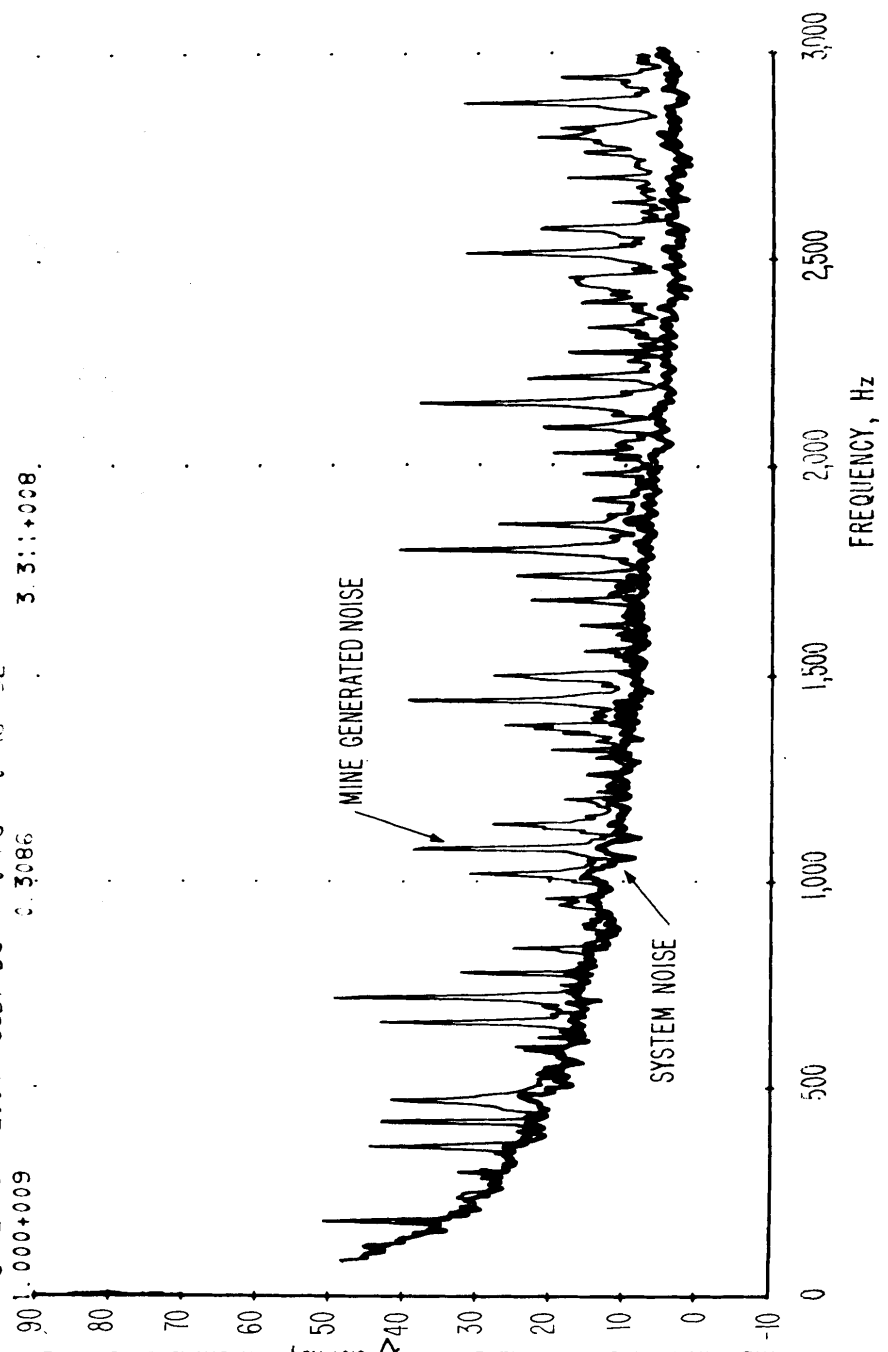


Figure 3-10 Spectrum of magnetic field strength obtained on a loop antenna 100 Hz to 3 kHz, McElroy Mine, location B, no equipment operating, antenna sensitive axis vertical, 1:00 p.m., April 10, 1973. Spectral resolution is 3.91 Hz.

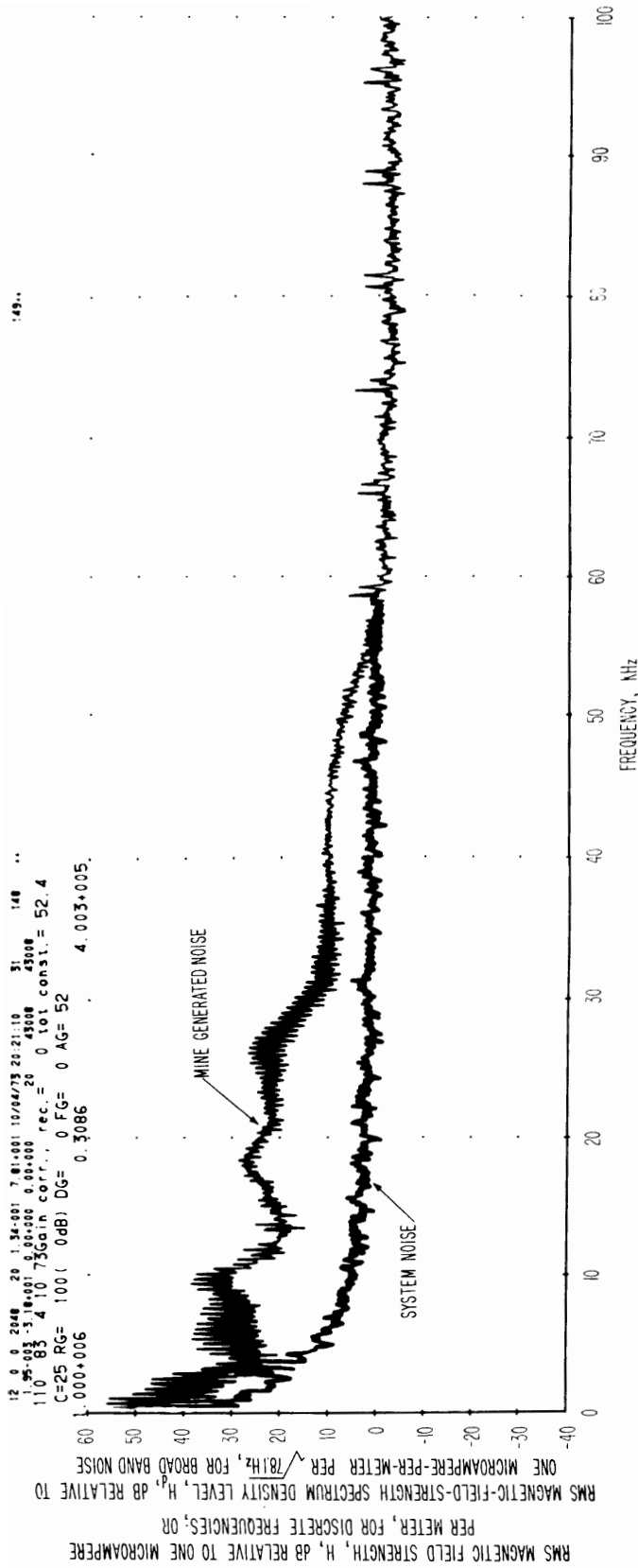


Figure 3-11 Spectrum of magnetic field strength obtained on a loop antenna 1 kHz to 100 kHz, McElroy Mine, location B, 15 meters behind operating miner and loader, antenna sensitive axis vertical, 2:00 p.m., April 10, 1973. Spectral resolution is 78.1 Hz.

12 0 0 2048 20 2.69+000 3.91+000 04/23/74 20:32:25 31 147
 1.95-003 -4.30+001 0.00+000 0.00+000 43008 43008
 30 112 4 10 73Gain corr., rec.= 0 tot const.= 52.4
 C=42 RG= 100(0dB) DG= 0 FG= 0 AG= 52
 1.000+010 0.3086 1.415+009.

RMS MAGNETIC FIELD STRENGTH, H, dB RELATIVE TO ONE MICROAMPERE
 PER METER, FOR DISCRETE FREQUENCIES; OR
 RMS MAGNETIC-FIELD-STRENGTH SPECTRUM DENSITY LEVEL, H, dB RELATIVE TO
 ONE MICROAMPERE-PER-METER PER $\sqrt{391}$ Hz, FOR BROAD BAND NOISE

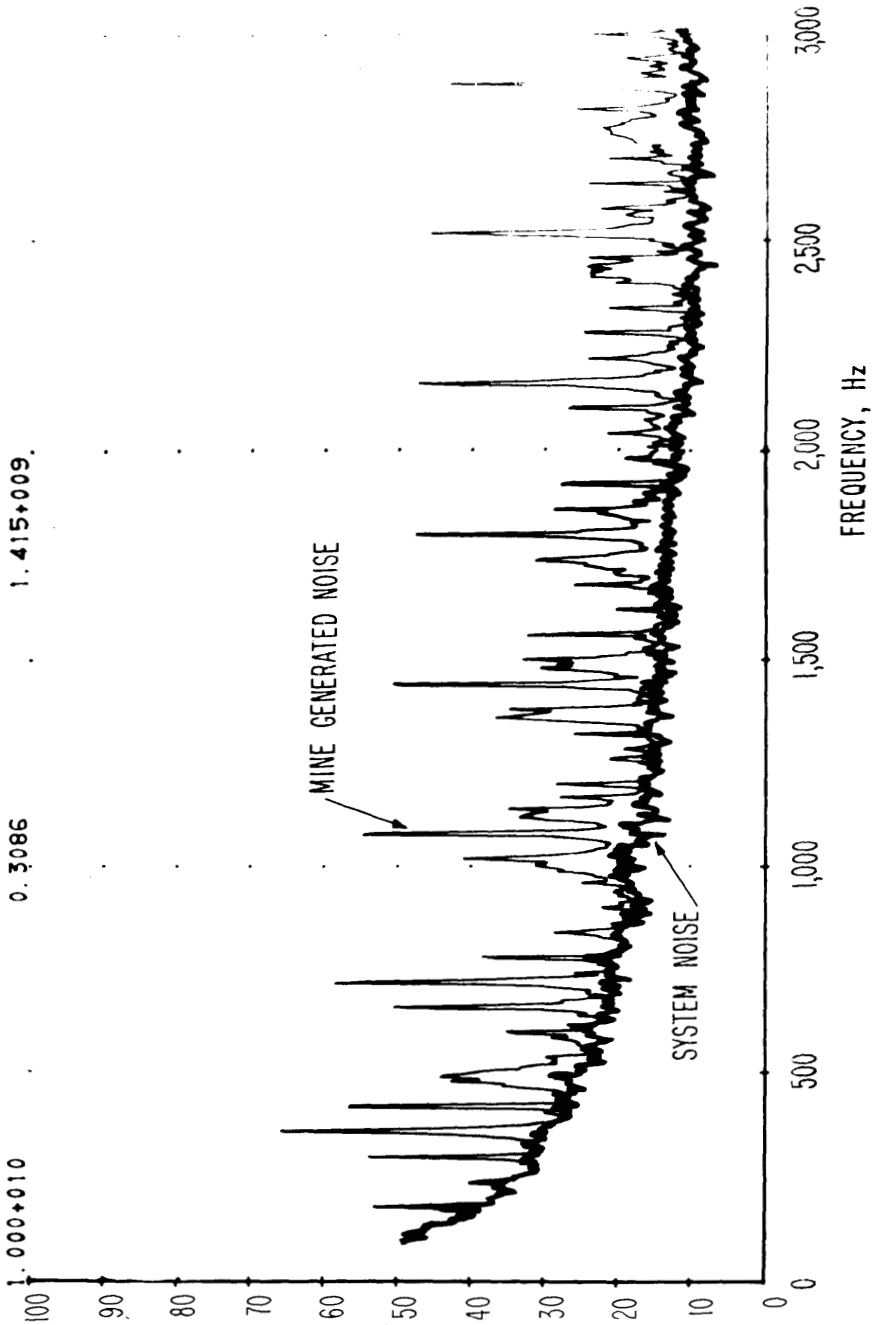


Figure 3-12 Spectrum of magnetic field strength obtained on a loop antenna
 100 Hz to 3 kHz, McElroy Mine, location B, 15 meters behind
 operating miner and loader, antenna sensitive axis vertical,
 2:00 P.m., April 10, 1973. Spectral resolution is 3.91 Hz.

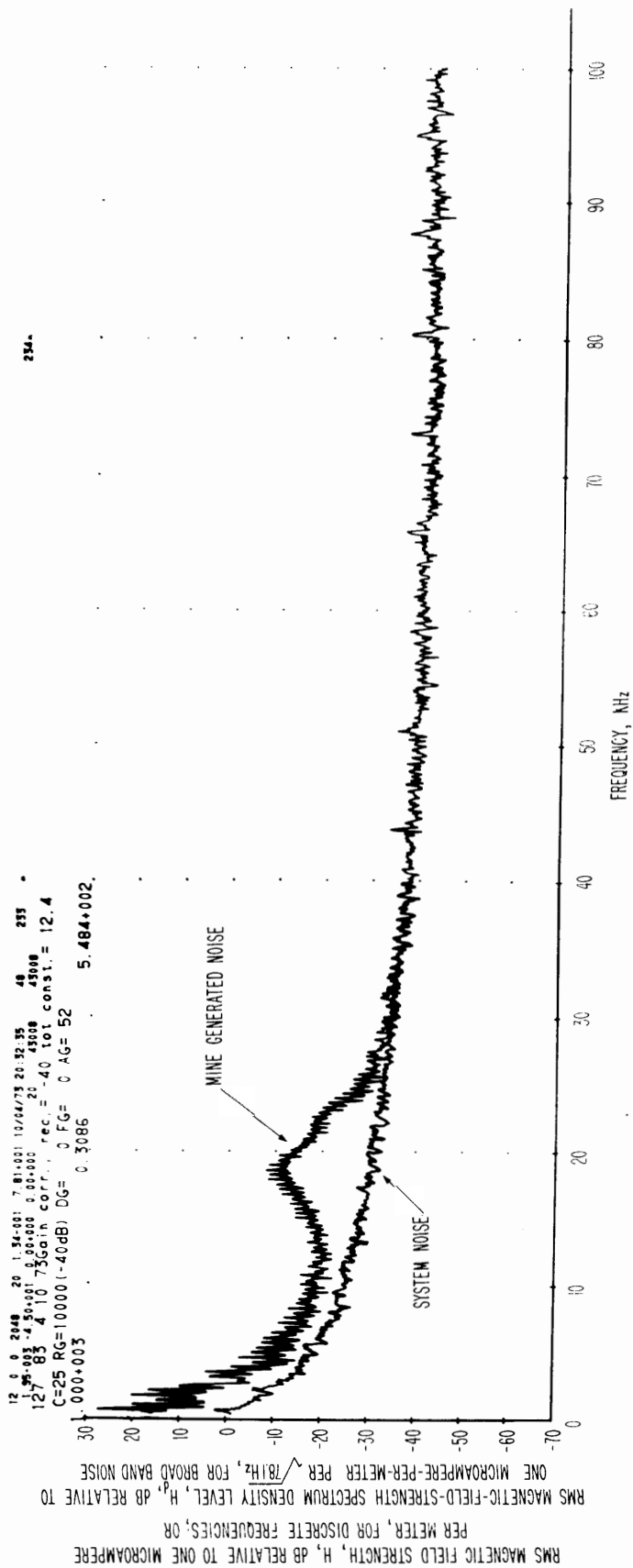


Figure 3-13 Spectrum of magnetic field strength obtained on a loop antenna 1 kHz to 100 kHz, McElroy Mine, location F, return entry, antenna sensitive axis horizontal, parallel to entry, 4:00 p.m., April 10, 1973. Spectral resolution is 78.1 Hz.

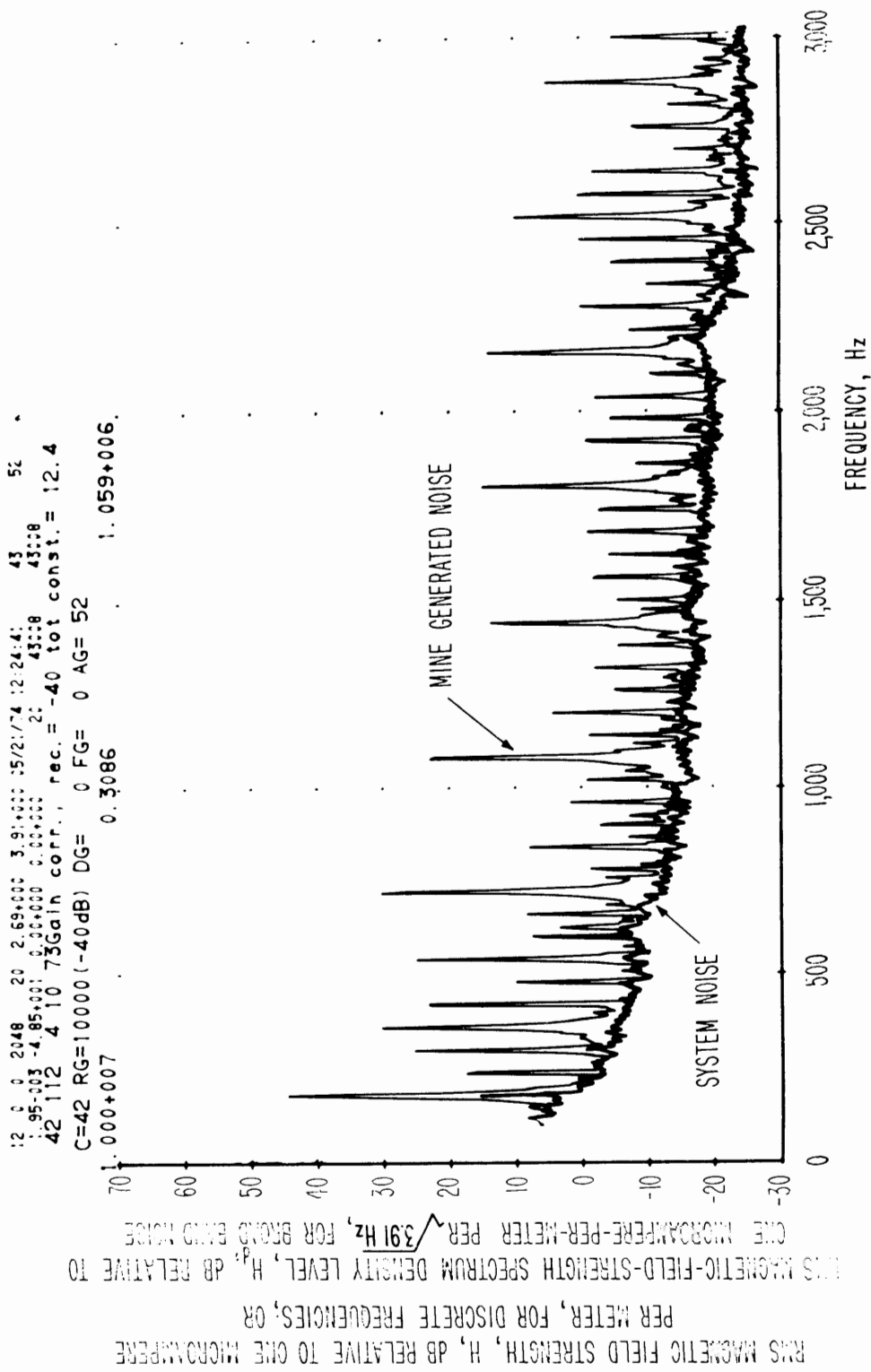


Figure 3-14 Spectrum of magnetic field strength obtained on a loop antenna 100 Hz to 3 kHz, McElroy Mine, location G, return entry, antenna sensitive axis horizontal, parallel to entry, 4:00 p.m., April 10, 1973. Spectral resolution is 3.91 Hz.

12 0 0 2048 20 6.72+002 1.56+012 14.20774 10.35:13 61 152
 1.95-003 -3.02+001 3.00+001 3.00+001 43:08 43:08
 60 92 4 12 73Gain corr. rec. 6 tot const. = 58.0
 C=33 RG= 50 (6dB) DG= 0 FG= 0 AG= 52
 1.000+008 0.3085 1.639+007.

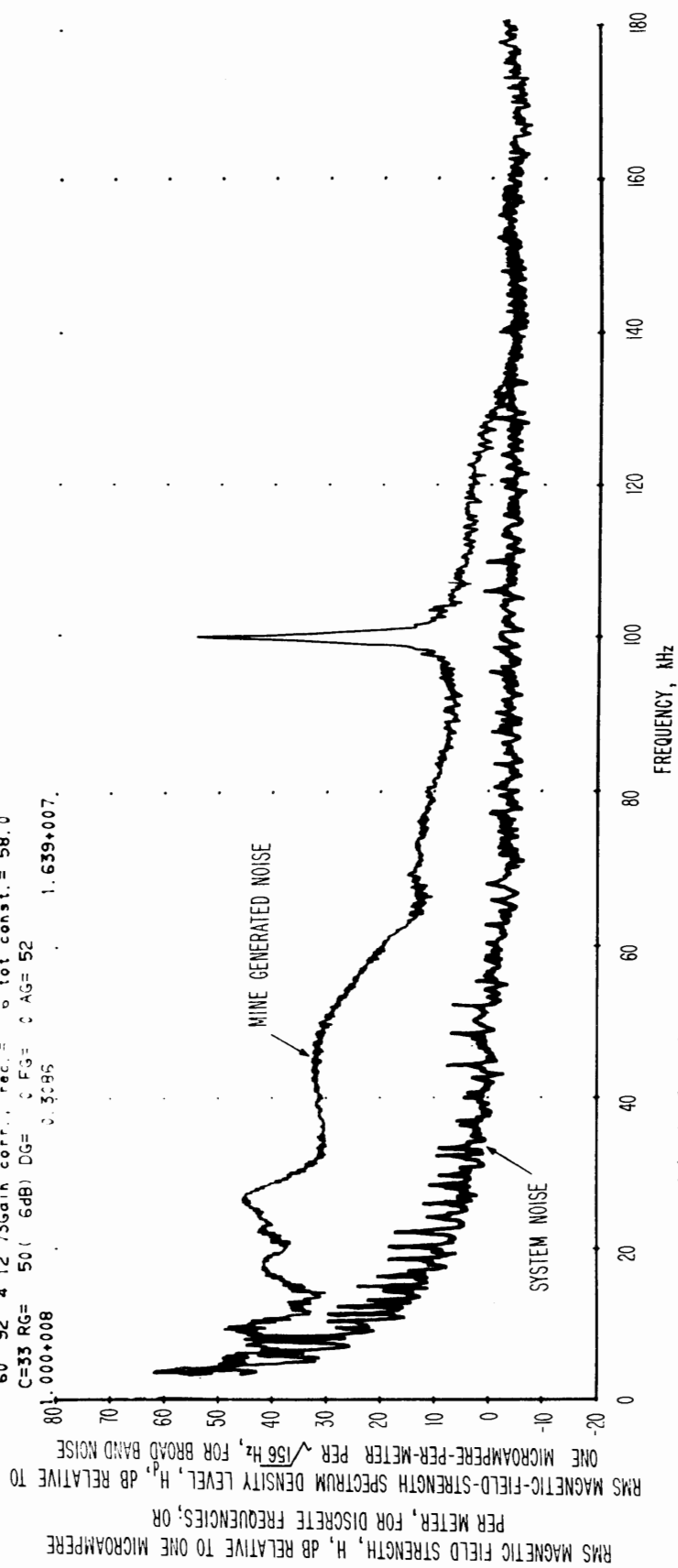


Figure 3-15 Spectrum of machinery-generated, vertical, magnetic field noise at location A, fig. 3-2, McElroy Mine, April 12, 1973, 1:02 p.m. The spectrum is calibrated from 3 to 180 kHz and the spectral resolution is 156 Hz.

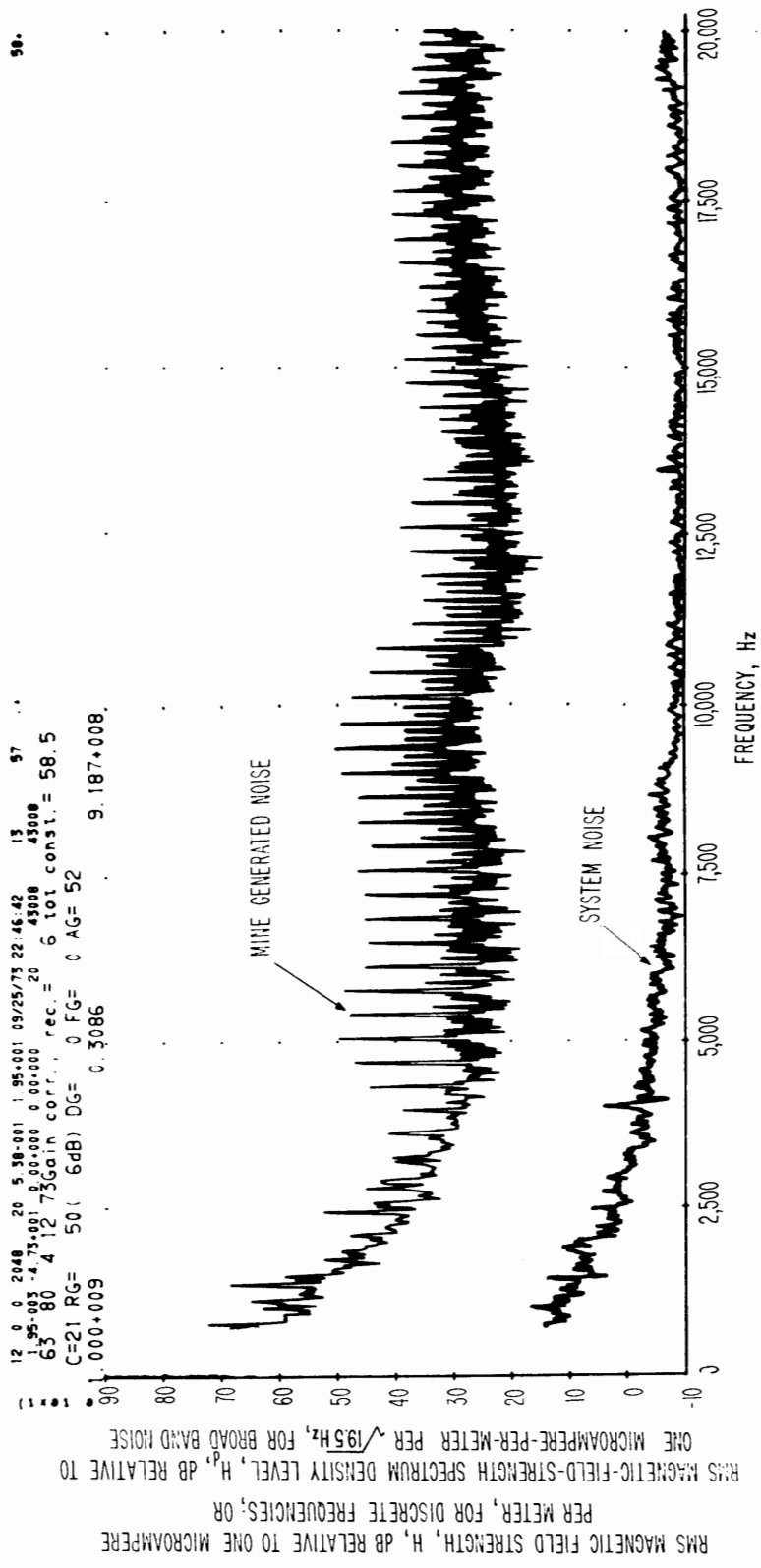


Figure 3-16 Spectrum of machinery-generated, vertical, magnetic-field noise at location A, fig. 3-2, McElroy Mine, April 12, 1973, 1:02 p.m. Spectrum is calibrated from 750 Hz to 20 kHz, and spectral resolution is 19.5 Hz.

12 0 0 2048 26 6.72-502 1.56+002 24/25/74 07:40:39 21 222
 1.95-003 -1.32+000 3.00+000 0.00+000 43008 43008
 70 92 4 12 73Gain corr. rec. = 14 tot const. = 66.0
 C=33 RG= 20 (14dB) DG= 0 FG= 0 AG= 52
 .000+008 .0.3086 9.564+007.

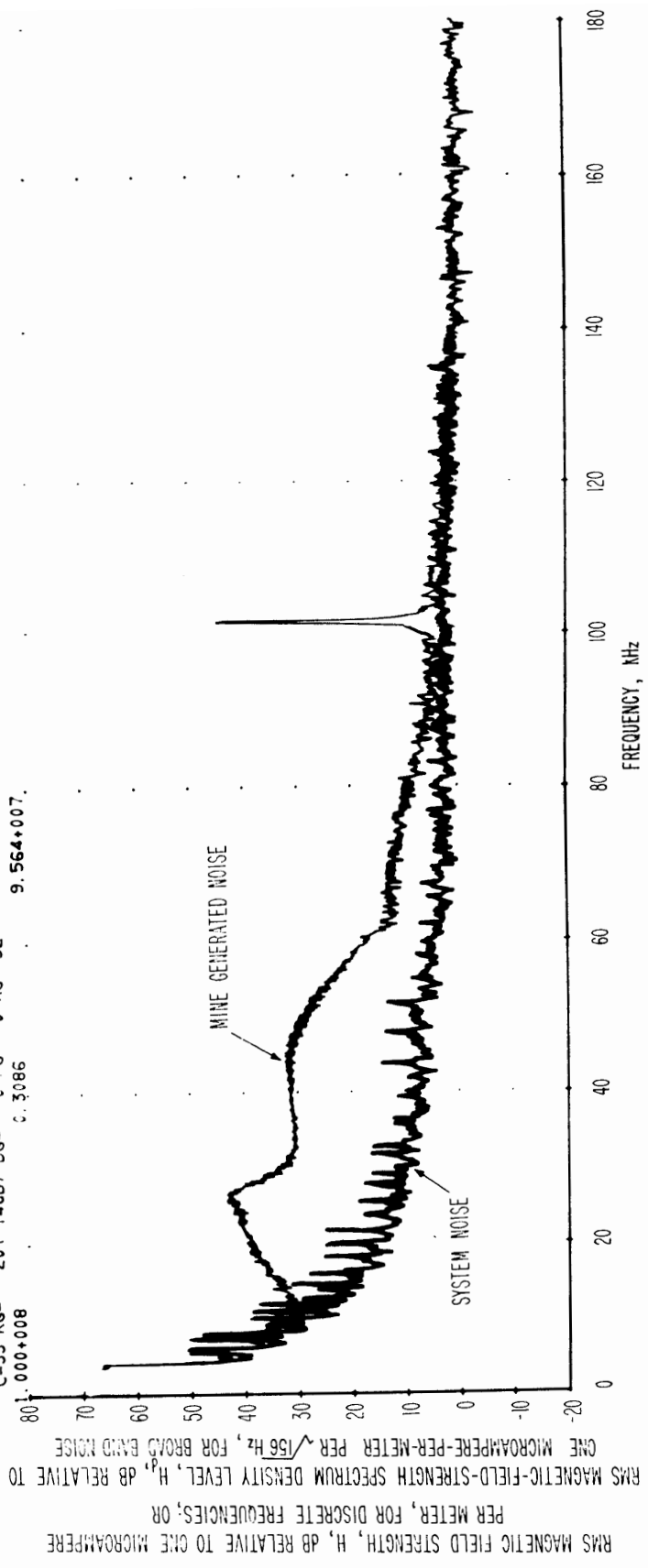


Figure 3-17 Spectrum of machinery-generated, vertical, magnetic-field noise at location A, fig. 3-2, McElroy Mine, April 12, 1973, 1:28 p.m. The spectrum is calibrated from 3 to 180 kHz and the spectral resolution is 156 Hz.

12 0 0 2048 20 6.72-002 1.56+002 04/23/74 05:42:46 74 217
 1.95-003 -2.37+000 0.00+000 0.00+000 20 43008 43008
 75 92 4 12 75Gain corr. rec.= 0 tot const.= 52.0
 C=33 RG= 100(0dB) DG= 0 FG= 0 AG= 52
 0.000+007 0.3086 4.804+006.

RMS MAGNETIC FIELD STRENGTH, H, DB RELATIVE TO ONE MICROAMPERE PER METER, FOR DISCRETE FREQUENCIES, OR
 RMS MAGNETIC-FIELD-STRENGTH SPECTRUM DENSITY LEVEL, H, DB RELATIVE TO ONE MICROAMPERE-PER-METER PER $\sqrt{156}$ Hz, FOR BROAD BAND NOISE

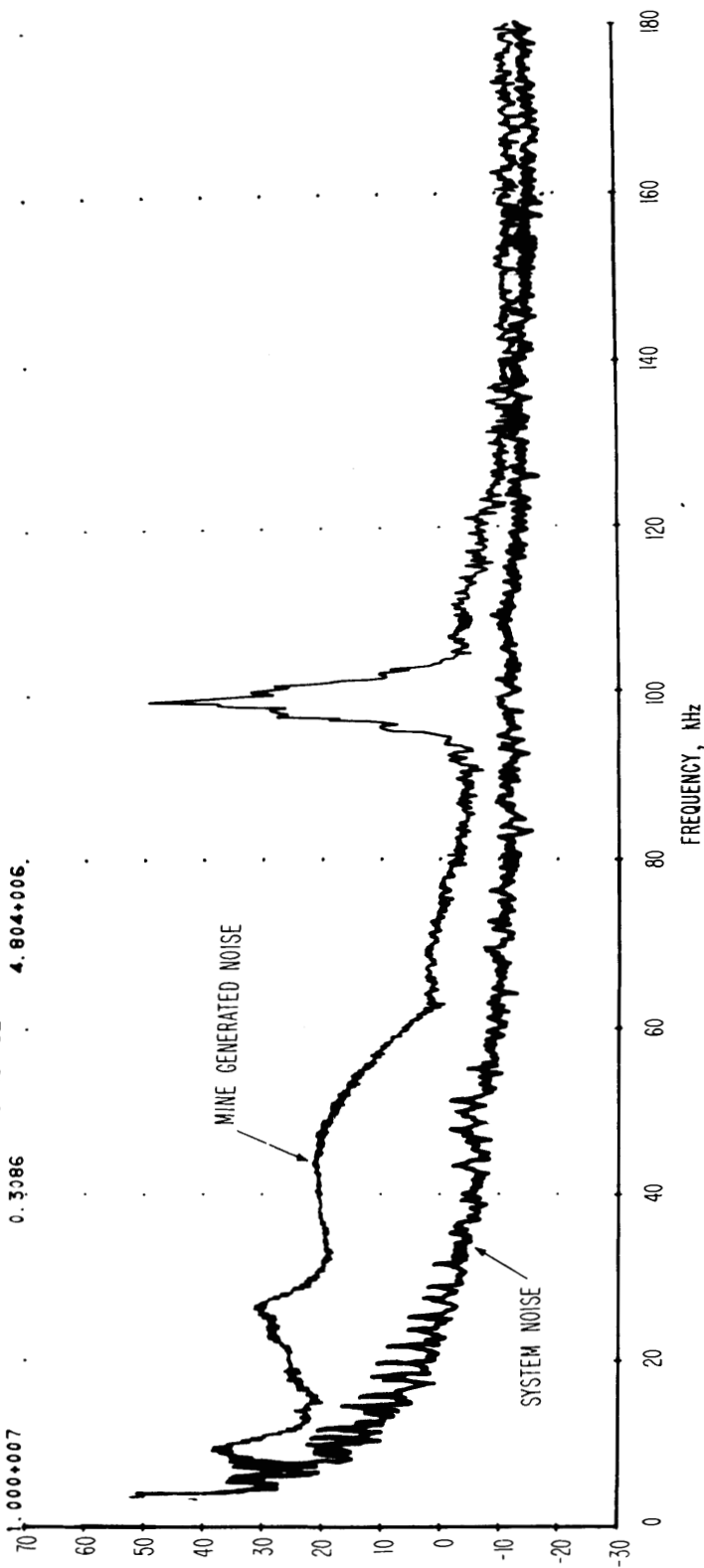


Figure 3-18 Spectrum of machinery-generated, horizontal (E-W), magnetic-field noise at location A, fig. 3-2, McElroy Mine, April 12, 1973, 1:28 p.m. Note modulated, 100 kHz trolley-phone signal. The spectrum is calibrated from 3 to 180 kHz and the spectral resolution is 156 Hz.

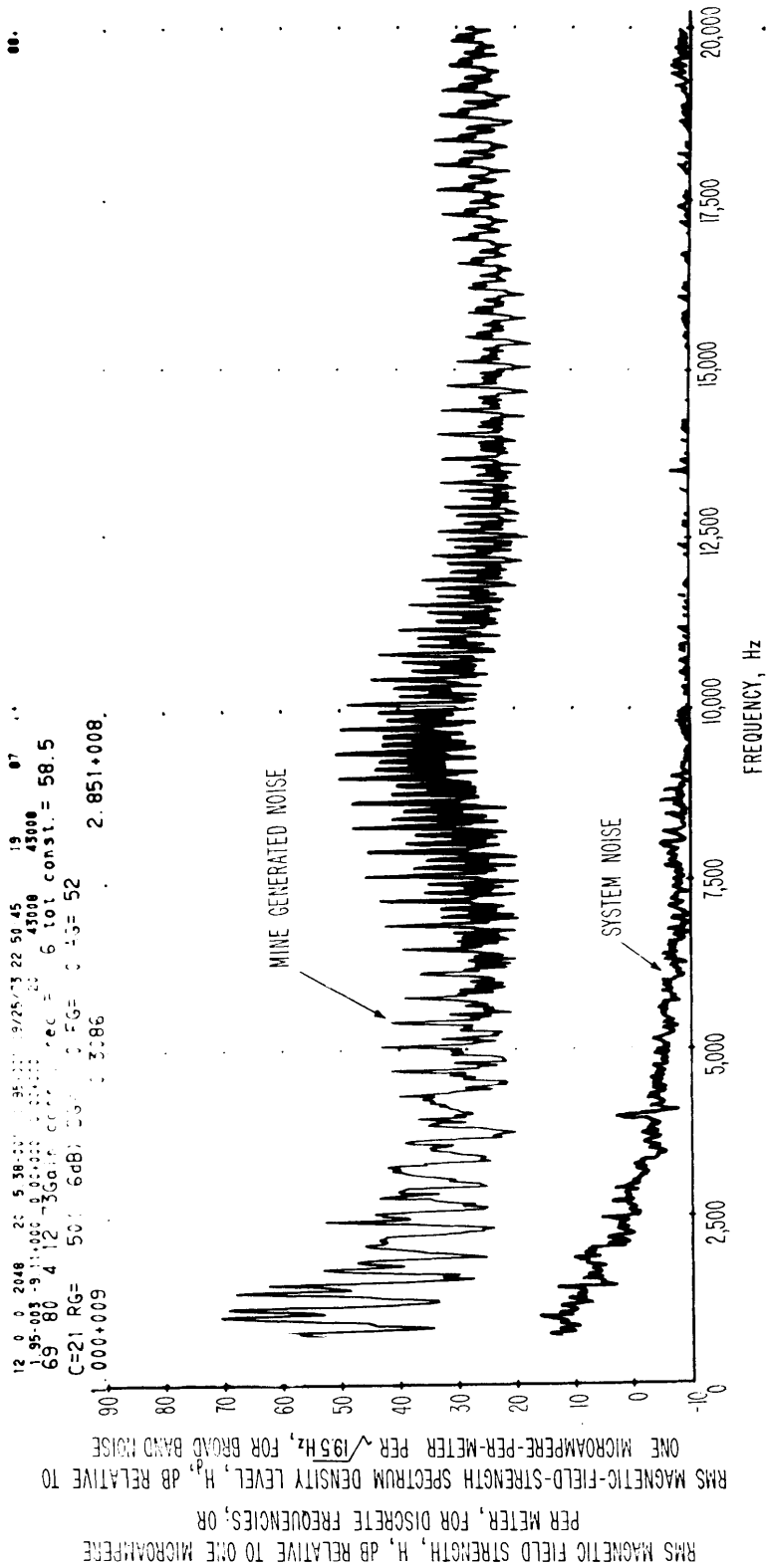


Figure 3-19 Spectrum of machinery-generated, vertical, magnetic-field noise at location A, fig. 3-2, McElroy Mine, April 12, 1973, 1:28 p.m. The spectrum is calibrated from 750 Hz to 20 kHz and spectral resolution is 19.5 Hz.

12 0 0 2048 20 6 72-122 1.56-122 2472774 11:34:35 63 162
 1.95-003 -2.43+003 43778 43778
 62 92 4 12 75Gain corr. rec = 6 tot const. = 58.0
 C=33 RG= 50 (6dB) DG= 0 FG= 0 AG= 52
 1.000+008 0.3686 1.205+007.

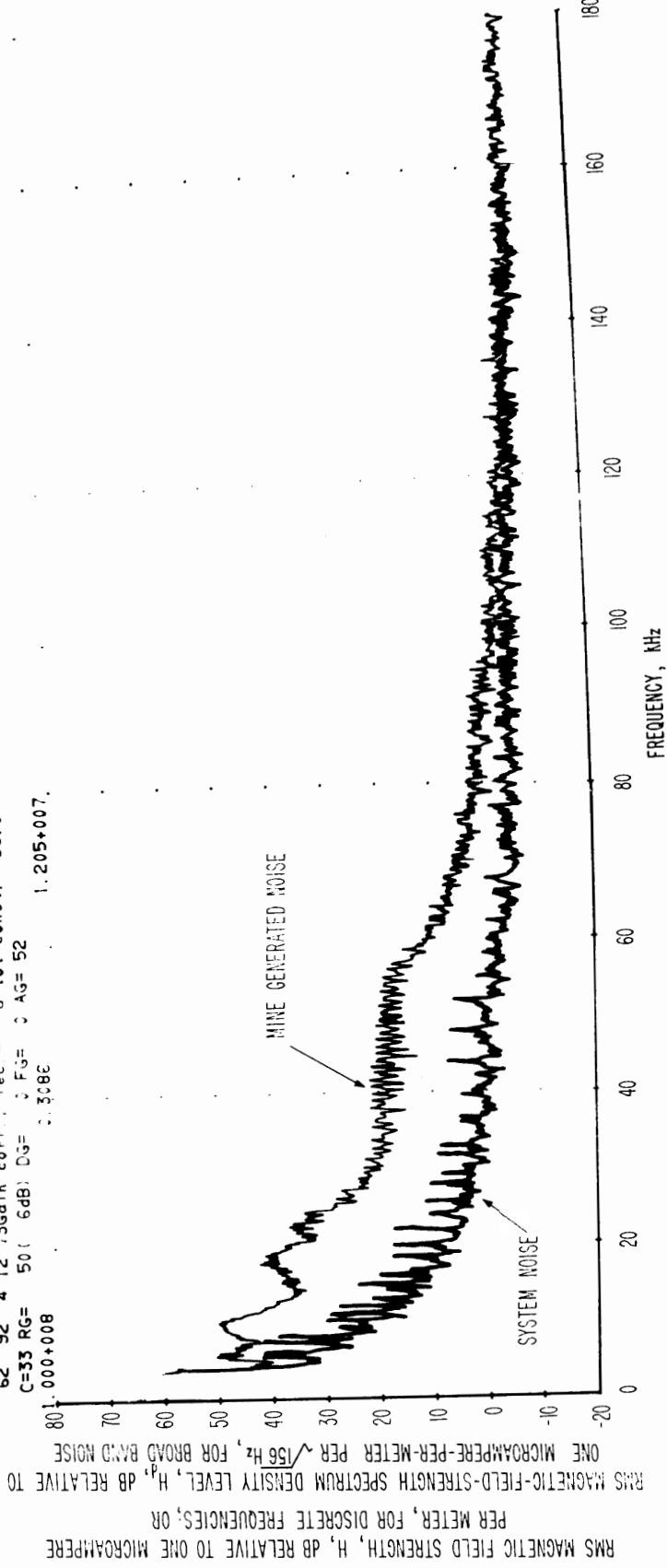


Figure 3-20 Spectrum of machinery-generated, vertical, magnetic-field noise at location A, fig. 3-2, McElroy Mine, April 12, 1973, 12:56 p.m. The spectrum is calibrated from 3 to 180 kHz and the spectral resolution is 156 Hz.

150

12 0 2048 20 6.72-022 1.56+022 14.22/74 003533 64 167
 1.95-003 -2.87+000 0.000000 0.000000 2 43008 43008
 63 92 4.12 75Gain corr, rec. = 0 tot const. = 52.0
 C=33 RG= 100(0dB) DG= 0 FG= 0 AG= 52
 1.000+007 0.3086 3.070+006

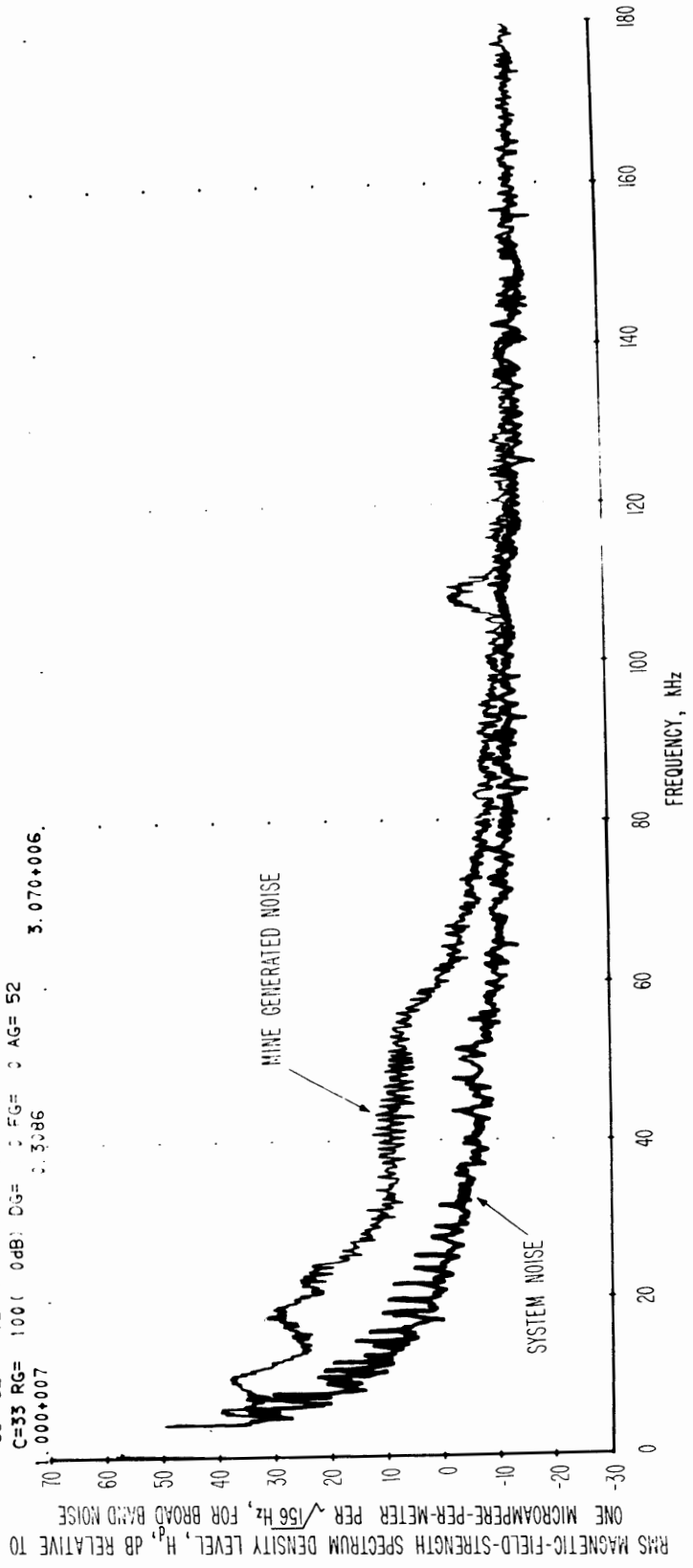


Figure 3-21 Spectrum of machinery-generated, horizontal (E-W), magnetic-field noise at location A, fig. 3-2, McElroy Mine, April 12, 1973, 12:56 p.m. The spectrum is calibrated from 3 to 180 kHz and the spectral resolution is 156 Hz.

12 0 0 2048 20 5.38-001 1.95+001 09/25/73 22:47:22 14 62 ..
 1.95-003 -2.58+000 0.00+000 0.00+000 43608 43608
 64 80 4 12 73 Gain corr., rec. = 6 tot const. = 58.5
 C=21 RG= 50 (6dB) DG= 0 FG= 0 AG= 52 3.484+007.
 0.000+008 0.3086

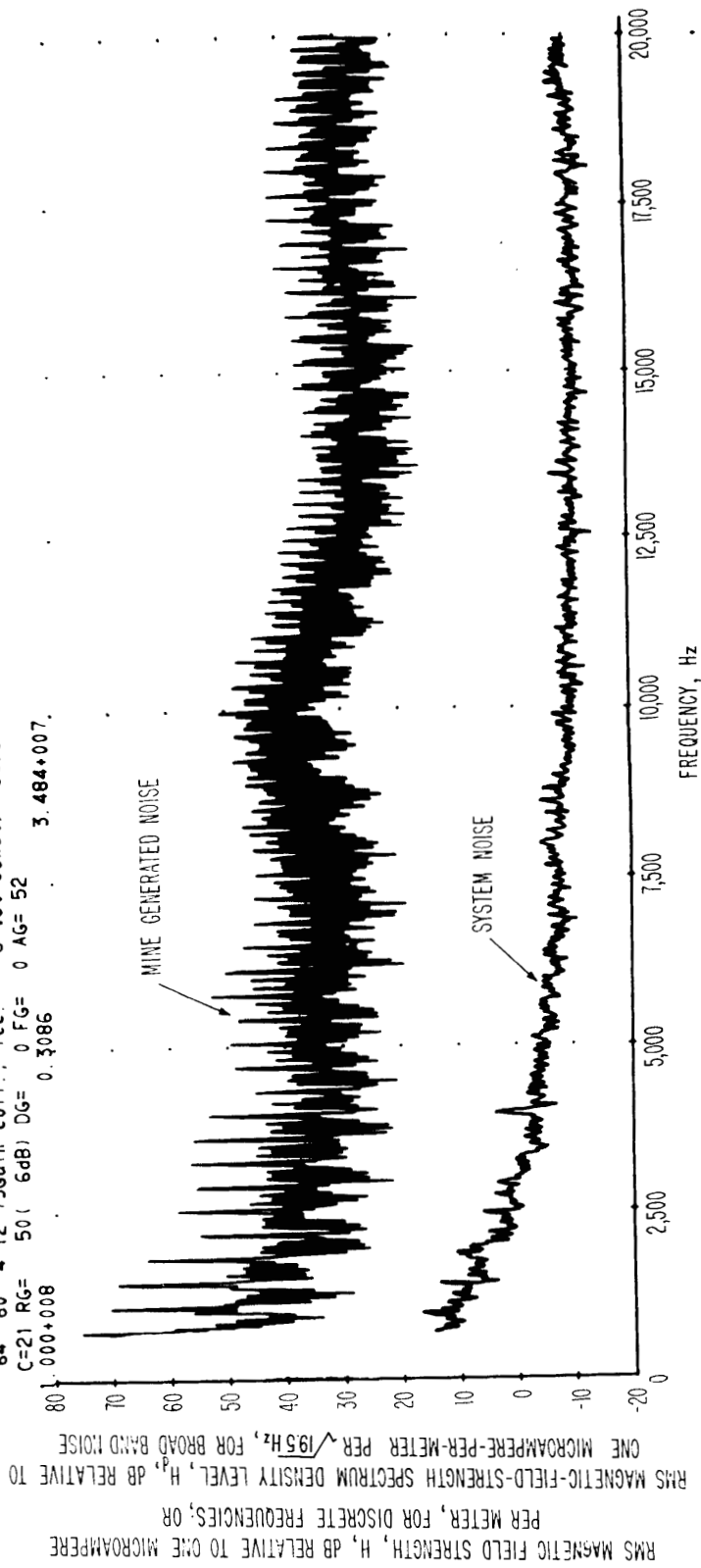


Figure 3-22 Spectrum of machinery generated, vertical, magnetic-field noise, location A, fig. 3-2, McElroy Mine, April 12, 1973, 12:56 p.m. The spectrum is calibrated from 750 Hz to 20 kHz and spectral resolution is 19.5 Hz.

123.

12 0 0 2048 20 5.72-002 1.56-002 04/20/74 00:28:22 55 122 "

1.95-003 -1.87-000 0.00+000 0.00+000 43000 43000

54 92 4 12 75Gain corr., rec.= 14 tot const.= 66.0

C=33 RG= 20 (14dB) DG= 0 FG= 0 AG= 52

0.000+008 0.3086 6.947+007.

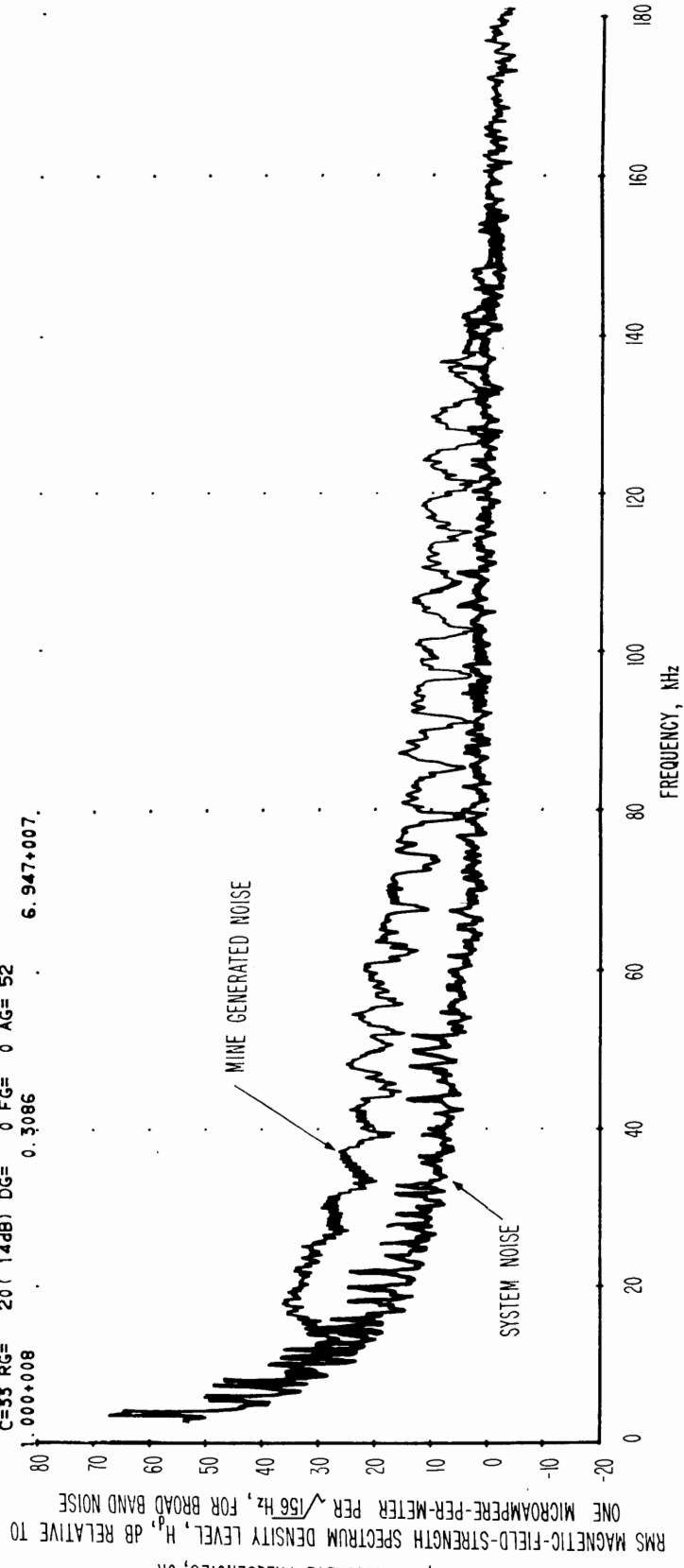


Figure 3-23 Spectrum of impulse, location A, fig. 3-2, McElroy Mine, April 12, 1973, 12:08 p.m. The spectrum is calibrated from 3 to 180 kHz and the spectral resolution is 156 Hz.

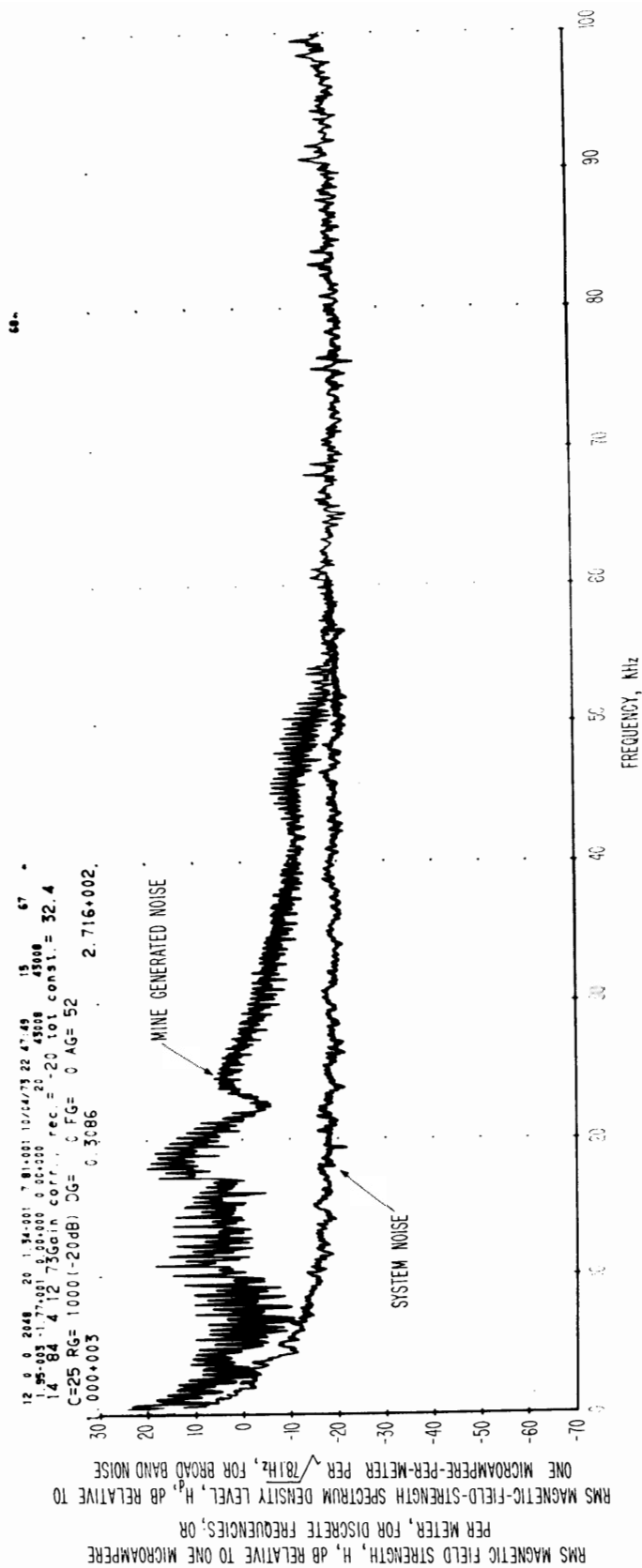


Figure 3-24 Spectrum of magnetic field strength obtained on a loop antenna 1 kHz to 100 kHz, McElroy Mine, in haulageway near bottom of elevator shaft, antenna sensitive axis vertical, 9:43 a.m., April 12, 1973. Spectral resolution is 78.1 Hz.

12 0 0 2048 20 2.69+000 3.91+000 04/24/74 23:25:54 51 91 *
 1.95-003 -3.18+001 0.00+000 0.00+000 20 43008 43008
 50 112 4 10 73Gain corr., rec. = -20 tot const. = 32.4
 C=42 RG= 1000(-20dB) DG= 0 FG= 0 AG= 52
 1.000+007 0.3086 7.356+006.

RMS MAGNETIC FIELD STRENGTH, H, DB RELATIVE TO ONE MICROAMPERE PER METER, FOR DISCRETE FREQUENCIES; OR
 RMS MAGNETIC-FIELD-STRENGTH SPECTRUM DENSITY LEVEL, H², DB RELATIVE TO ONE MICROAMPERE-PER-METER PER $\sqrt{391}$ Hz, FOR BROAD BAND NOISE

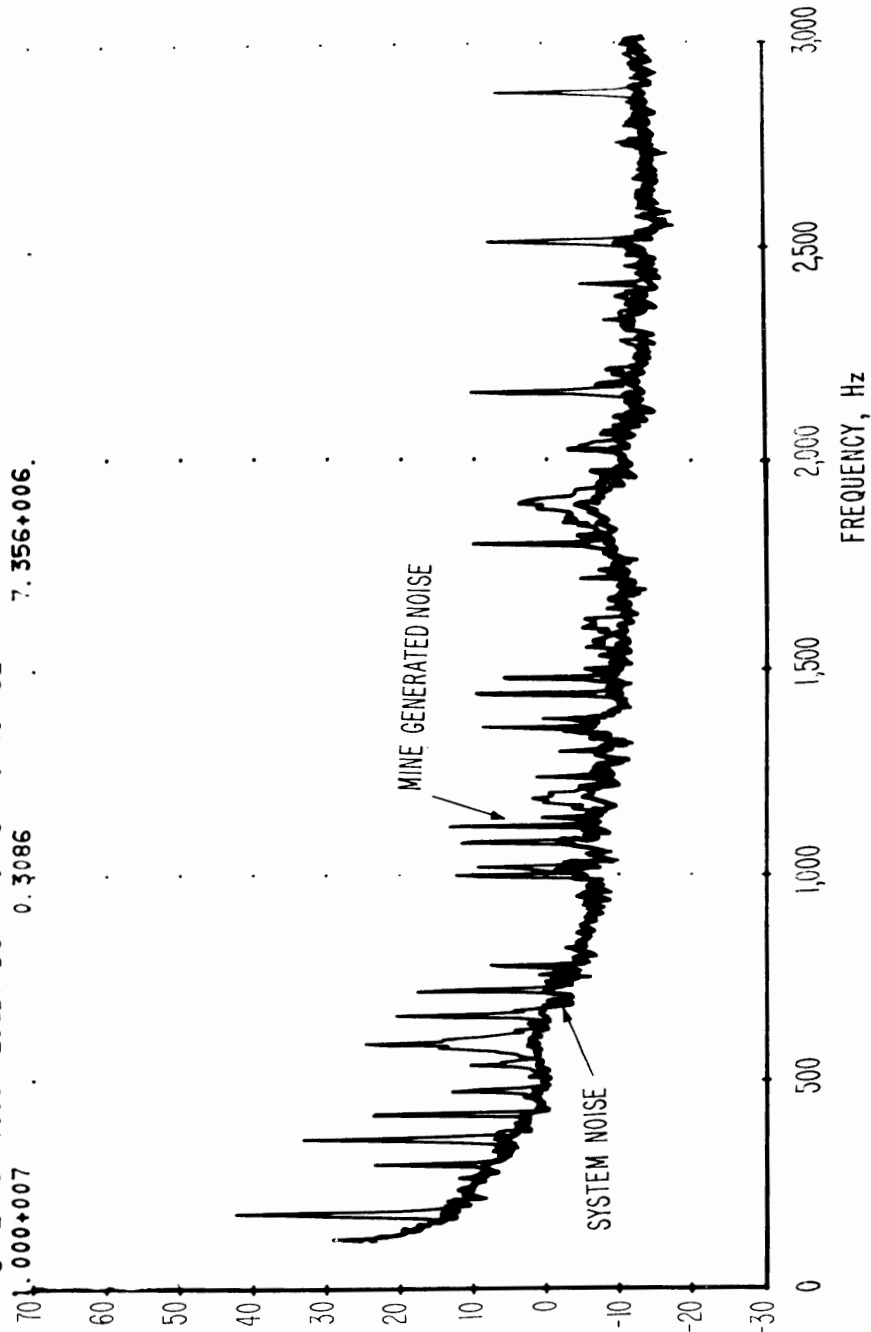


Figure 3-25 Spectrum of magnetic field strength obtained on a loop antenna 100 Hz to 3 kHz, McElroy Mine, haulageway, antenna sensitive axis vertical, 9:43 a.m., April 12, 1973. Spectral resolution is 3.91 Hz.

12 0 2248 20 154000 80000 10/24/73 03 17 45 55 257
 1 95 03 03 02 03 02 03 02 21 45 08 45 08
 54 84 4 12 3Gain corr rec = 1.4 1.01 corr = 39.4
 C=25 PG= 500 14dB; CG= 1.5G= 1.43= 52
 000.008 0.3386 5.112407

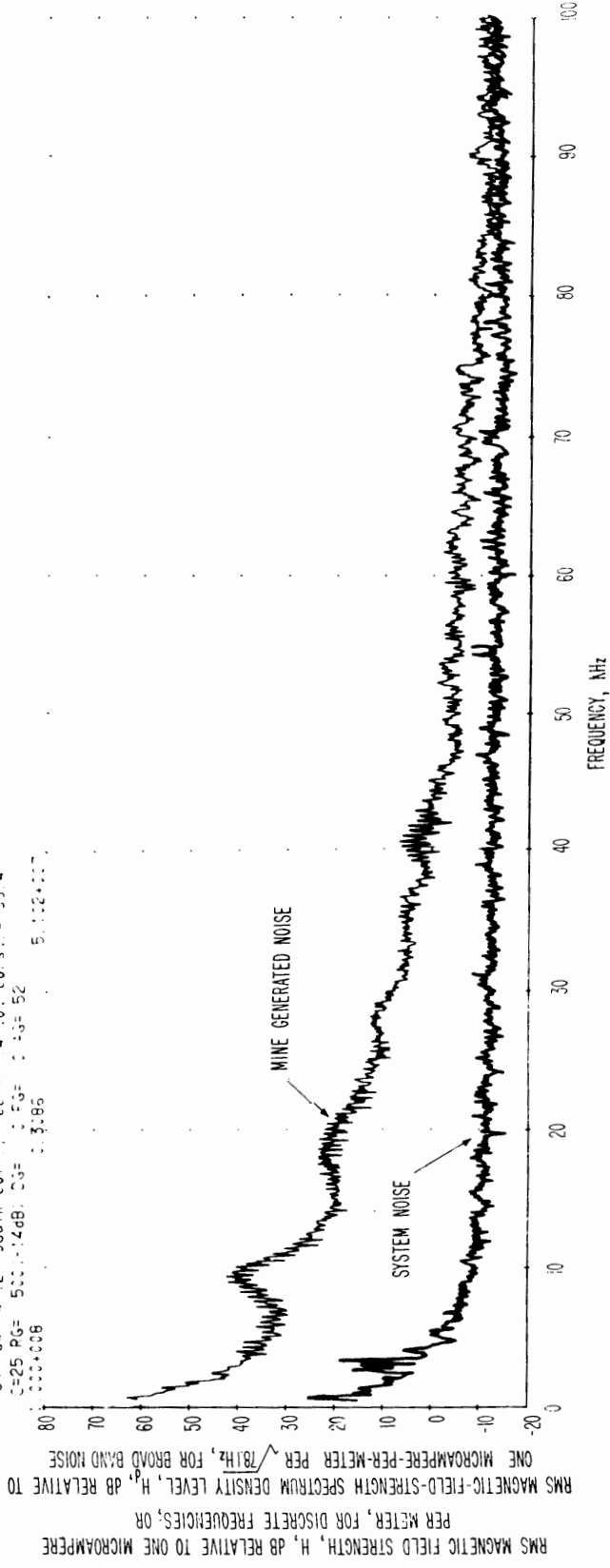


Figure 3-26 Spectrum of magnetic field strength obtained on a loop antenna 1 kHz to 100 kHz, McElroy Mine, location B, train going by, antenna sensitive axis vertical, 2:13 p.m., April 12, 1973. Spectral resolution is 78.1 Hz.

12 6 0 2048 20 2.69+000 3.0+000 05/31/74 21:59:50 9 37
 1.95-003 -1.29+000 5.00+000 43:08
 20 113 4 10 73Gain const., rec. = -14 tot const. = 38.4
 C=42 RG= 500 (-14dB) CS= 0 FG= 0 AG= 52
 200+011 1.3086 1.057+010.

RMS MAGNETIC FIELD STRENGTH, H, dB RELATIVE TO ONE MICROAMPERE
 PER METER, FOR DISCRETE FREQUENCIES; OR
 RMS MAGNETIC-FIELD-STRENGTH SPECTRUM DENSITY LEVEL, H², dB RELATIVE TO
 ONE MICROAMPERE-PER-METER PER $\sqrt{391}$ Hz, FOR BROAD BAND NOISE

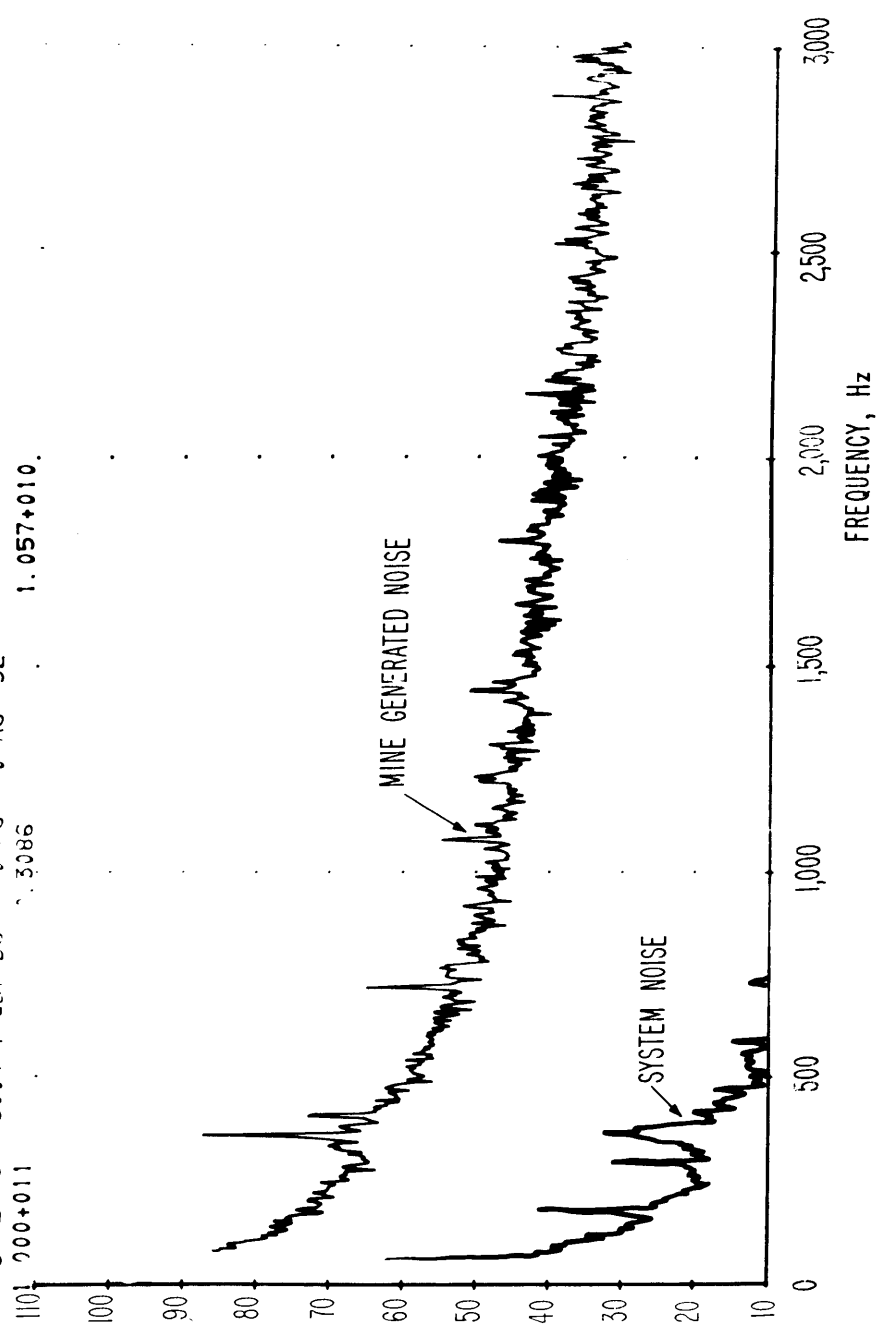


Figure 3-27 Spectrum of magnetic field strength obtained on a loop antenna 100 Hz to 3 kHz, McElroy Mine, location B, train going by, antenna sensitive axis vertical, 2:13 p.m., April 12, 1973. Spectral resolution is 3.91 Hz.

12 0 2048 20 2.69+000 3.51+000 05/13/74 21:58:15 8 32
 1.95+003 -3.52+000 0.00+000 0.00+000 20 43008 43008
 19 113 4 10 73Gain corr., rec. = -14 tot const. = 38.4
 C=42 RG= 500 (-14dB) DG= 0 FG= 0 AG= 52
 1.000+008 0.3086 4.676+007.

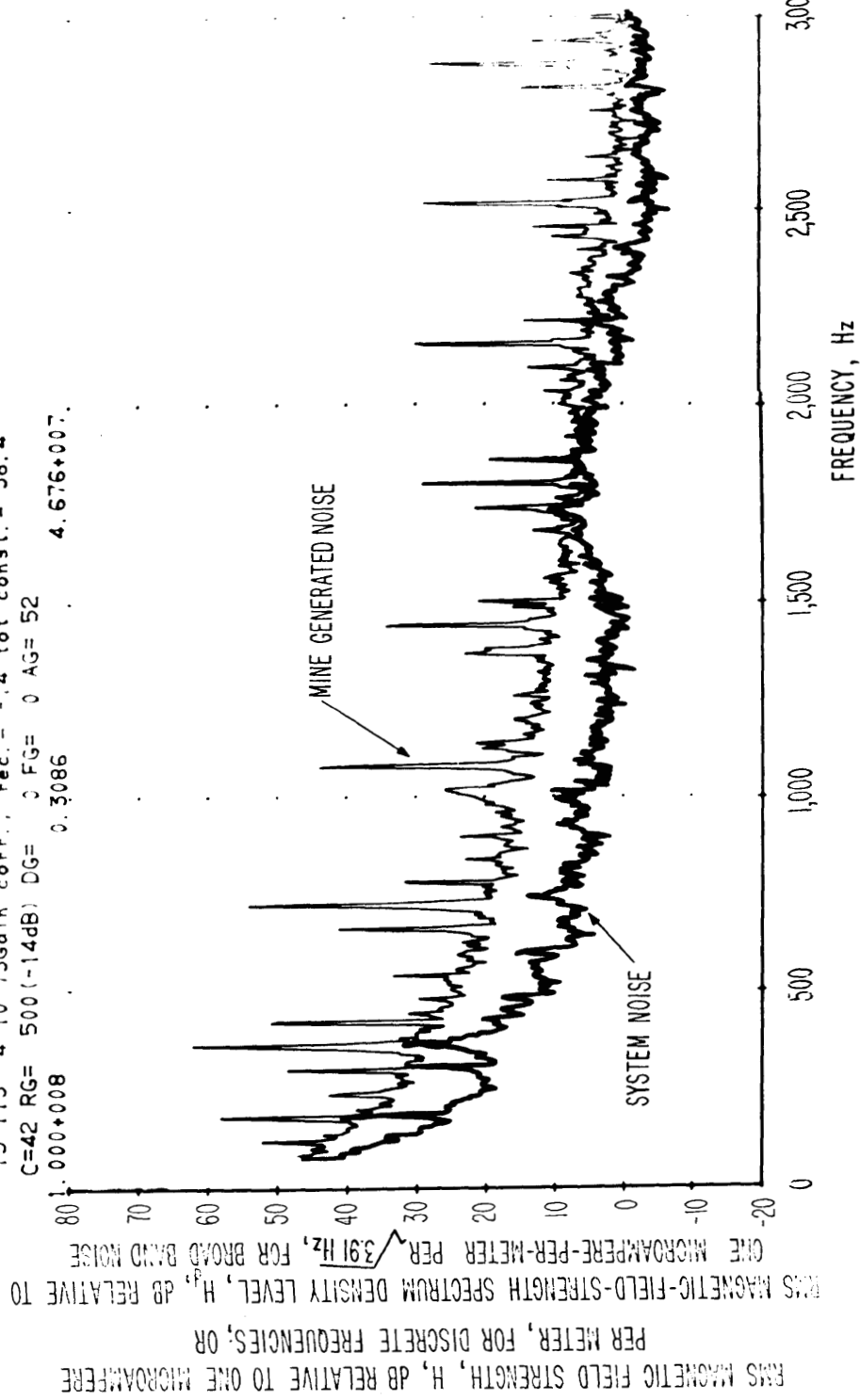


Figure 3-28 Spectrum of magnetic field strength obtained on a loop antenna 100 Hz to 3 kHz, McElroy Mine, location B, empty train passing by, antenna sensitive axis vertical, 2:10 p.m., April 12, 1973. Spectral resolution is 3.91 Hz.

12 0 0 2046 20 1 54-001 7.81+001 10/04/75 23 12:38 48 232 *
 1.55-003 -1.39+001 -0.00+000 0.00+000 20 43008 43008
 47 84 4 12 75Gain corr. rec. = -14 tot const. = 38.4
 C=25 RG= 500(-14dB) DG= 0 FG= 0 AG= 52
 1.000+006 0 3086 1.352+005.

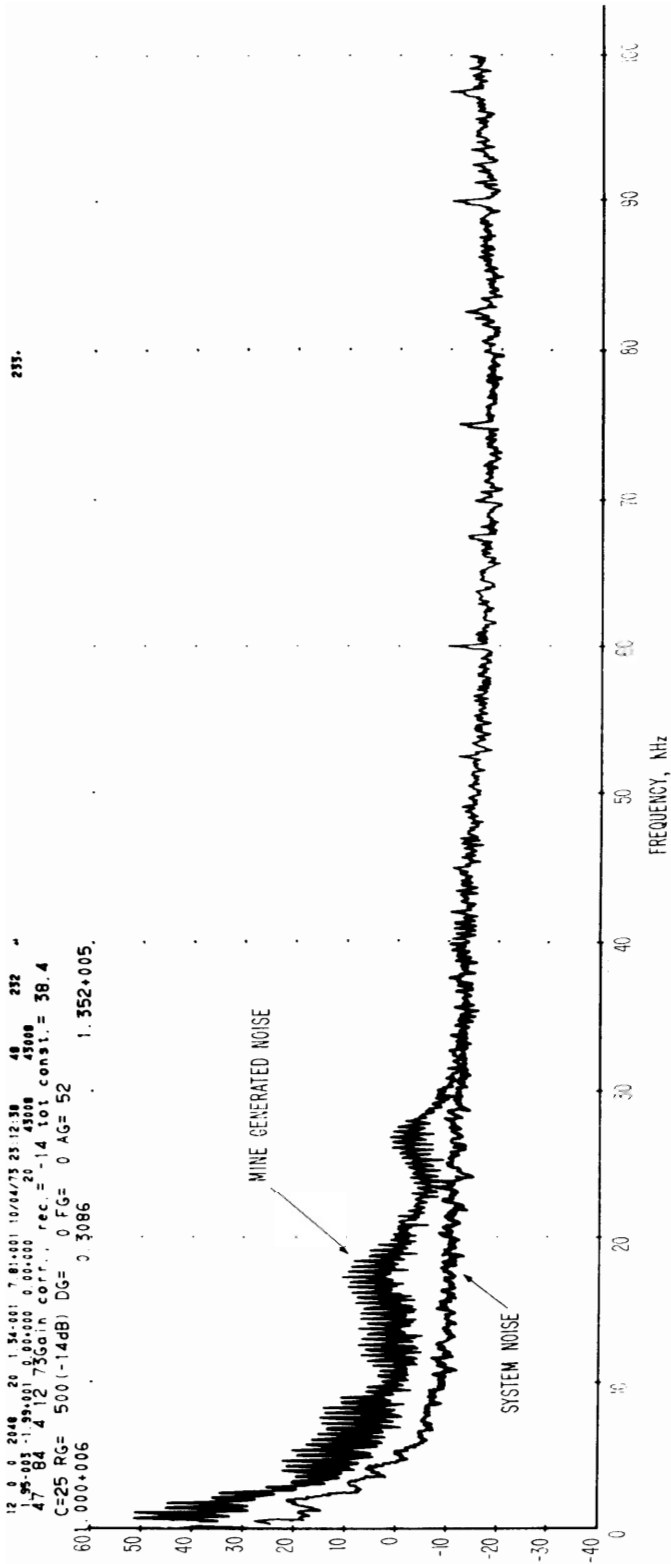


Figure 3-29 Spectrum of magnetic field strength obtained on a loop antenna 1 kHz to 100 kHz, McElroy Mine, location C, at head piece with conveyor and car-pull operating, antenna sensitive axis vertical, 1:40 p.m., April 12, 1973. Spectral resolution is 78.1 Hz.

12 0 0 2048 20 2.69000 3.91000 15/374 21:57:14 6 22
 1.95-003 -2.91000 5.00000 0.00000 2: 43008 43008
 17 113 4 10 75Gain corr., rec. = -14 tot const. = 38.4
 C=42 RG= 500 (-14dB) DG= 0 FG= 0 AG= 52
 0.000+008 0.3086 2.426+007.

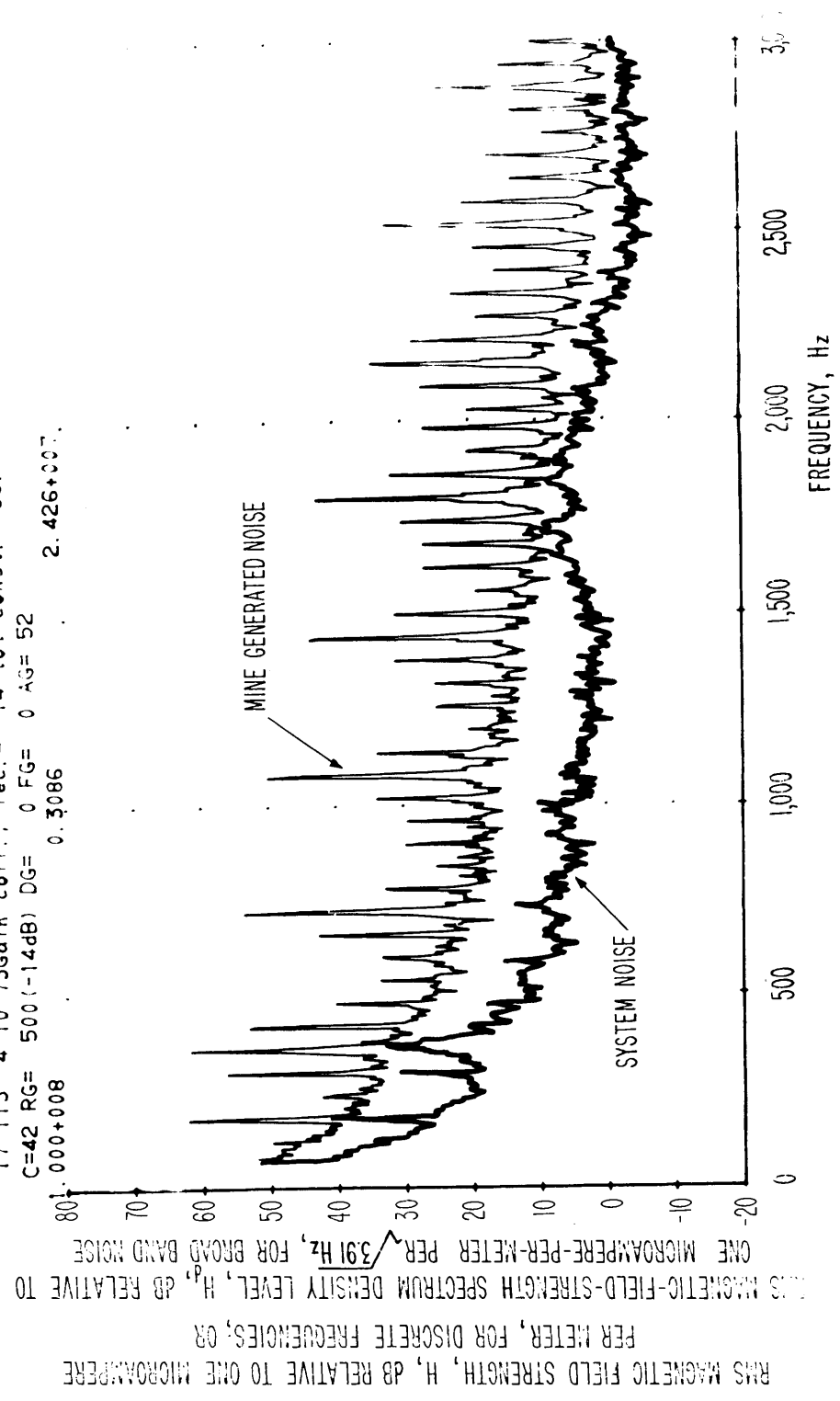


Figure 3-30 Spectrum of magnetic field strength obtained on a loop antenna 100 Hz to 3 kHz, McElroy Mine, location C, at head piece with conveyor and car-pull operating, antenna sensitive axis vertical, 1:40 p.m., April 12, 1973. Spectral resolution is 3.91 Hz.

12 0 0 2048 20 6.72-002 1.56+002 04/20/74 00:16:57 39 42
 1.95-003 -1.10+000 0.00+000 0.00+000 21 43628 43508
 38 92 4.10 736gain corr., rec. = -20 tot const. = 32.0
 C=33 RG= 1000 (-20dB) DG= 0 FG= 0 AG= 52
 1.000+005 0.3086 2.867+004.

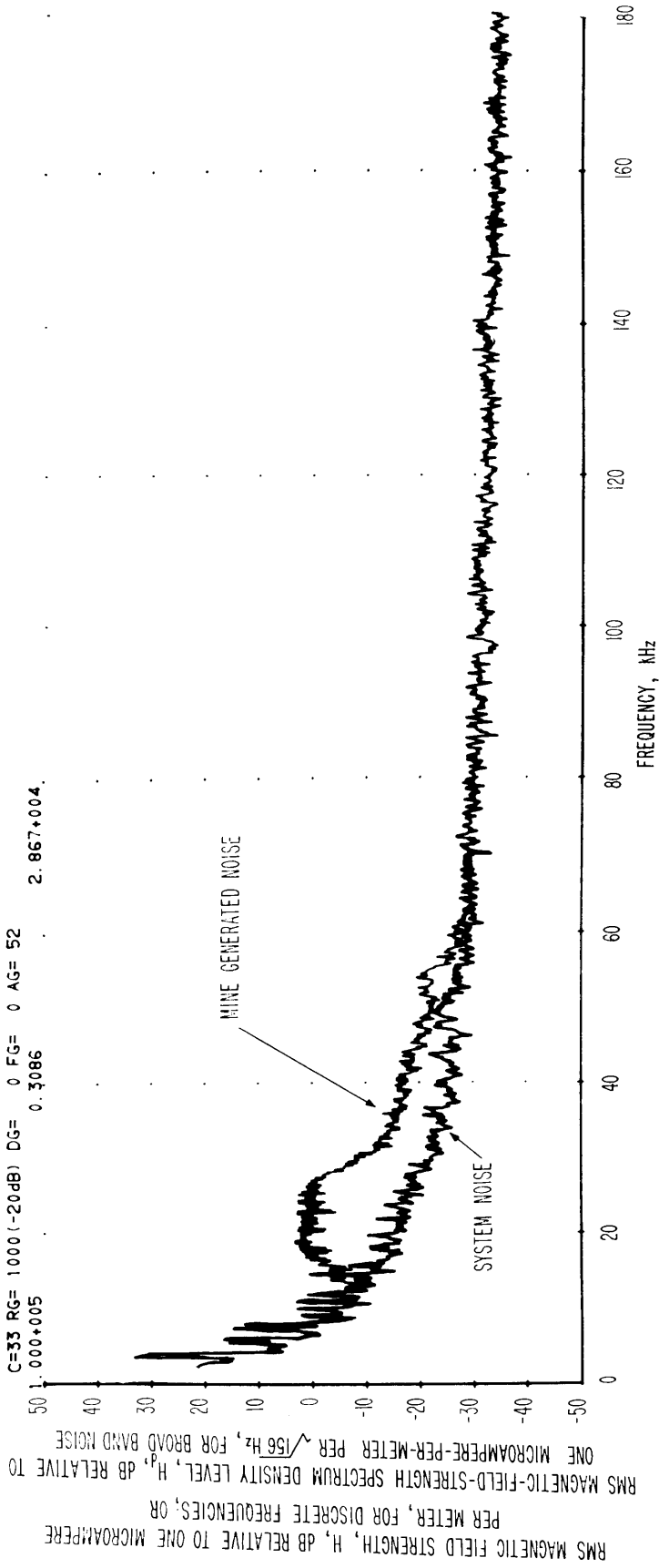


Figure 3-31 Spectrum of haulageway, magnetic-field noise at location A on fig. 3-1, in McElroy Mine, April 10, 1973, 12:15 p.m. The spectrum is calibrated from 3 to 180 kHz and the spectral resolution is 156 Hz.

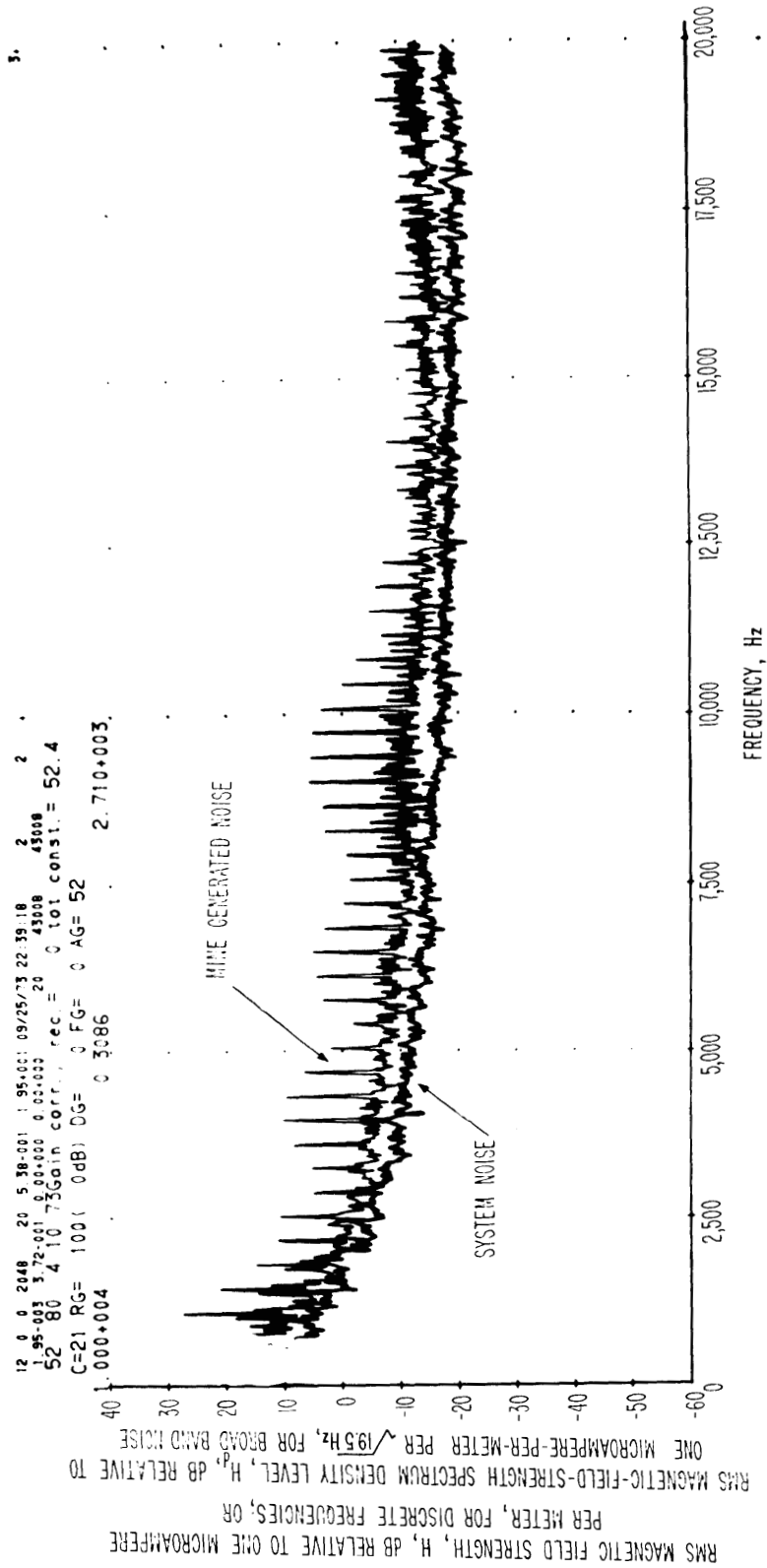


Figure 3-32 Spectrum of haulageway, magnetic-field noise at location A, fig. 3-1, McElroy Mine, April 10, 1973, 12:15 p.m. The spectrum is calibrated from 750 Hz to 20 kHz and spectral resolution is 19.5 Hz.

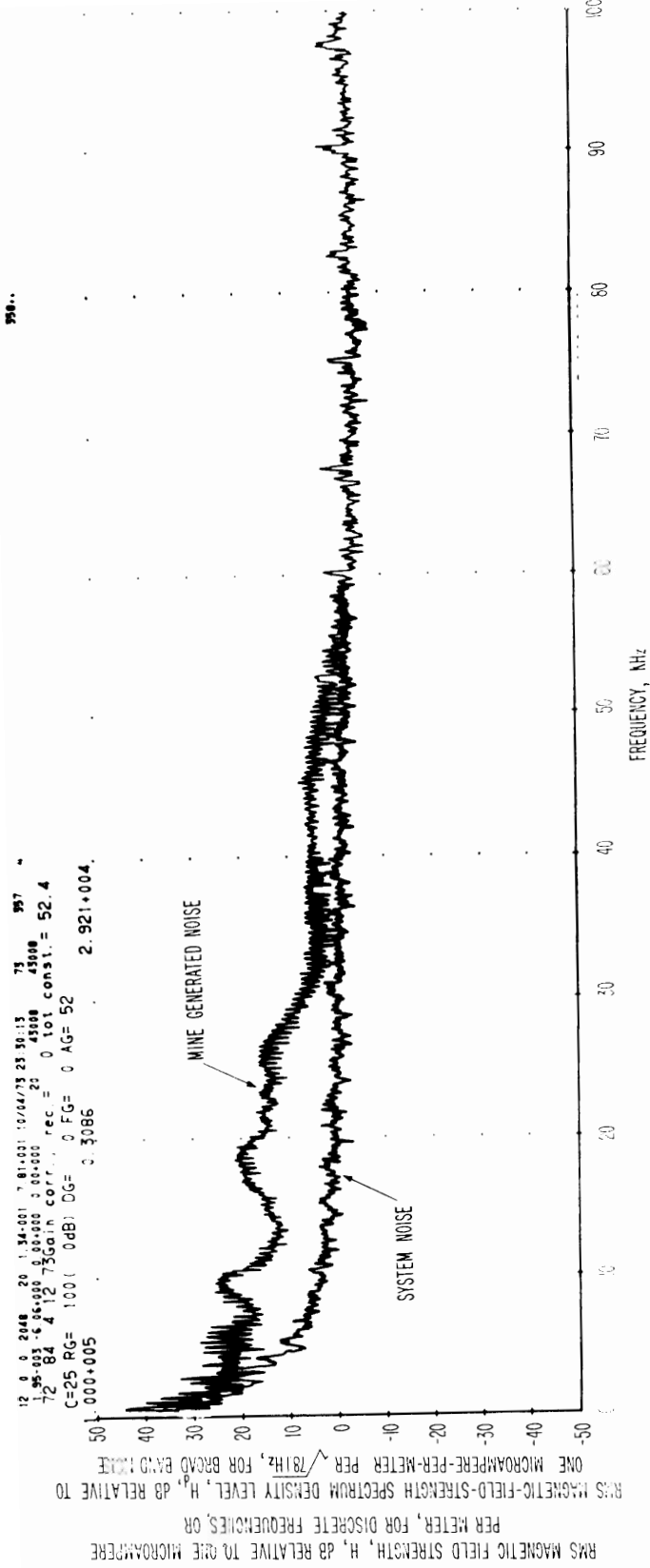


Figure 3-33 Spectrum of magnetic field strength obtained on a loop antenna 1 kHz to 100 kHz, McElroy Mine, location A, highest measured noise on this day, antenna sensitive axis vertical, 3:15 p.m., April 12, 1973. Spectral resolution is 78.1 Hz.

378

```

12 2 5 2248 20 1 34... 78... 10/28 23 30 52 ... 377
7.8-82 ... 48:28
16 84 4 12 300m con... rec= 0 001 const1= 52.4
C=25 RG= 100 0dB: CG= 5 FG= 0 LG= 52
0.000+005 0.3286 3.370+004

```

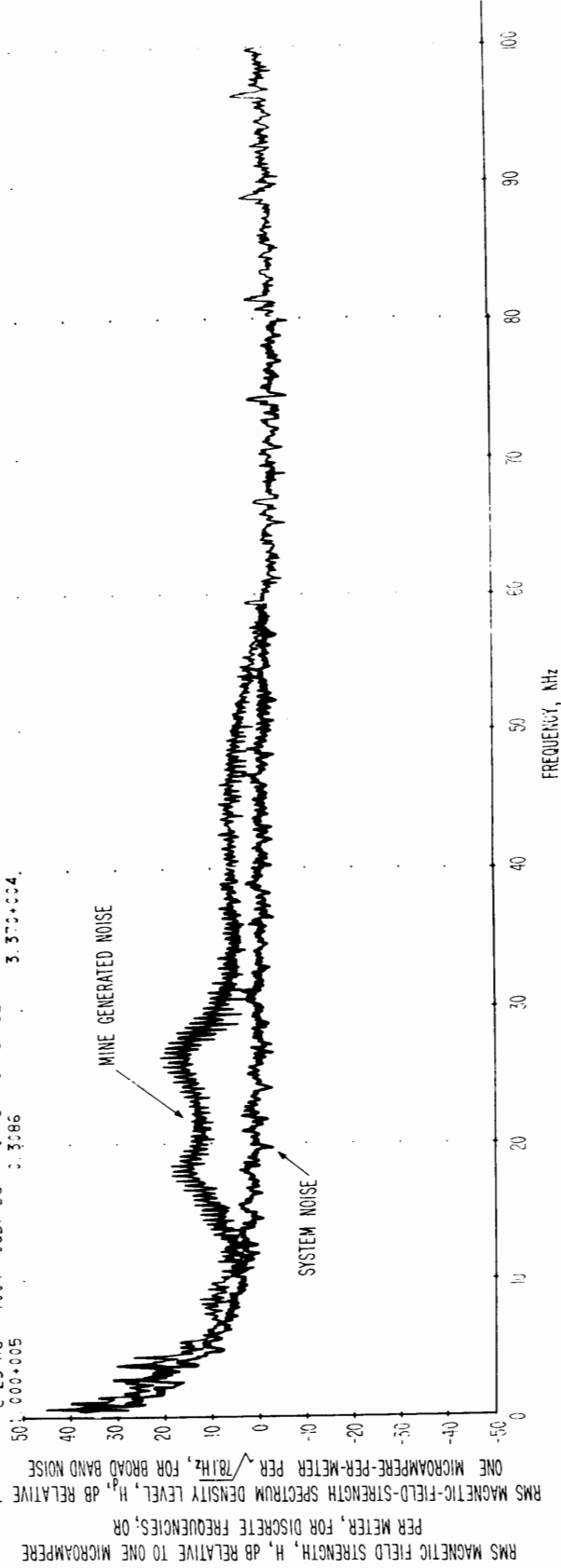


Figure 3-34 Spectrum of magnetic field strength obtained on a loop antenna 1 kHz to 100 kHz, McElroy Mine, operating arc welder 15 meters away, antenna sensitive axis vertical, 3:25 p.m., April 12, 1973. Spectral resolution is 78.1 Hz.

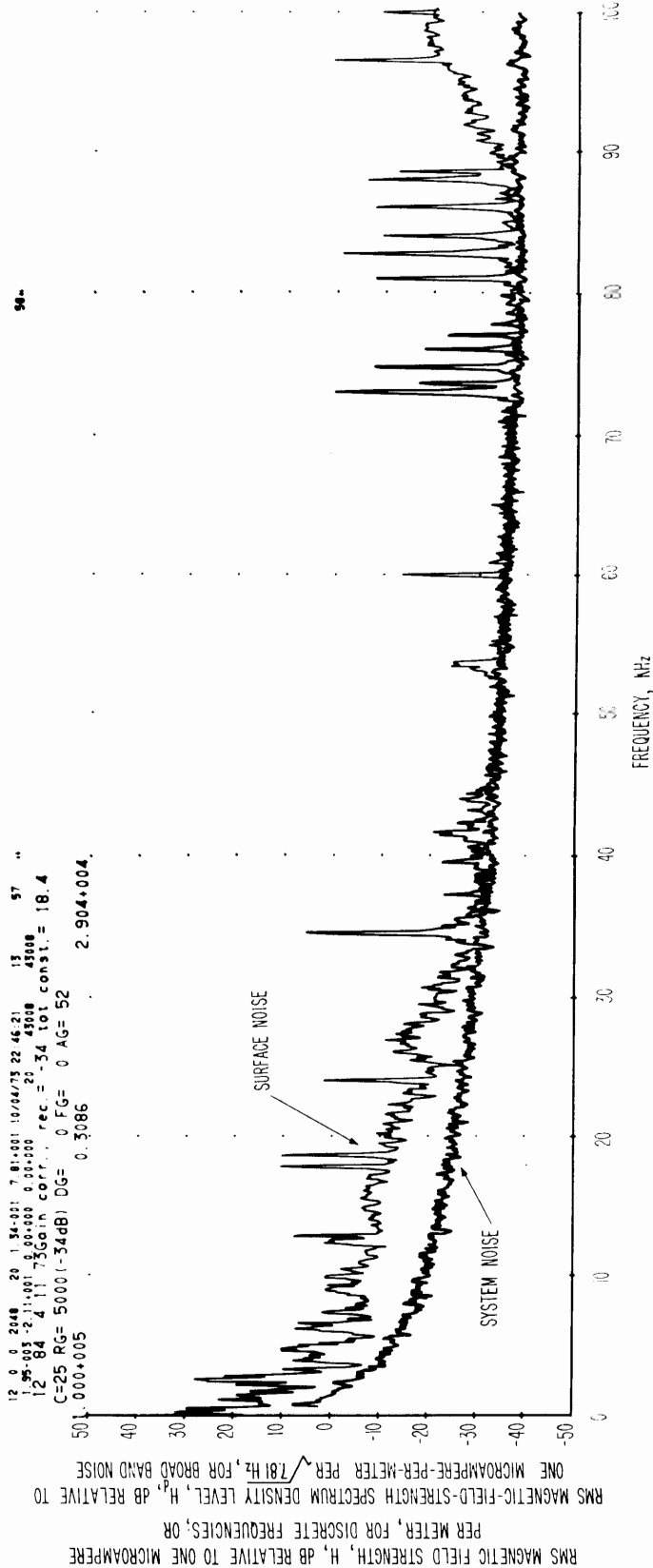


Figure 3-35 Spectrum of magnetic field strength obtained on a loop antenna 1 kHz to 100 kHz, surface above McElroy Mine, antenna sensitive axis parallel to powerline (horizontal N-S), 5:25 p.m., April 11, 1973. Spectral resolution is 78.1 Hz.

12 0 0 2048 20 2.69+000 3.91+000 06/14/74 11:07:52 47 12
 1.95-003 -4.38+001 0.00+000 0.00+000 20 43008 43008
 49 112 4 10 73Gain corr., rec. = -34 tot const. = 18.4
 C=42 RG= 5000 (-34dB) DG= 0 FG= 0 AG= 52
 1.000+007 0.3086 3.404+006.

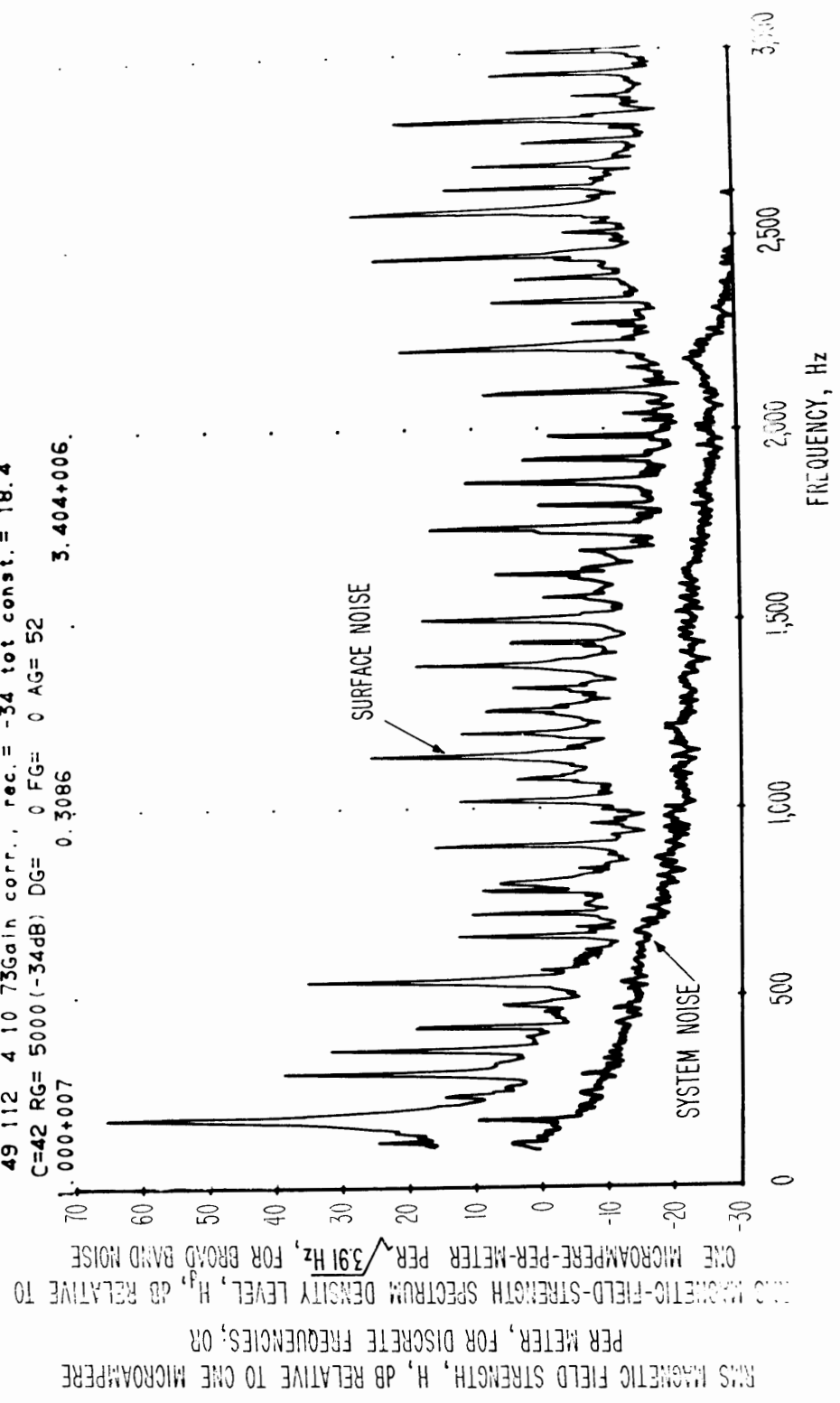


Figure 3-36 Spectrum of magnetic field strength obtained on a loop antenna 100 Hz to 3 kHz, surface above McElroy Mine, antenna sensitive axis parallel to powerline (horizontal N-S), 5:25 p.m., April 11, 1973. Spectral resolution is 3.91 Hz.

12 3 2048 20 6.72-032 1.56-032 04/20/74 00:19:09 42 5
 1 95-003 6.51-005 0.00-000 0.00-000 20 43008 43008
 41 92 4 10 73Gain corr., rec. = -34 tot const. = 18.0
 C=33 RG= 5000 (-34dB) DG= 0 FG= 0 AG= 52
 0.000+004 0.3086 1.664+003

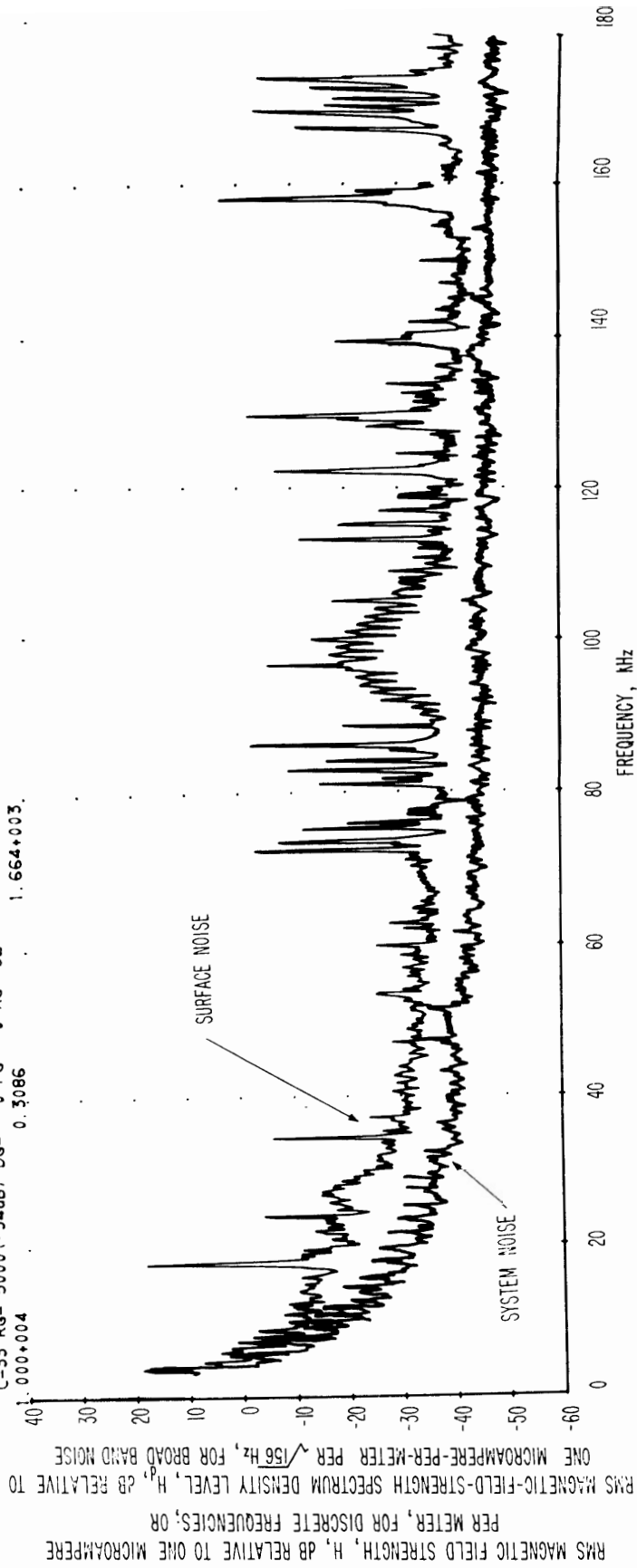


Figure 3-37 Spectrum of surface, horizontal (E-W), magnetic-field noise over 1 Left, 1 North, McElroy Mine, April 17, 1973, 5:00 p.m. The spectrum is calibrated from 3 to 180 kHz and the spectral resolution is 156 Hz.

```

:2 0 0 2148 25 6.72+02 1.55+02 24/27/74 00:21:18 45 72
1.95+03 -2.27+00 0.00+00 0.00+00 20 43:08 43:08
44 92 4 10 73Gain corr., rec.= -34 tot const.= 18.0
C=33 RG= 5000(-34dB) DG= 0 FG= 0 AG= 52
1.000+004 0.3086 1.647+003

```

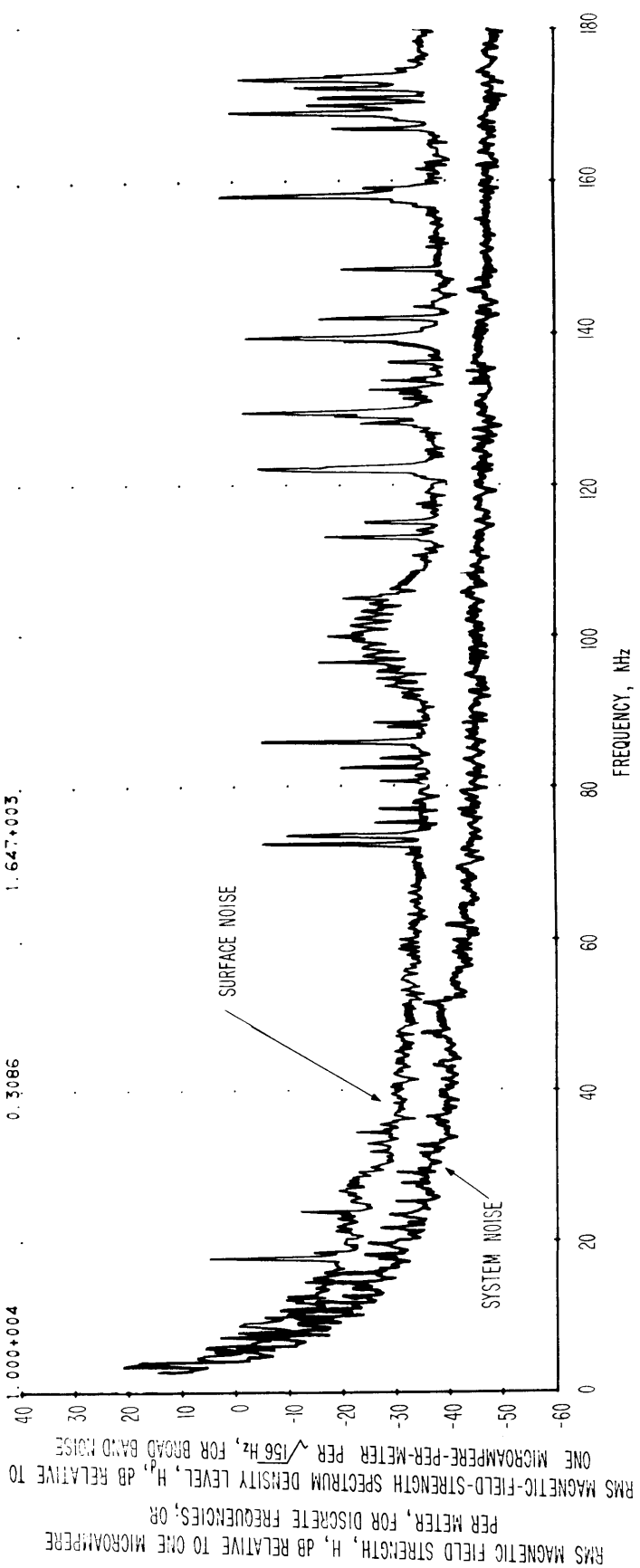


Figure 3-38 Spectrum of surface, vertical, magnetic field noise over 1 Left, 1 North, McElroy Mine, April 11, 1973, 5:00 p.m. The spectrum is calibrated from 3 to 180 kHz and the spectral resolution is 156 Hz.

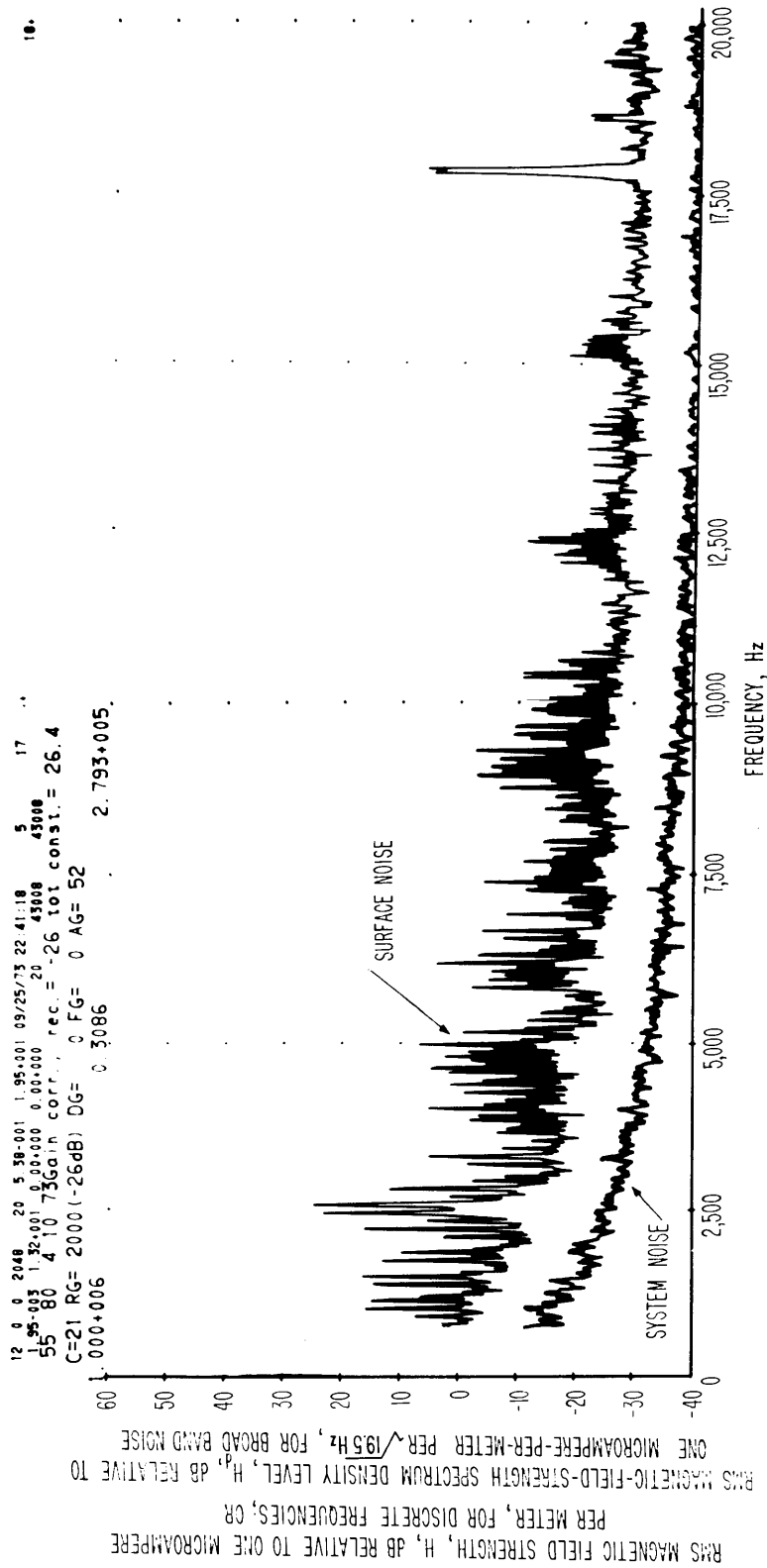


Figure 3-39 Spectrum of surface, vertical, magnetic-field noise over 1 Left, 1 North of McElroy Mine, April 11, 1973, 5:00 p.m. The spectrum is calibrated from 750 Hz to 20 kHz and spectral resolution is 19.5 Hz.


```

12 0 0 2048 20 2.69+000 3.91+000 05/21/74 12:26:30 45 52
1.95+003 9.34+001 0.00+000 0.00+000 20 43:08 43:08
44 112 4 10 73Gain corr., rec.= 0 tot const.= 52.4
C=44 RG= 100( 0dB) DG= 0 FG= 0 AG= 52
.000+004 . 0.3086 . 2.421-003.

```

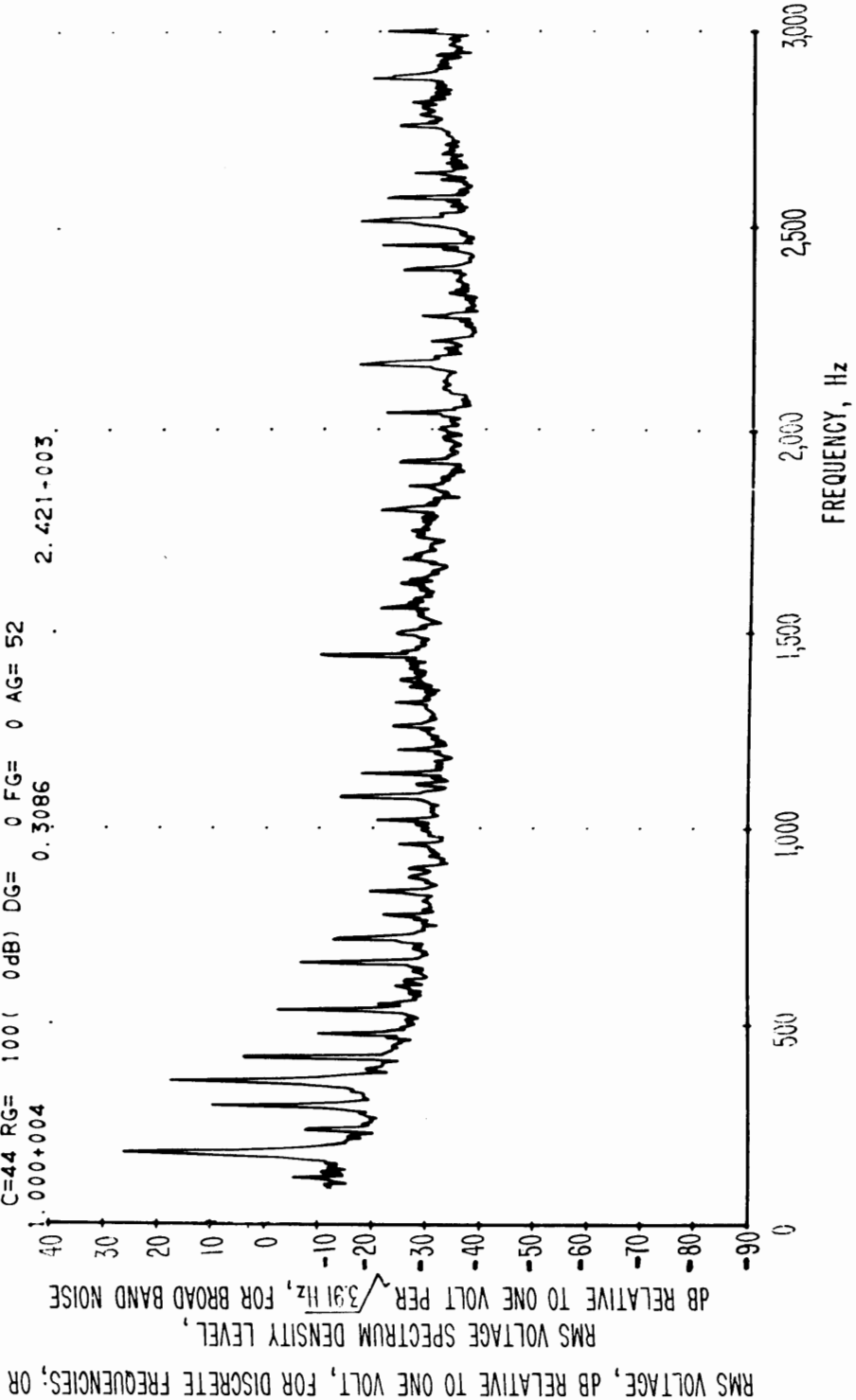


Figure 3-41 Voltage spectrum obtained from roof bolts located 21.7 meters apart, 100 Hz to 3 kHz, McElroy Mine, 4:10 p.m., April 10, 1973. Spectral resolution is 3.91 Hz.

12 3 5 2048 20 2.69+000 3.91+000 05/21/74 12:27:22 45 6
 1.95+003 0.55+001 0.00+000 0.00+000 43:08 43:08
 45 112 4 10 75Gain corr., rec.= 0 tot const.= 52.4
 C=44 RG= 100(0dB) DG= 0 FG= 0 AG= 52
 1.000+003 0.3086 6.364+002.

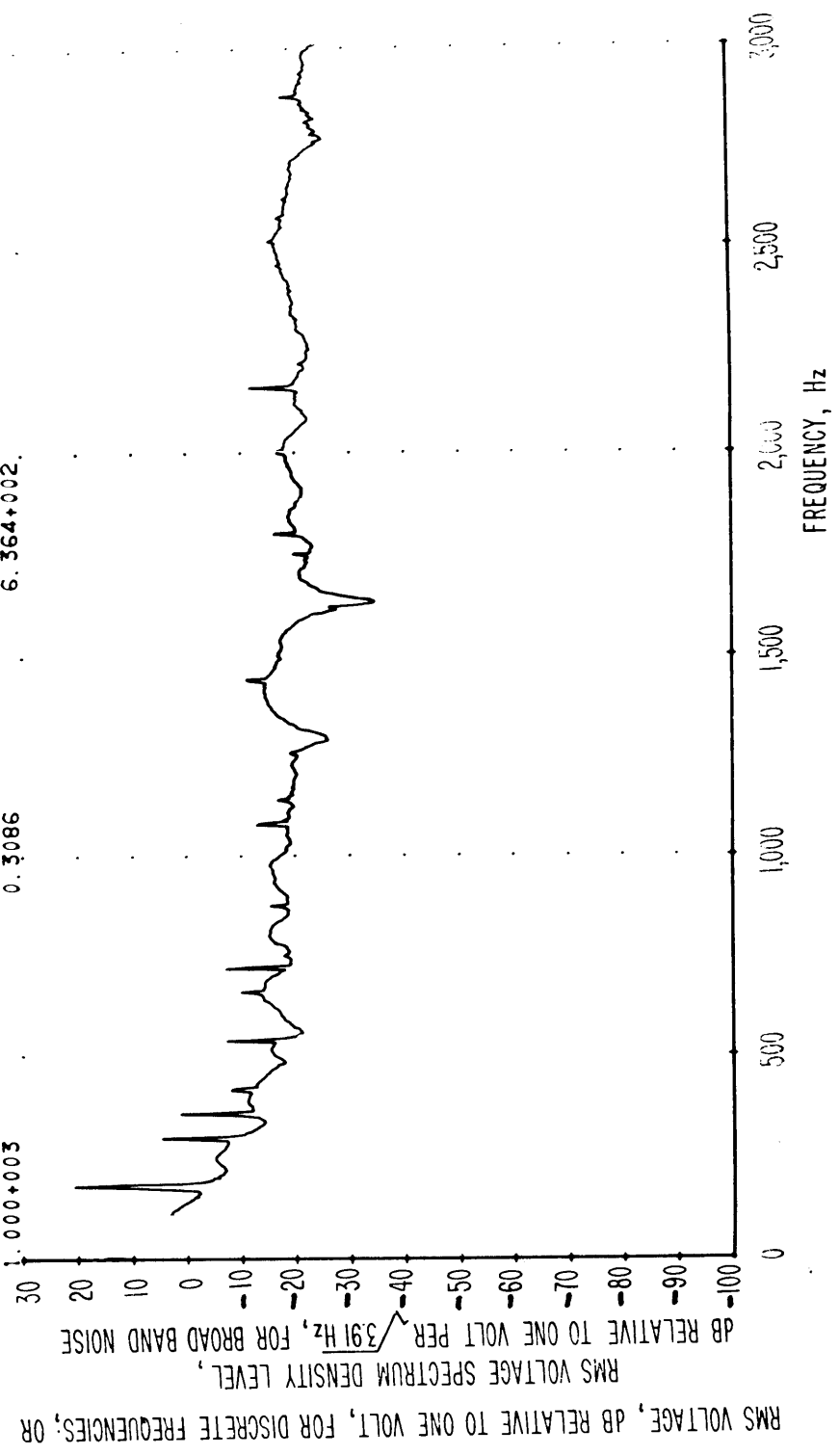


Figure 3-42 Voltage spectrum obtained from roof bolts located 11.2 meters apart, 100 Hz to 3 kHz, McElroy Mine, 4:30 p.m., April 10, 1973. Spectral resolution is 3.91 Hz.

12 0 0 2048 20 2.69+000 3.91+011 14/23/74 20:30:45 29 137
 1.95-003 -4.04+001 0.00+000 0.00+000 20 43:08 43:08
 28 112 4 10 75Gain corr., rec.= 20 tot const.= 72.4
 C=42 RG= 10 (20dB) DG= 0 FG= 0 AG= 52
 1.000+012 0.3086 1.257+011.

RMS MAGNETIC FIELD STRENGTH, H, DB RELATIVE TO ONE MICROAMPERE
 PER METER, FOR DISCRETE FREQUENCIES; OR
 RMS MAGNETIC FIELD-STRENGTH SPECTRUM DENSITY LEVEL, H_p, DB RELATIVE TO
 ONE MICROAMPERE-PER-METER PER $\sqrt{391}$ Hz, FOR BROAD BAND NOISE

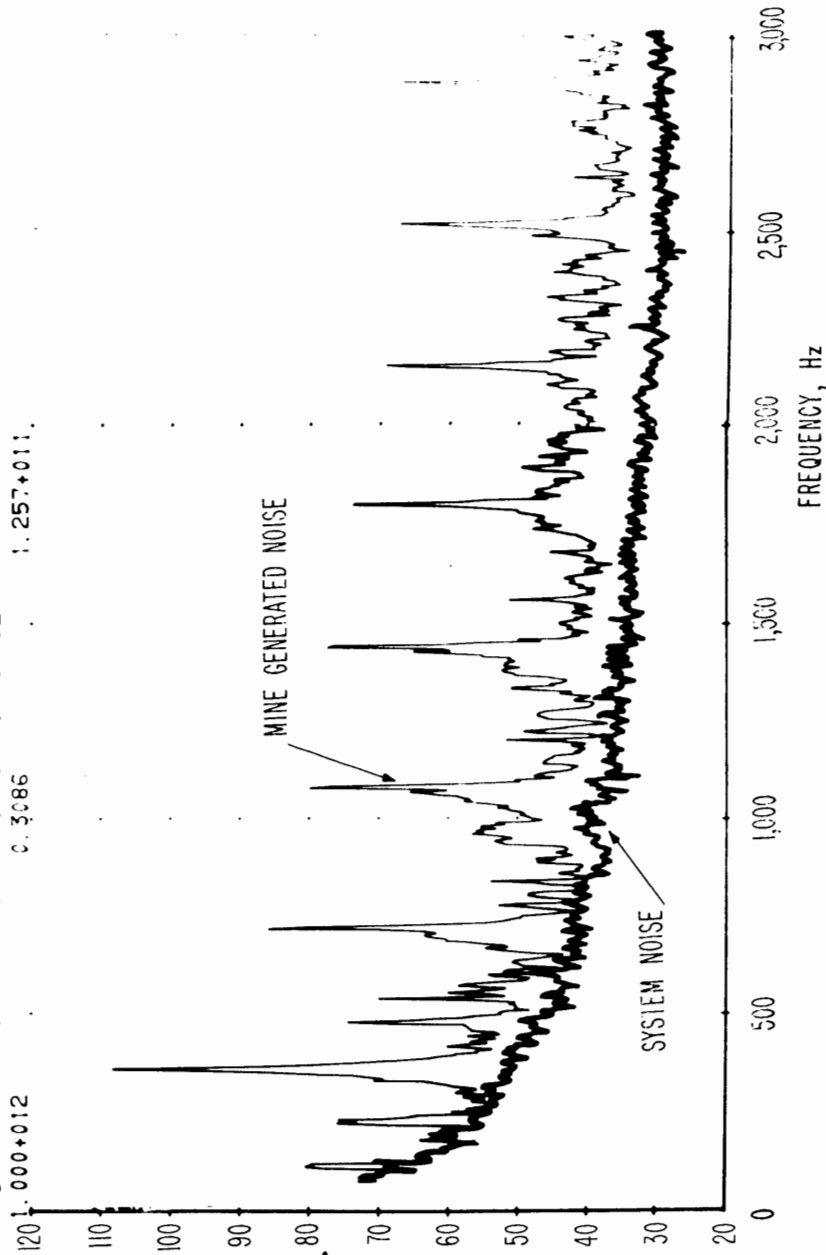


Figure 3-43 Spectrum of magnetic field strength obtained on a loop antenna 100 Hz to 3 kHz, McElroy Mine, antenna placed on top of current carrying cables, 1:50 p.m., April 10, 1973. Spectral resolution is 3.91 Hz.

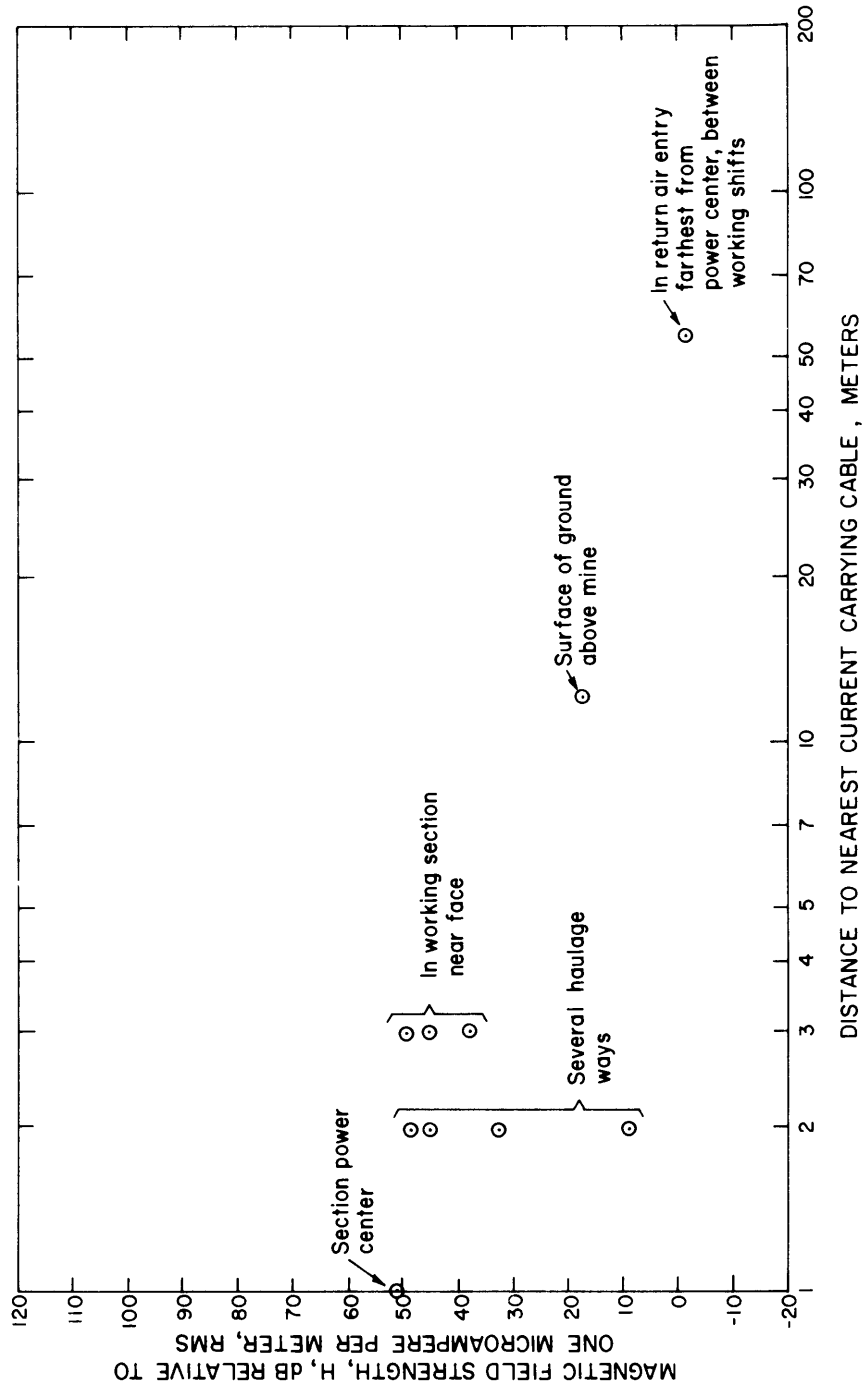


Figure 3-44 Logarithmic average magnetic field strength in McElroy Coal Mine in the frequency range 1080 Hz to 2880 Hz, produced usually by power line harmonics 3 through 8 of 360 Hz. Antenna sensitive axis orientation is vertical (up-down).

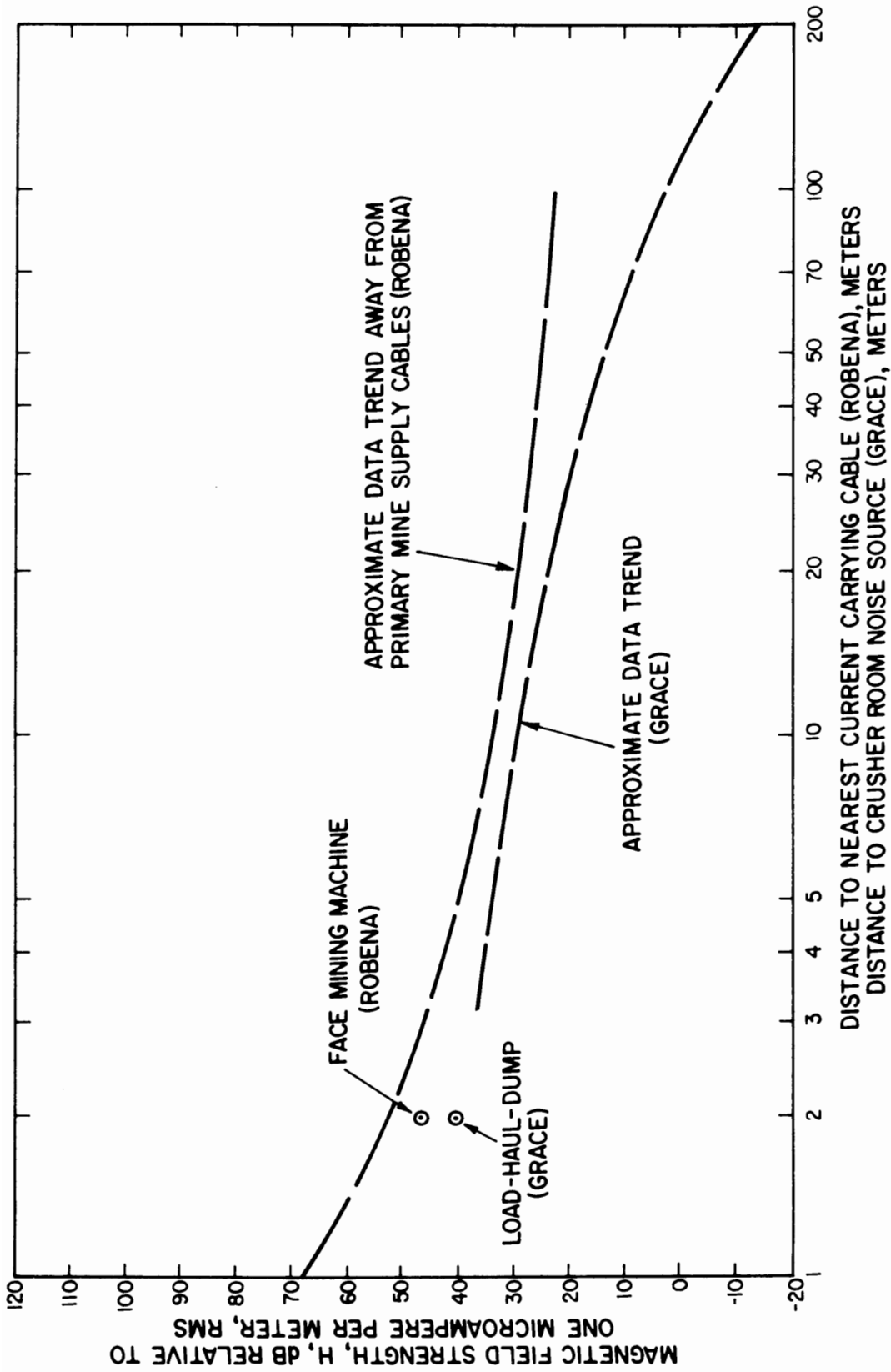


Figure 3-45 Comparison of magnetic field strengths of Grace and Robena Mines as a function of distance from noise source.

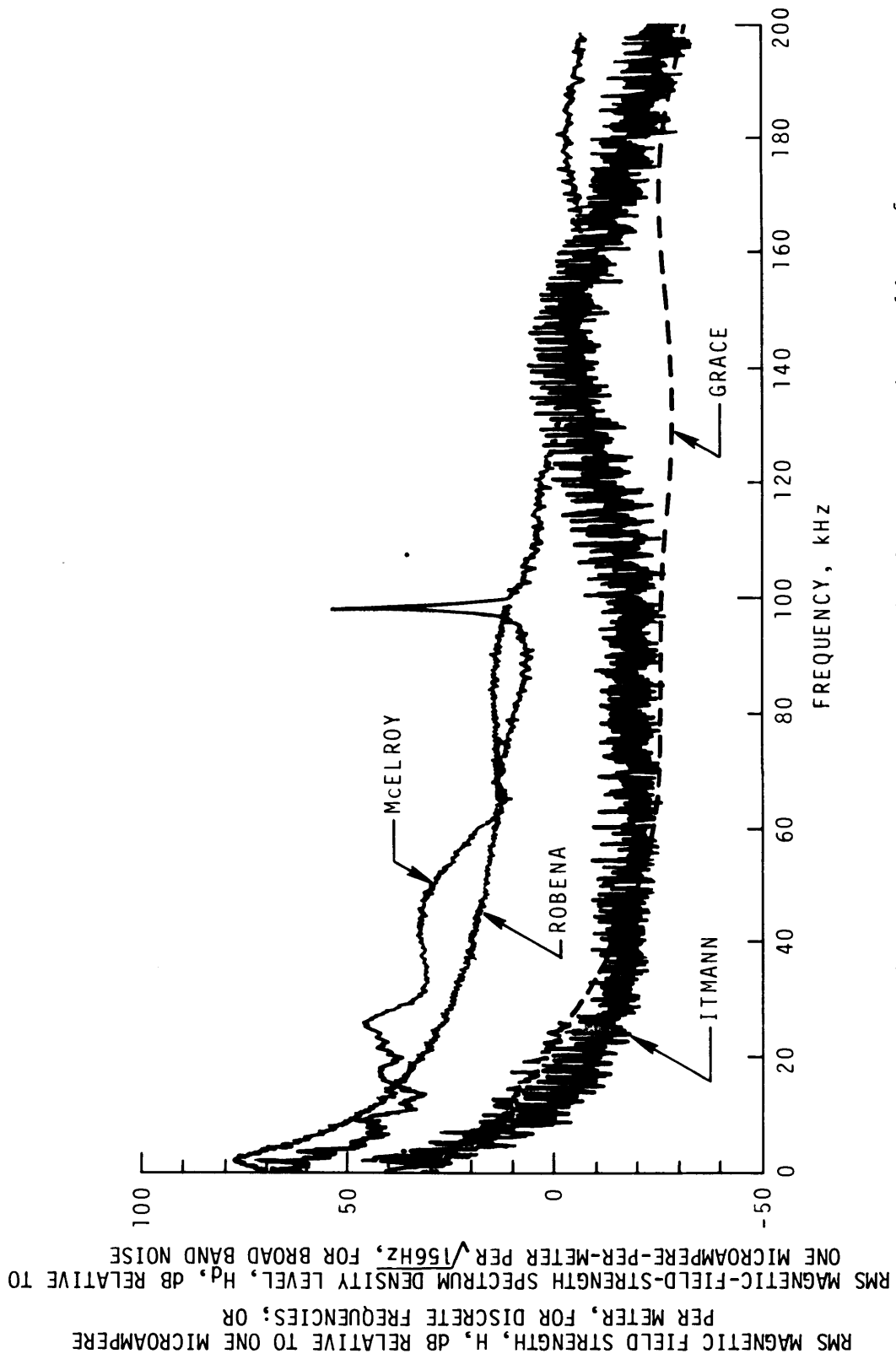


Figure 3-46 Comparison of E-M noise levels near operating machinery from four mines. Vertical magnetic-field components are shown. Broken sections of the curves represent system noise.

RMS MAGNETIC FIELD STRENGTH, H, DB RELATIVE TO ONE MICROAMPERE PER METER, FOR DISCRETE FREQUENCIES; OR
 RMS MAGNETIC-FIELD-STRENGTH SPECTRUM DENSITY LEVEL, H, DB RELATIVE TO ONE MICROAMPERE-PER-METER PER $\sqrt{156}$ HZ, FOR BROAD BAND NOISE

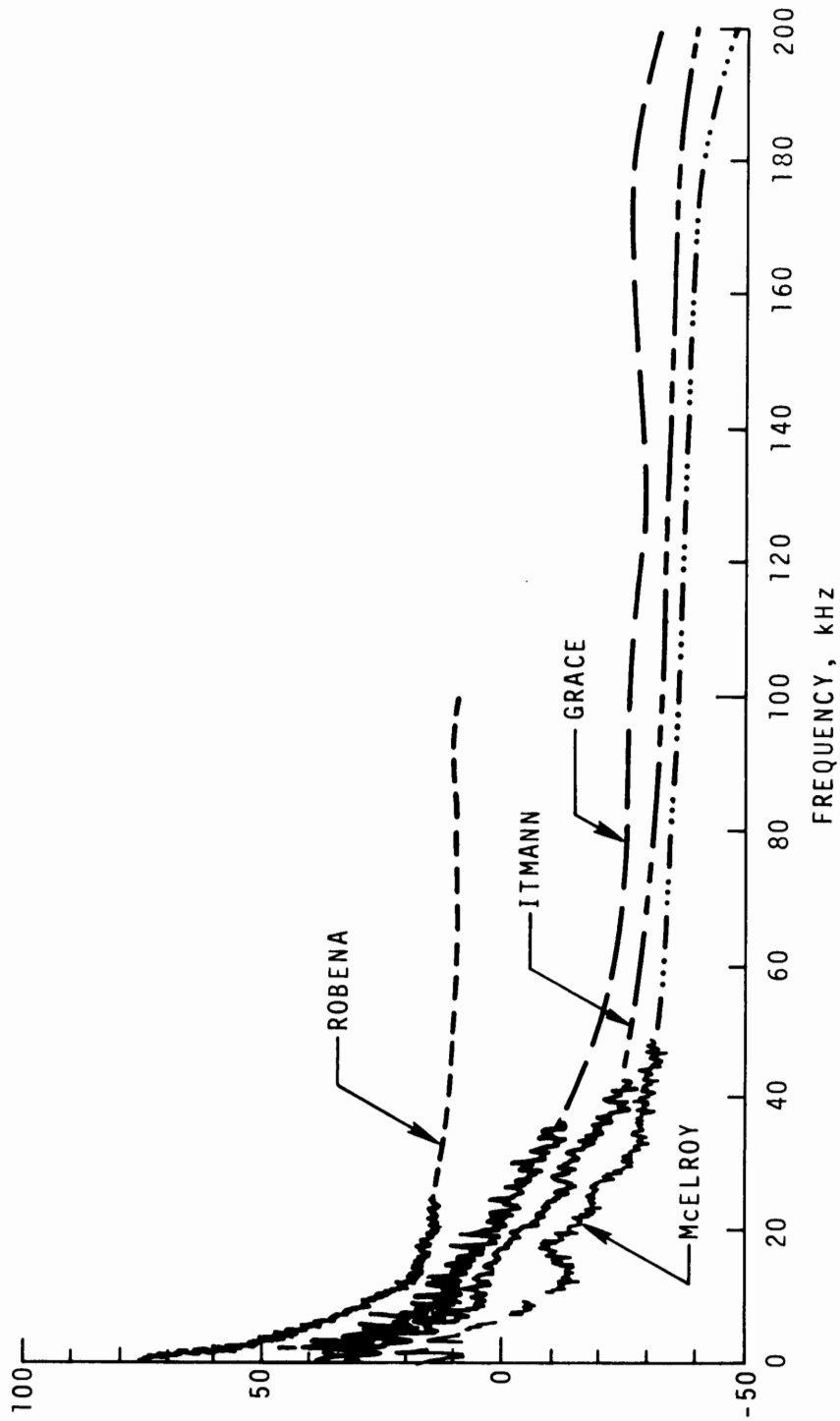


Figure 3-47 Comparison of E-M noise levels along haulageways in four mines. Vertical magnetic-field components are shown. Broken sections of the curves represent measurement-system noise levels.

4. AMPLITUDE PROBABILITY DISTRIBUTION MEASUREMENTS

4.1 Introduction and Uncertainties

Statistical representations are required since the variations of field strength are, in general, random. The amplitude probability distribution (APD) of the received noise envelope is one of the most useful statistical descriptions of the noise process for the design and evaluation of a telecommunications system operating in a noisy environment [5,6,7].

By plotting the cumulative APD on Rayleigh graph paper, one can show clearly the fraction of time that the noise envelope exceeds various levels. Rayleigh graph paper is chosen with scales such that a Rayleigh distribution (i.e., envelope distribution of Gaussian noise) plots as a straight line with slope of $-1/2$. Noise with rapid large changes in amplitude (e.g., impulsive noise) then has a much steeper slope, typically -4 or -5 , depending on the impulsiveness of the noise and the receiver bandwidth.

With the exception of the roof-support bolt measurements, all APD measurements are reported in absolute quantities.

The estimated limits of error for the APD noise measurements are ± 5 dB. Several sources of error that are critical to the overall accuracy of our measurements are listed below:

1. Use of a discrete, digital level counter (levels are 6 dB apart) contributes ± 1 -dB quantization error limit. One-decibel step attenuators are used to achieve the \pm one decibel.
2. The system, i.e., recording, data transcribing, and data processing, has a calibration uncertainty of ± 0.5 dB [3].
3. The estimated uncertainty involved in using the portable and the laboratory tape recorders for record and playback is ± 0.5 dB due to harmonic distortion, flutter, dropout, cross-talk, etc.

4. The gain instability during measurements, gain changes between measurements and calibration, and the non-linearity of electromagnetic interference and field strength (EIFS) meters and mixers, all combined, contribute ± 0.5 dB uncertainty.
5. The gain instability and non-linearity of the digital level counter, the tuned frequency converter, the amplifier, and attenuators, all combined, contribute ± 0.5 dB uncertainty.
6. Connector losses and BNC cable losses, particularly at higher frequencies above 100 kHz, contribute ± 2.0 dB uncertainty.

Some additional uncertainty beyond the stated measurement system uncertainty is caused by the in-mine environment. Care was taken to provide at least one meter separation from metallic objects wherever possible. However, coal, rock, or earth was sometimes immediately adjacent to a loop antenna. In all observed cases, this had no effect at frequencies up to 1 MHz. Above 1 MHz, earth and other reflections did in some cases cause ± 1 dB variations, even with a shielded, balanced loop antenna. An estimate is that an additional ± 5 dB uncertainty might be advisable. However, due to the complexity of the shielded loop in the mine environment, this uncertainty cannot be rigorously bounded without substantial additional analysis.

4.2 Results

4.2.1 Introduction

APD measurements were made on April 10 and 12, 1973, during operation in the McElroy Coal Mine located near Moundsville, West Virginia. Descriptions of McElroy Mine are given in section 1.2. APD measurements were made at four locations. The first set of APD measurements of about eleven different frequencies was made on April 10, 1973, at

location B in figure 3-1. The second set of APD measurement of about eight different frequencies was made on April 10, 1973, at location A in figure 3-1. In these two sets of APD measurements, both the vertical and horizontal components of magnetic field were measured.

The third set of APD measurements of about nine frequencies was made on April 12, 1973, at location B in figure 3-2. The fourth set of APD measurements of about nine frequencies was made on April 12, 1973, at location A in figure 3-2. In these two sets of APD measurements, only the vertical components of magnetic field were measured.

In addition to these four sets of measurements, APD measurements were made during a quiet time at locations A and B in figure 3-1. APD measurements between roof-support bolts were performed on April 10, 1973, at location B in figure 3-1.

4.2.2 Measurement Results

Figures 4-1 through 4-11 show the APD's of vertical components of magnetic field noise and figures 4-12 through 4-23 show the APD's of horizontal components (NE-SW) of magnetic field noise measured at location B of figure 3-1 on April 10, 1973. APD's measured at quiet time at location B of figure 3-1 are shown in figures 4-24 through 4-27. Here only the vertical component of magnetic noise was measured at four frequencies ranging from 10 kHz to 150 kHz. Above 250 kHz, the magnetic noise measured in the mine was below the system noise (i.e., 60 dB or more below one microampere per meter) since EIFS meter readings with and without an antenna were the same.

Figures 4-28 through 4-36 show APD's of the vertical component of magnetic field noise and figures 4-37 through 4-43 show APD's of the horizontal component of magnetic field noise measured at location A in figure 3-1 on April 10,

1973. APD measurements made at a quiet time at location A in figure 3-1 are also shown in figures 4-44 through 4-48. Again, only the vertical component of magnetic noise was measured at five frequencies ranging from 10 kHz to 160 kHz. Above 250 kHz, the magnetic noise measured in the mine was below the system noise (i.e., 60 dB or more below one microampere per meter) since EIFS meter readings with and without an antenna were the same.

Figures 4-49 through 4-58 show the APD's of magnetic field noise measured at location B in figure 3-2. Figures 4-59 through 4-68 show the APD's of magnetic field noise measured at location A in figure 3-2 on April 12, 1973. Only the vertical component of the magnetic field was measured at ten frequencies ranging from 10 kHz to 32 kHz.

Figures 4-69 through 4-70 show results of the roof-support bolt measurements made at location B in figure 3-1 on April 10, 1973. The separation between the two roof-support bolts was 3 meters. The APD's were measured using non-shielded copper wire clipped to the roof-support bolts. It is not easy to analyze what was measured using non-shielded copper wire. It was a combination of electric field through a dipole with a lossy surrounding medium (i.e., coal), of magnetic field through a lossy loop antenna, and of voltage induced by current flowing through the medium between the roof bolts. Therefore, relative voltage is the parameter given. The rms value is arbitrarily assigned the value 0 dB.

4.2.3 RMS and Average Values

The APD's are integrated to give rms and average values of the field strength, according to the equations

$$H_{avg} = - \int_0^{\infty} H dp(H)$$

and

$$H_{\text{rms}} = \left(\int_0^{\infty} H^2 dp(H) \right)^{\frac{1}{2}},$$

where H represents the magnetic field strength of the noise, and p is the probability that the measured field strength exceeds the value H. These quantities are also dependent upon the measurement bandwidth, the length of the data run, and possibly other parameters. Finite series are actually used for the numerical integration. The rms and average values so arrived at are identified on each graph and are time averages (23 minutes) of these time-dependent parameters. If the tapes are played into ordinary rms-reading meters, the meter readings will vary 10 to 20 dB over fractions of a second depending on the averaging time constants of the meter. The rms value is directly relatable to noise power.

4.2.4 Summary Curves

Excursions of field strength between 0.001 and 99 percent, as well as rms and average values, are shown in figures 4-71 through 4-78. The predetection bandwidth for these APD measurements either is 1 kHz or is normalized to 1 kHz. Figures 4-1 through 4-11 (vertical, near the power distribution center) are summarized on figure 4-71; figures 4-12 through 4-23 (horizontal, near the power distribution center) are summarized on figure 4-72; figures 4-24 through 4-27 (vertical, quiet time, near the power distribution center) are summarized on figure 4-73. Figures 4-28 through 4-36 (vertical, near end of rail haulage) are summarized on figure 4-74; figures 4-37 through 4-43 (horizontal, near end of rail haulage) are summarized on figure 4-75; figures 4-44 through 4-48 (vertical, quiet time near end of rail haulage) are summarized on figure 4-76. Figures 4-49 through 4-58 (near intersection of main haulage and conveyor belt) are summarized in figure 4-77.

Figures 4-59 through 4-68 (near operating continuous miner) are summarized on figure 4-78. Magnetic field strength generally decreases monotonically with increasing frequency at 20 dB per decade. Some long-term fluctuations in values occur because of different operating conditions during different times of the day. Although 20 minutes was determined to be a sufficient time to give validity to the statistics in a mine-section environment where the work cycle is two to four minutes, 20 minutes may not be sufficient in other locations where longer cycles may exist. Perhaps this should be considered further.

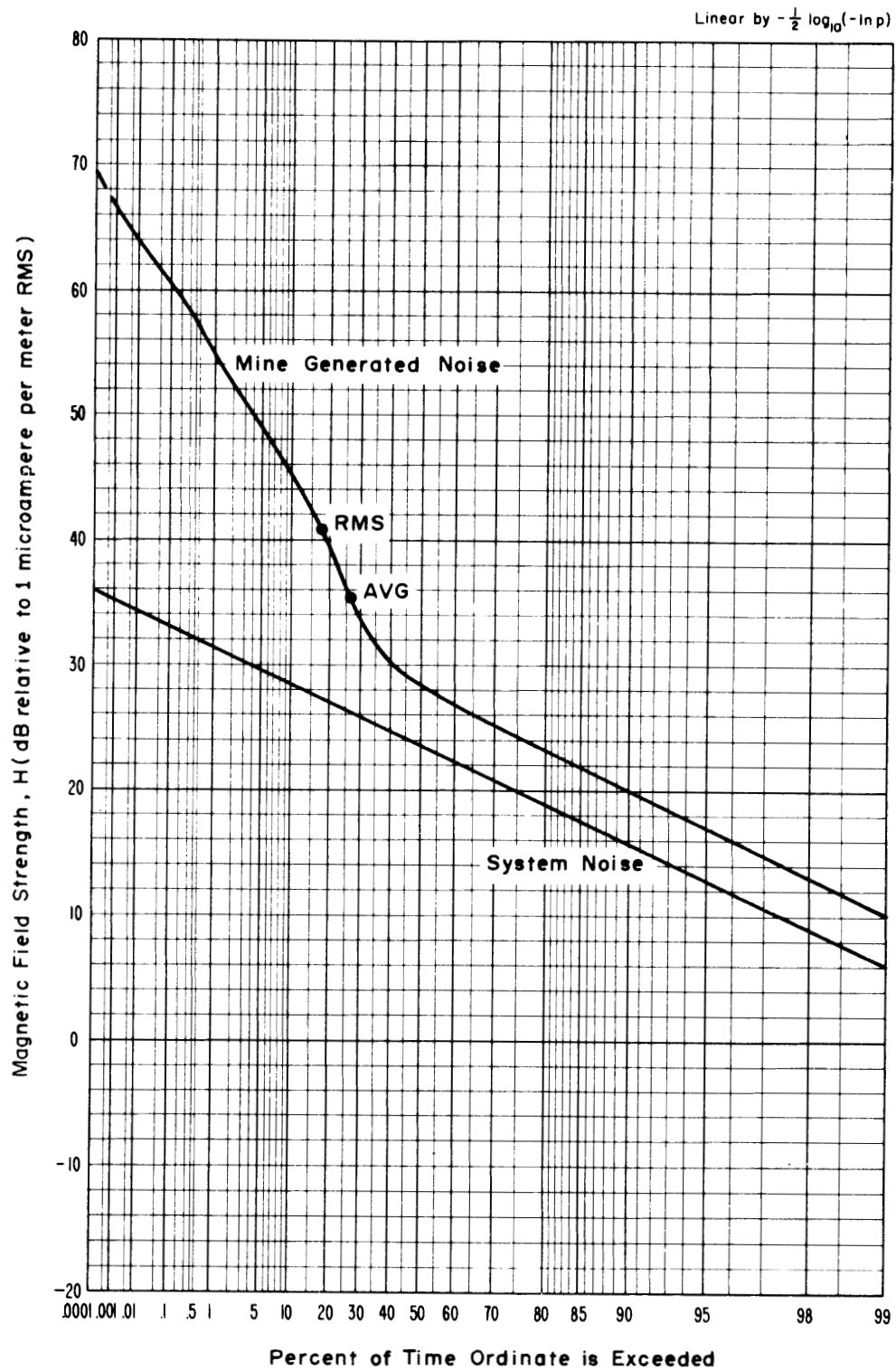


Figure 4-1 APD, 10 kHz, vertical component, 1.0 kHz predetection bandwidth, April 10, 1973, 11:40 a.m., McElroy Mine.

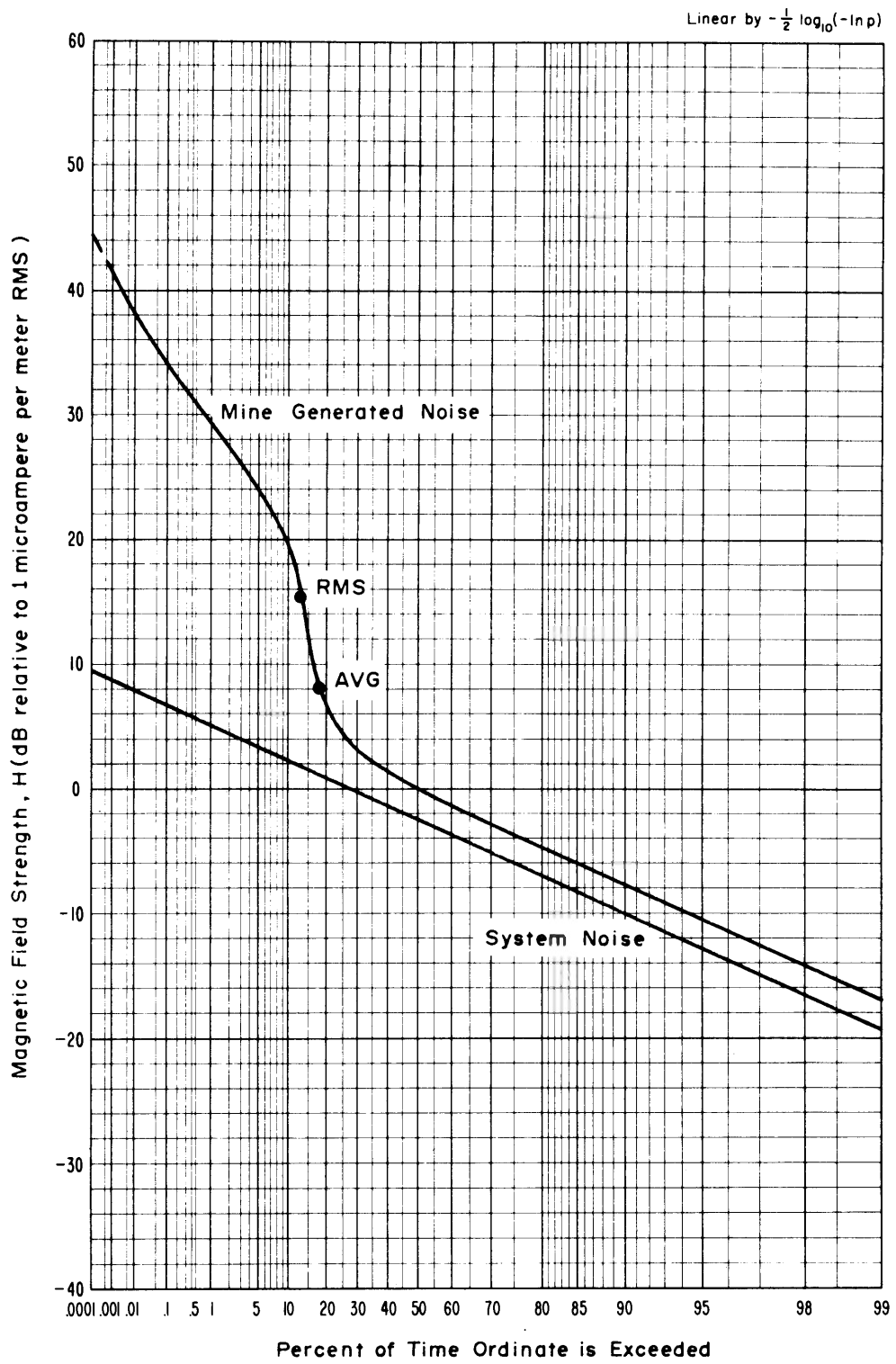


Figure 4-2 APD, 30 kHz, vertical component, 1.0 kHz predetection bandwidth, April 10, 1973, 1:10 p.m., McElroy Mine.

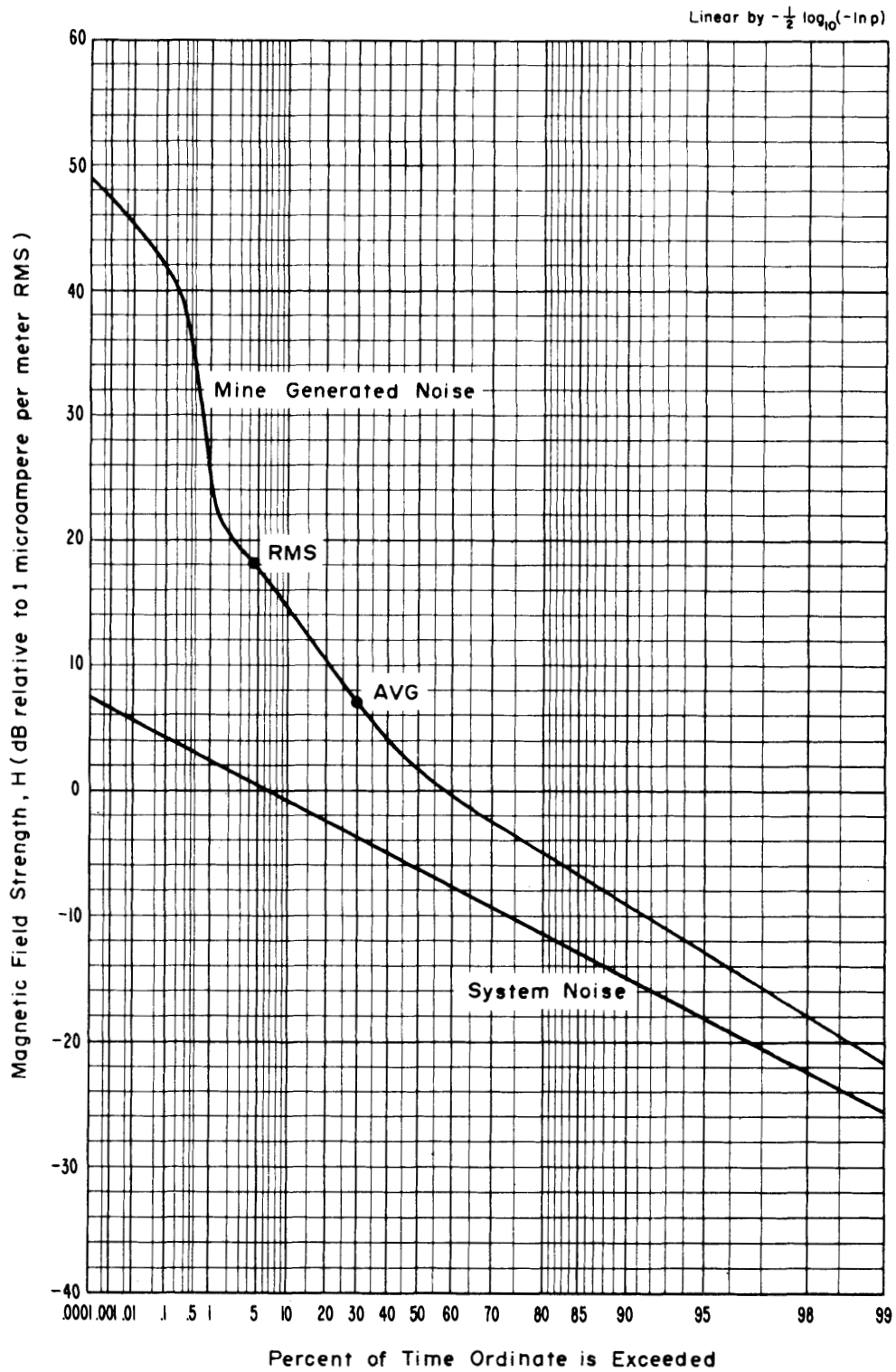


Figure 4-3 APD, 70 kHz, vertical component, 1.0 kHz predetection bandwidth, April 10, 1973, 2:20 p.m., McElroy Mine.

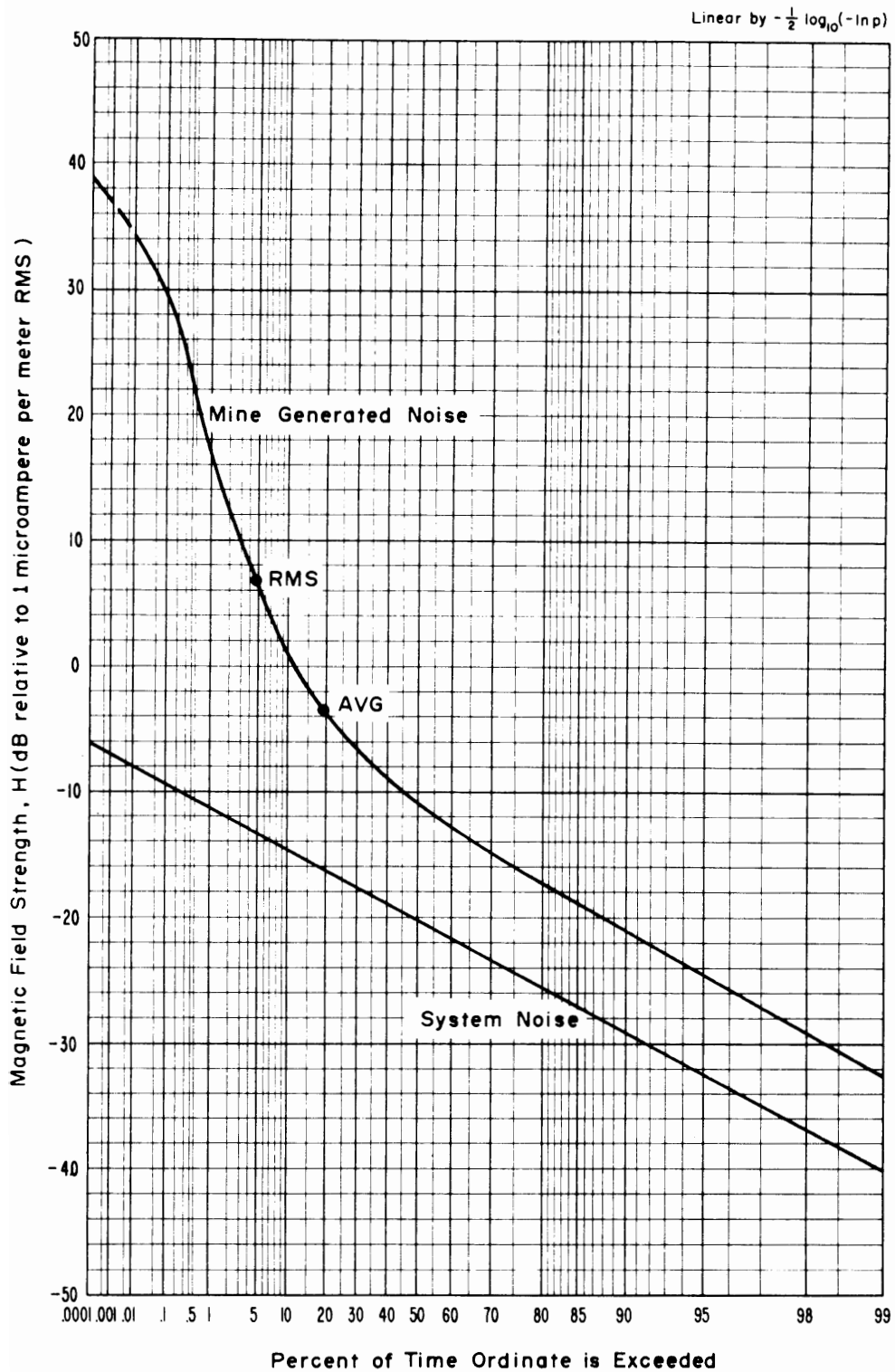


Figure 4-4 APD, 130 kHz, vertical component, 1.0 kHz predetection bandwidth, April 10, 1973, 3:25 p.m., McElroy Mine.

Linear by $-\frac{1}{2} \log_{10}(-\ln p)$

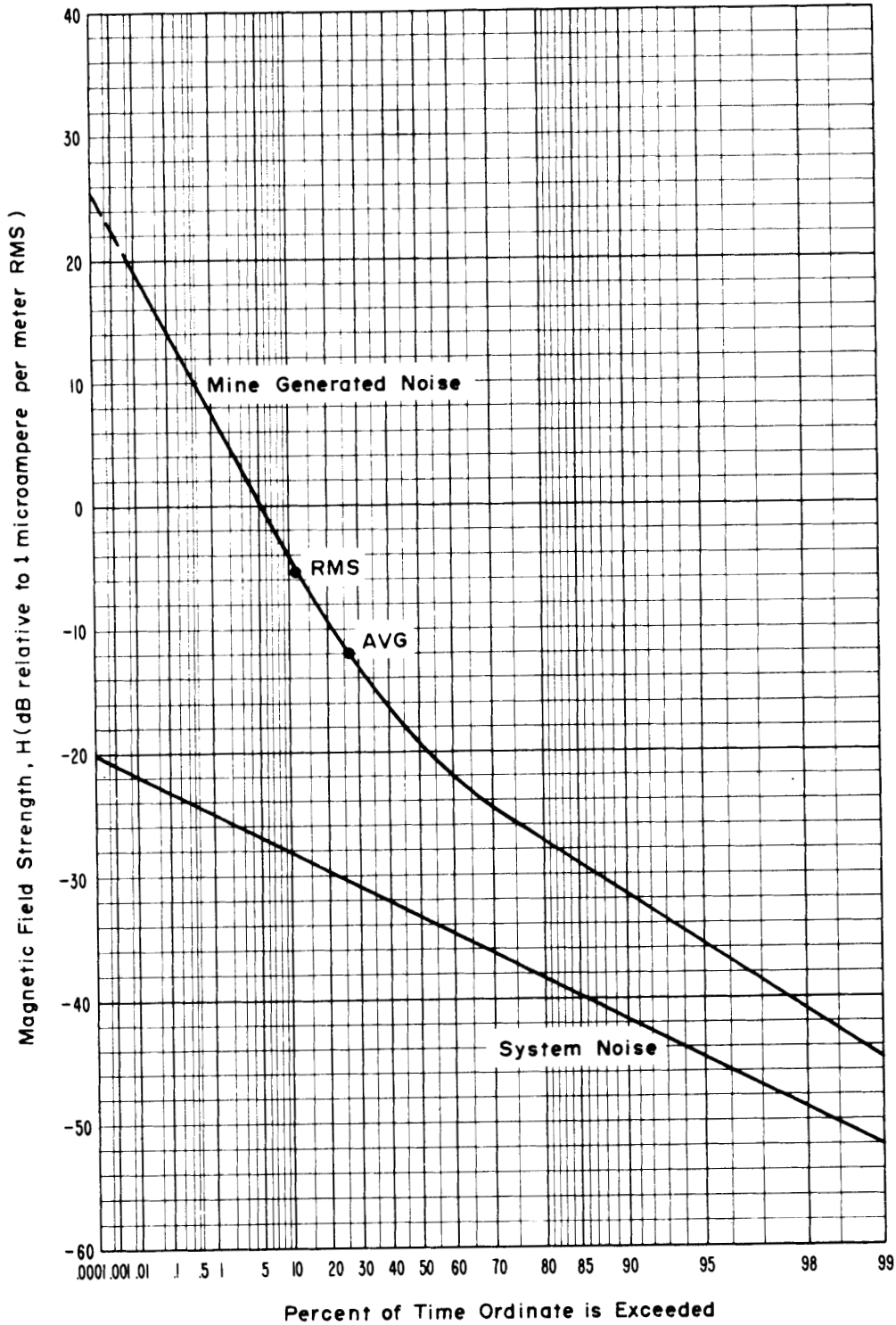


Figure 4-5 APD, 160 kHz, vertical component, 1.0 kHz predetection bandwidth, April 10, 1973, 5:30 p.m., McElroy Mine.

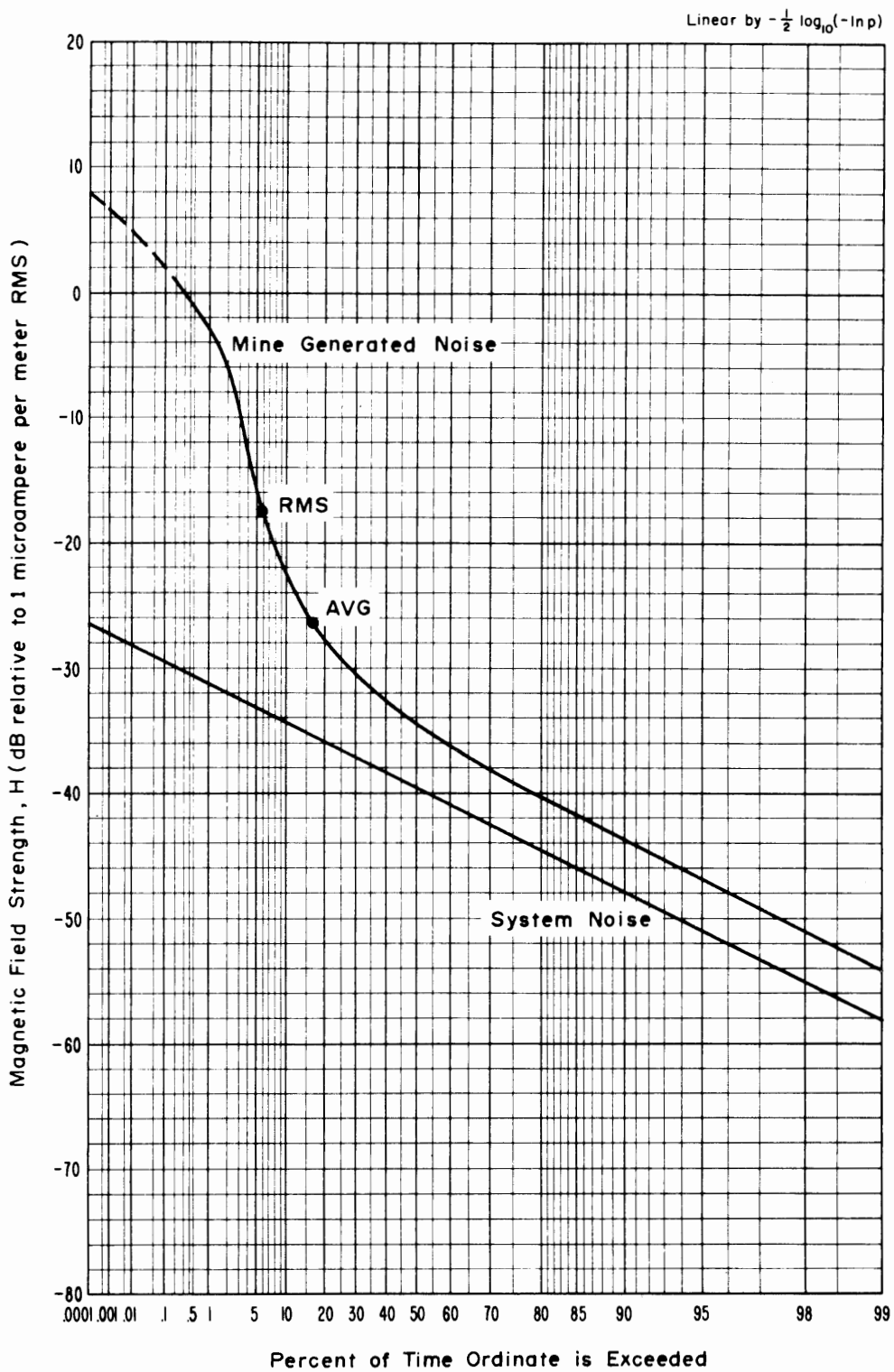


Figure 4-6 APD 250 kHz, vertical component, 1.0 kHz predetection bandwidth, April 10, 1973, 6:35 p.m., McElroy Mine.

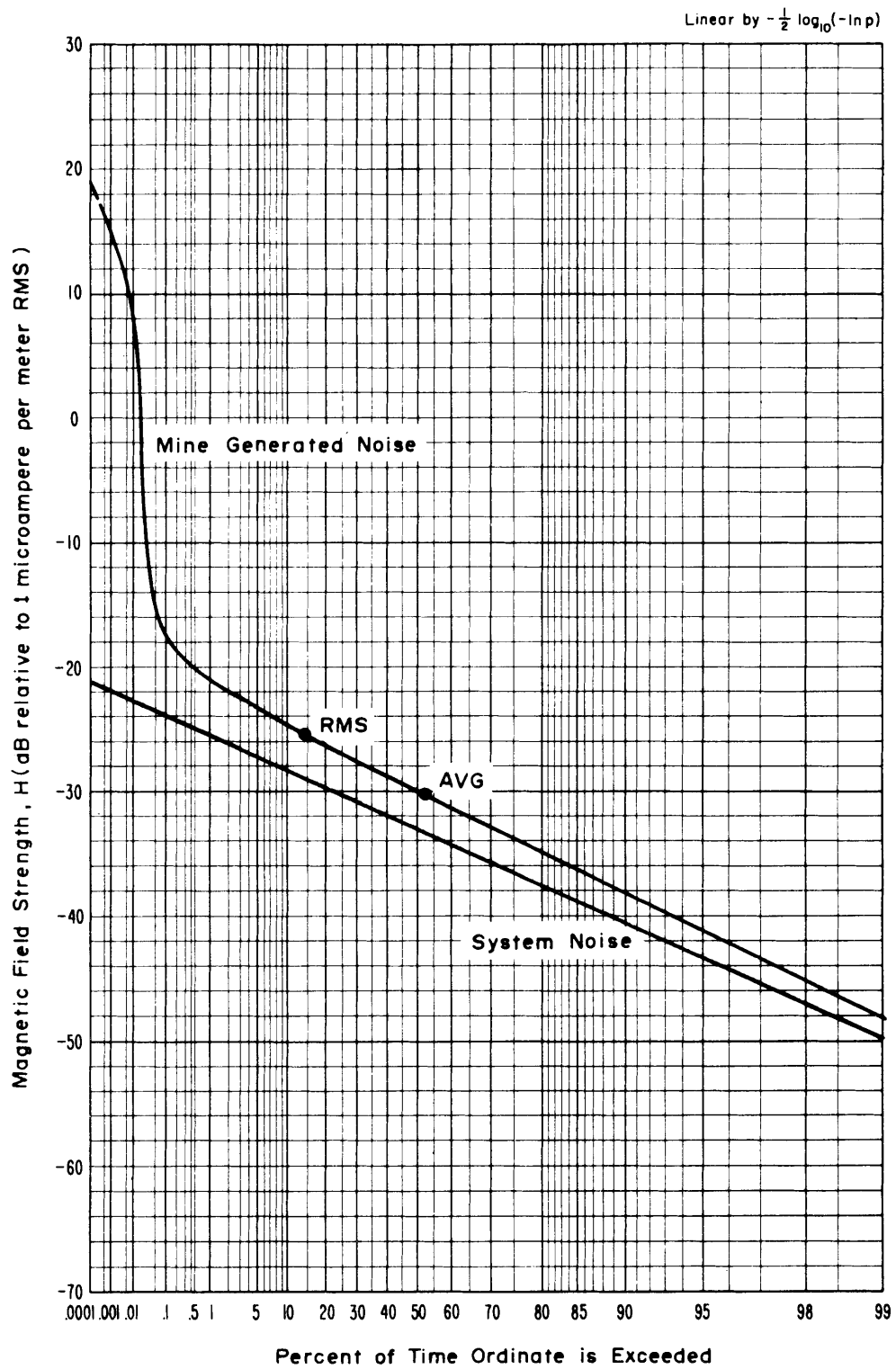


Figure 4-7 APD, 500 kHz, vertical component, 1.2 kHz predetection bandwidth, April 10, 1973, 11:40 a.m., McElroy Mine.

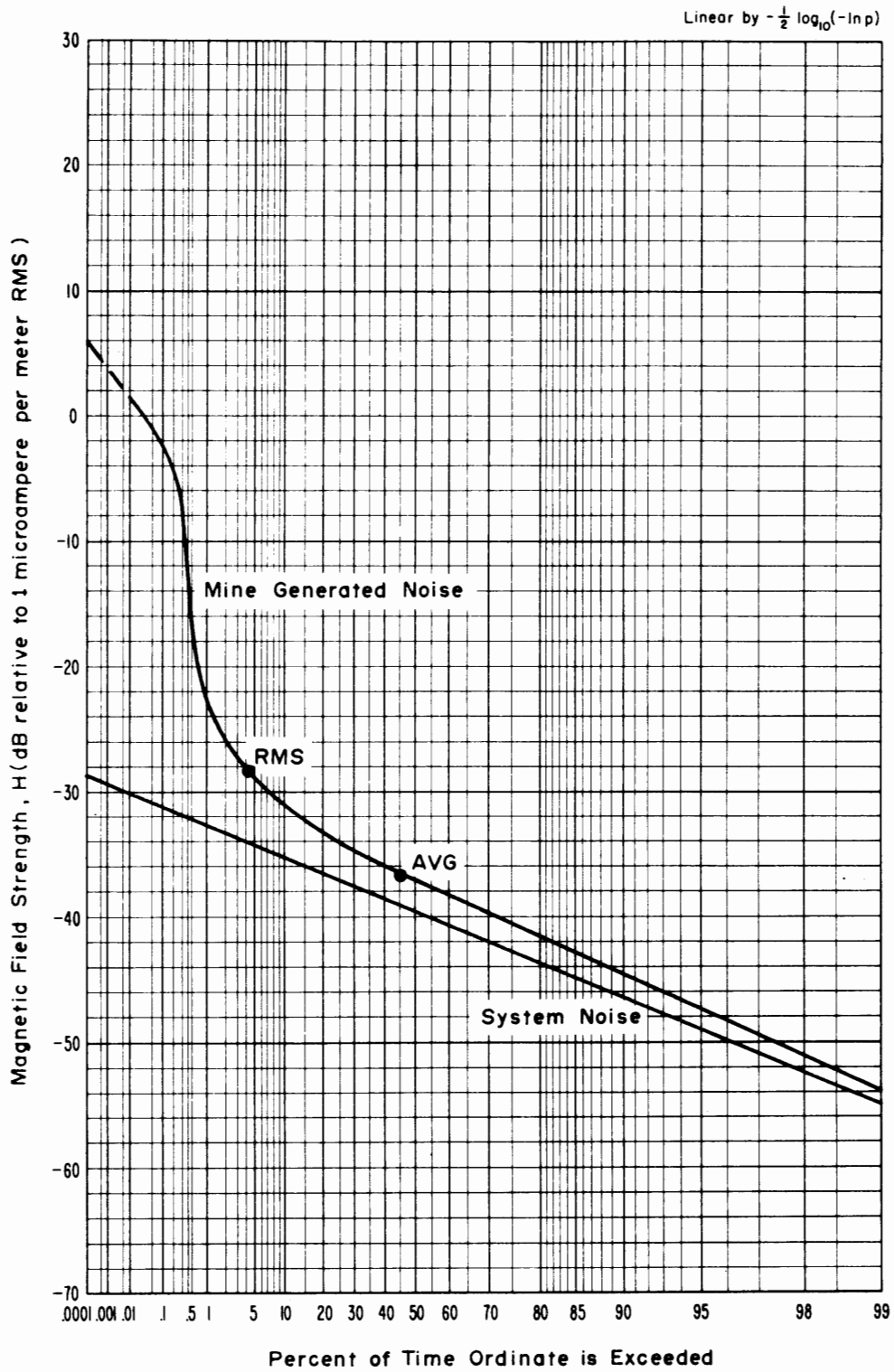


Figure 4-8 APD, 1 MHz, vertical component, 1.2 kHz predetection bandwidth, April 10, 1973, 1:10 p.m., McElroy Mine.

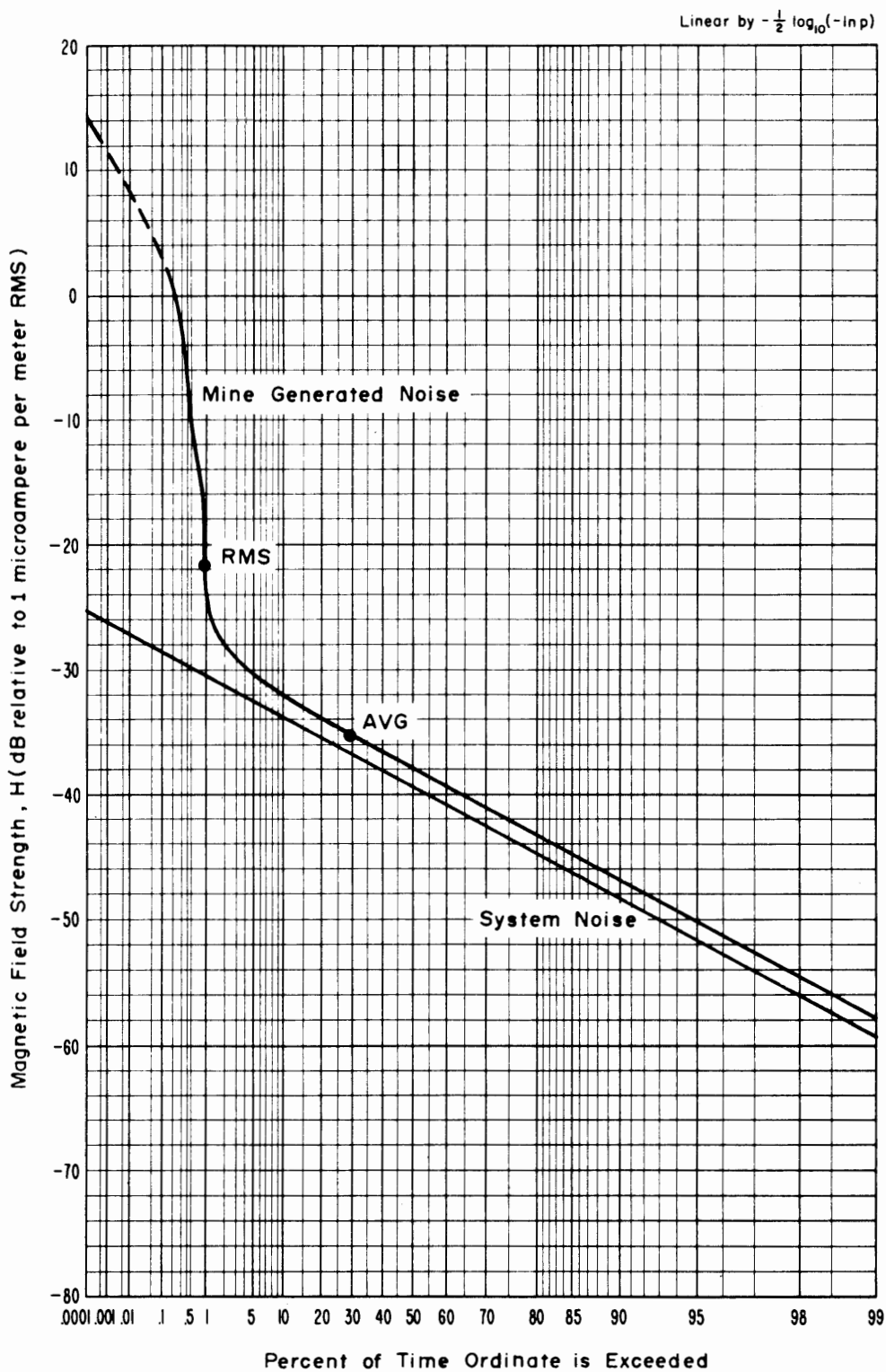


Figure 4-9 APD, 2 MHz, vertical component, 1.2 kHz predetection bandwidth, April 10, 1973, 2:20 p.m., McElroy Mine.

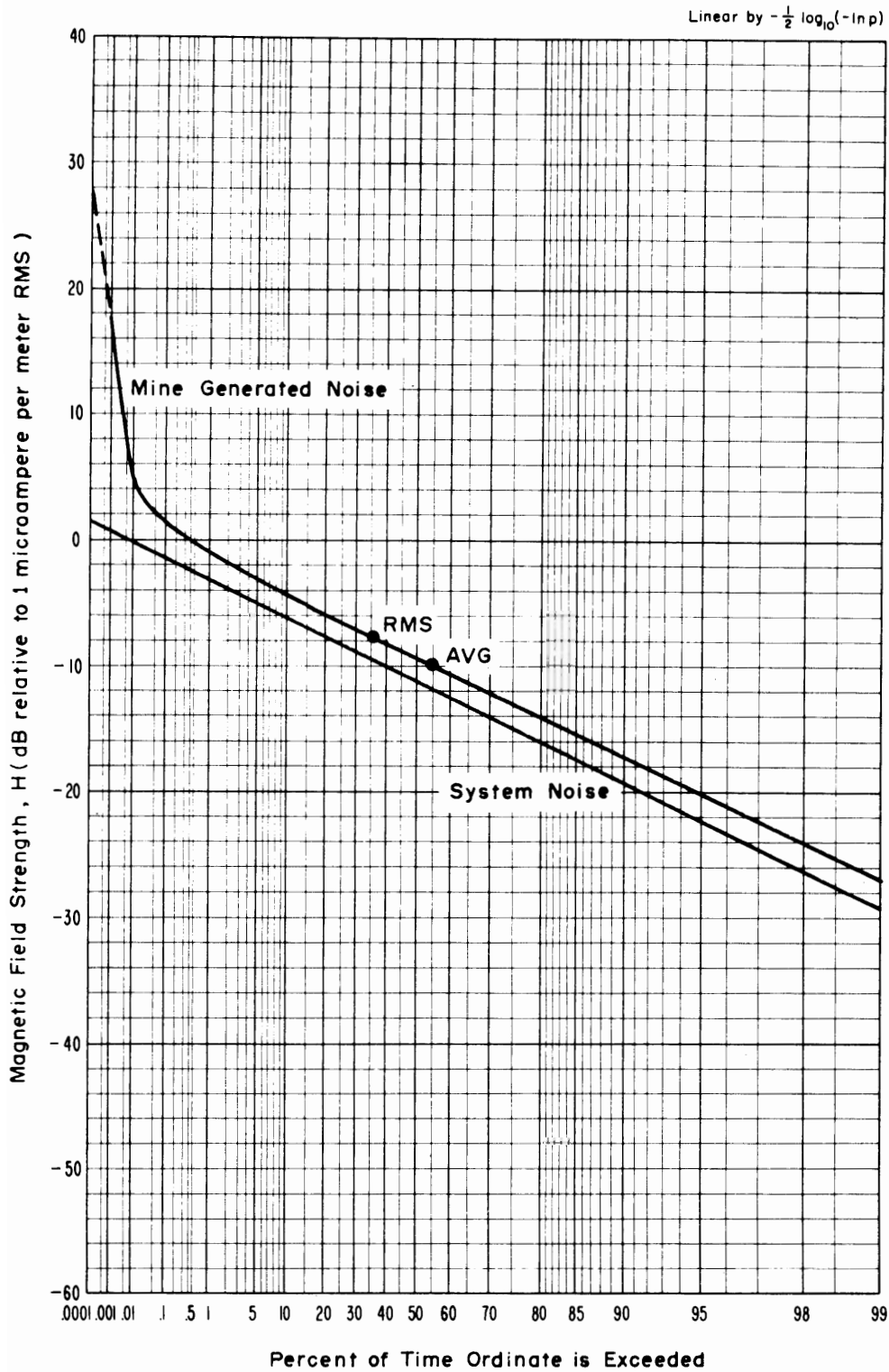


Figure 4-10 APD, 6 MHz, vertical component, 1.2 kHz predetection bandwidth, April 10, 1973, 3:25 p.m., McElroy Mine.

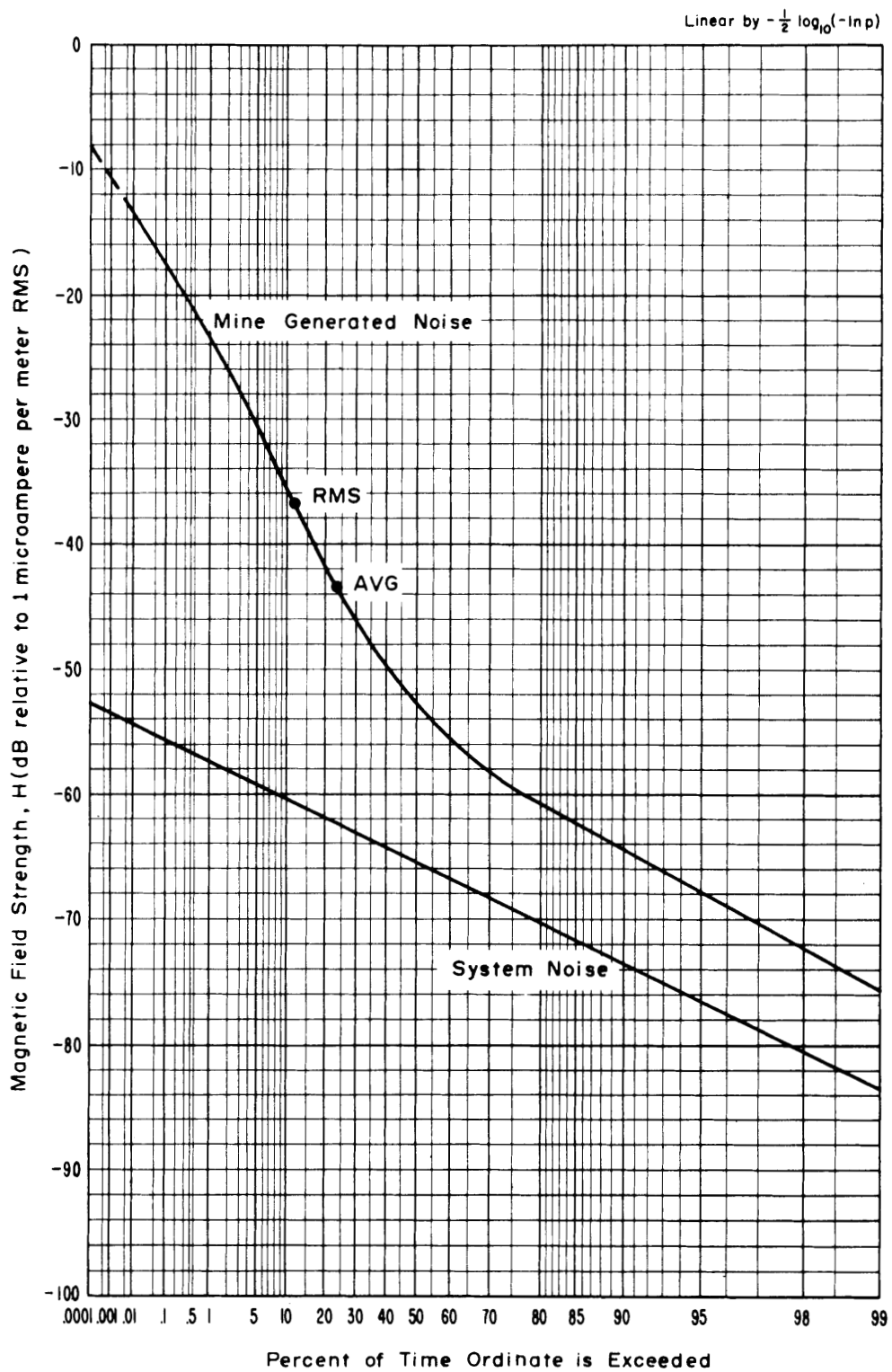


Figure 4-11 APD, 14 MHz, vertical component, 1.2 kHz predetection bandwidth, April 10, 1973, 5:30 p.m., McElroy Mine.

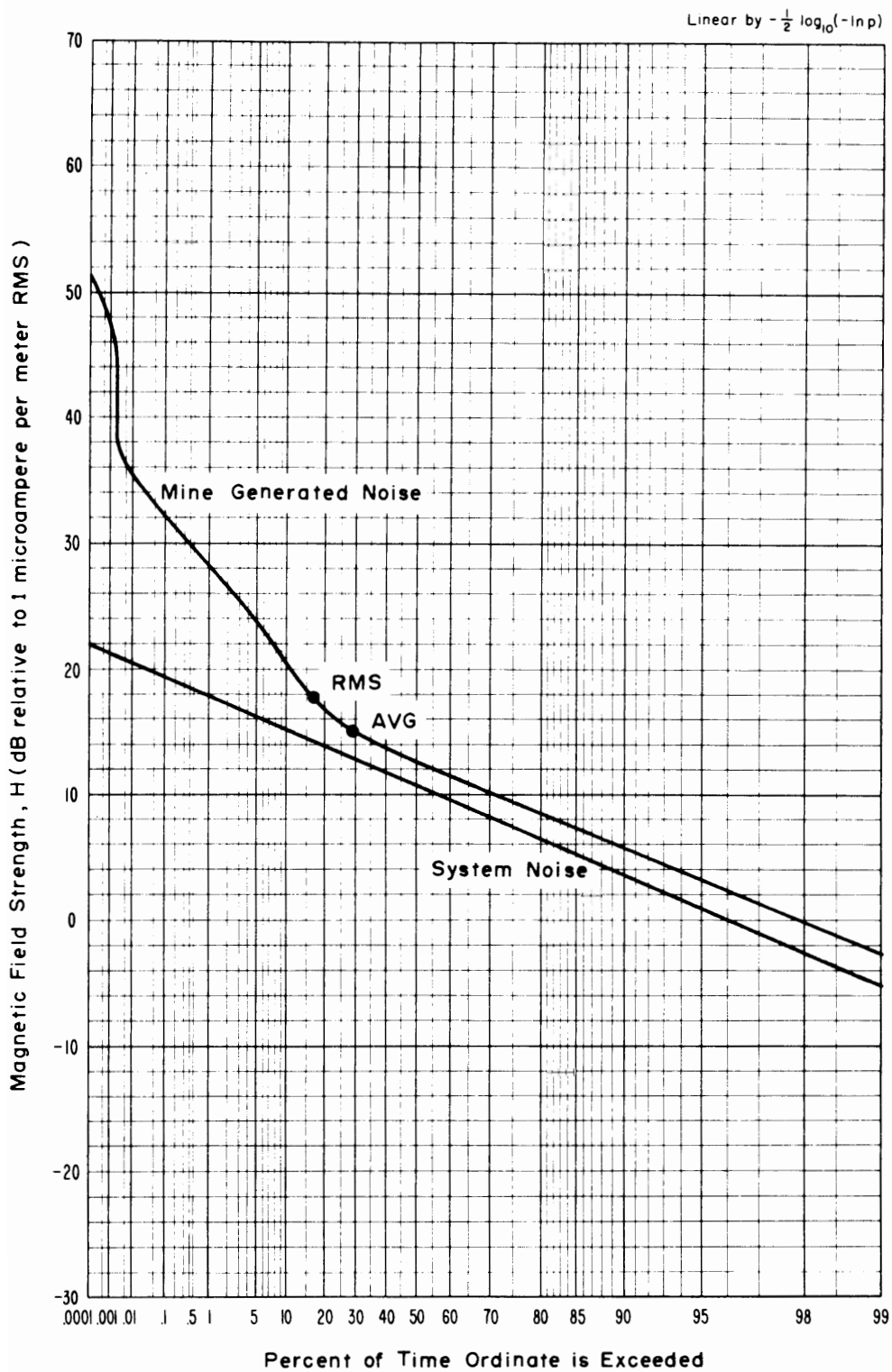


Figure 4-12 APD, 10 kHz, horizontal component (NE-SW), 1.0 kHz predetection bandwidth, April 10, 1973, 12:20 p.m., McElroy Mine.

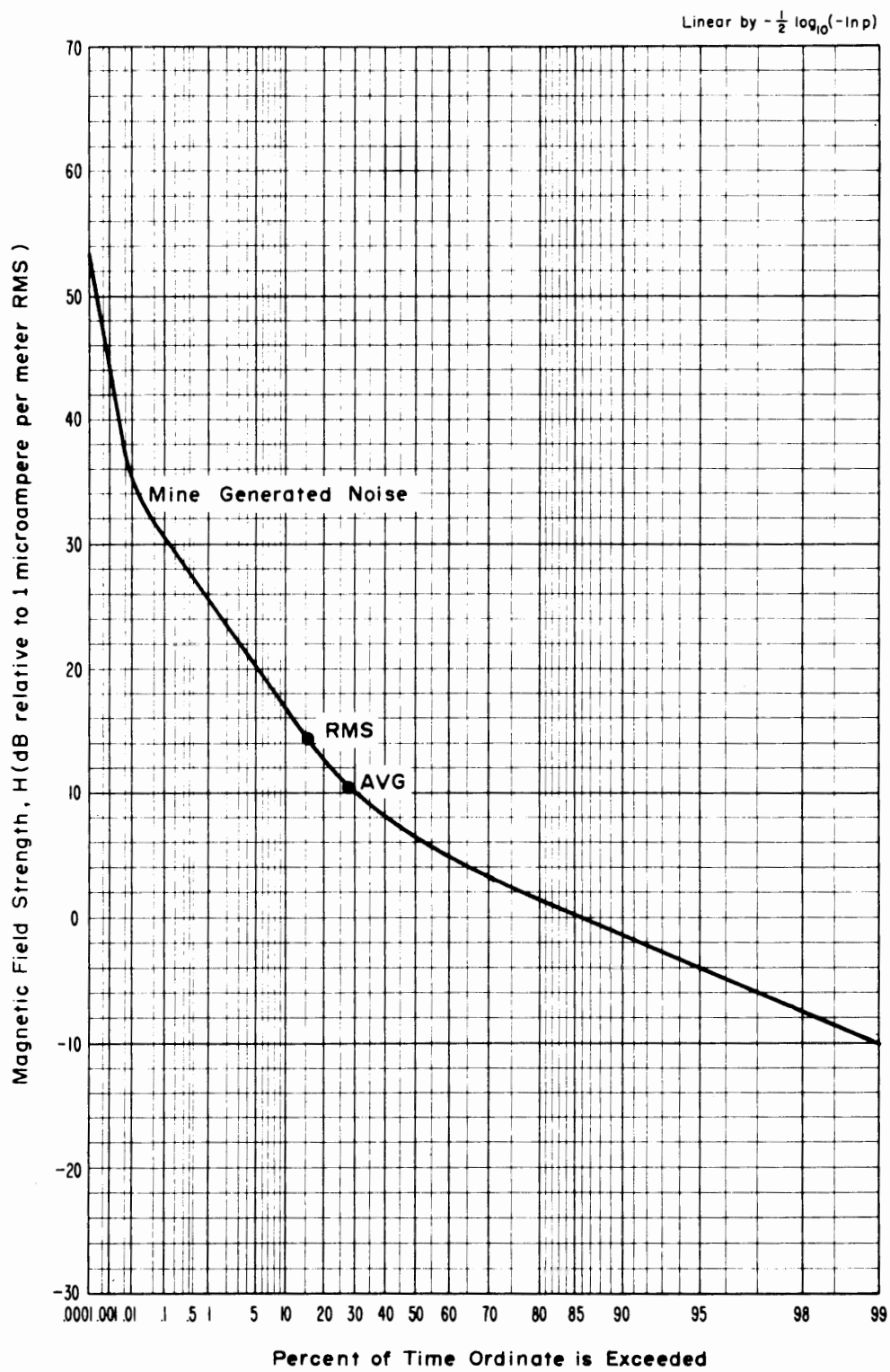


Figure 4-13 APD, 30 kHz, horizontal component, (NE-SW), 1.0 kHz predetection bandwidth, April 10, 1973, 1:50 p.m., McElroy Mine.

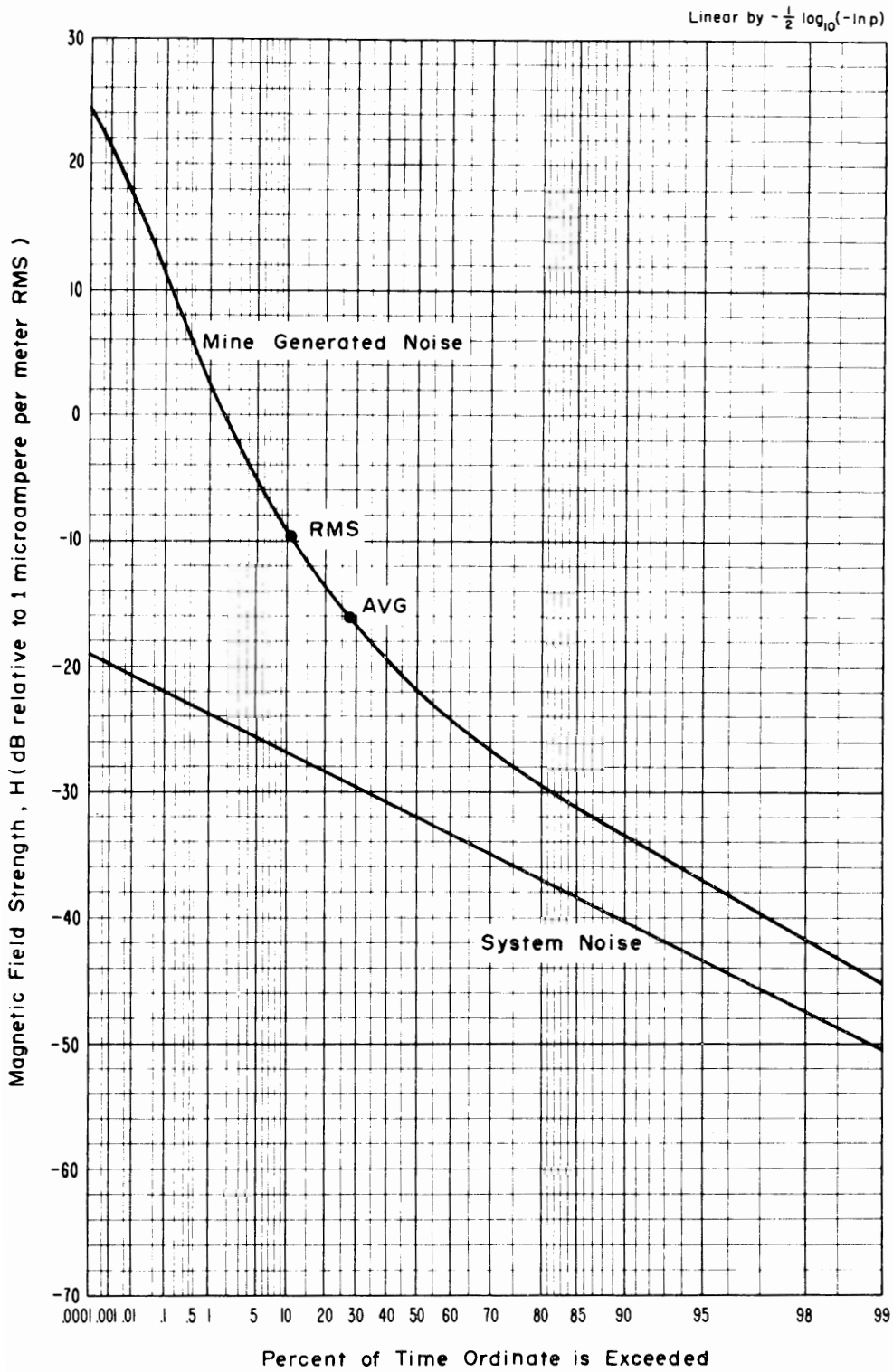


Figure 4-14 APD, 70 kHz, horizontal component (NE-SW), 1.0 kHz predetection bandwidth, April 10, 1973, 2:50 p.m., McElroy Mine.

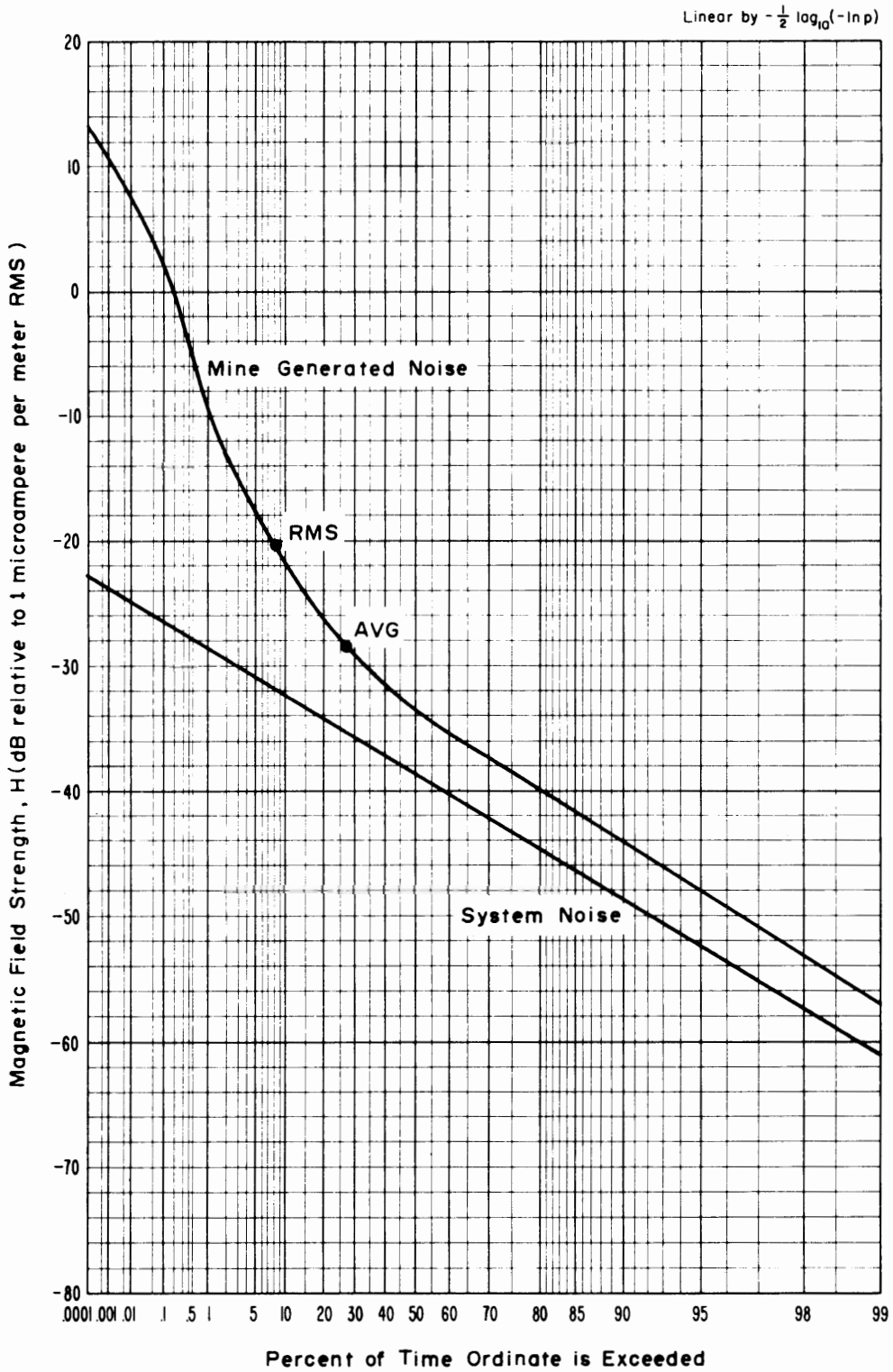


Figure 4-15 APD, 130 kHz, horizontal component (NE-SW), 1.0 kHz predetection bandwidth, April 10, 1973, 5:00 p.m., McElroy Mine.

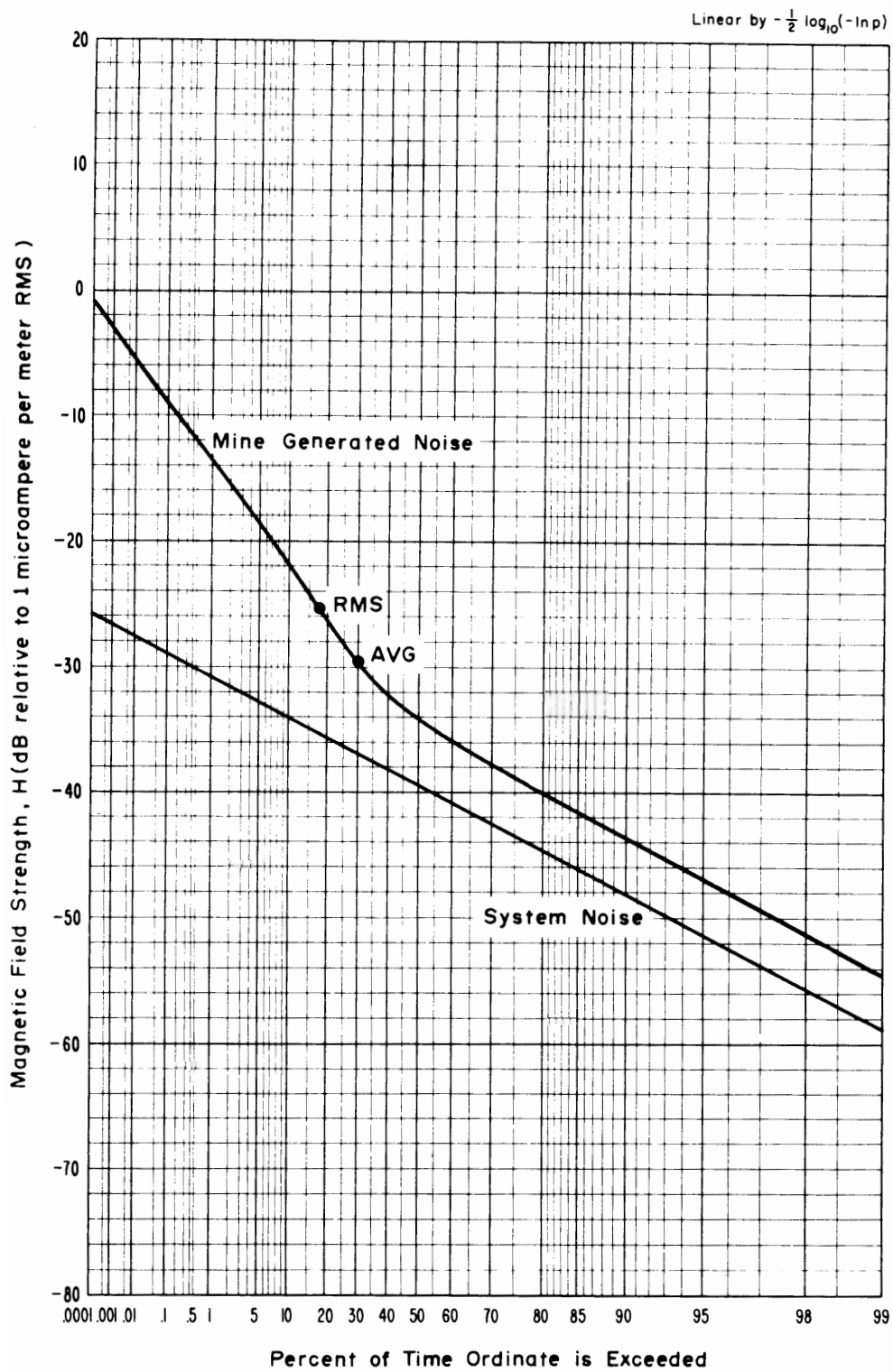


Figure 4-16 APD, 160 kHz, horizontal component(NE-SW), 1.0 kHz predetection bandwidth, April 10, 1973, 6:00 p.m., McElroy Mine.

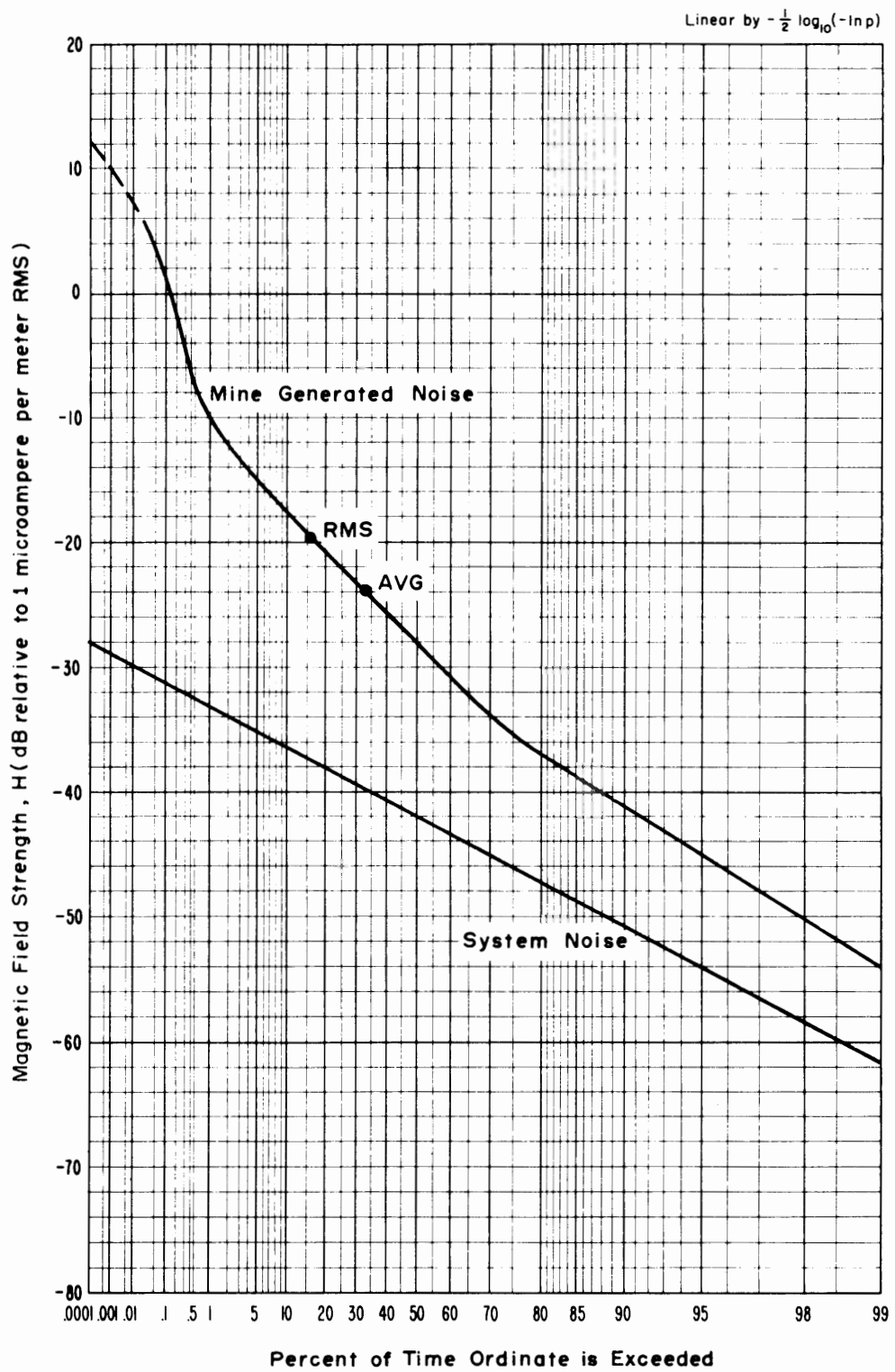


Figure 4-17 APD, 250 kHz, horizontal component (NE-SW), 1.0 kHz, predetection bandwidth, April 10, 1973, 7:00 p.m., McElroy Mine.

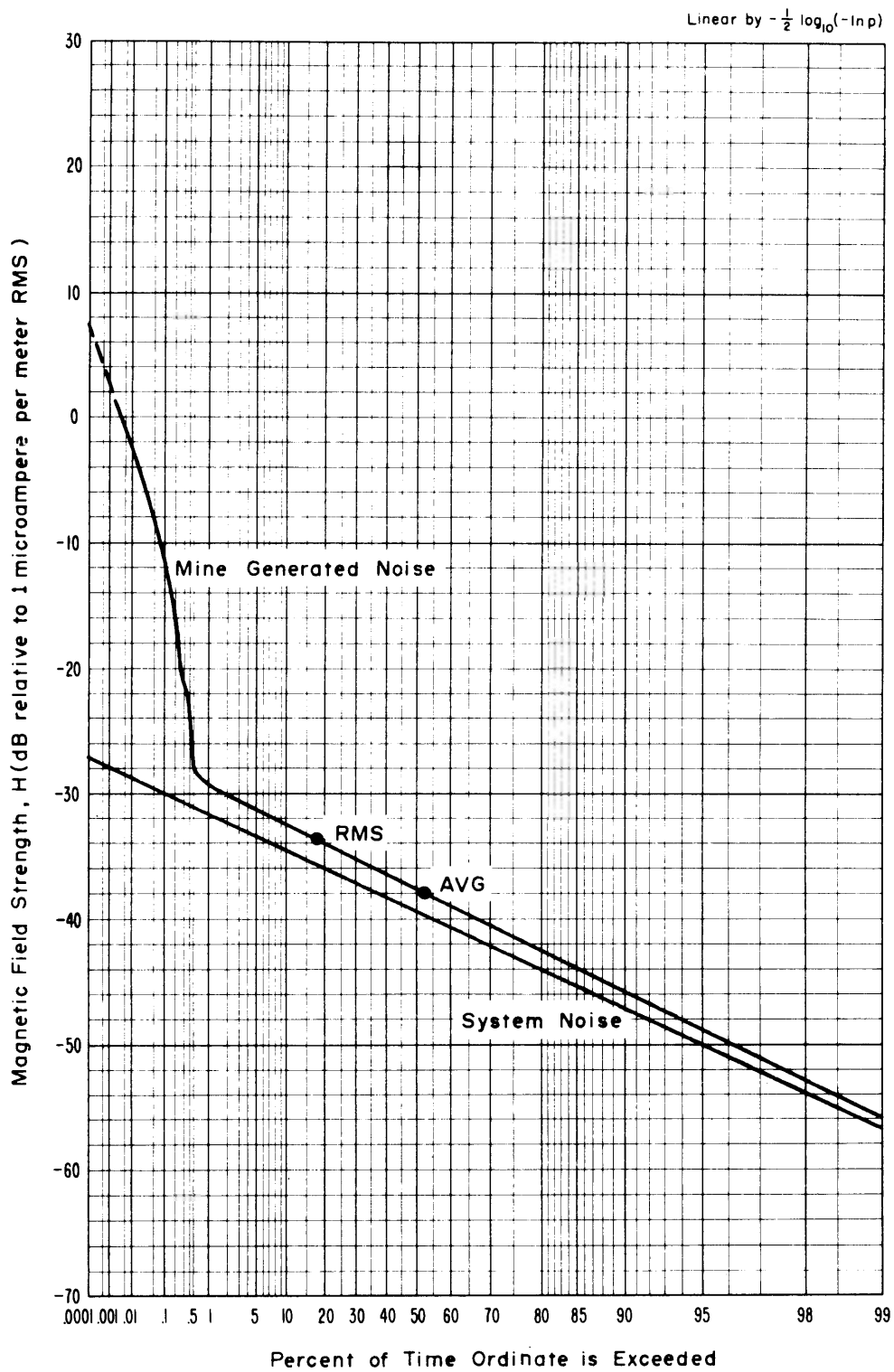


Figure 4-18 APD, 500 kHz, horizontal component (NE-SW), 1.2 kHz predetection bandwidth, April 10, 1973, 12:20 p.m., McElroy Mine.

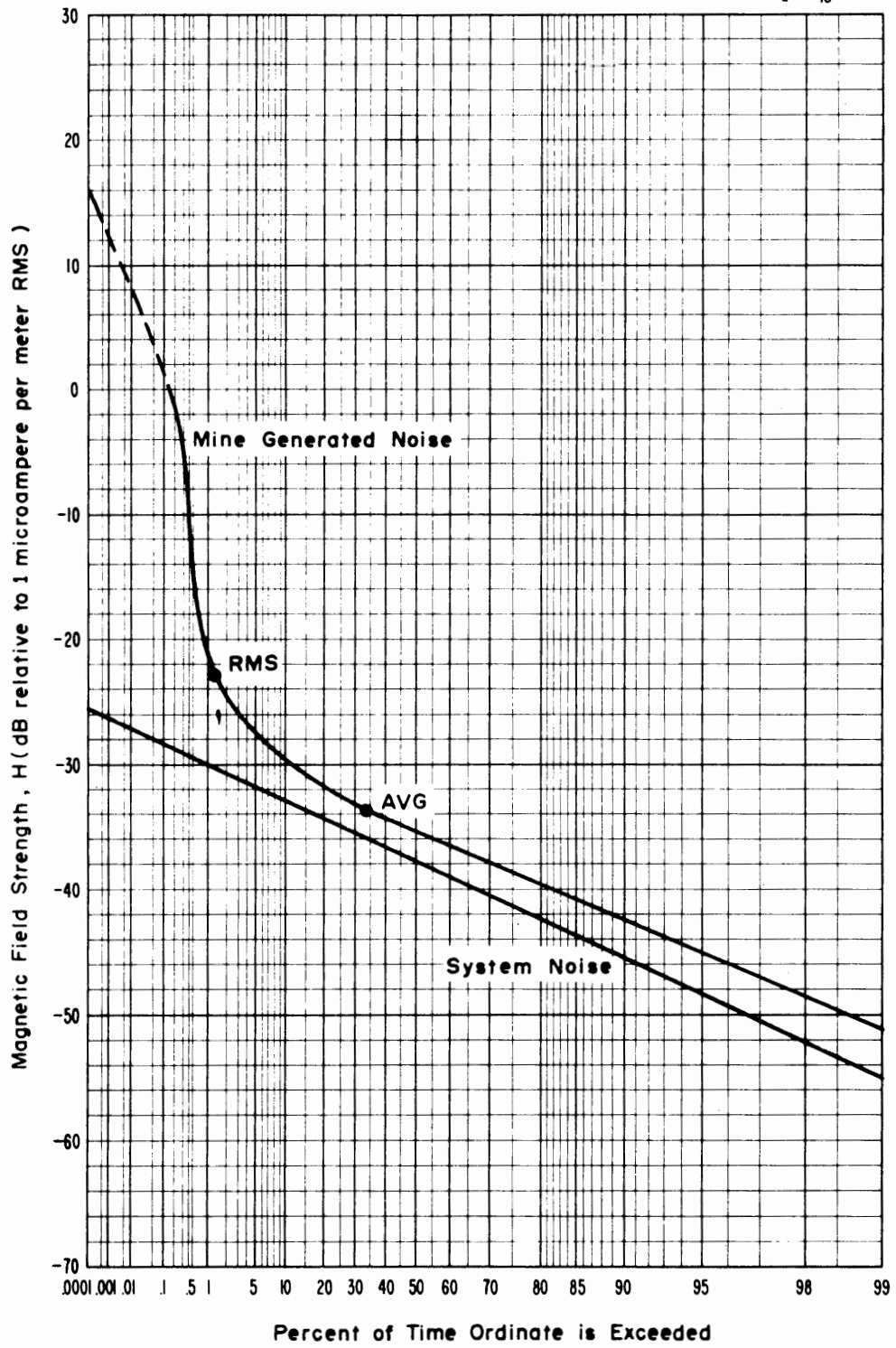


Figure 4-19 APD, 1 MHz, horizontal component (NE-SW), 1.2 kHz predetection bandwidth, April 10, 1973, 1:50 p.m., McElroy Mine.

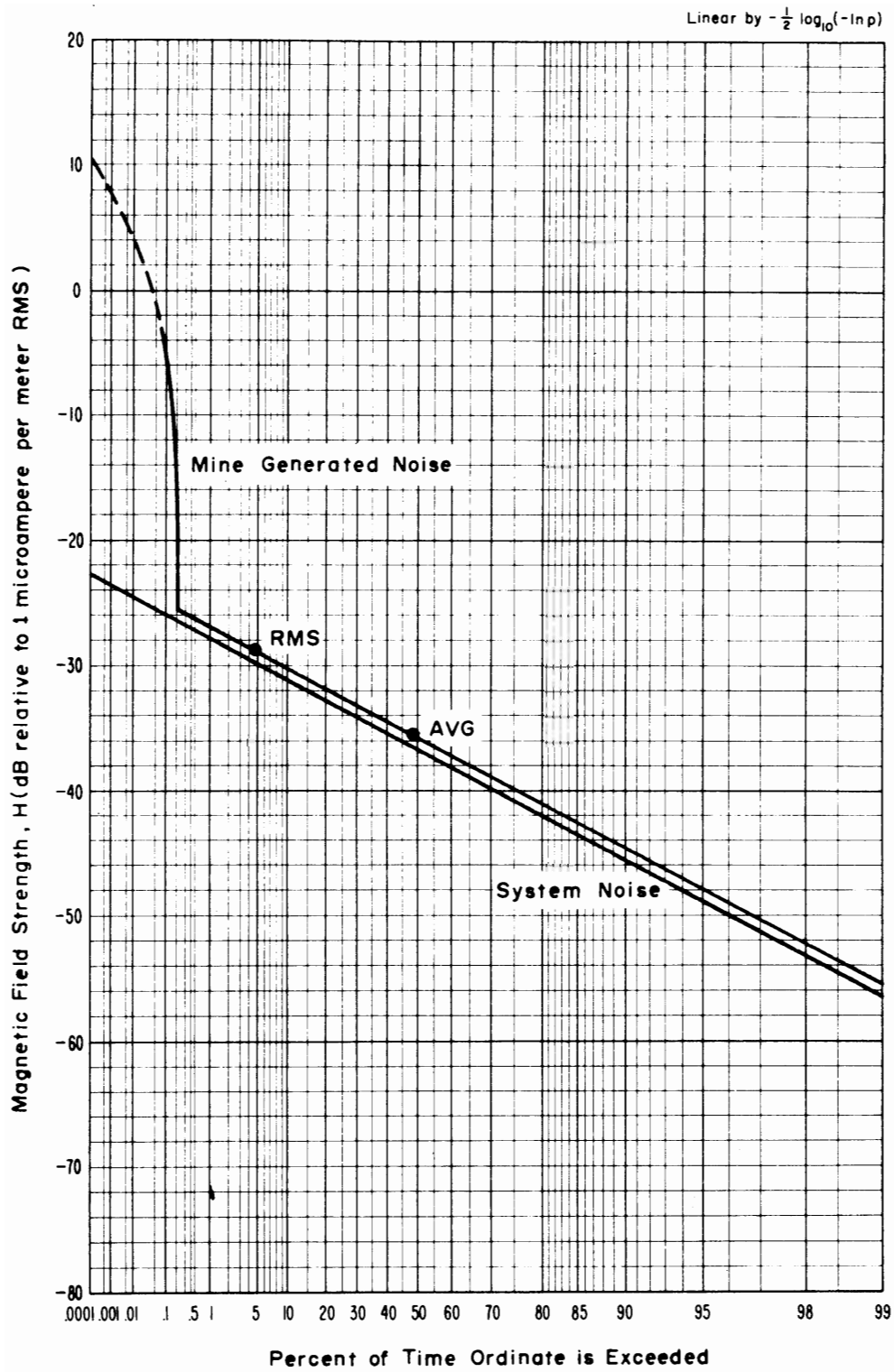


Figure 4-20 APD, 2 MHz, horizontal component (NE-SW), 1.2 kHz predetection bandwidth, April 10, 1973, 2:50 p.m., McElroy Mine.

Linear by $-\frac{1}{2} \log_{10}(-\ln p)$

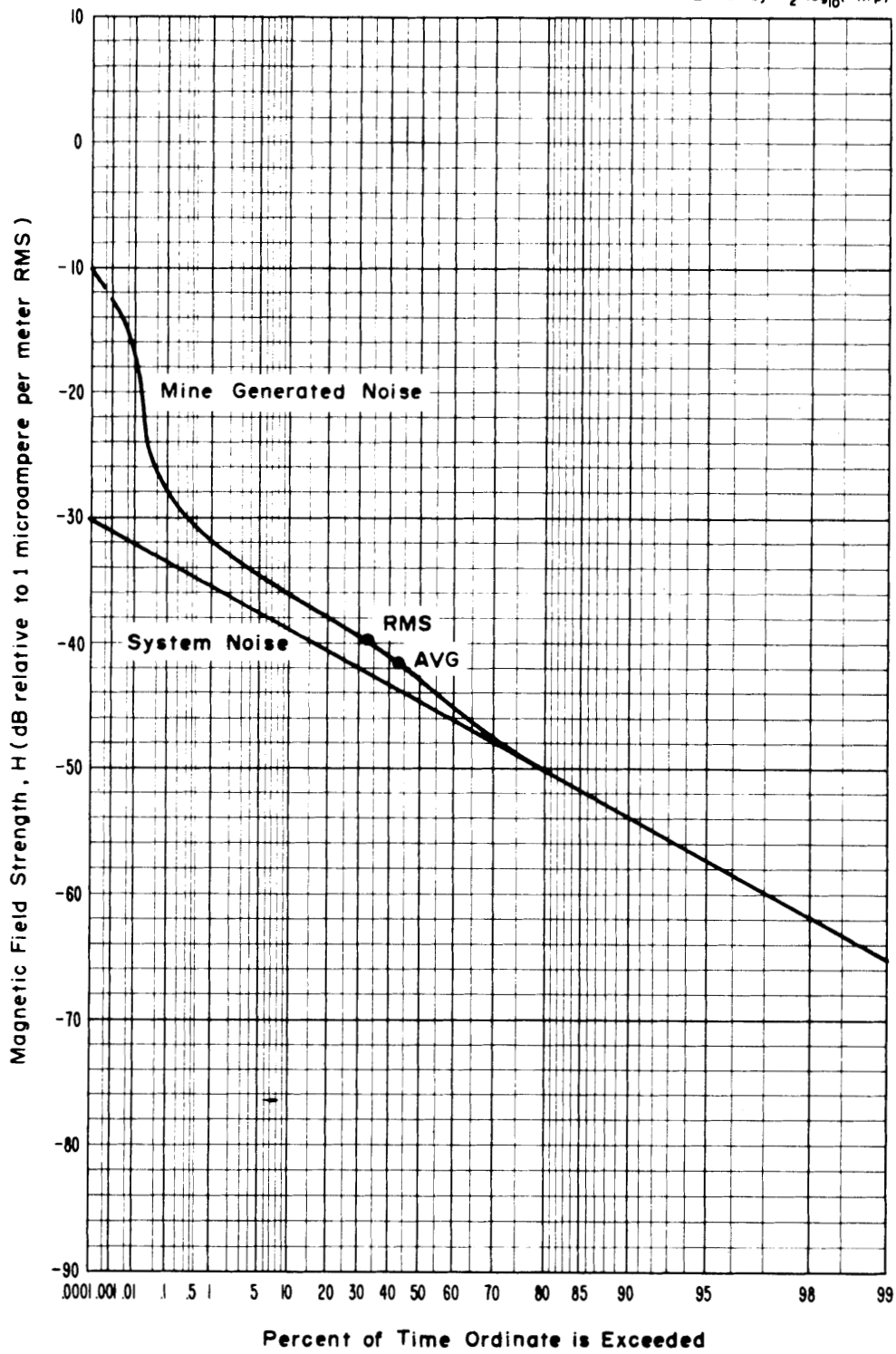


Figure 4-21 APD, 6 MHz, horizontal component (NE-SW), 1.2 kHz predetection bandwidth, April 10, 1973, 5:00 p.m., McElroy Mine.

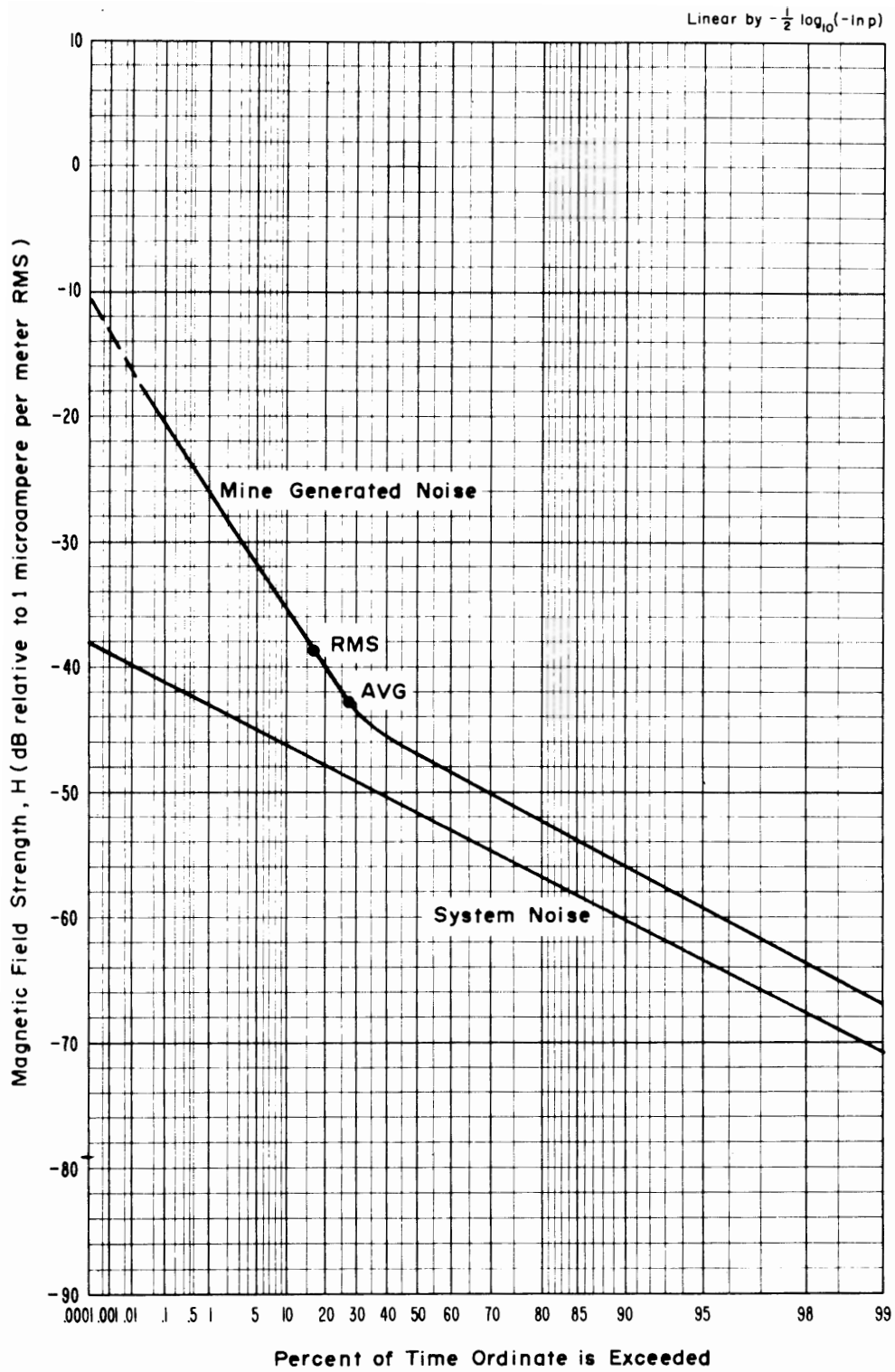


Figure 4-22 APD, 14 MHz, horizontal component (NE-SW), 1.2 kHz predetection bandwidth, April 10, 1973, 6:00 p.m., McElroy Mine.

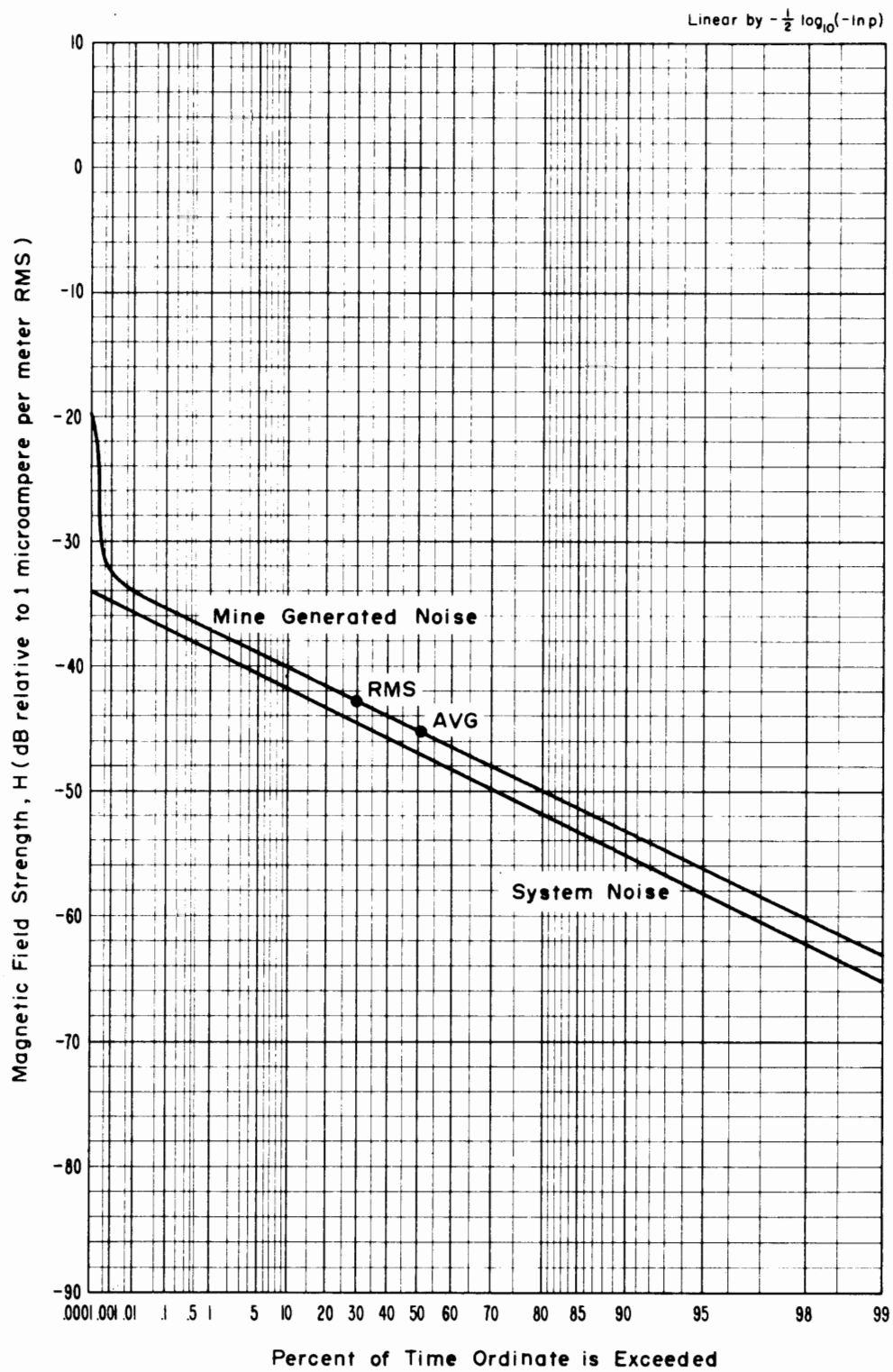


Figure 4-23 APD, 32 MHz, horizontal component (NE-SW), 1.2 kHz predetection bandwidth, April 10, 1973, 7:00 p.m., McElroy Mine.

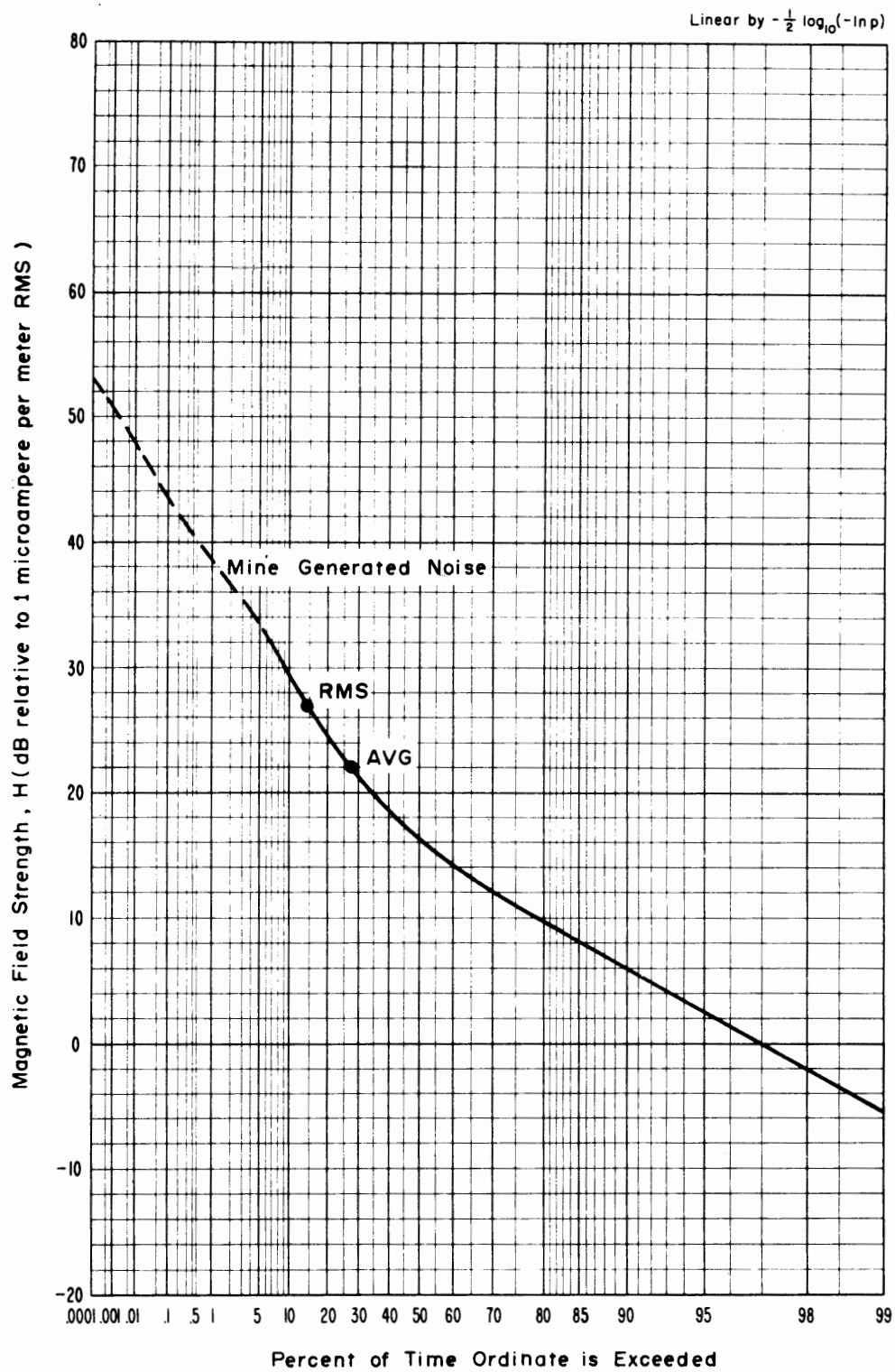


Figure 4-24 APD, 10 kHz, vertical component, 1.0 kHz predetection bandwidth, April 10, 1973, 4:00 p.m., quiet time measurements, McElroy Mine.

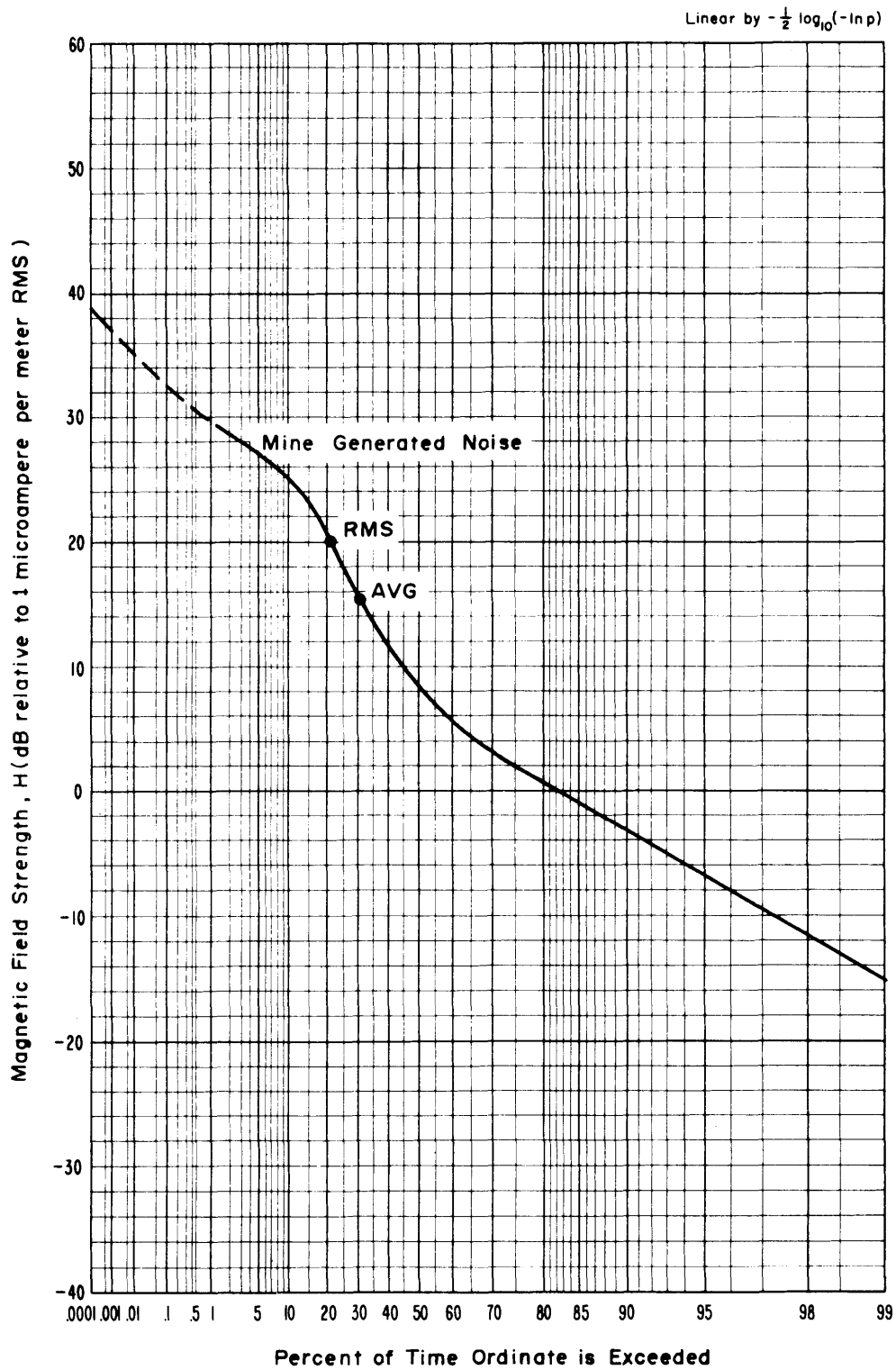


Figure 4-25 APD, 30 kHz, vertical component, 1.0 kHz predetection bandwidth, April 10, 1973, 4:10 p.m., quiet time measurements, McElroy Mine.

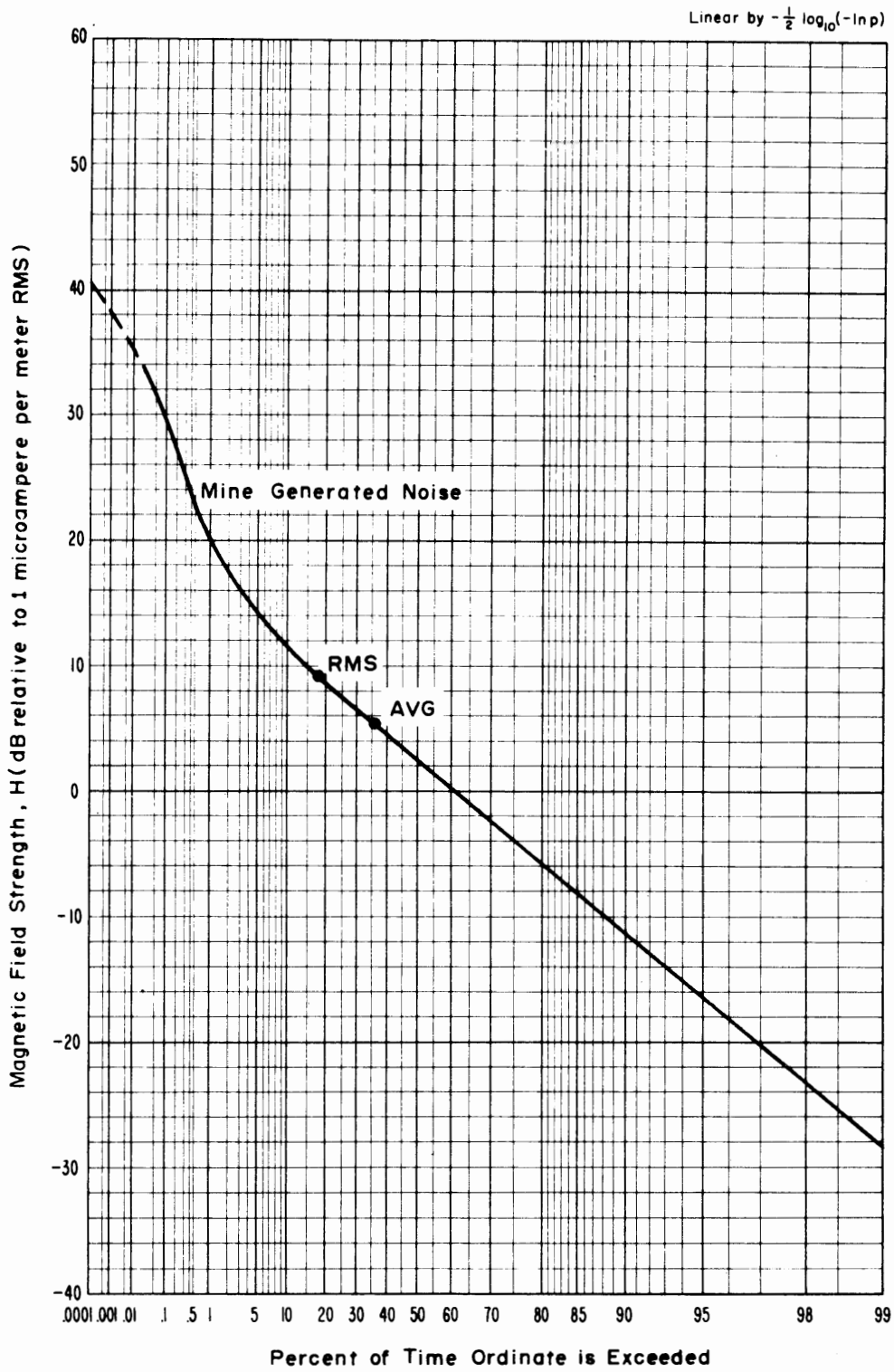


Figure 4-26 APD, 70 kHz, vertical component, 1.0 kHz predetection bandwidth, April 10, 1973, quiet time measurements, McElroy Mine.

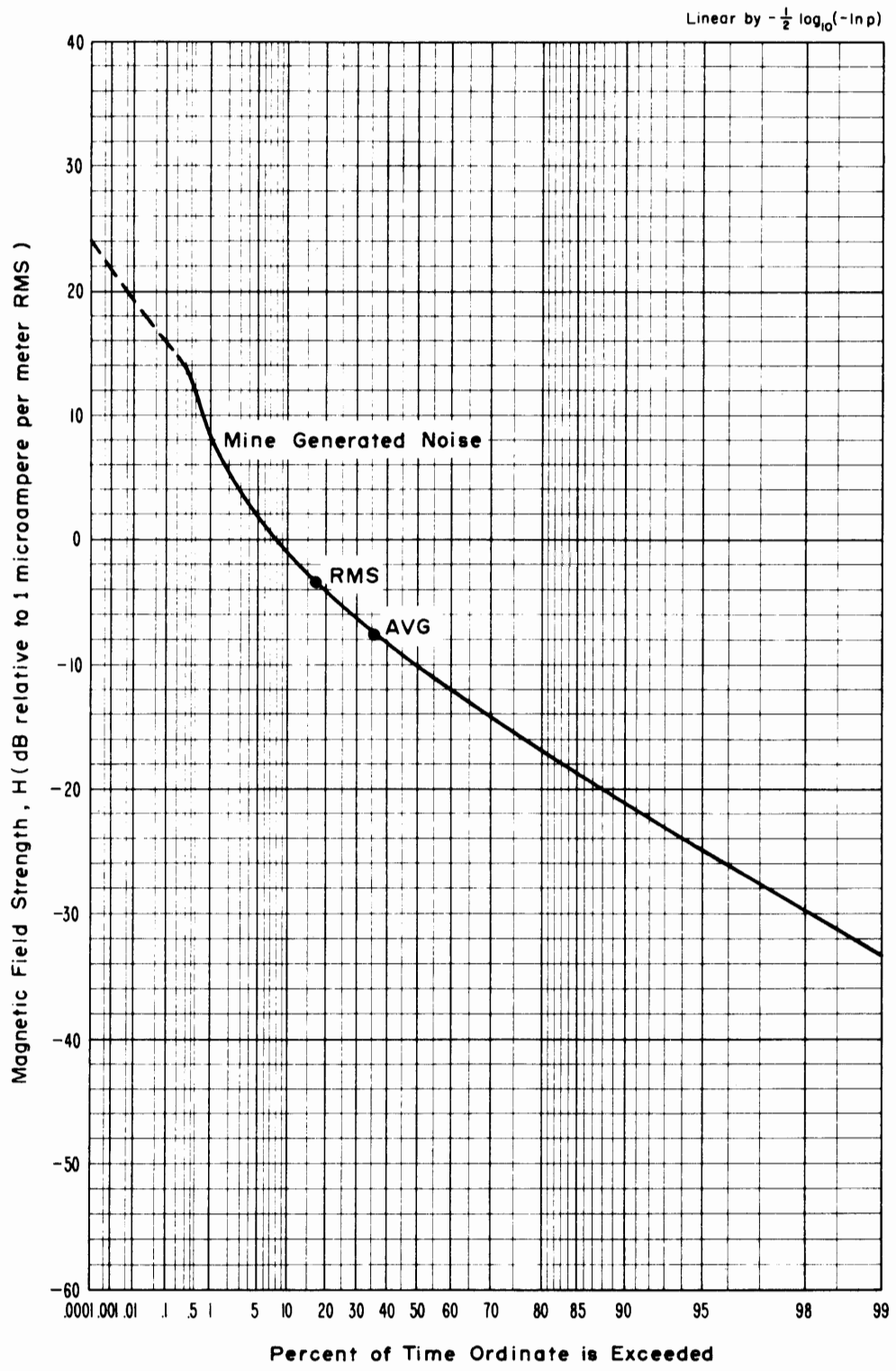


Figure 4-27 APD, 130 kHz, vertical component, 1.0 kHz predetection bandwidth, April 10, 1973, 4:30 p.m., quiet time measurement, McElroy Mine.

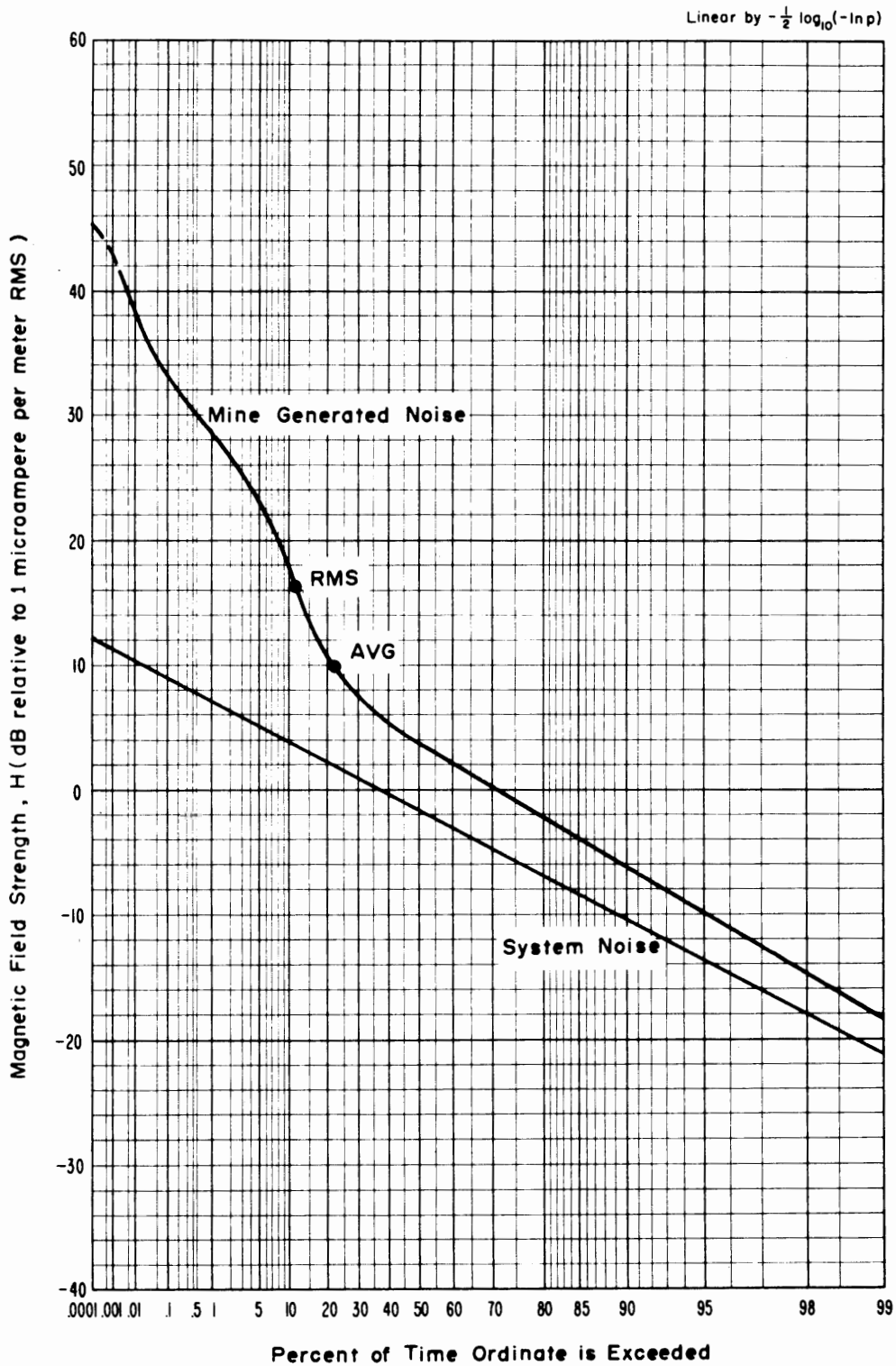


Figure 4-28 APD, 10 kHz, vertical component, 1.0 kHz predetection bandwidth, April 10, 1973, 1:00 p.m., McElroy Mine.

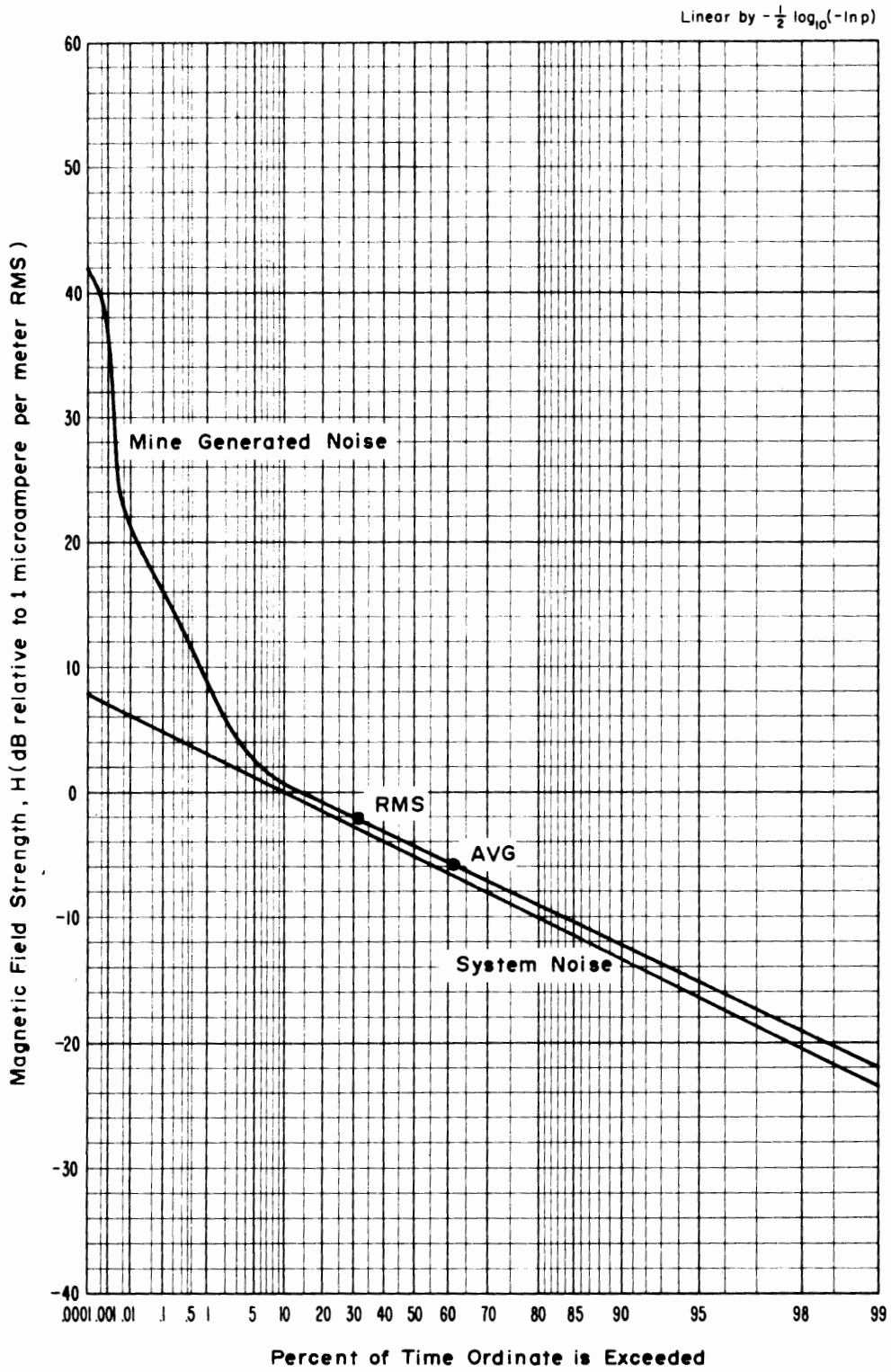


Figure 4-29 APD, 30 kHz, vertical component, 1.0 kHz predetection bandwidth, April 10, 1973, 2:30 p.m., McElroy Mine.

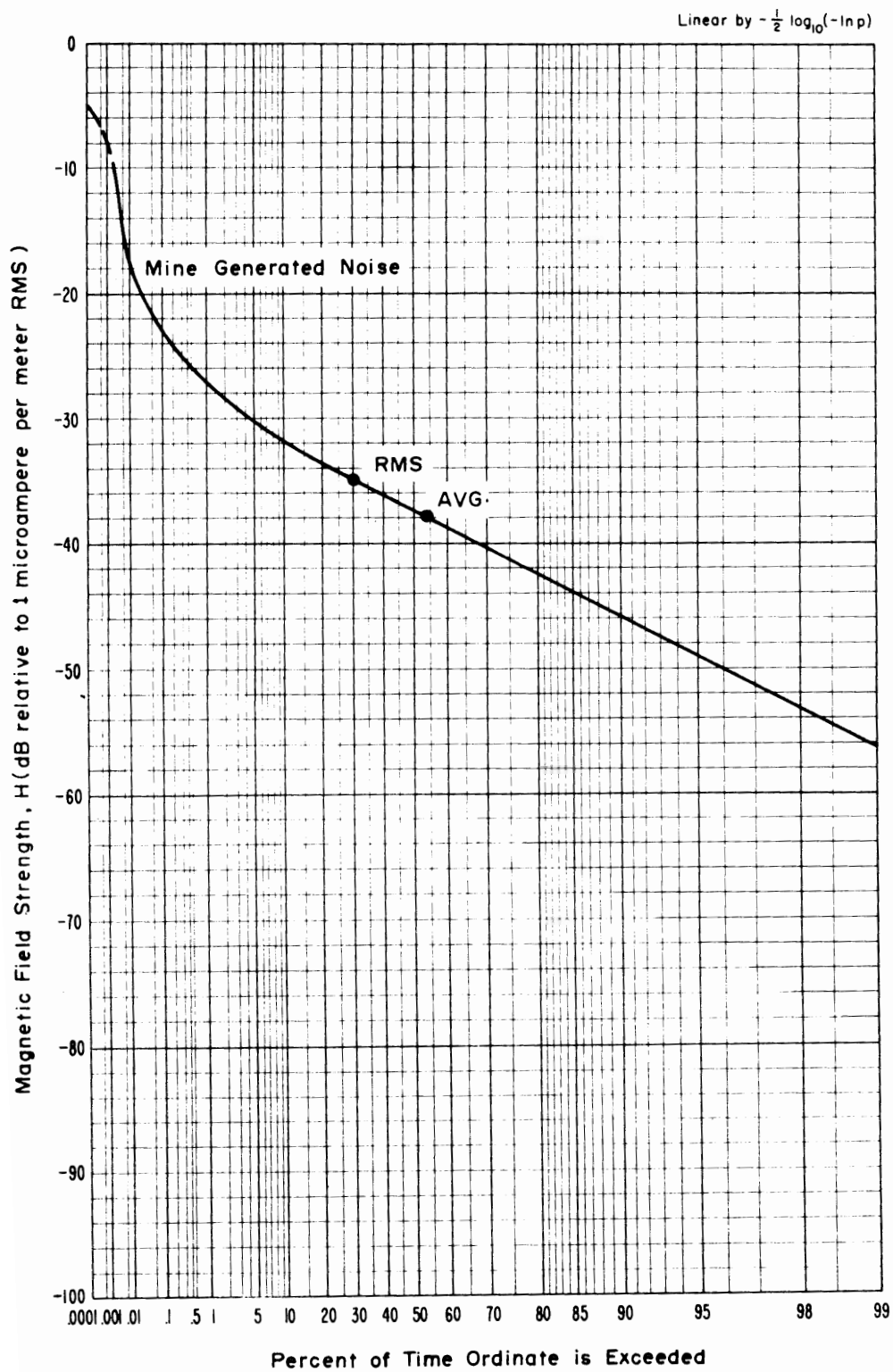


Figure 4-30 APD, 70 kHz, vertical component, 1.0 kHz predetection bandwidth, April 10, 1973, 5:15 p.m., McElroy Mine.

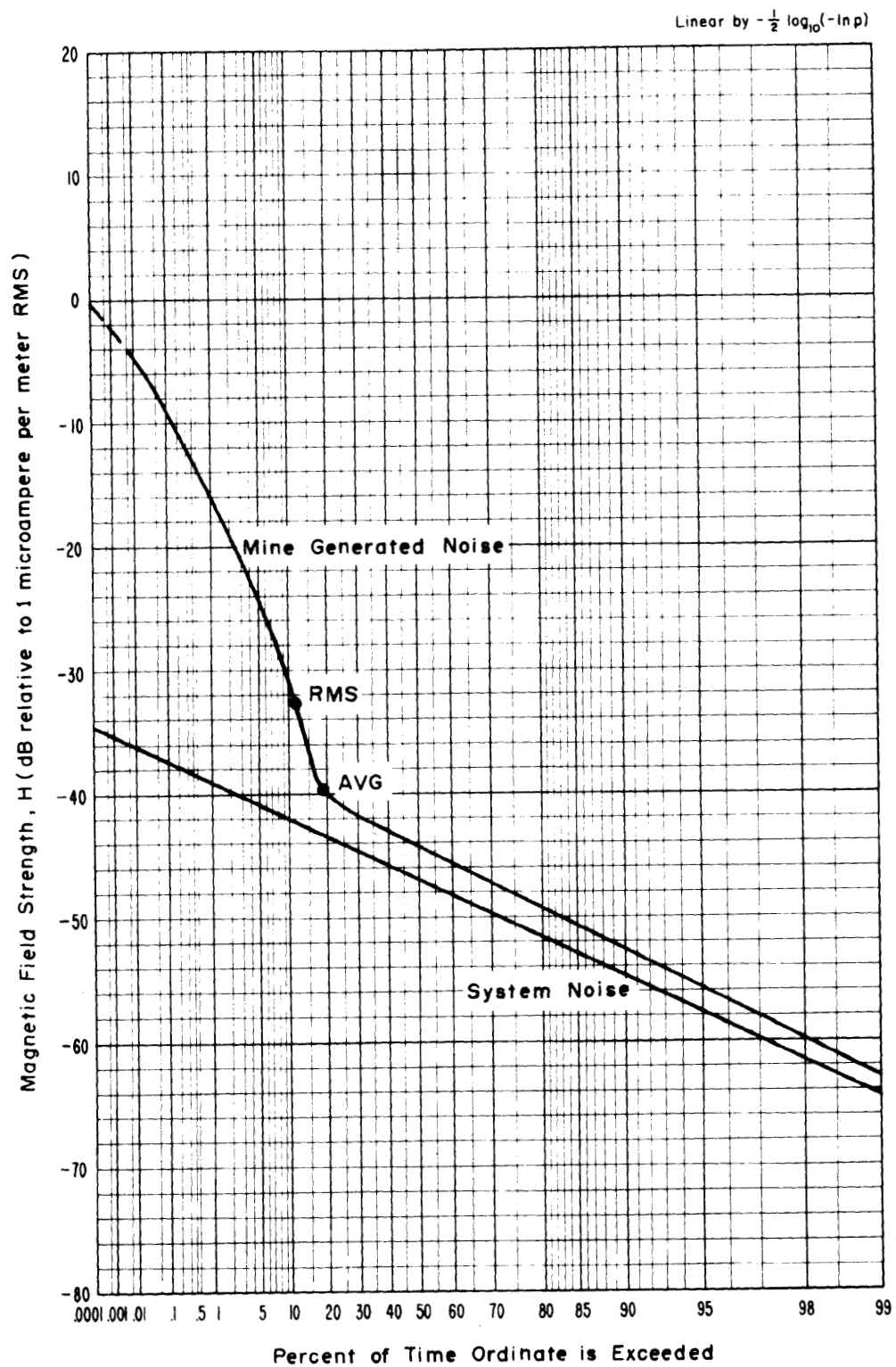


Figure 4-31 APD, 130 kHz, vertical component, 1.0 kHz predetection bandwidth, April 10, 1973, 7:30 p.m., McElroy Mine.

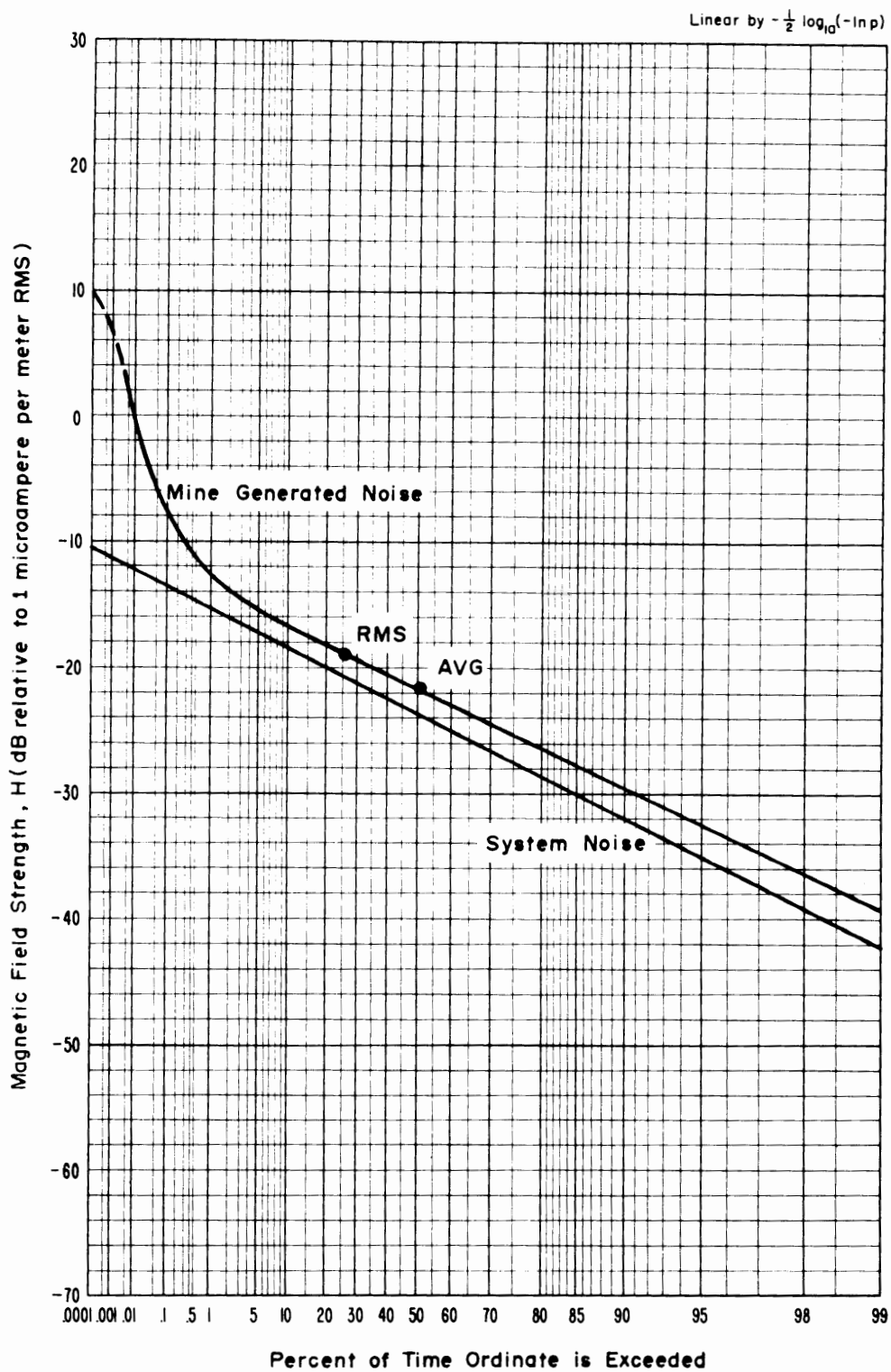


Figure 4-32 APD, 160 kHz, vertical component, 1.0 kHz predetection bandwidth, April 10, 1973, 6:45 p.m., McElroy Mine.

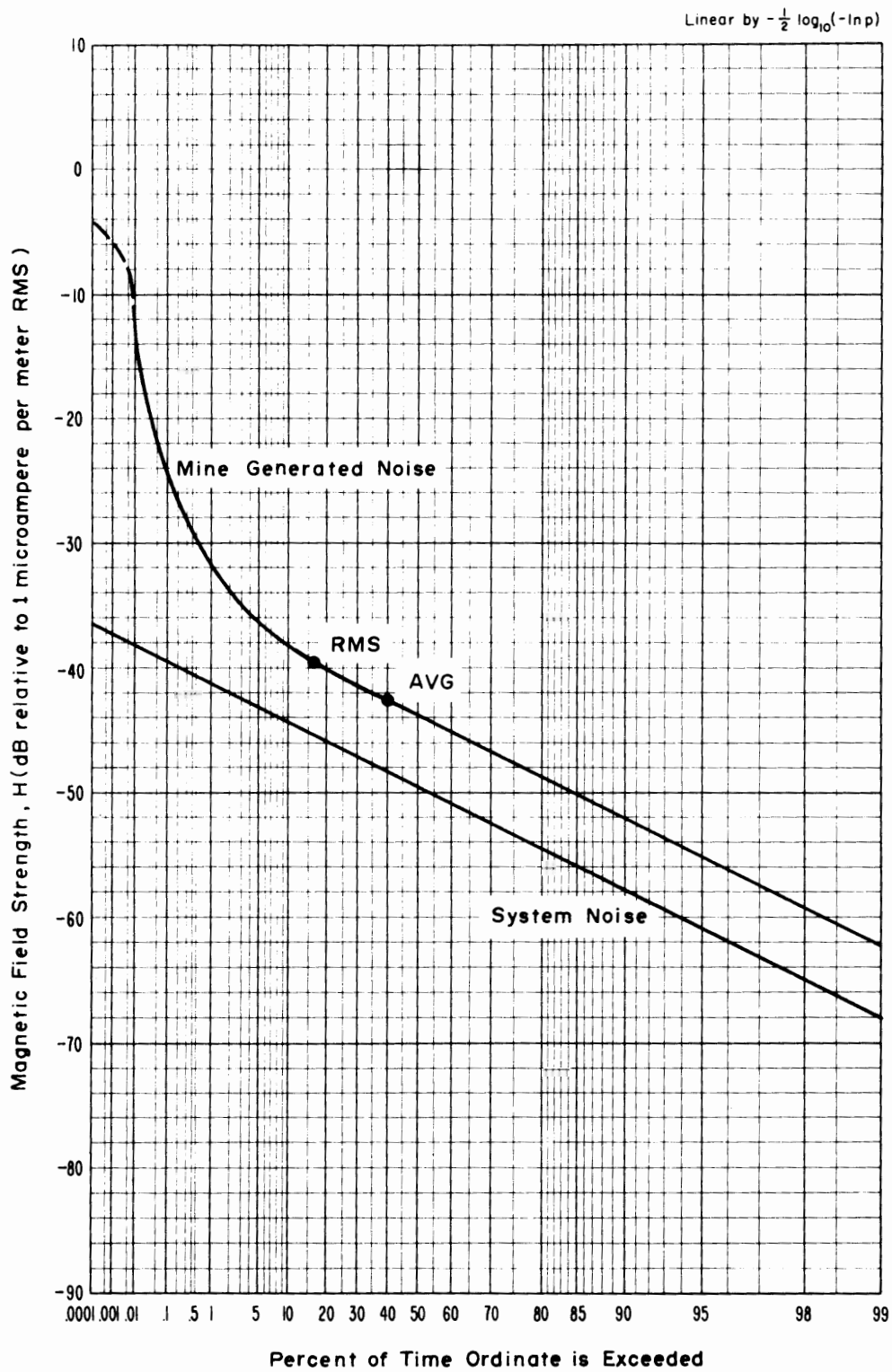


Figure 4-33 APD, 250 kHz, vertical component, 1.2 kHz predetection bandwidth, April 10, 1973, 7:30 p.m., McElroy Mine.

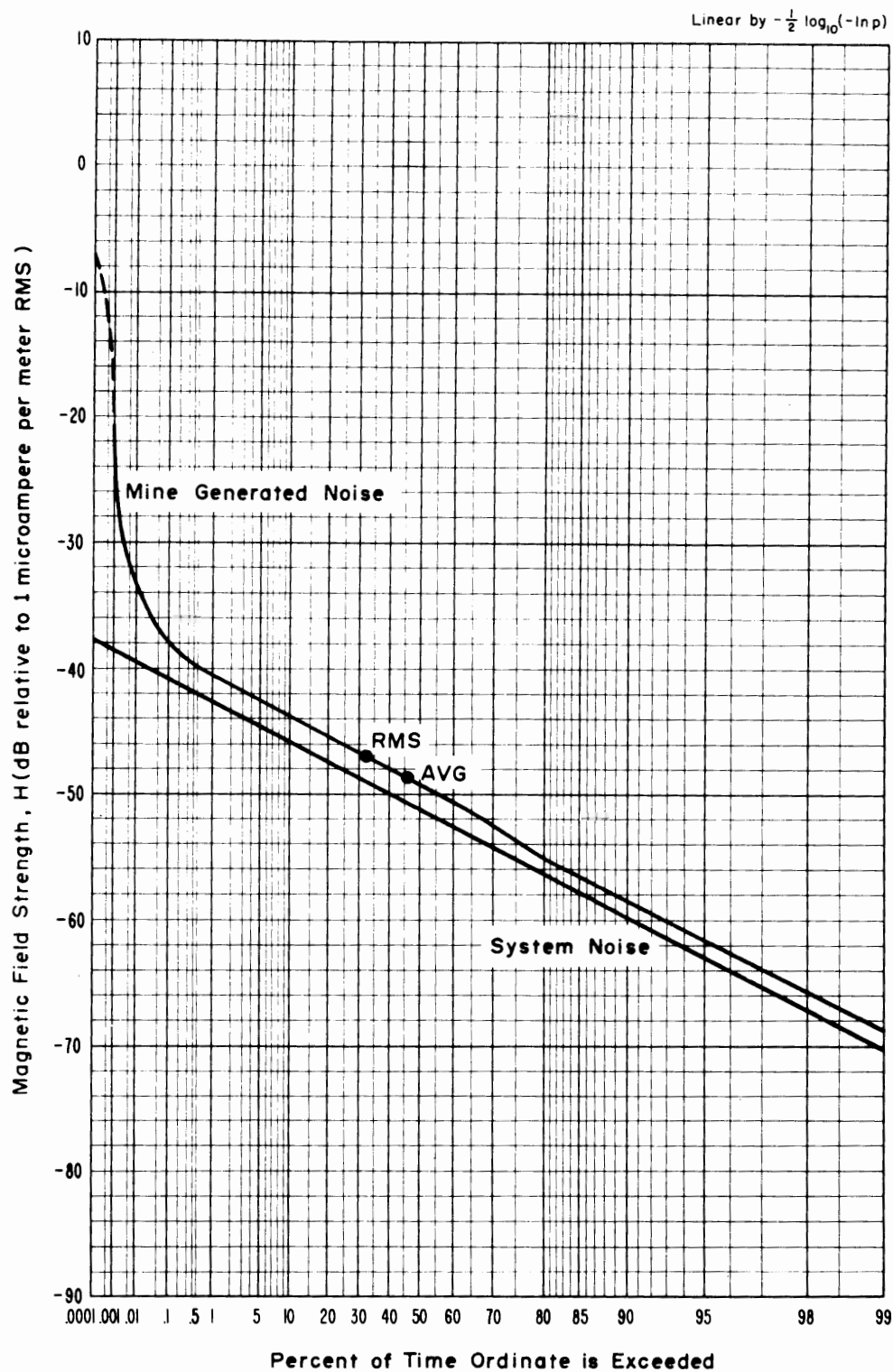


Figure 4-34 APD, 500 kHz, vertical component, 1.2 kHz predetection bandwidth, April 10, 1973, 1:00 p.m., McElroy Mine.

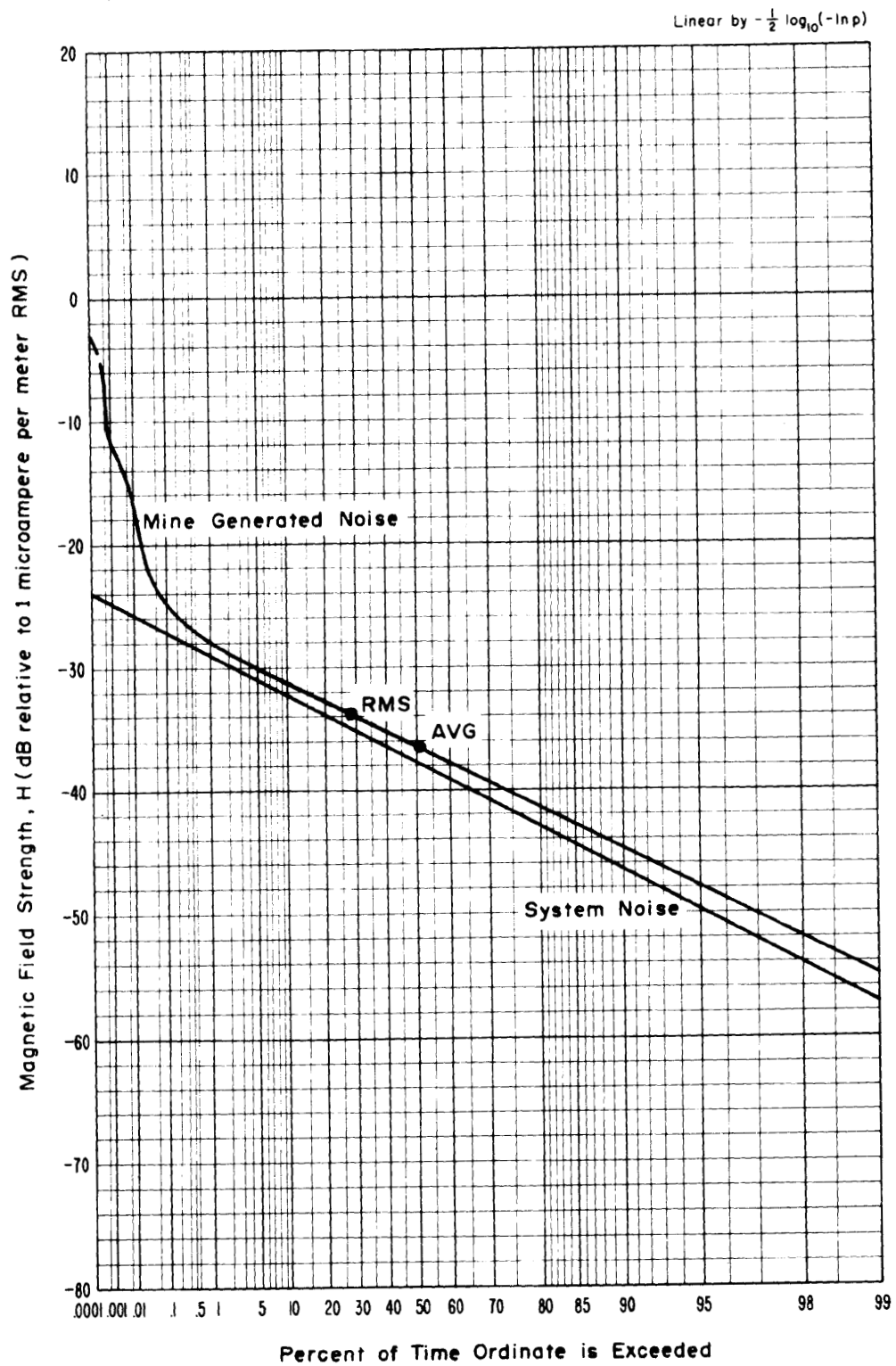


Figure 4-35 APD, 1 MHz, vertical component, 1.2 kHz predetection bandwidth, April 10, 1973, 2:30 p.m., McElroy Mine.

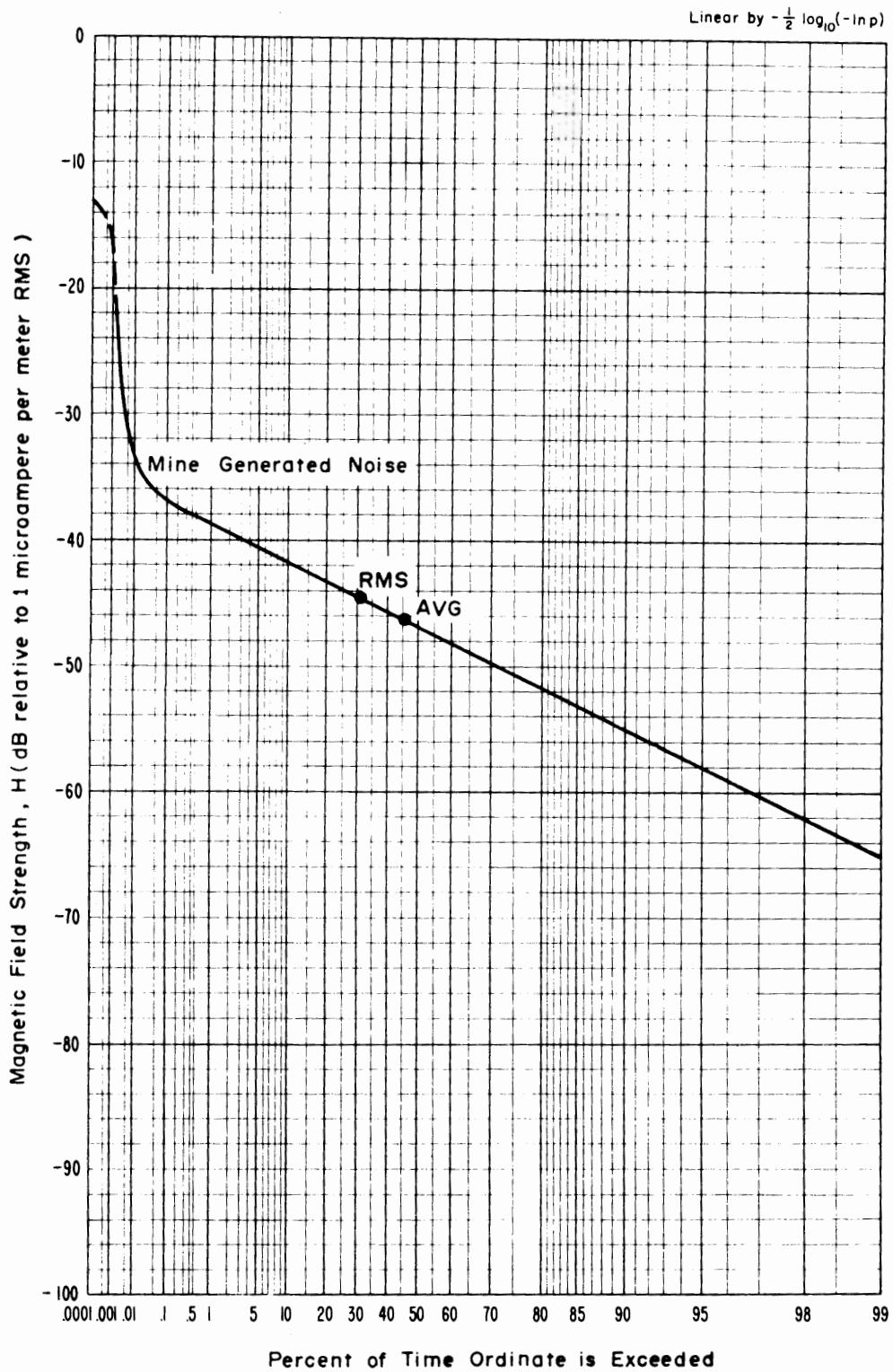


Figure 4-36 APD, 2 MHz, vertical component, 1.2 kHz predetection bandwidth, April 10, 1973, 5:15 p.m., McElroy Mine.

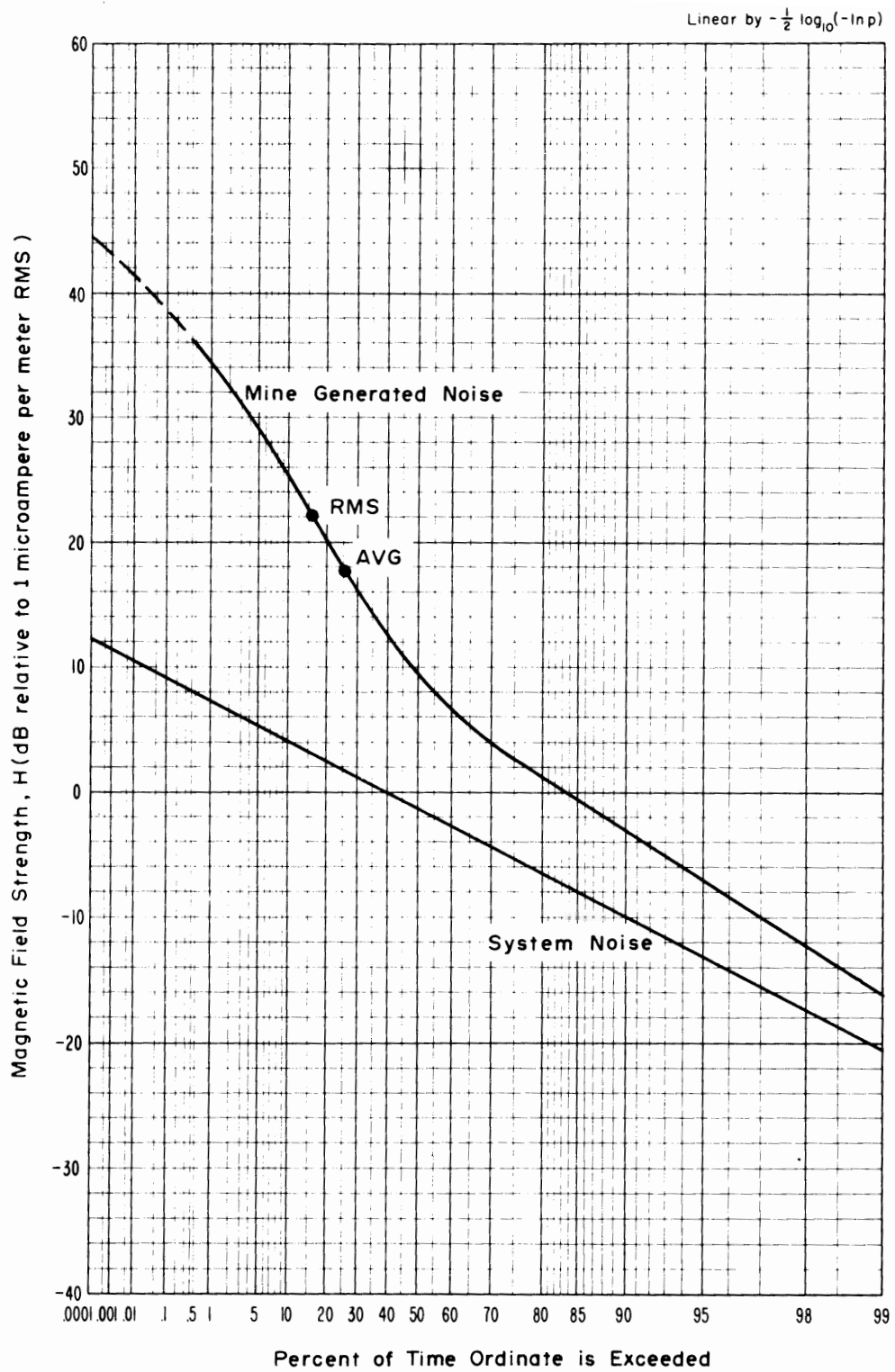


Figure 4-37 APD, 10 kHz, horizontal component (N-S), 1.0 kHz predetection bandwidth, April 10, 1973, 1:30 p.m., McElroy Mine.

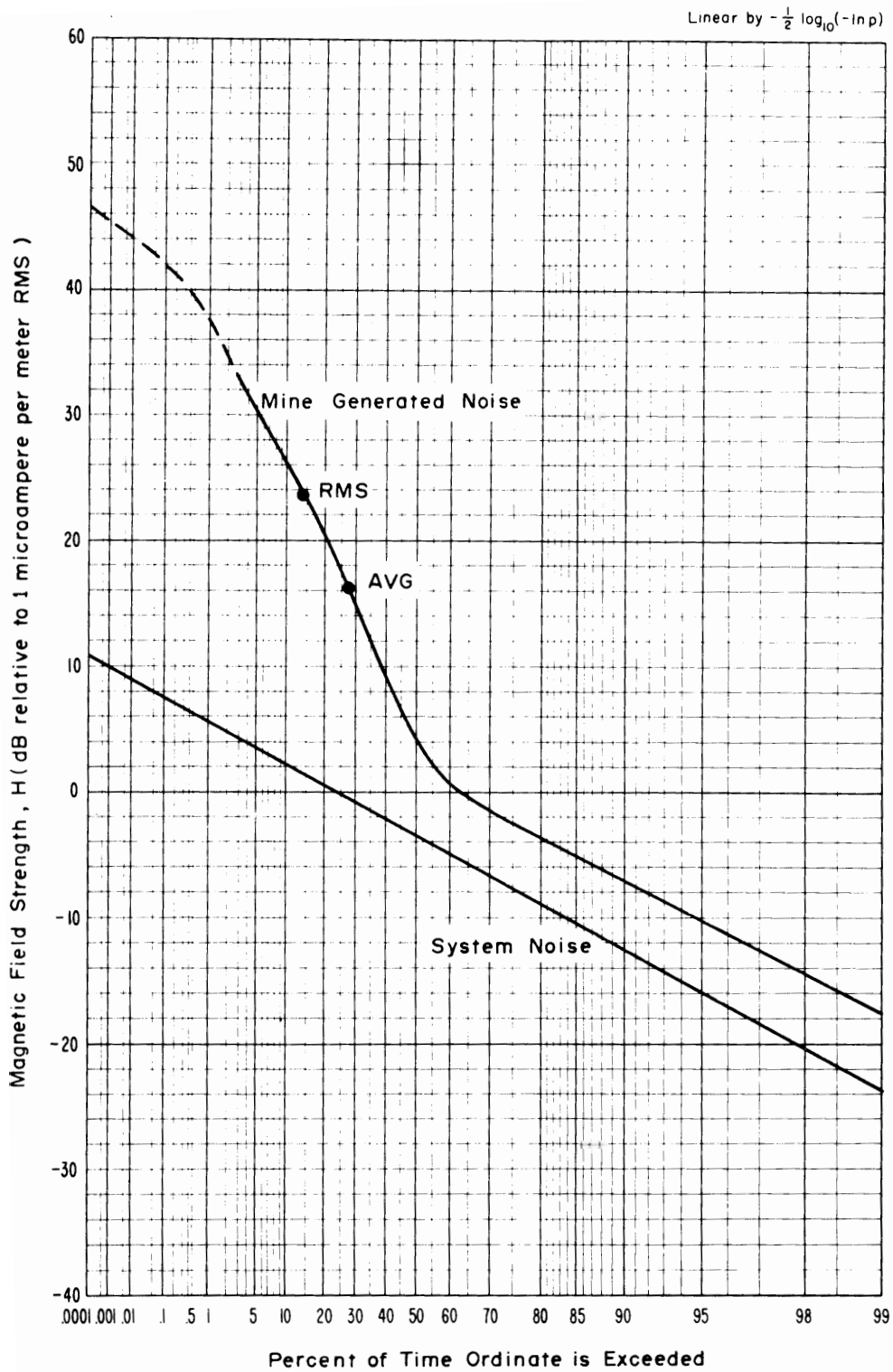


Figure 4-38 APD, 30 kHz, horizontal component (N-S), 1.0 kHz predetection bandwidth, April 10, 1973, 2:00 p.m., McElroy Mine.

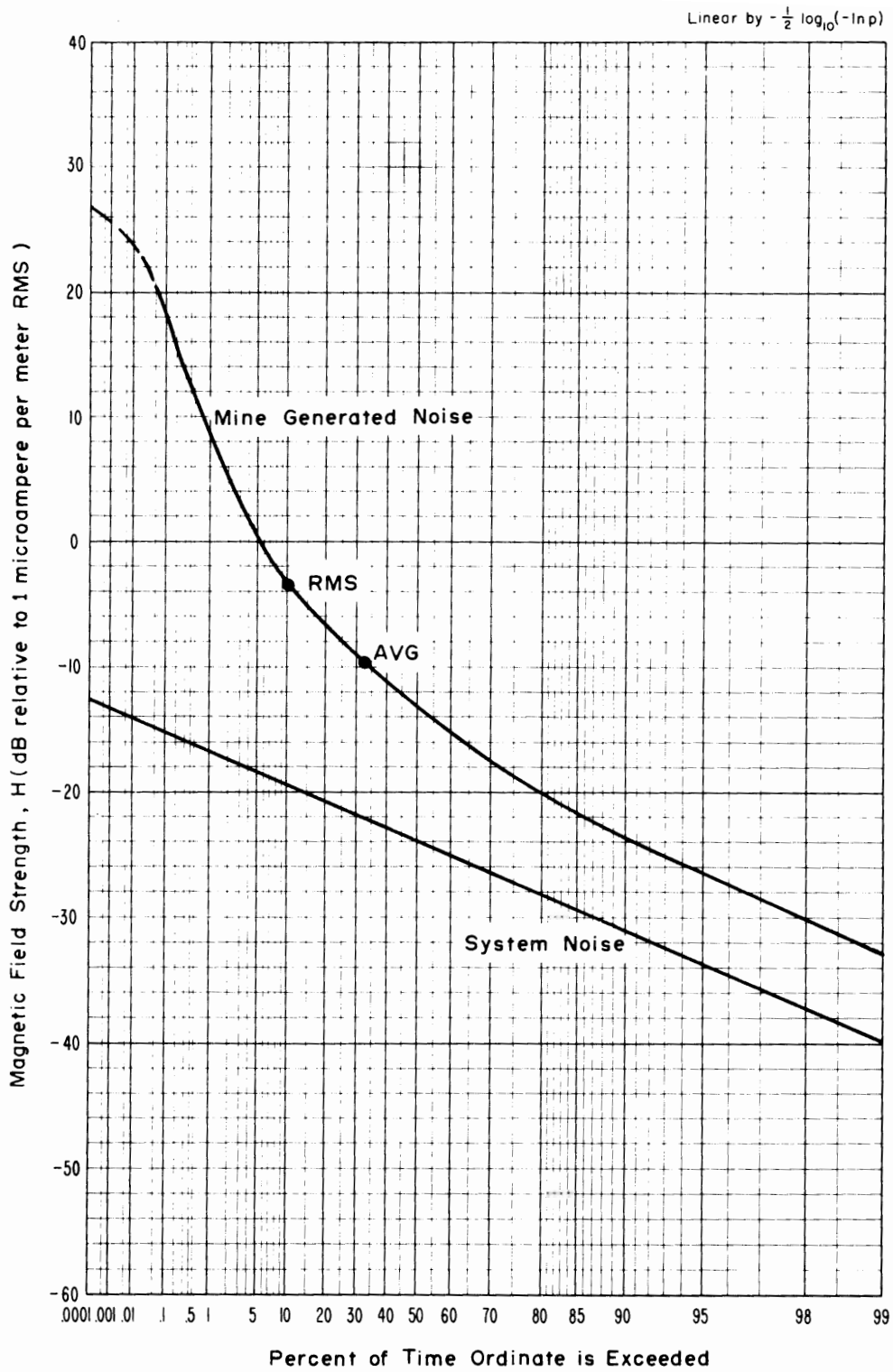


Figure 4-39 APD, 70 kHz, horizontal component (N-S), 1.0 kHz predetection bandwidth, April 10, 1973, 6:00 p.m., McElroy Mine.

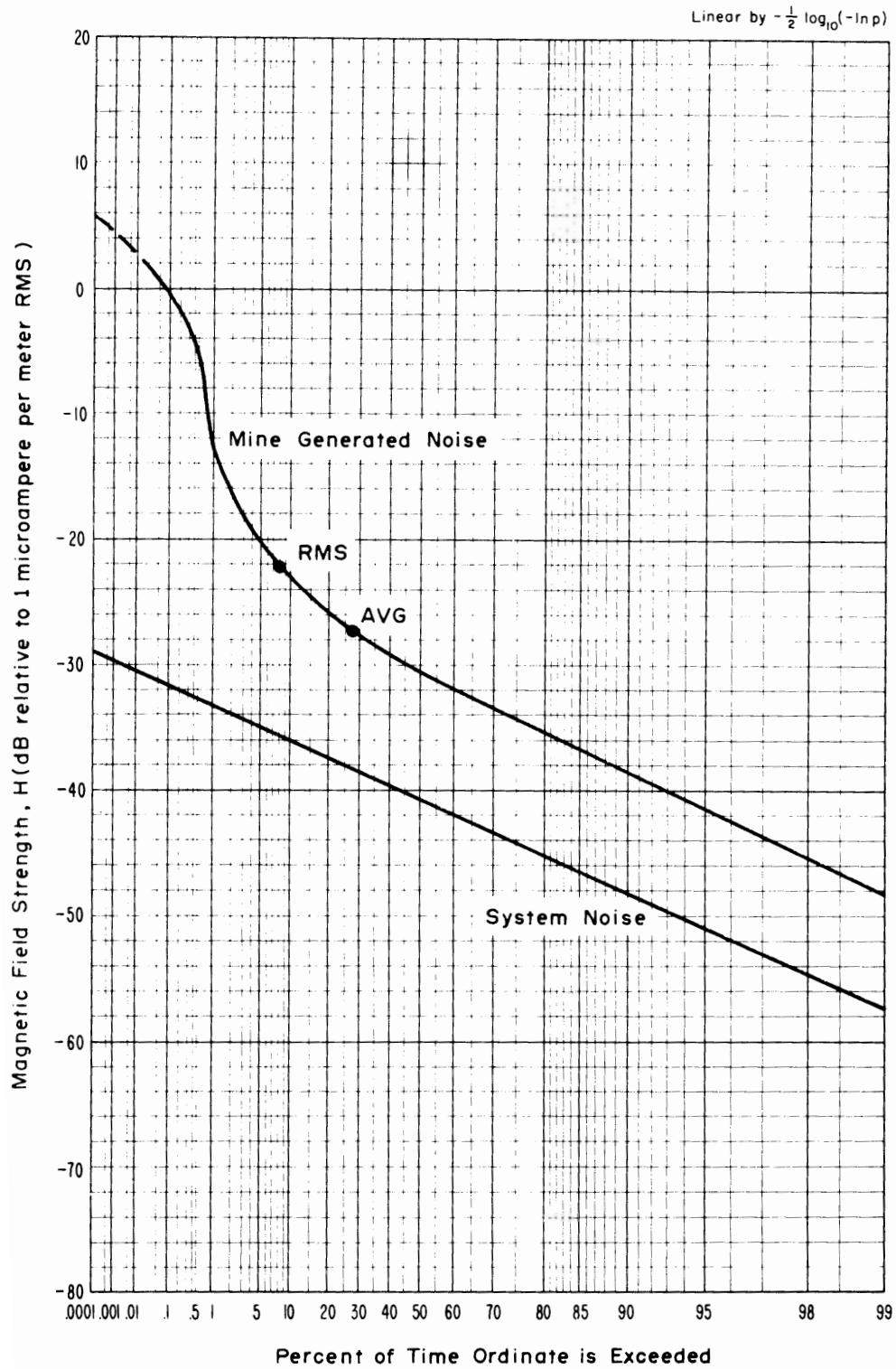


Figure 4-40 APD, 130 kHz, horizontal component (N-S), 1.0 kHz predetection bandwidth, April 10, 1973, 6:45 p.m., McElroy Mine.

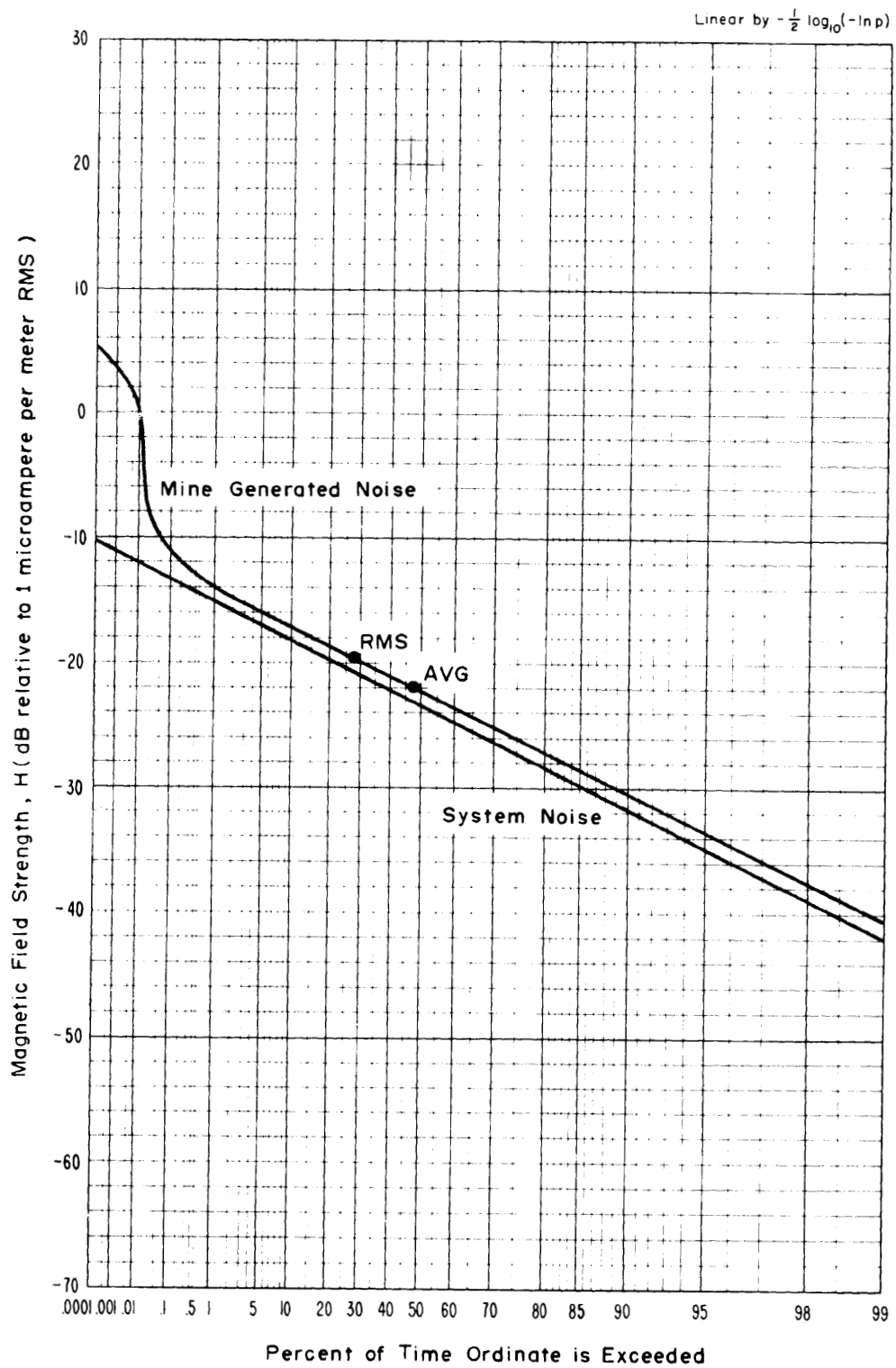


Figure 4-41 APD, 160 kHz, horizontal component (N-S), 1.0 kHz, predetection bandwidth, April 10, 1973, 6:00 p.m., McElroy Mine.

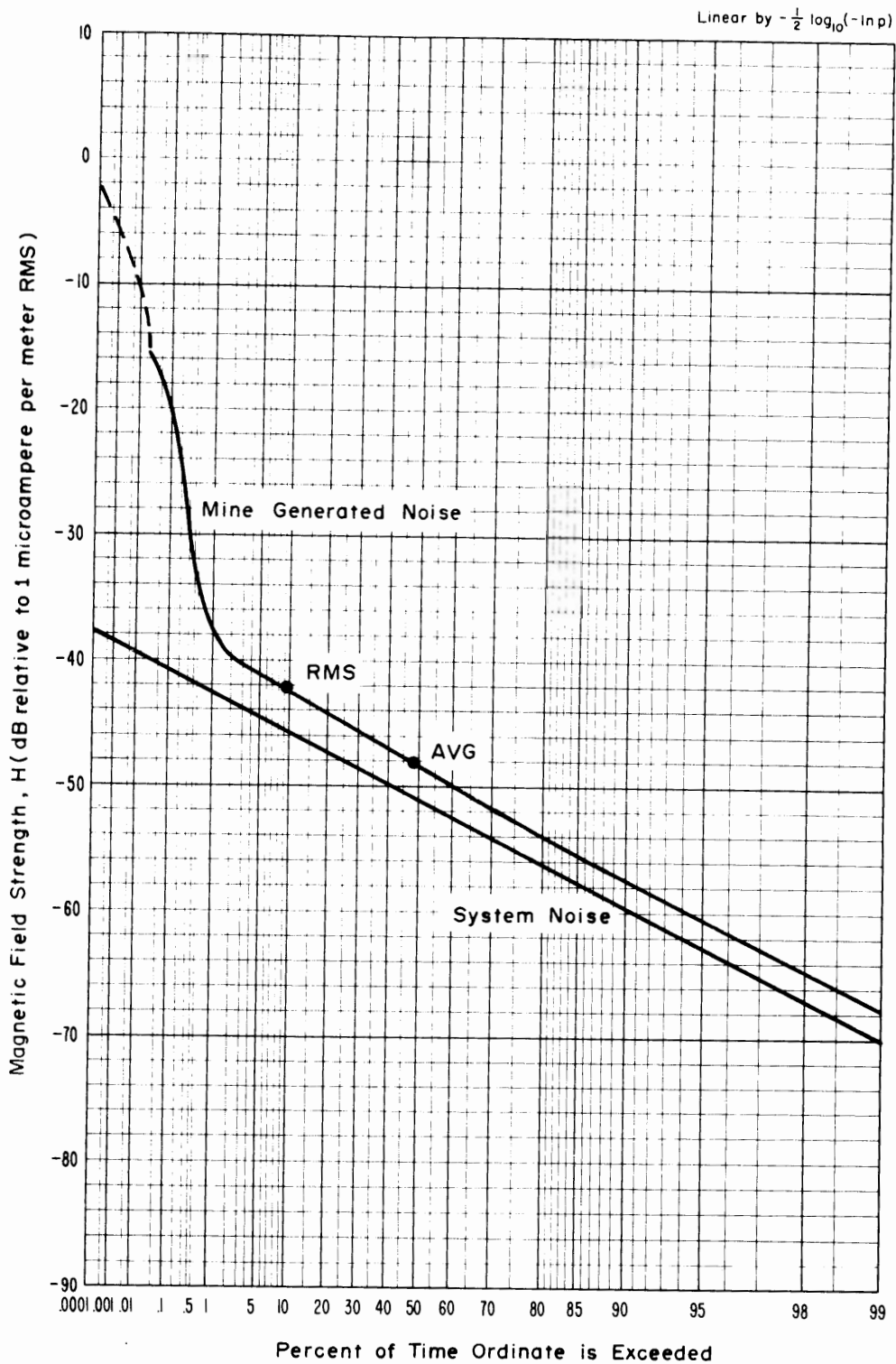


Figure 4-42 APD, 500 kHz, horizontal component(N-S), 1.2 kHz predetection bandwidth, April 10, 1973, 1:30 p.m., McElroy Mine.

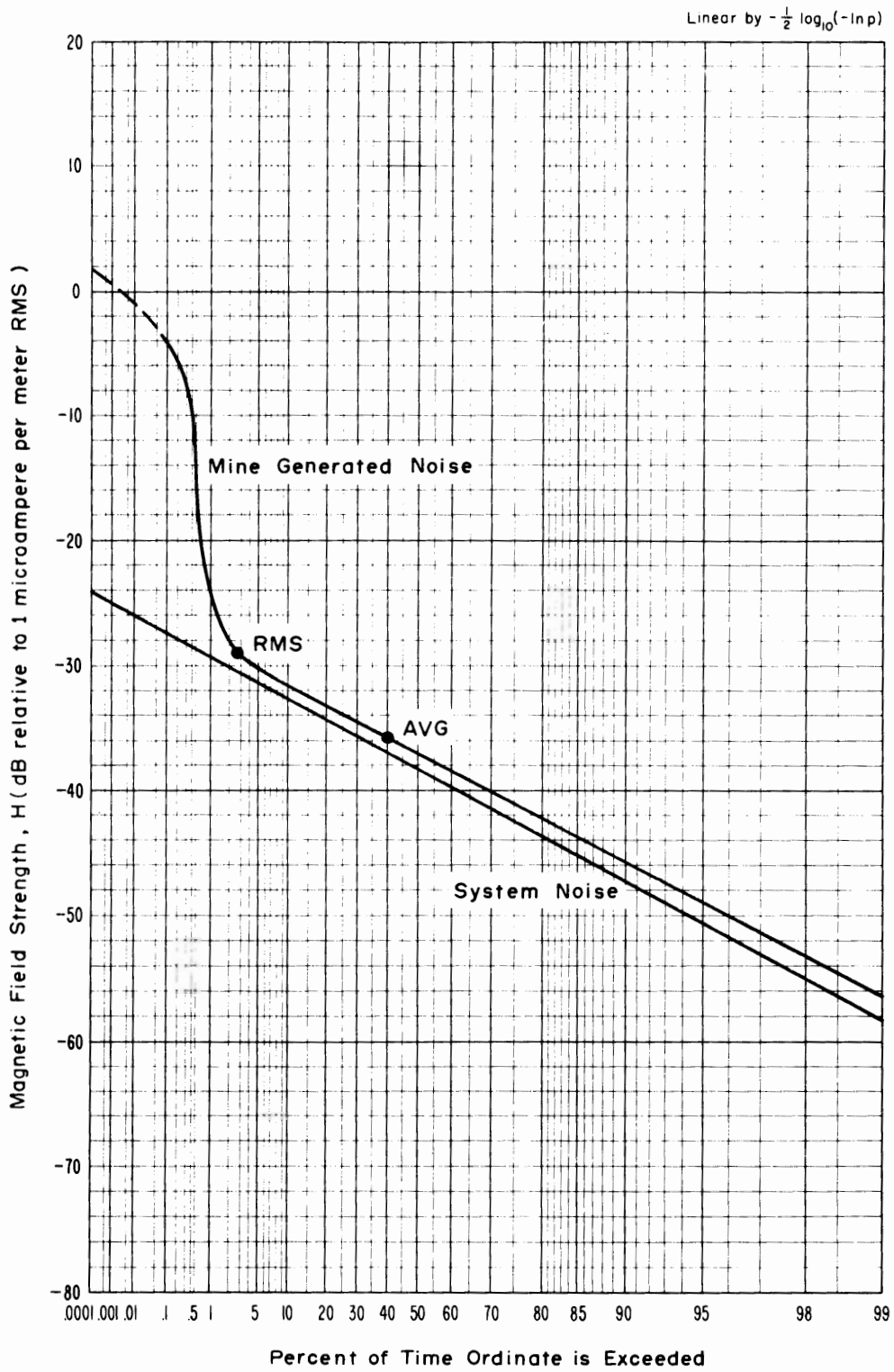


Figure 4-43 APD, 1 MHz, horizontal component (N-S), 1.2 kHz predetection bandwidth, April 10, 1973, 2:00 p.m., McElroy Mine.

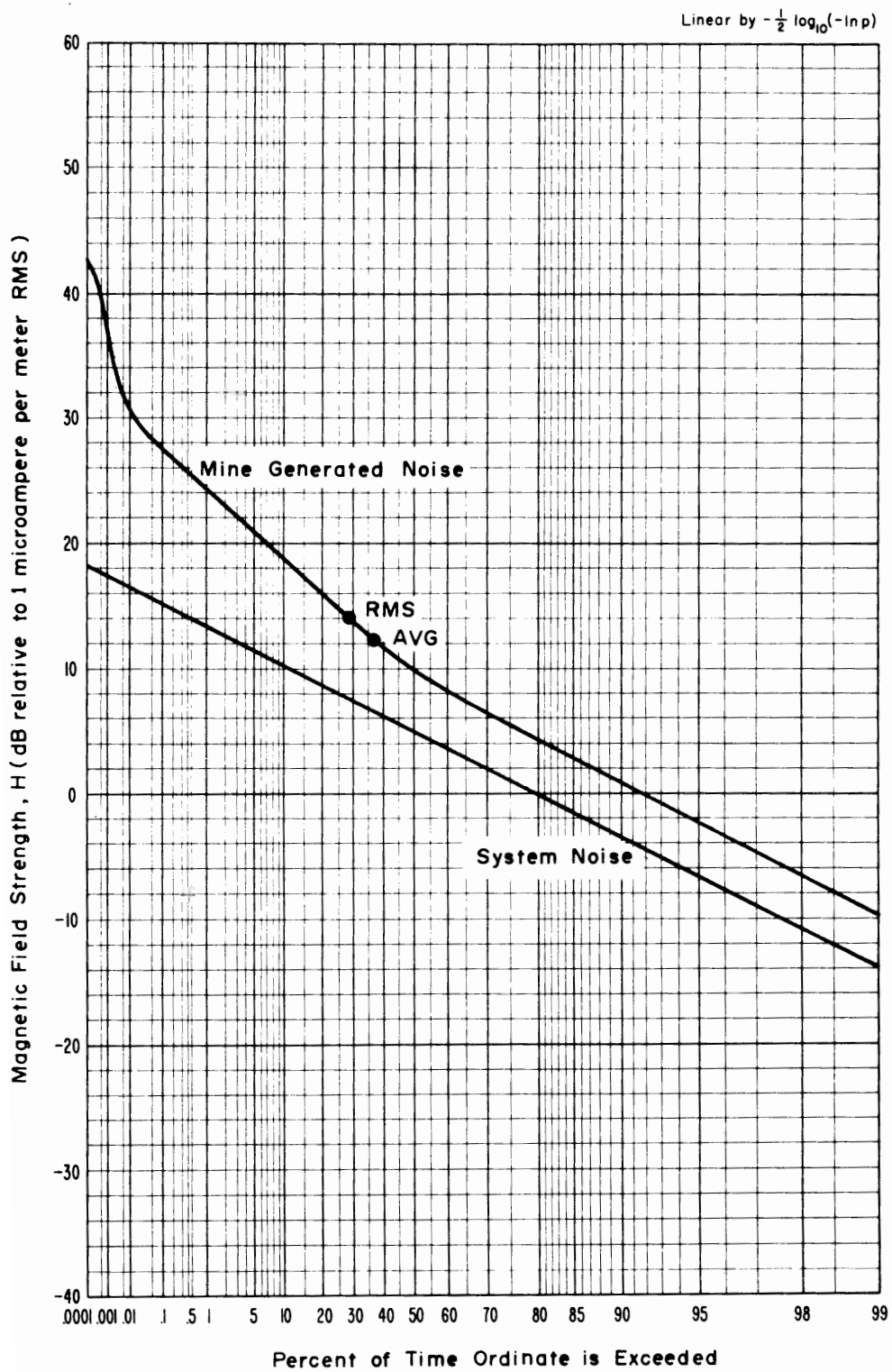


Figure 4-44 APD, 10 kHz, vertical component, 1.0 kHz predetection bandwidth, April 10, 1973, 4:00 p.m., quiet time measurements, McElroy Mine.

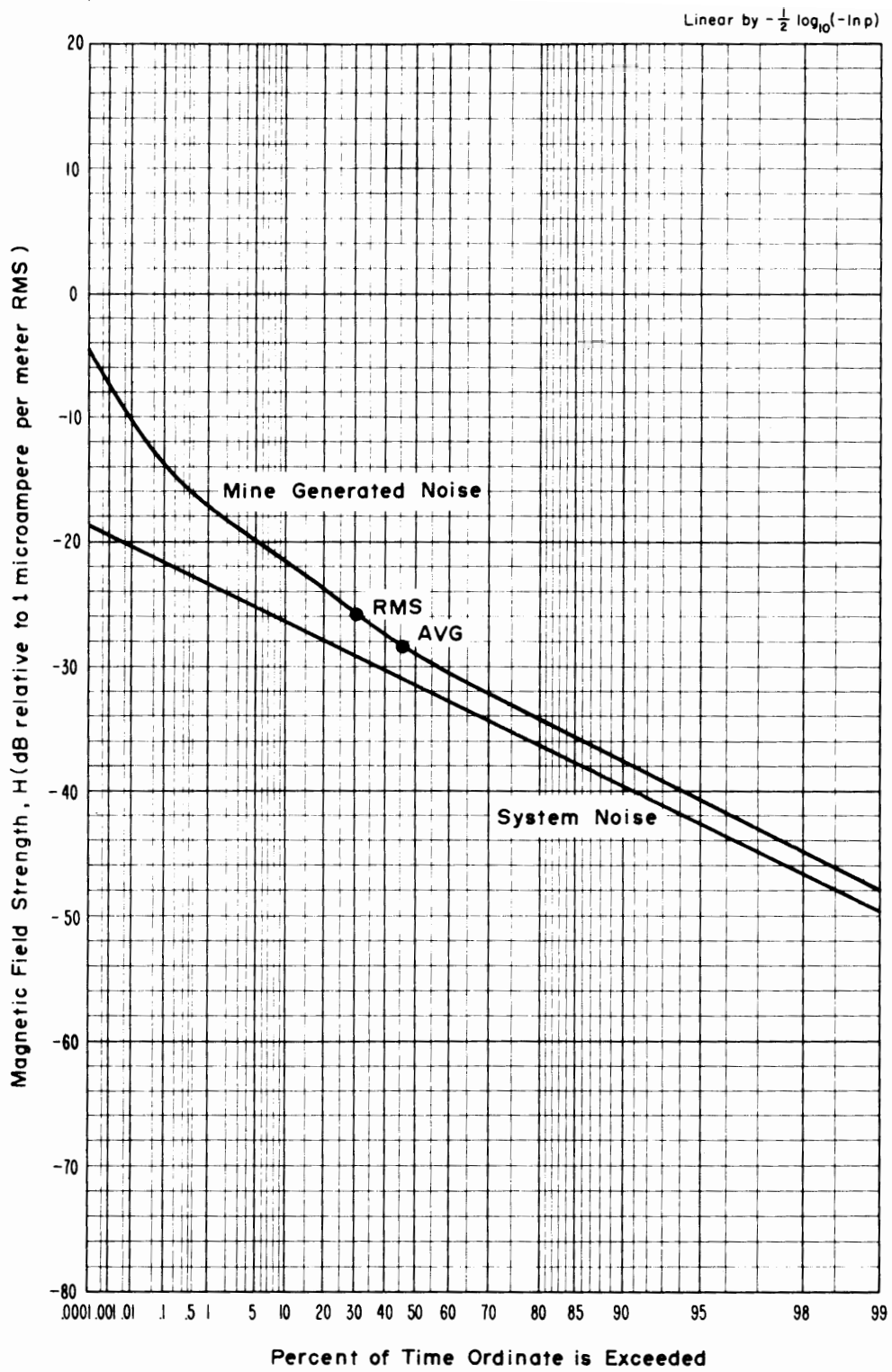


Figure 4-45 APD, 30 kHz, vertical component, 1.0 kHz predetection bandwidth, April 10, 1973, 4:05 p.m., quiet time measurements, McElroy Mine.

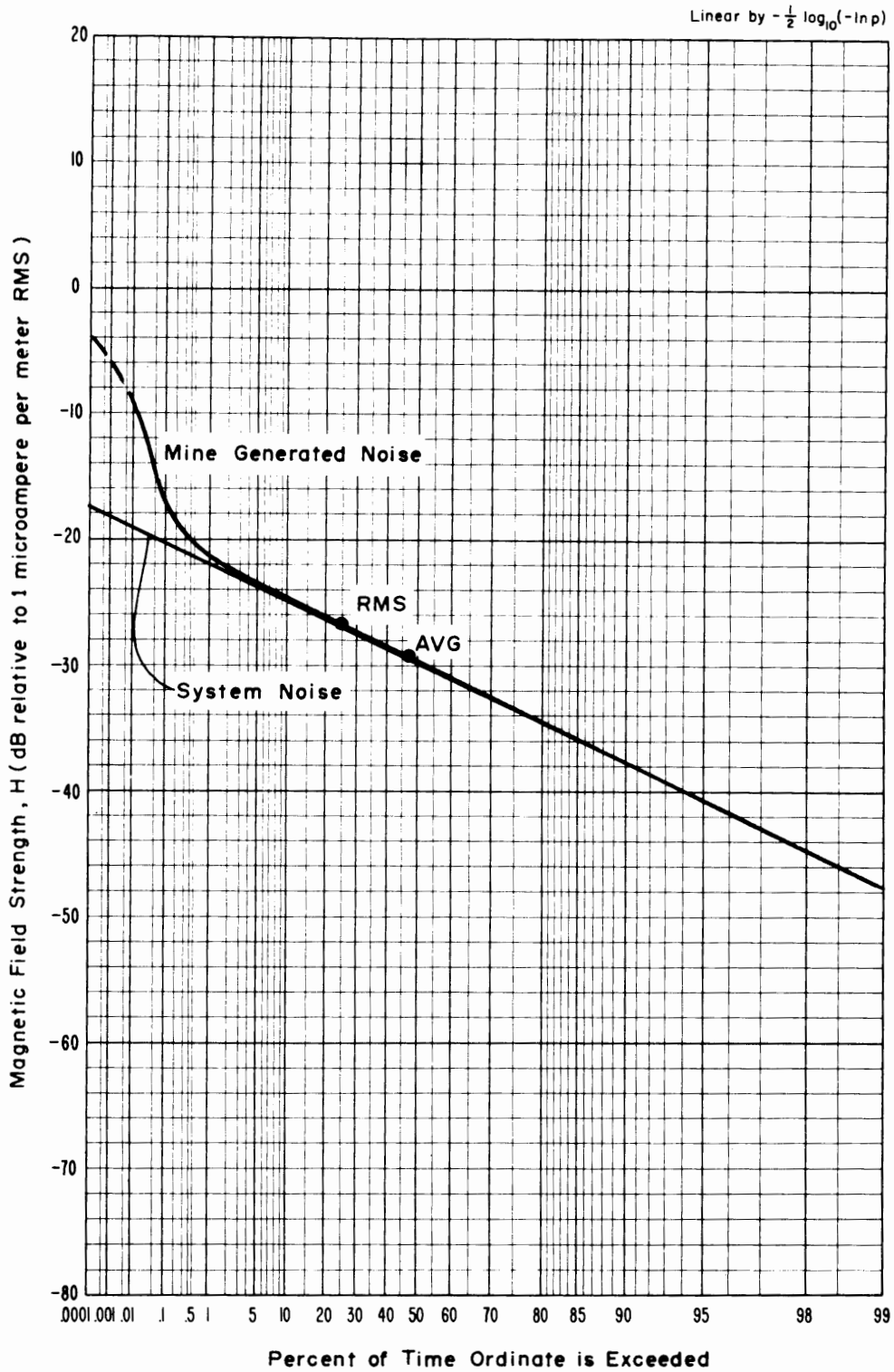


Figure 4-46 APD, 70 kHz, vertical component, 1.0 kHz predetection bandwidth, April 10, 1973, 4:15 p.m., quiet time measurements, McElroy Mine.

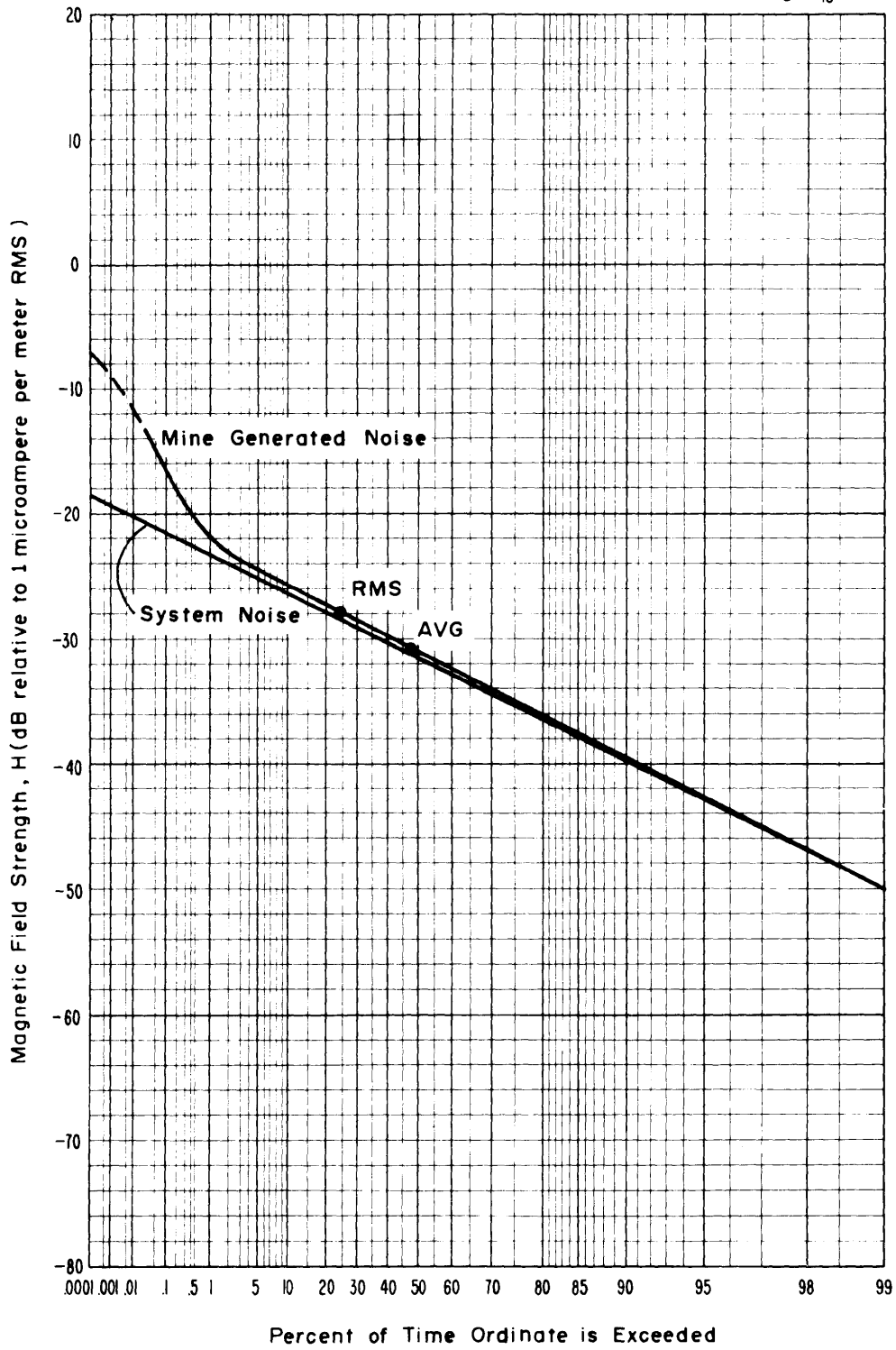


Figure 4-47 APD, 130 kHz, vertical component, 1.0 kHz predetection bandwidth, April 10, 1973, 4:20 p.m., quiet time measurements, McElroy Mine.

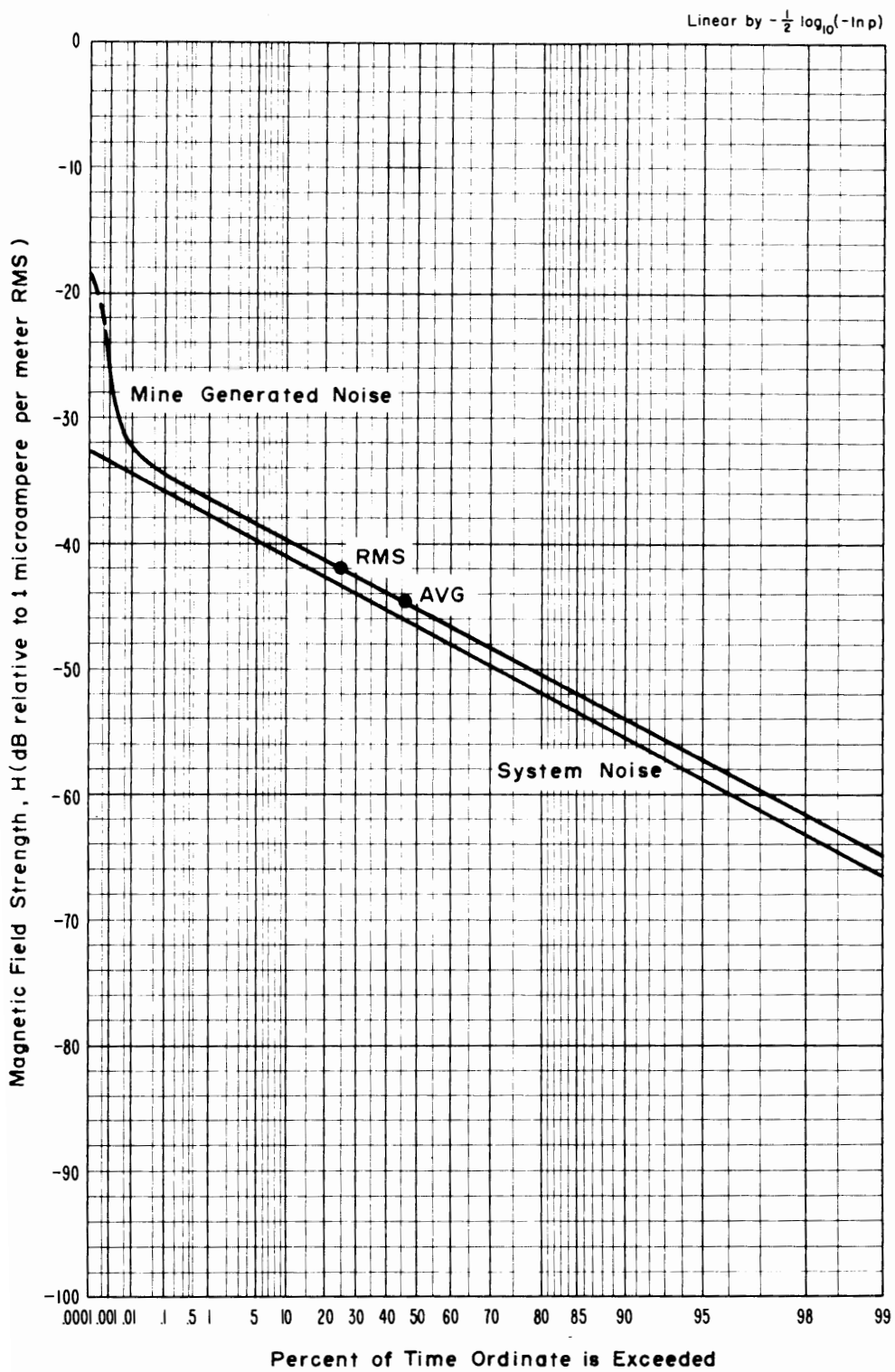


Figure 4-48 APD, 1 MHz, vertical component, 1.2 kHz predetection bandwidth, April 10, 1973, 4:05 p.m., quiet time measurements, McElroy Mine.

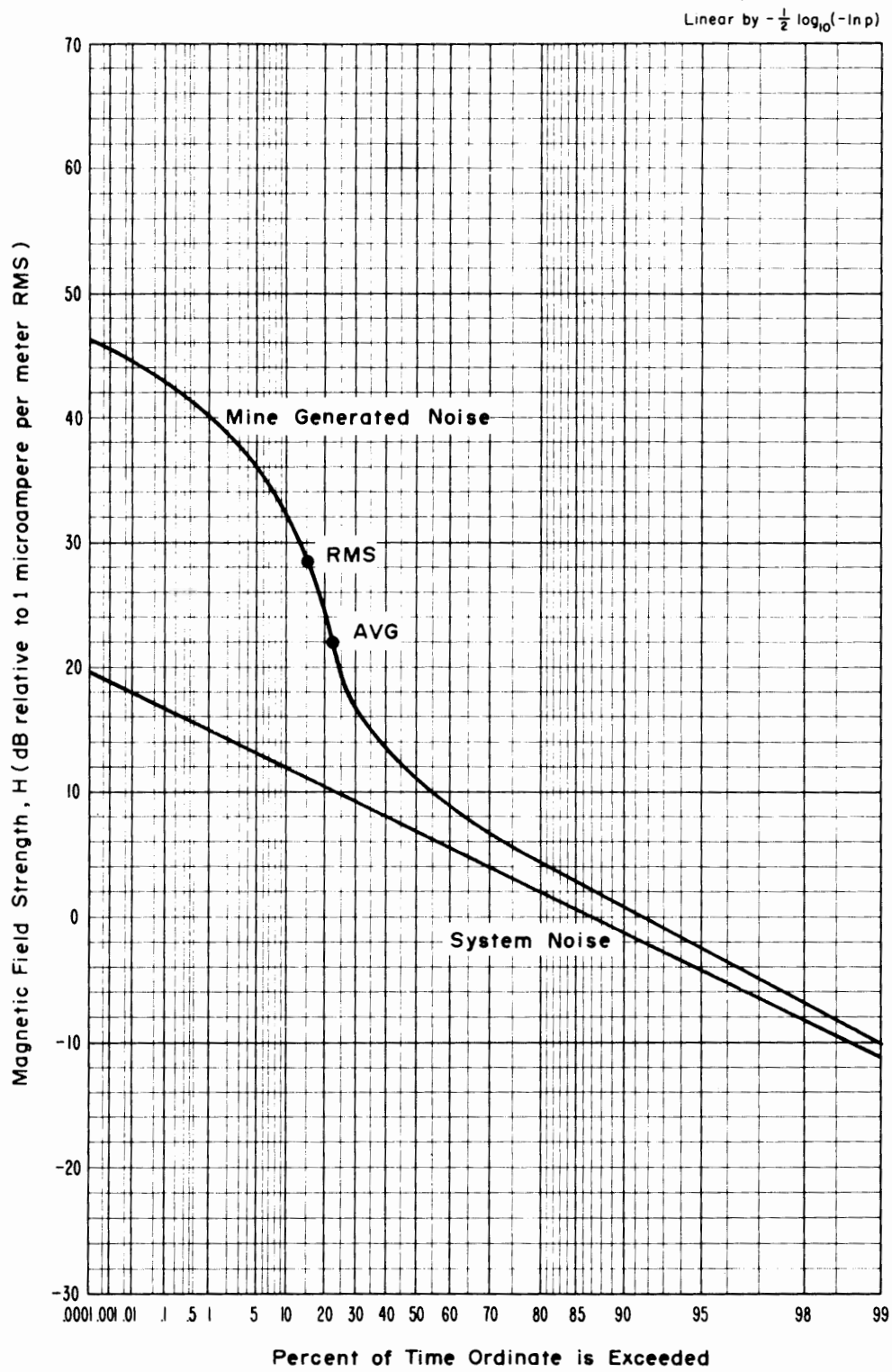


Figure 4-49 APD, 10 kHz, vertical component, 1.0 kHz predetection bandwidth, April 12, 1973, 11:50 a.m., McElroy Mine.

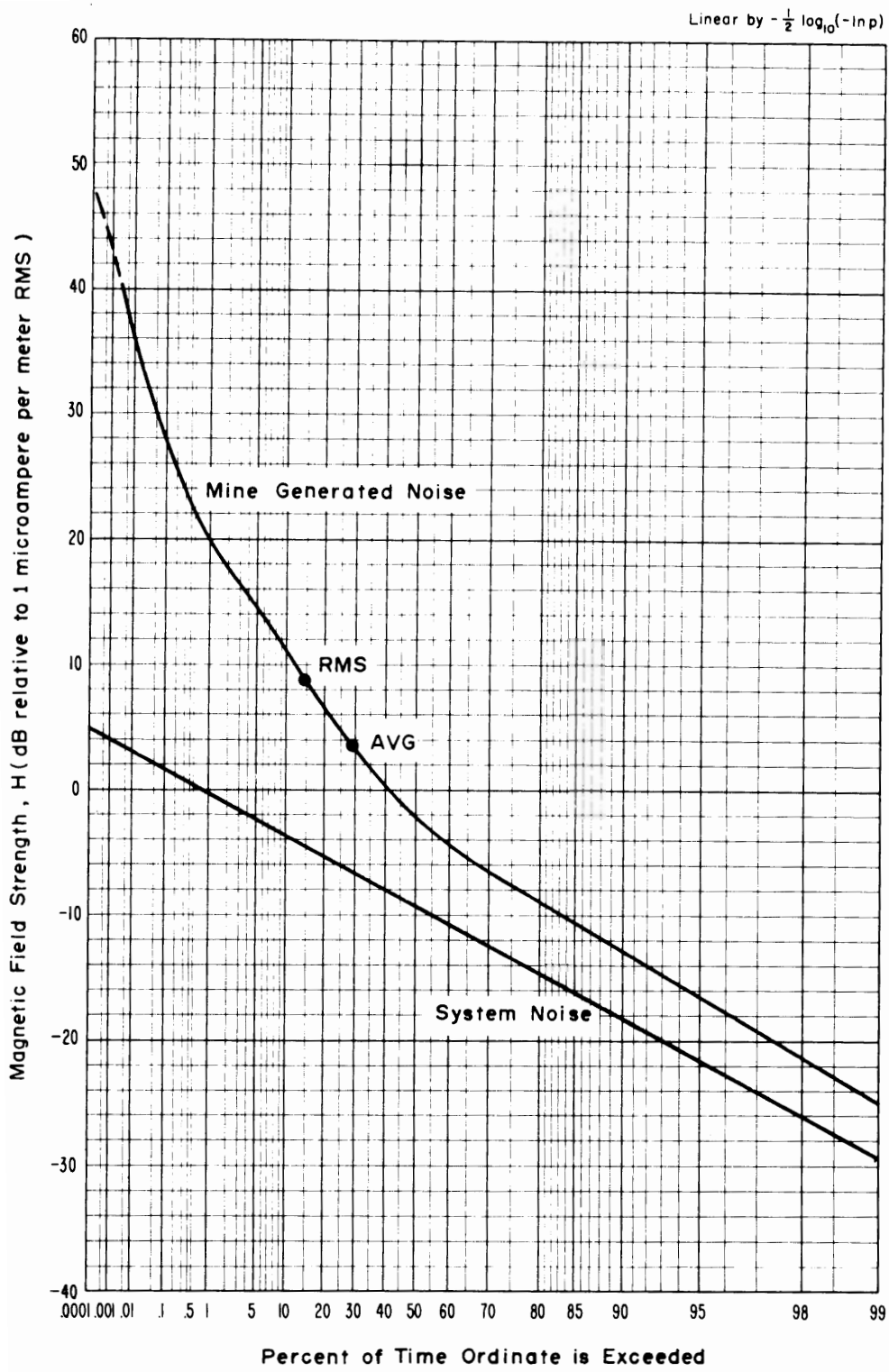


Figure 4-50 APD, 30 kHz, vertical component, 1.0 kHz predetection bandwidth, April 12, 1973, 12:25 p.m., McElroy Mine.

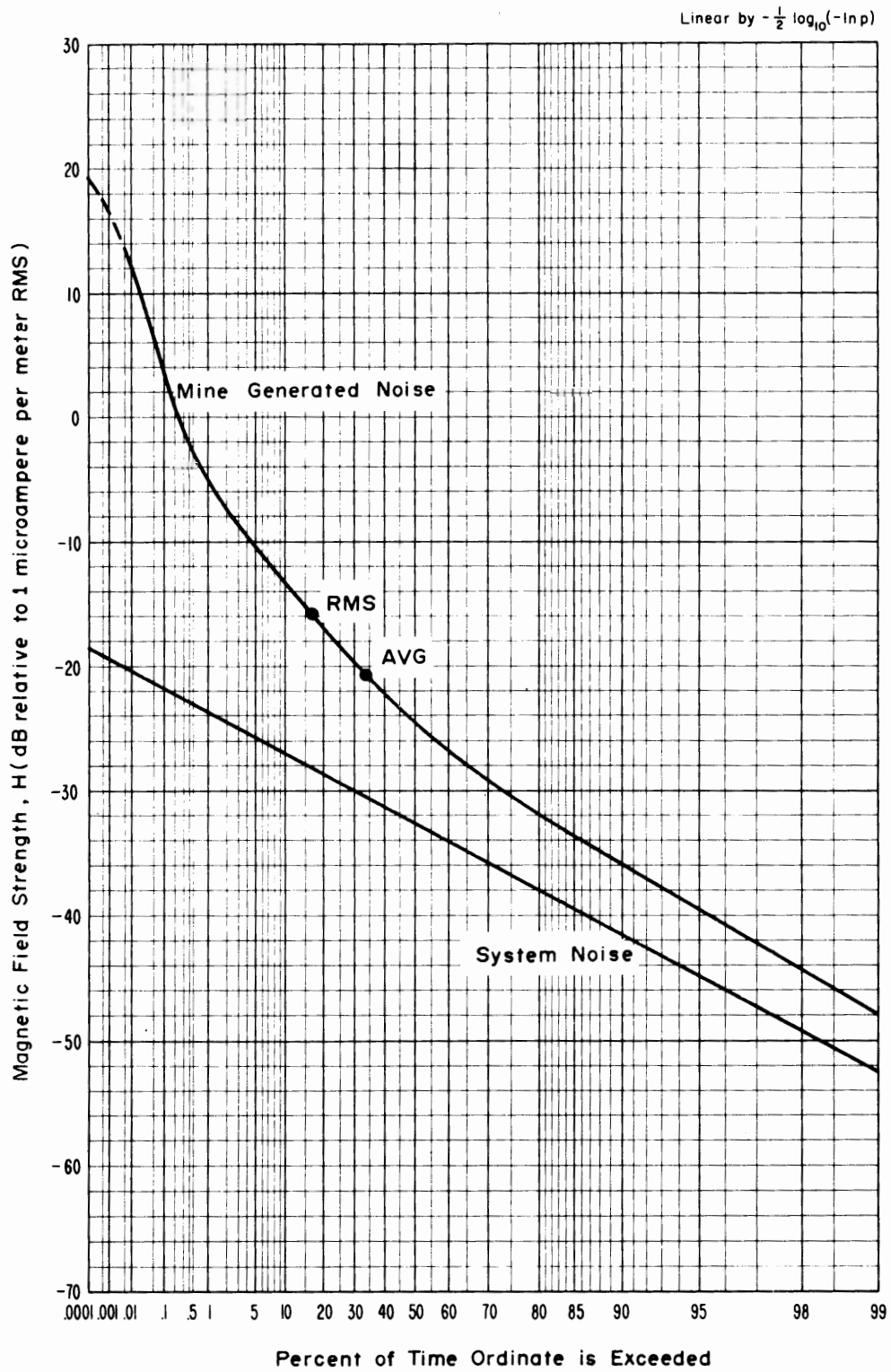


Figure 4-51 APD, 70 kHz, vertical component, 1.0 kHz predetection bandwidth, April 12, 1973, 12:50 p.m., McElroy Mine.

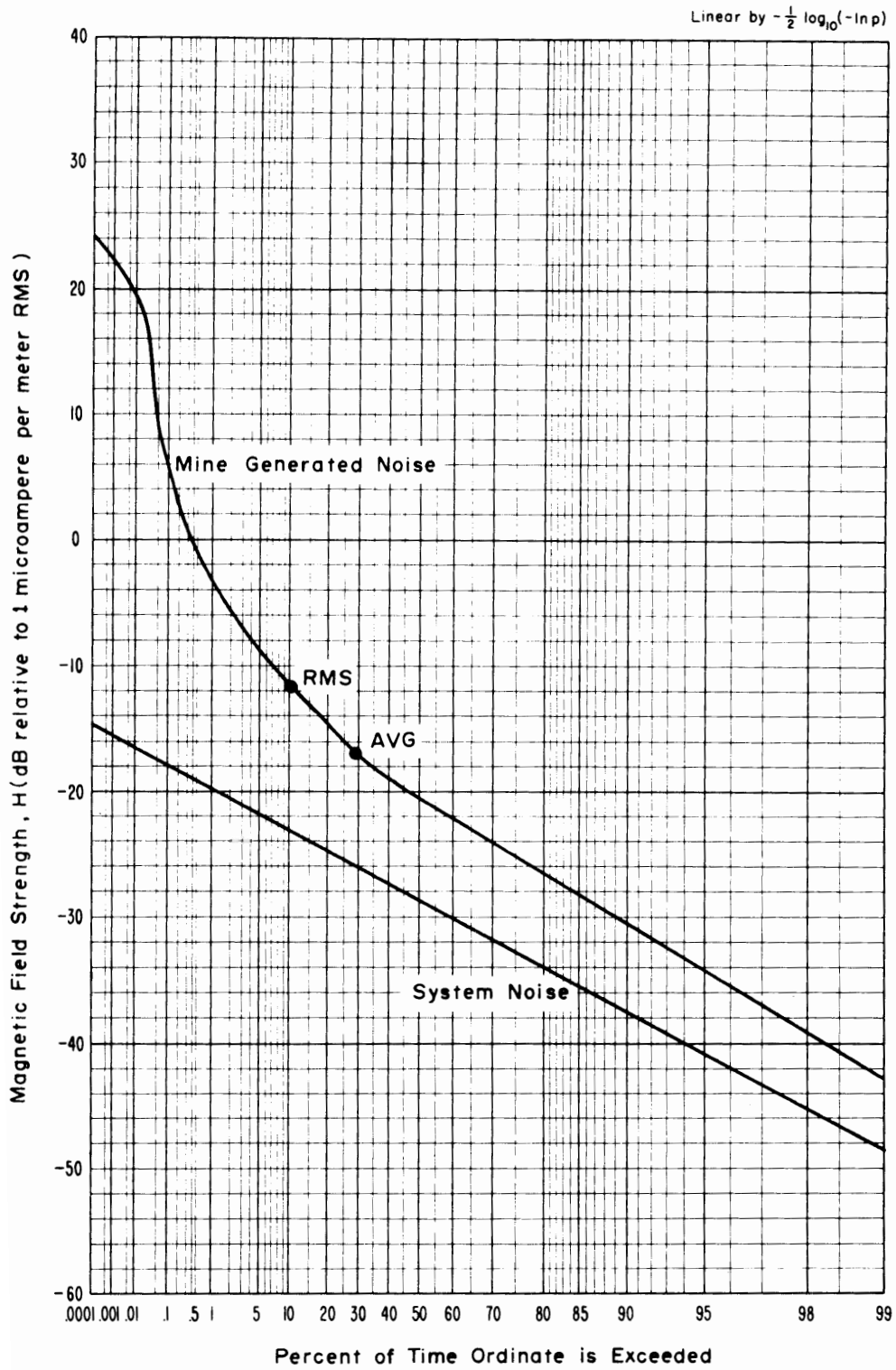


Figure 4-52 APD, 130 kHz, vertical component, 1.0 kHz predetection bandwidth, April 12, 1973, 1:30 p.m., McElroy Mine.

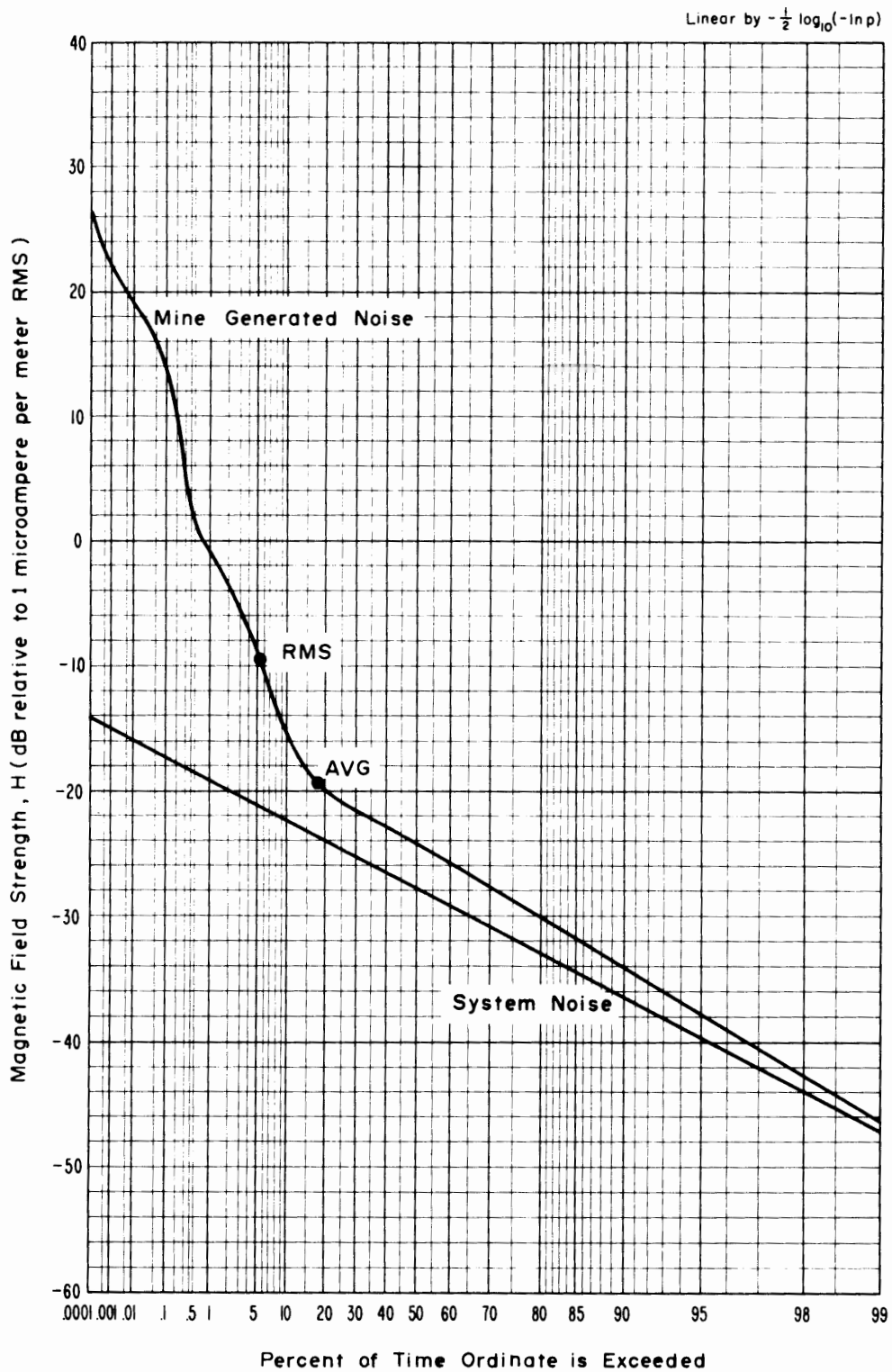


Figure 4-53 APD, 160 kHz, vertical component, 1.0 kHz predetection bandwidth, April 12, 1973, 2:10 p.m., McElroy Mine.

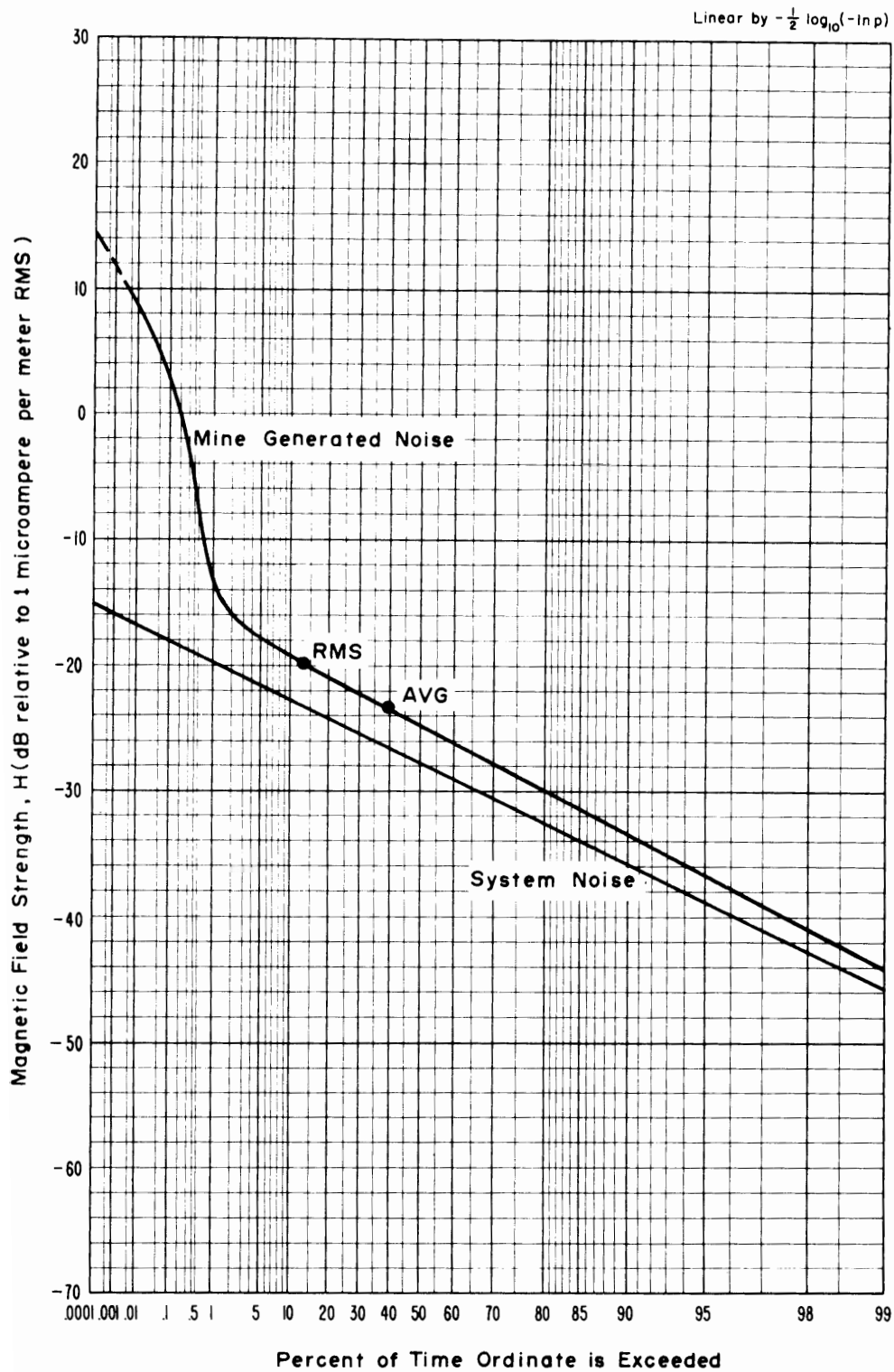


Figure 4-54 APD, 500 kHz, vertical component, 1.2 kHz predetection bandwidth, April 12, 1973, 11:50 a.m., McElroy Mine.

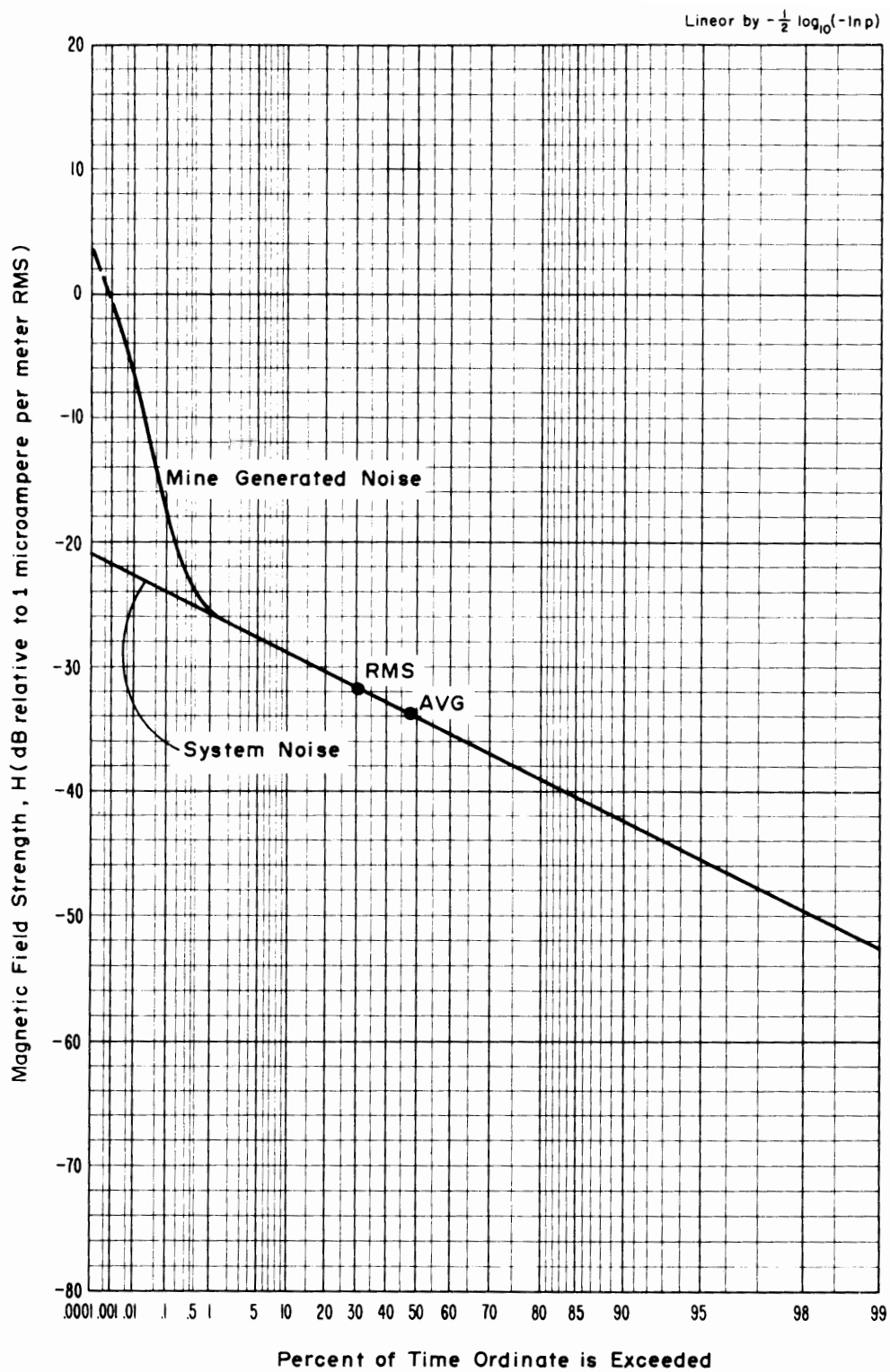


Figure 4-55 APD, 1 MHz, vertical component, 1.2 kHz predetection bandwidth, April 12, 1973, 12:25 p.m., McElroy Mine.

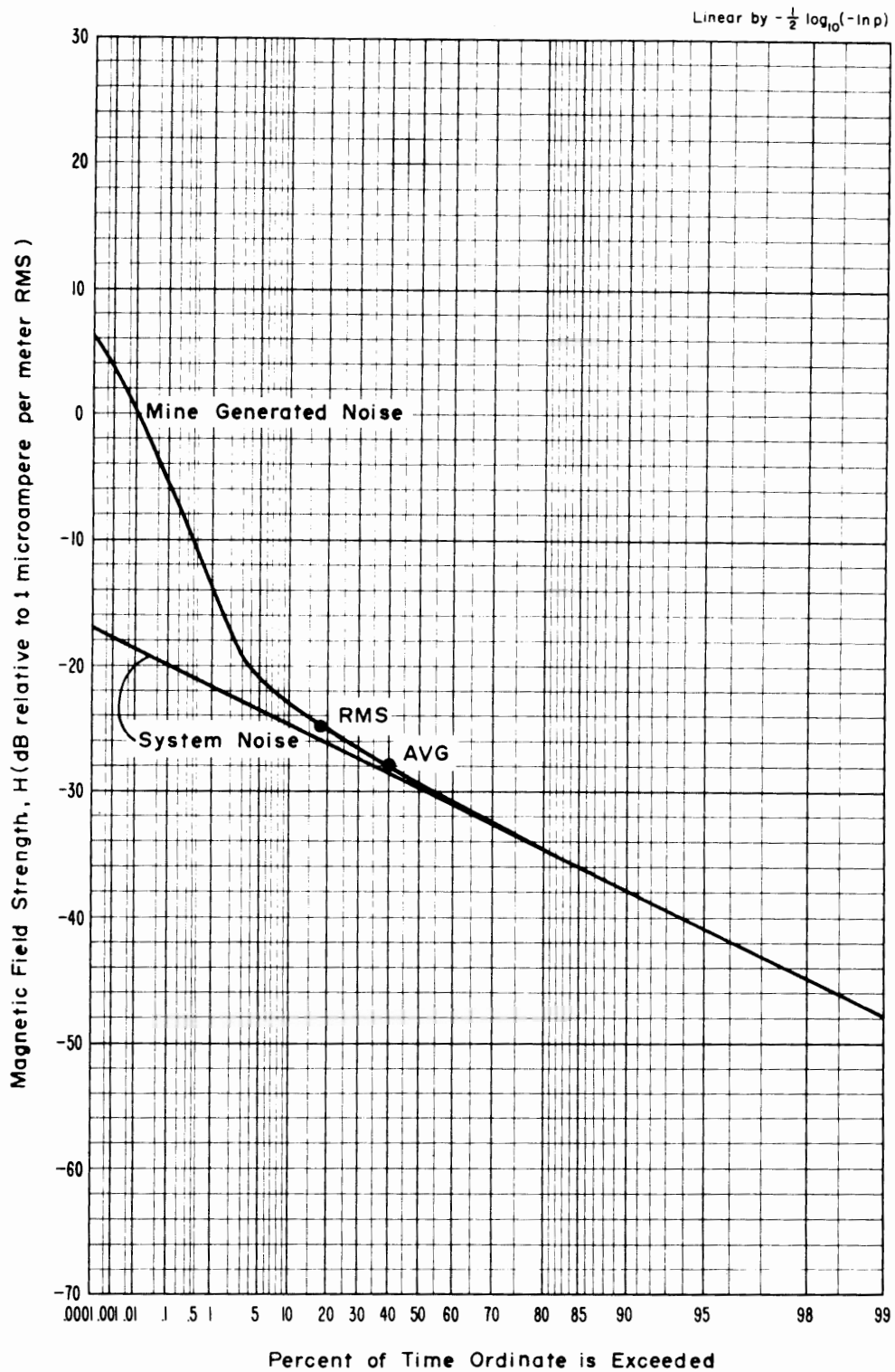


Figure 4-56 APD, 2 MHz, vertical component, 1.2 kHz predetection bandwidth, April 12, 1973, 12:50 p.m., McElroy Mine.

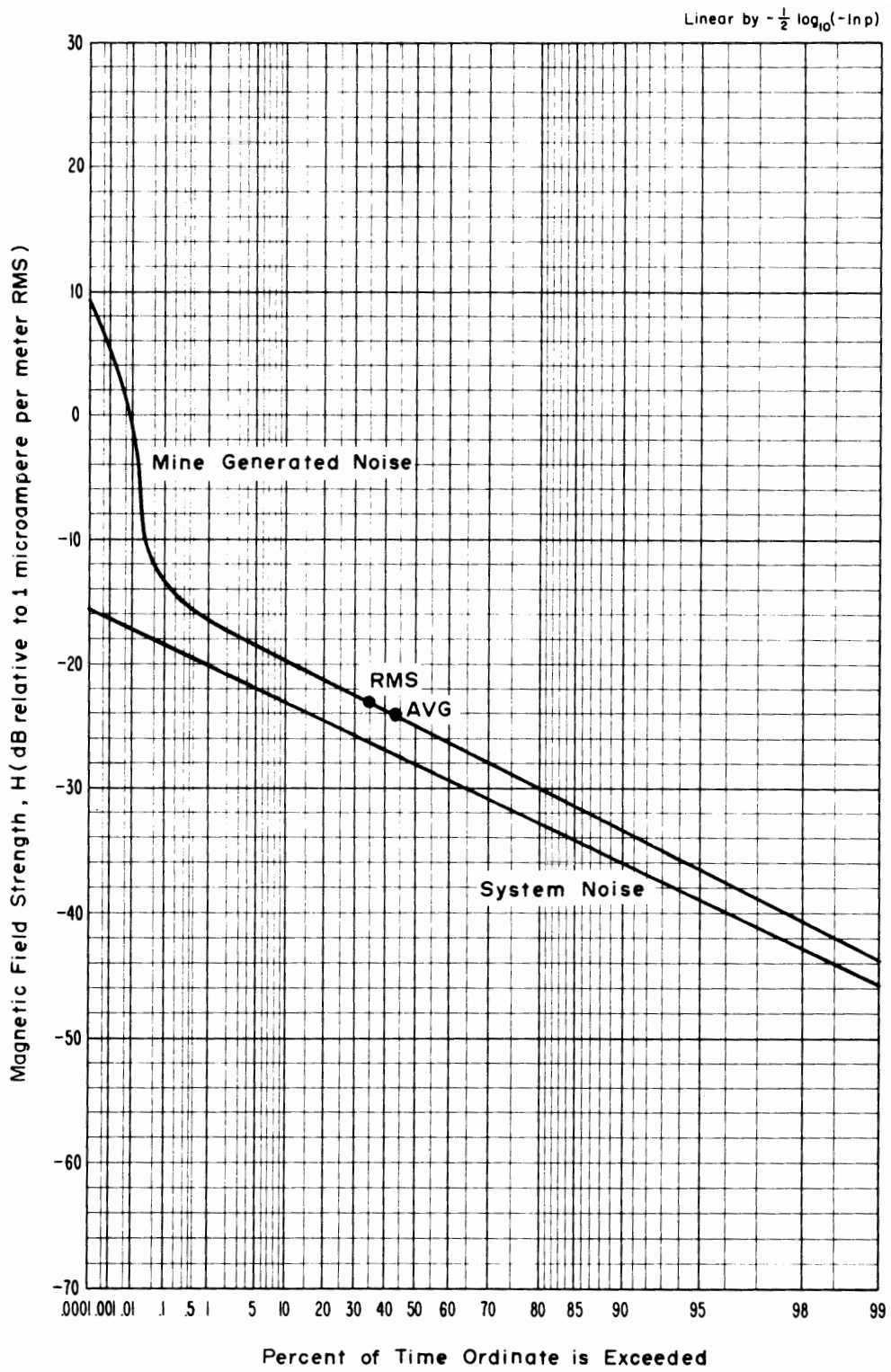


Figure 4-57 APD, 6 MHz, vertical component, 1.2 kHz predetection bandwidth, April 12, 1973, 1:30 p.m., McElroy Mine.

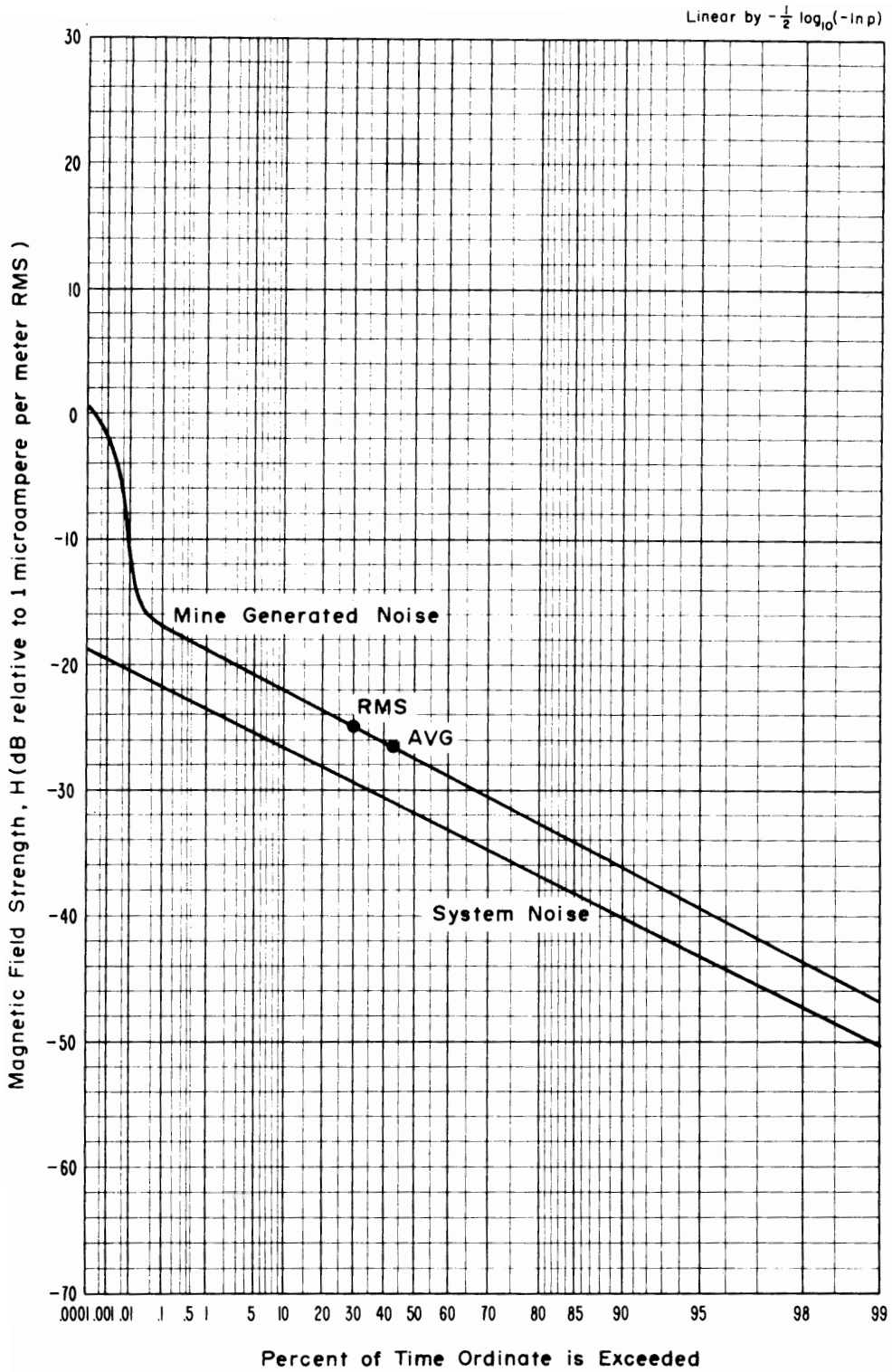


Figure 4-58 APD, 14 MHz, vertical component, 1.2 kHz predetection bandwidth, April 12, 1973, 2:10 p.m., McElroy Mine.

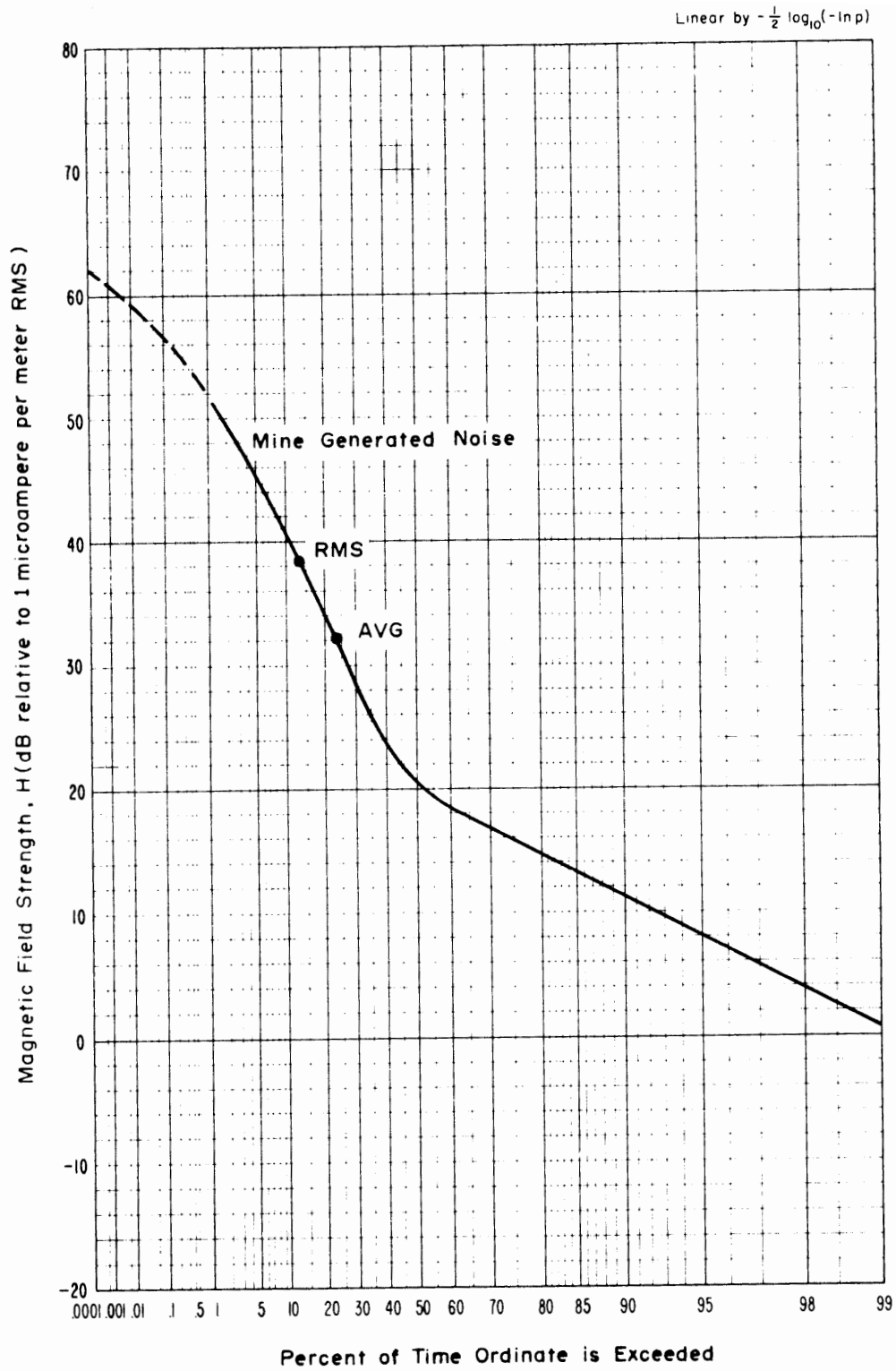


Figure 4-59 APD, 10 kHz, vertical component, 1.0 kHz predetection bandwidth, April 12, 1973, 11:30 a.m., McElroy Mine.

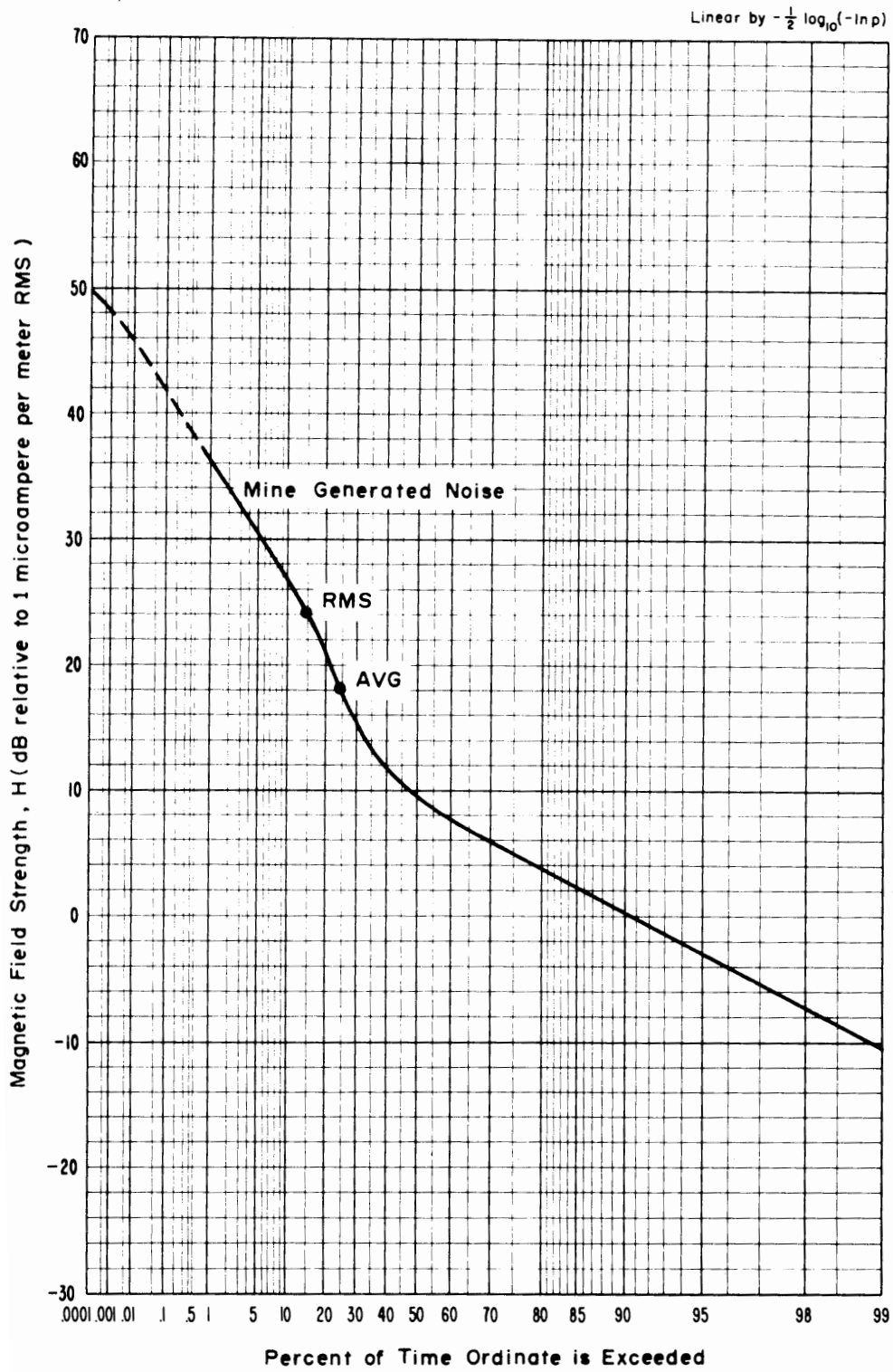


Figure 4-60 APD, 30 kHz, vertical component, 1.0 kHz predetection bandwidth, April 12, 1973, 12:15 p.m., McElroy Mine.

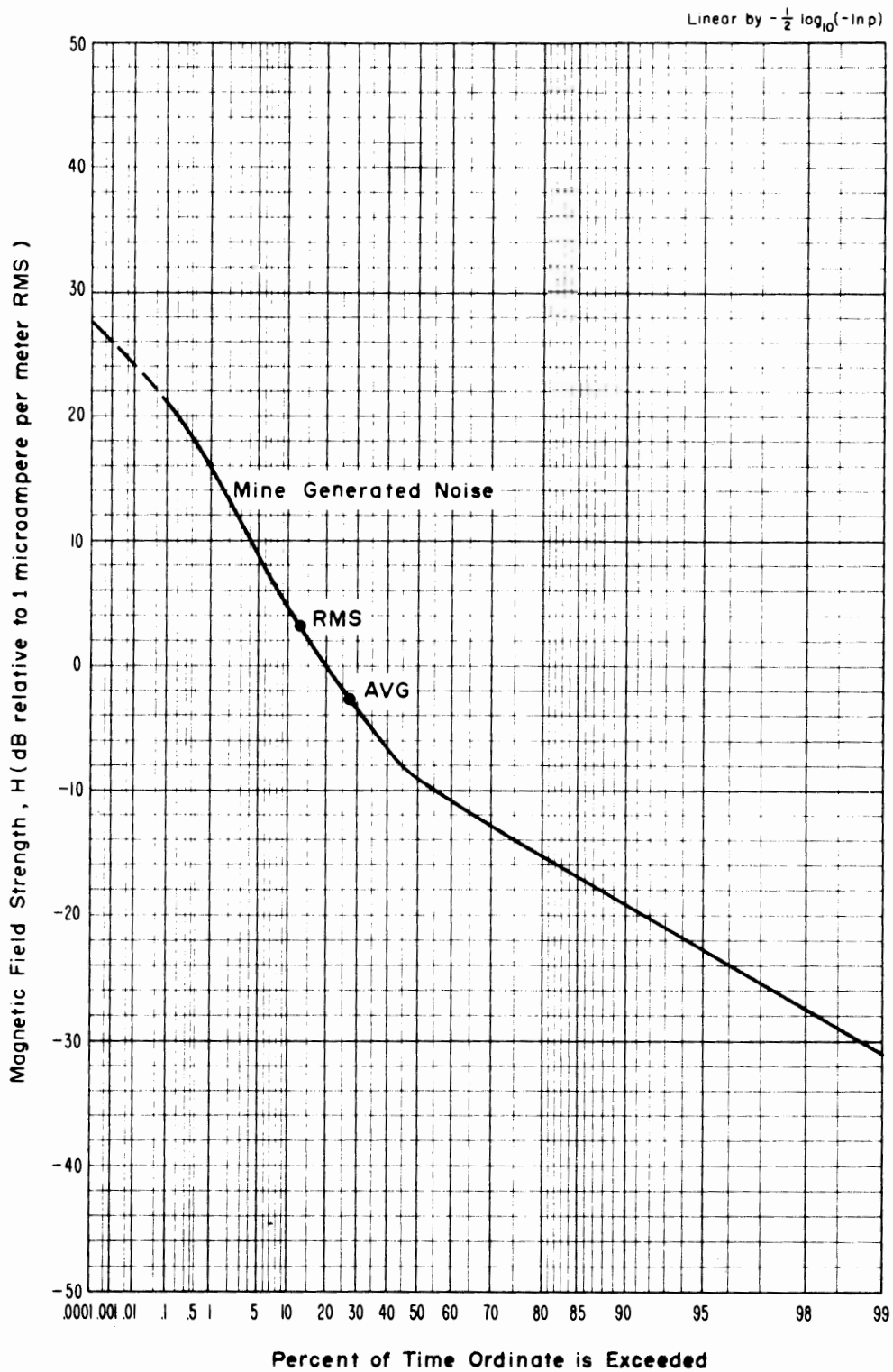


Figure 4-61 APD, 70 kHz, vertical component, 1.0 kHz predetection bandwidth, April 12, 1973, 1:00 p.m., McElroy Mine.

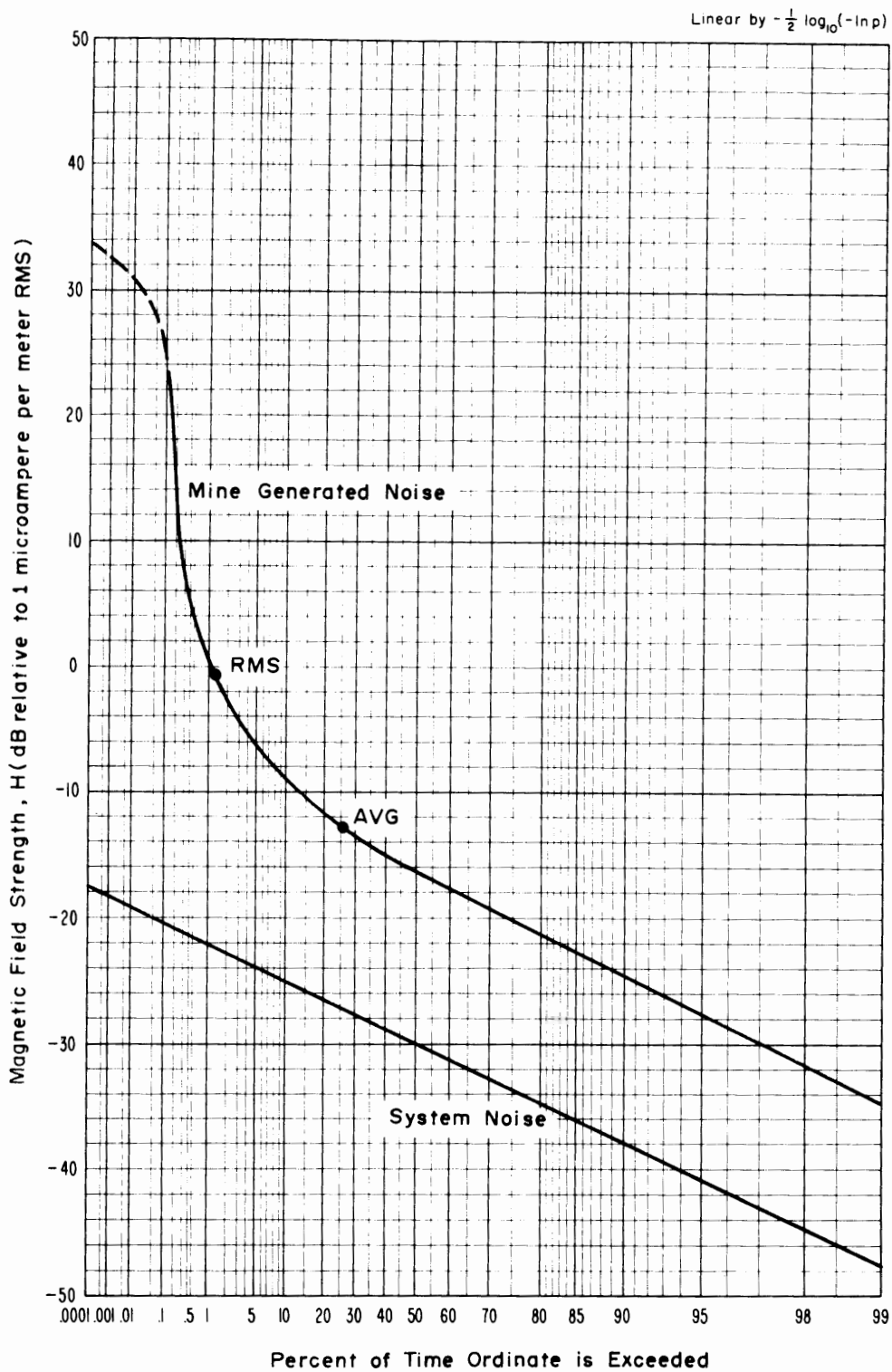


Figure 4-62 APD, 130 kHz, vertical component, 1.0 kHz predetection bandwidth, April 12, 1973, 1:30 p.m., McElroy Mine.

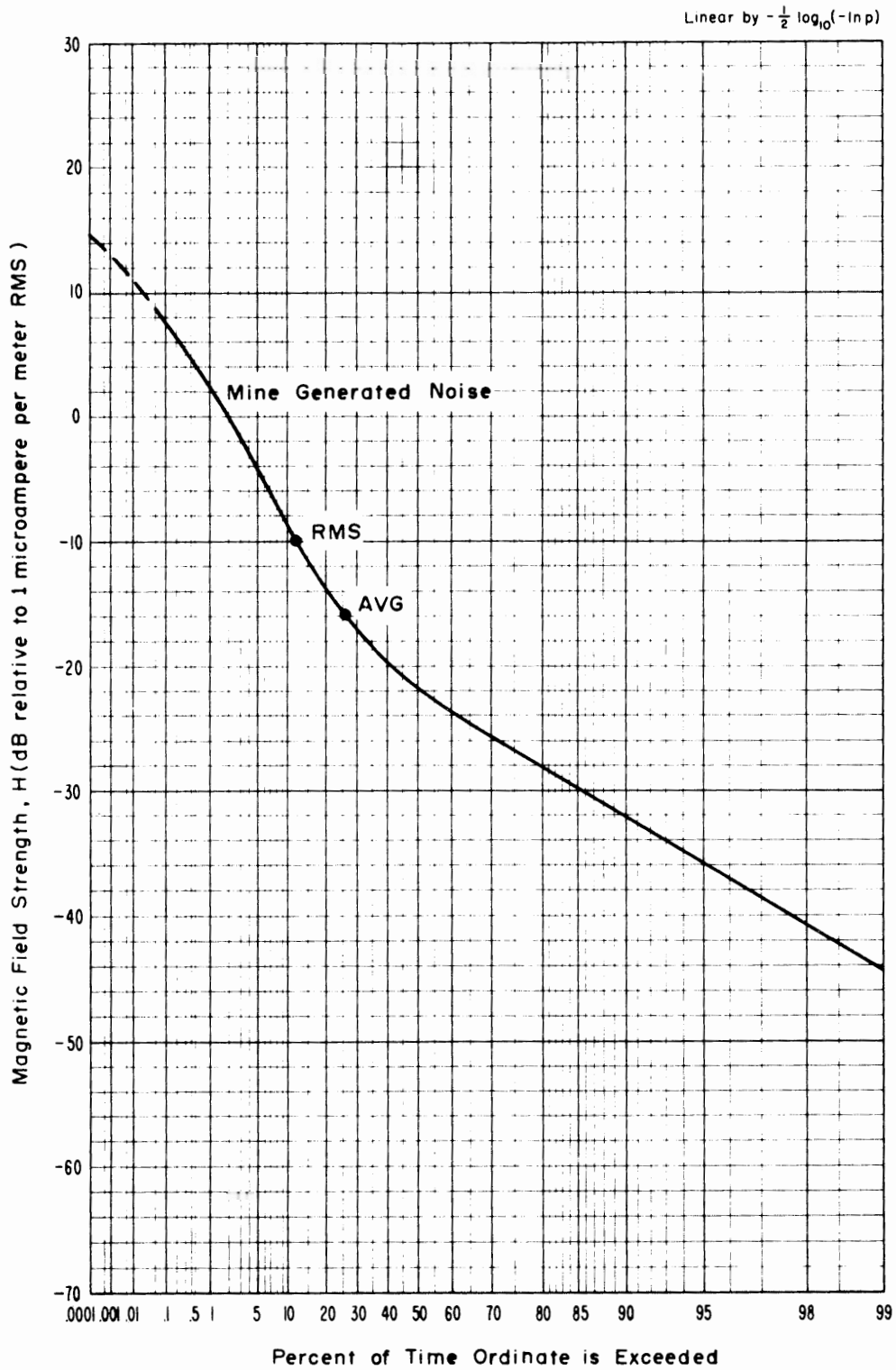


Figure 4-63 APD, 160 kHz, vertical component, 1.0 kHz predetection bandwidth, April 12, 1973, 2:15 p.m., McElroy Mine.

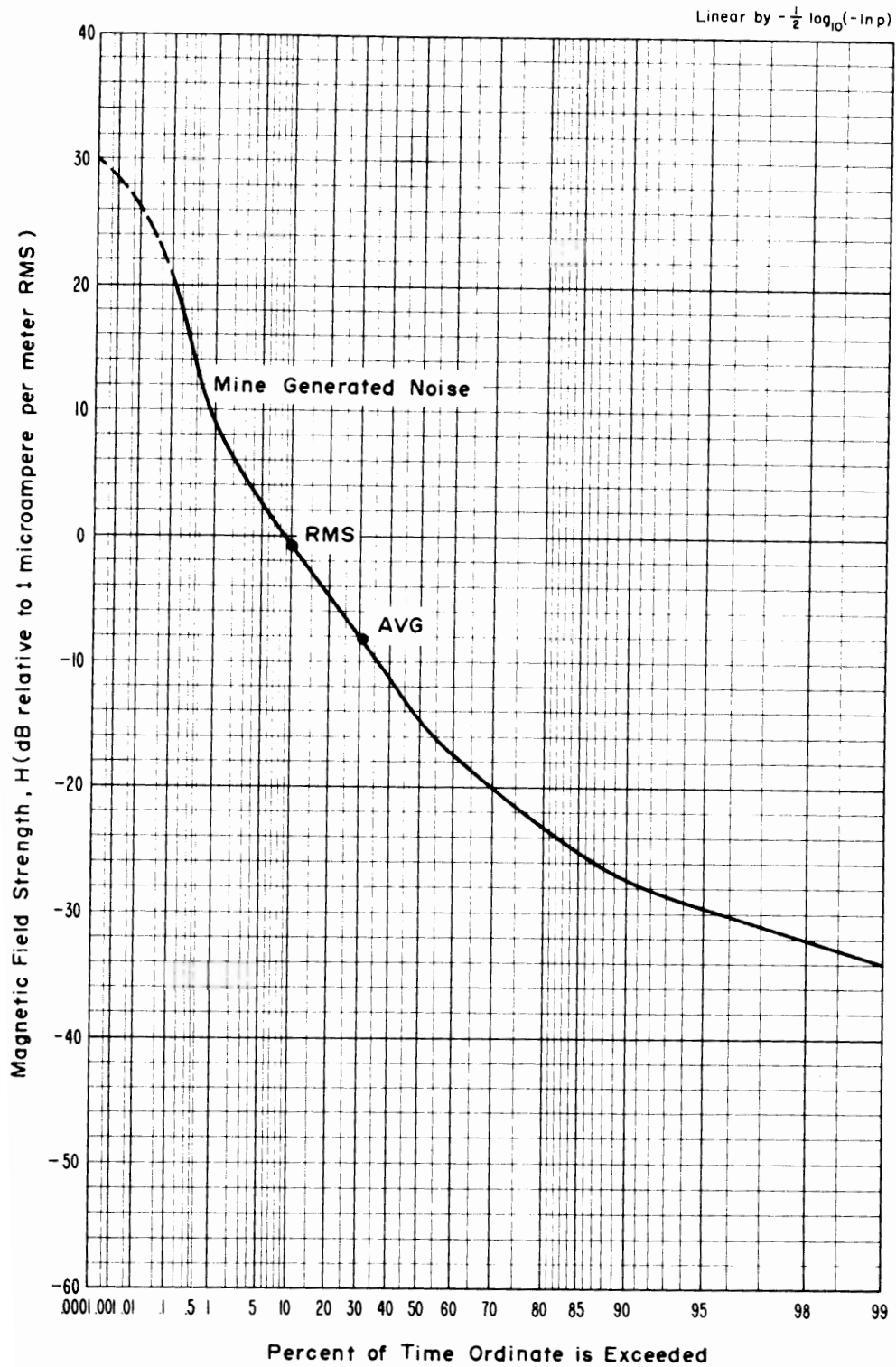


Figure 4-64 APD, 250 kHz, vertical component, 1.2 kHz predetection bandwidth, April 12, 1973, 11:30 p.m., McElroy Mine.

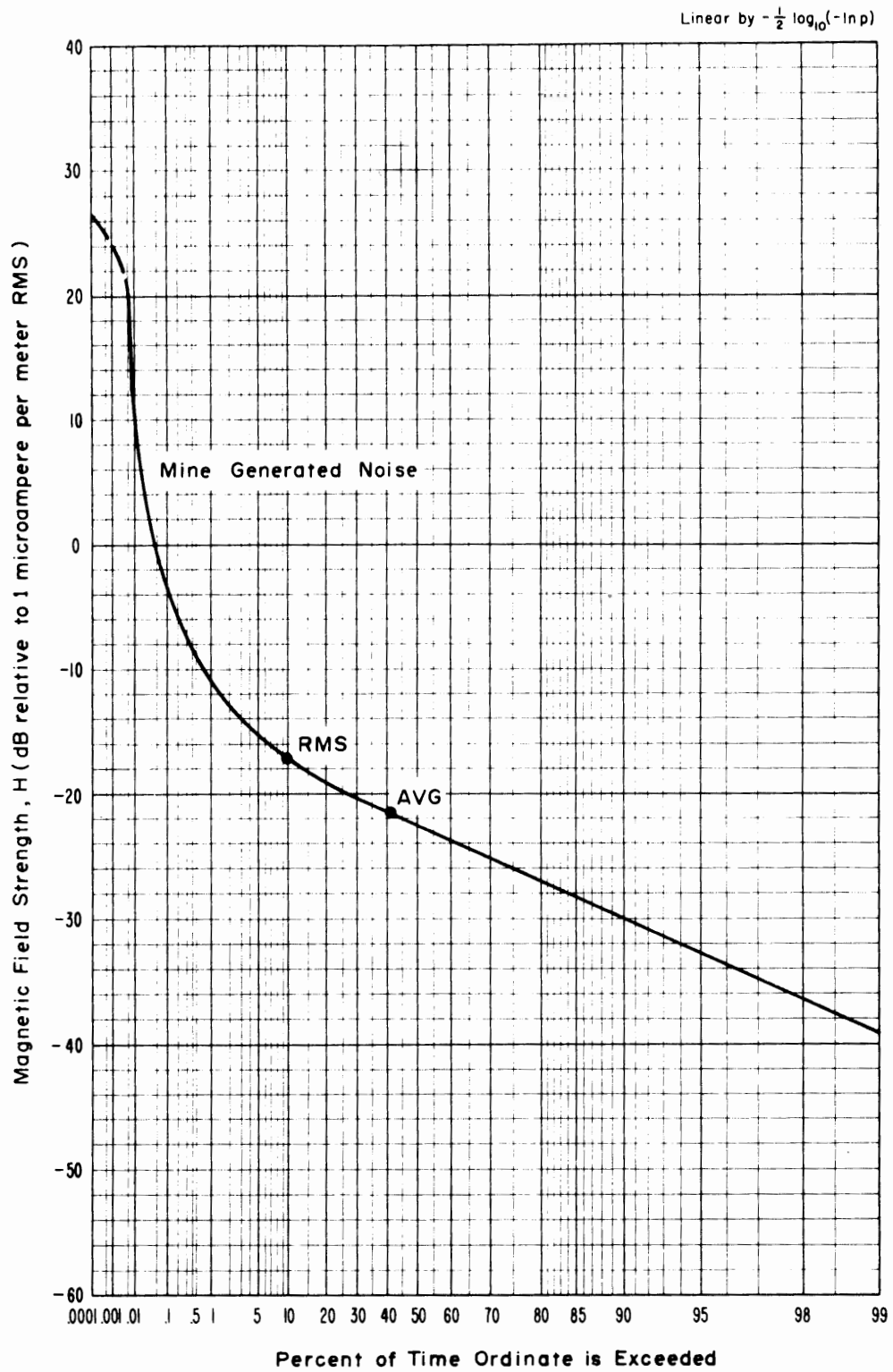


Figure 4-65 APD, 500 kHz, vertical component, 1.2 kHz predetection bandwidth, April 12, 1973, 12:15 p.m., McElroy Mine.

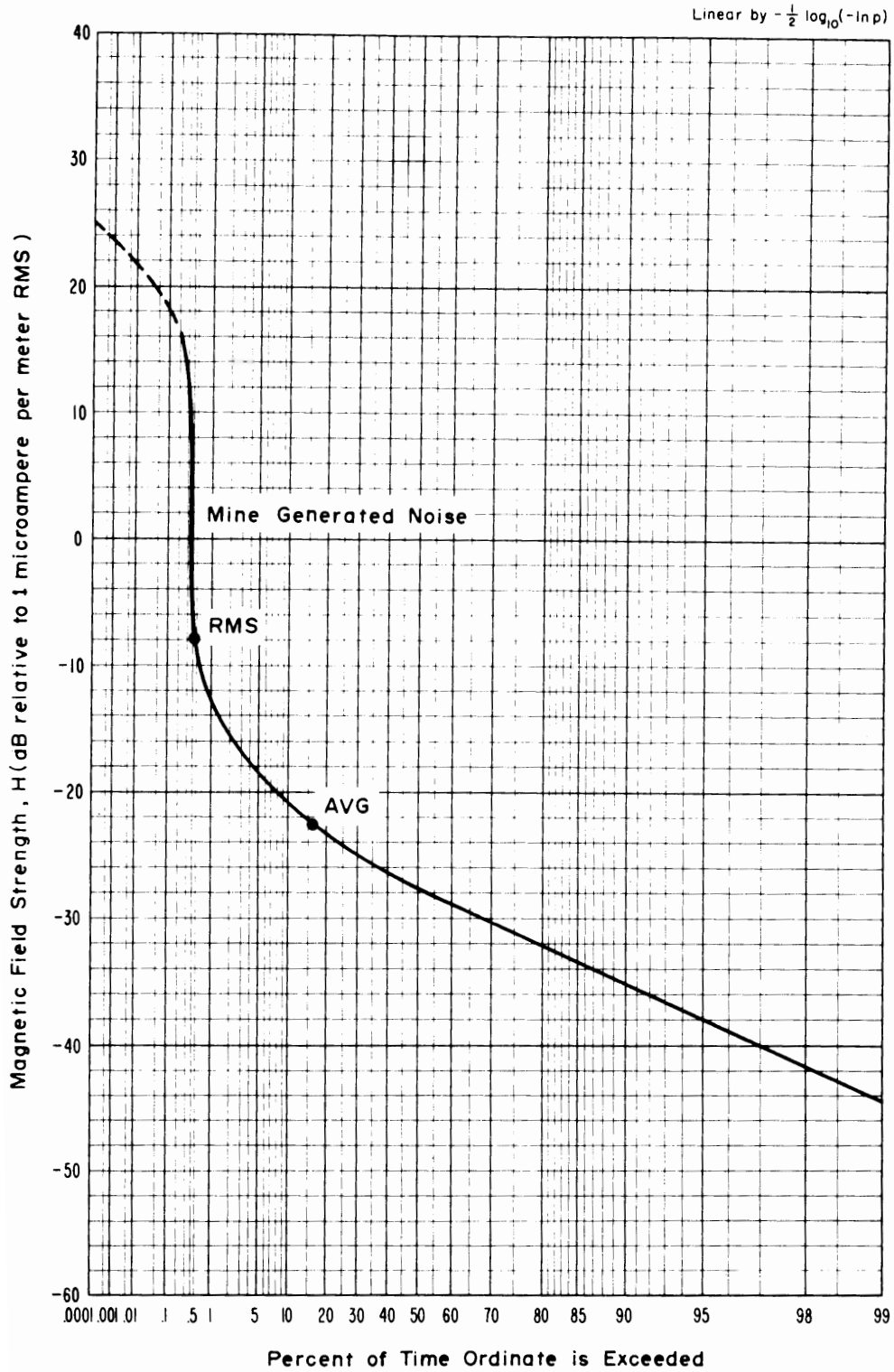


Figure 4-66 APD, 1 MHz, vertical component, 1.2 kHz predetection bandwidth, April 12, 1973, 1:00 p.m., McElroy Mine.

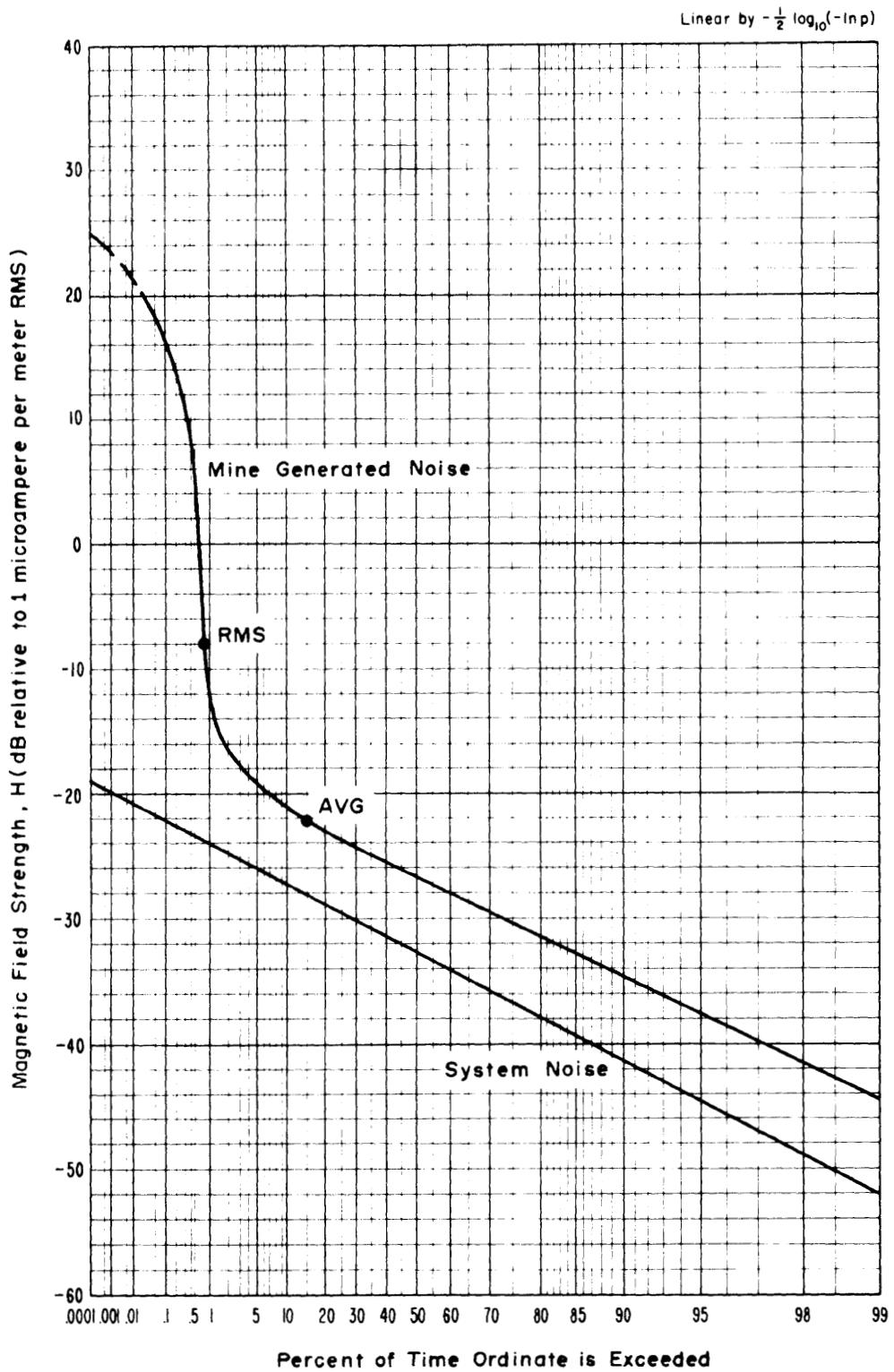


Figure 4-67 APD, 2 MHz, vertical component, 1.2 kHz predetection bandwidth, April 12, 1973, 1:30 p.m., McElroy Mine.

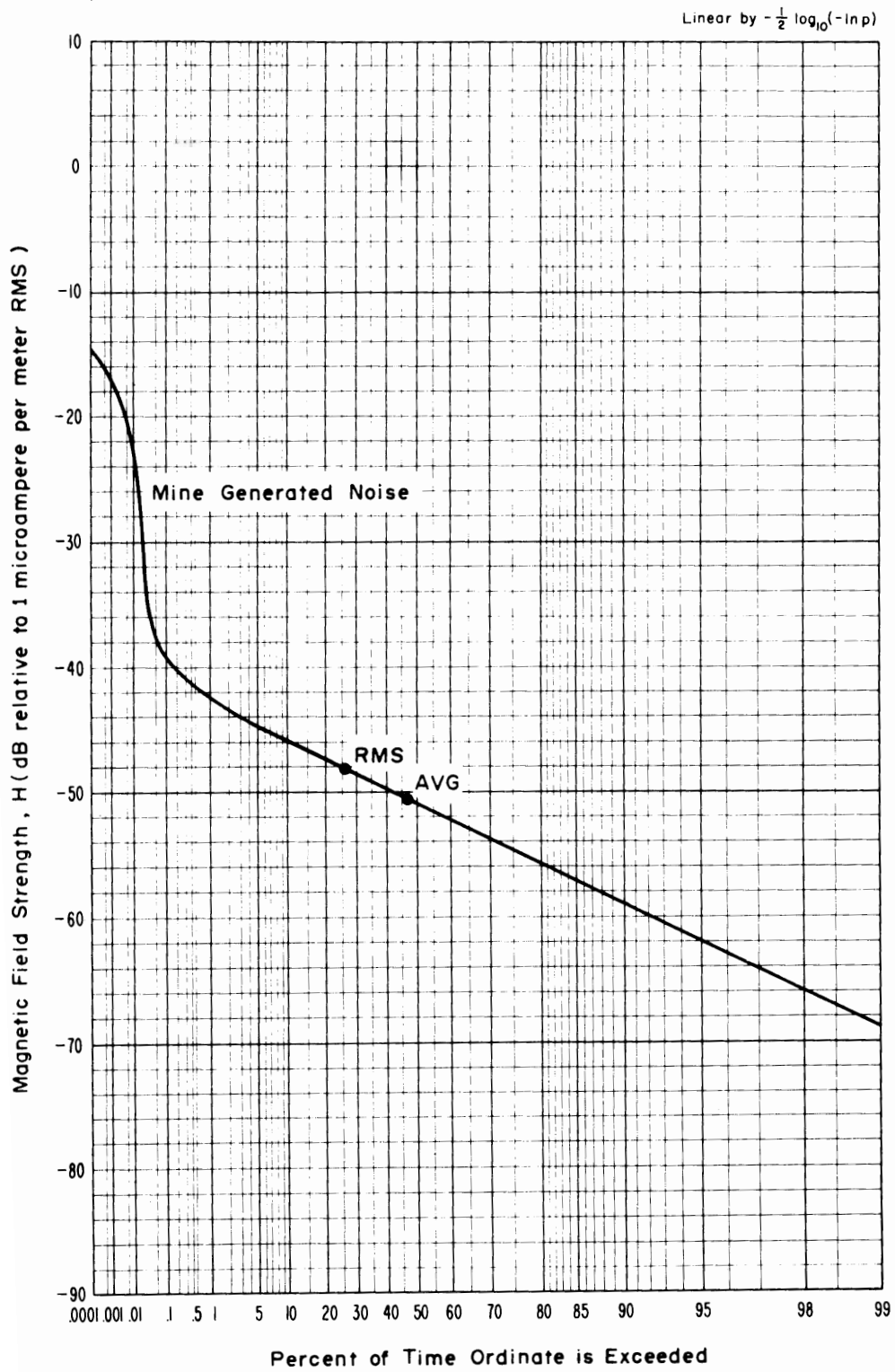


Figure 4-68 APD, 6 MHz, vertical component, 1.2 kHz predetection bandwidth, April 12, 1973, 2:15 p.m., McElroy Mine.

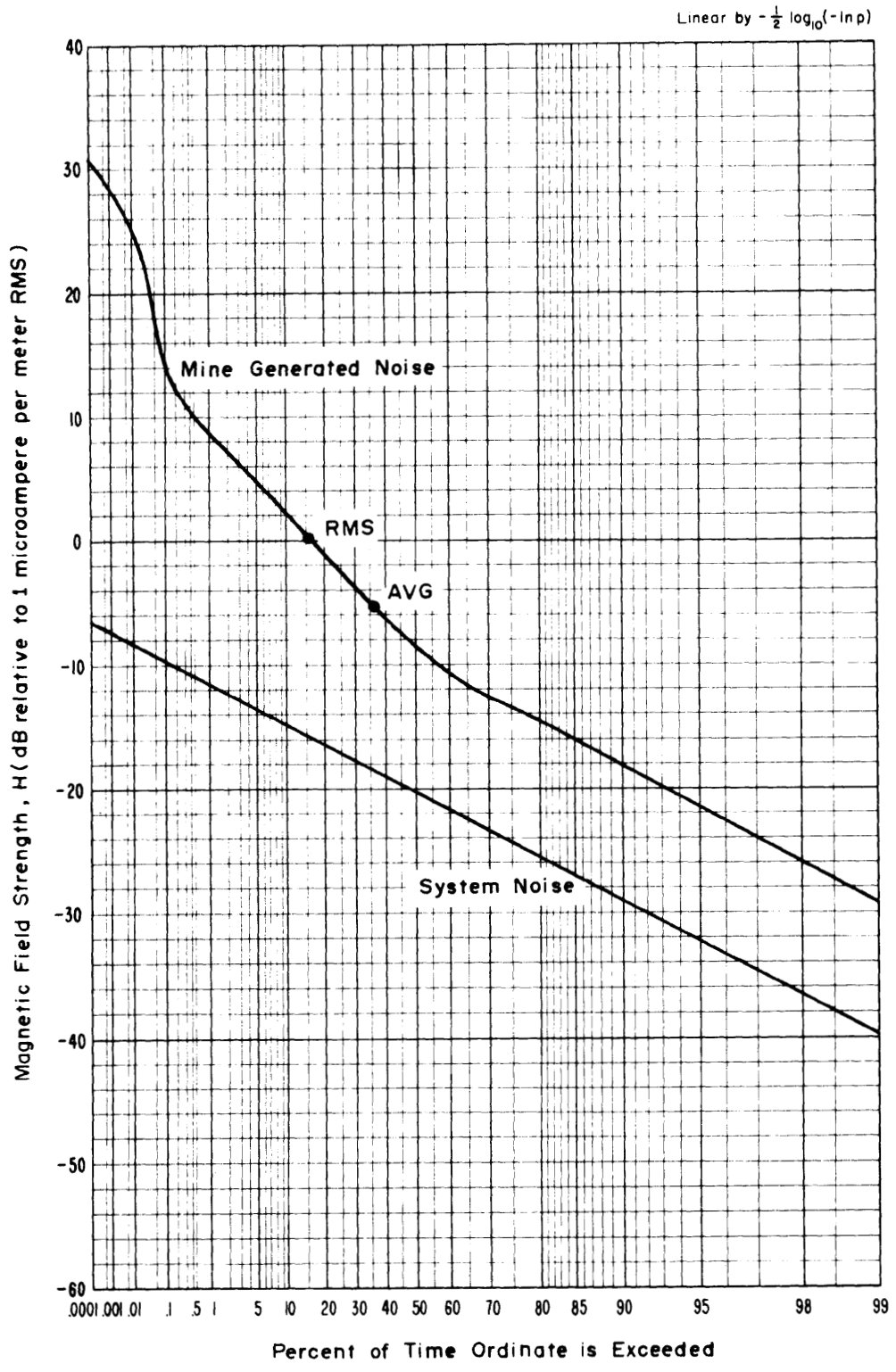


Figure 4-69 APD, 10 kHz, roof bolt measurements, 1.0 kHz predetection bandwidth, April 12, 1973, 2:45 p.m., McElroy Mine.

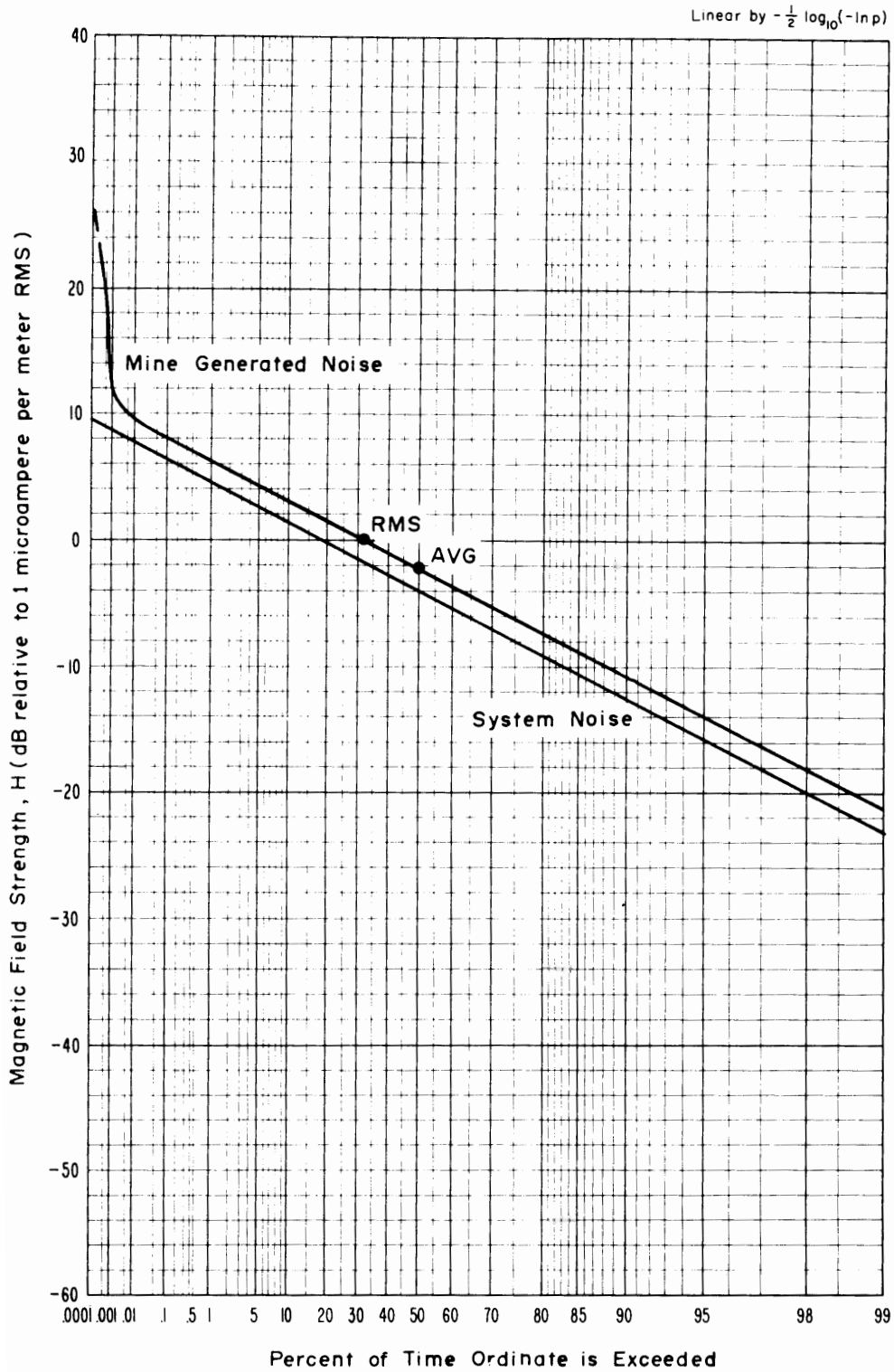


Figure 4-70 APD, 150 kHz, roof bolt measurements, 1.2 kHz predetection bandwidth, April 12, 1973, 2:45 p.m., McElroy Mine.

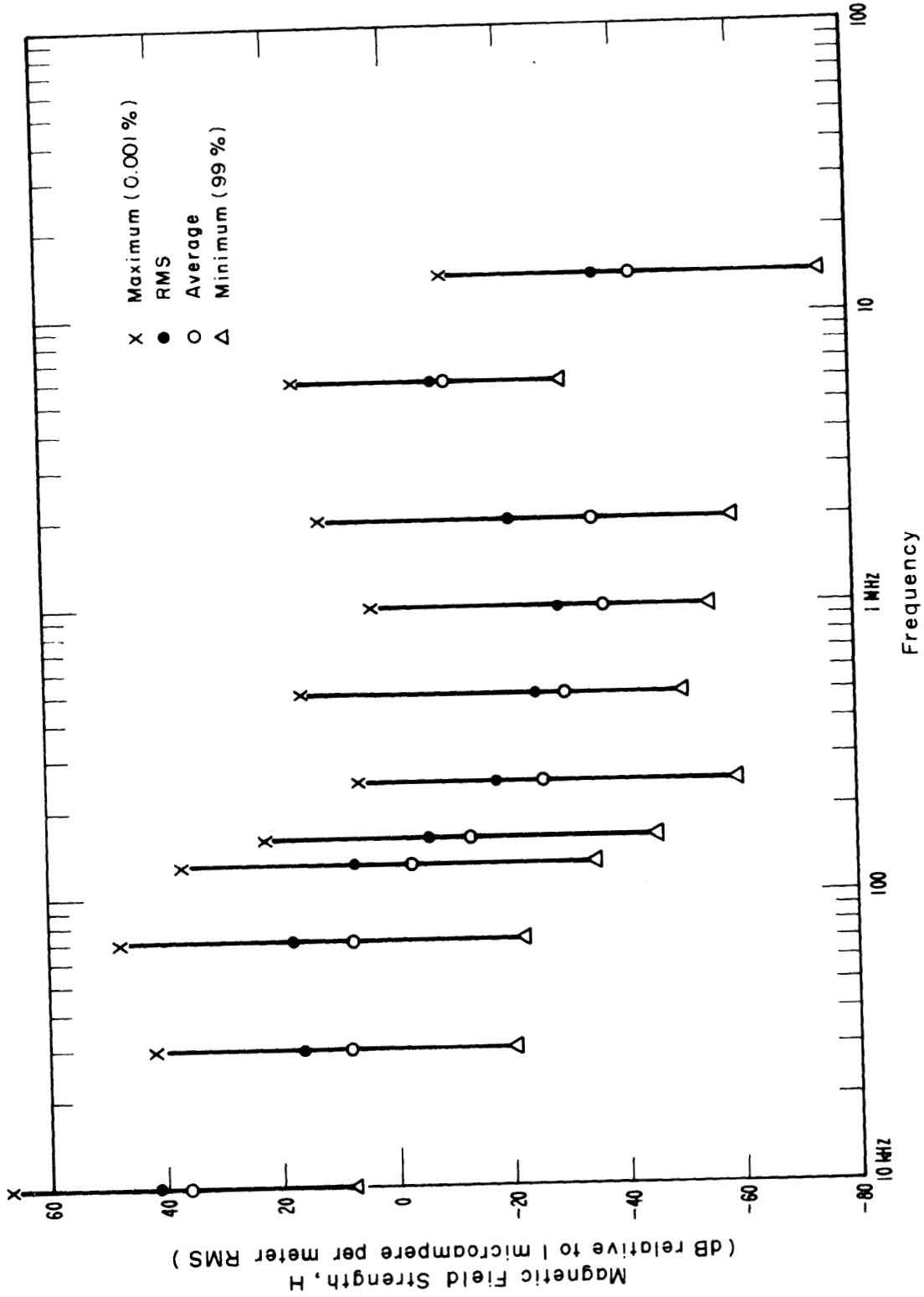


Figure 4-71 Field strength excursions between 0.001% and 99% of the time as a function of frequency, vertical component, location B on figure 3-1, 1 kHz predetection bandwidth, April 10, 1973, McElroy Mine.

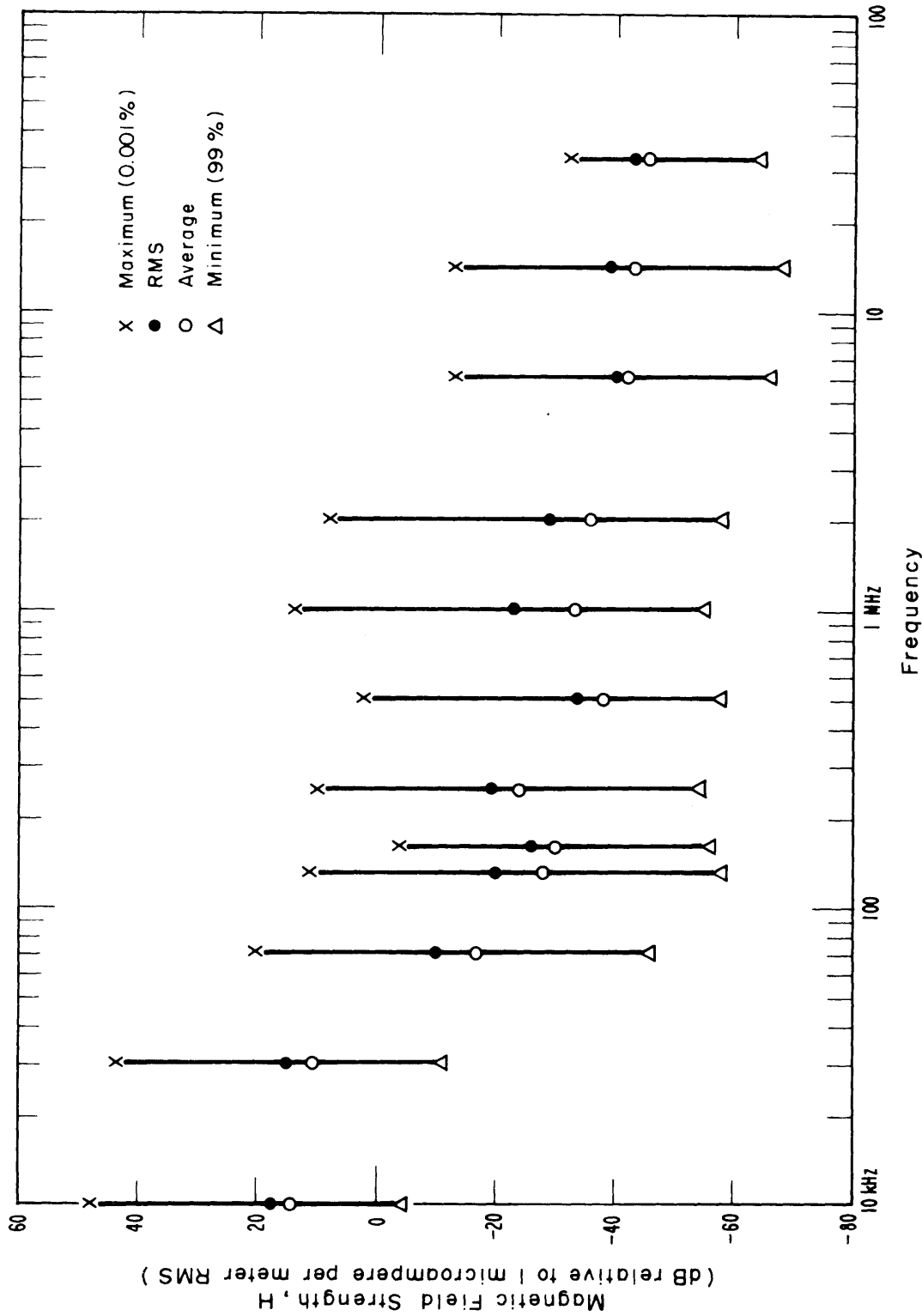


Figure 4-72 Field strength excursions between 0.001% and 99% of the time as a function of frequency, horizontal component (NE-SW), location B on figure 3-1, 1 kHz predetection bandwidth, April 10, 1973, McElroy Mine.

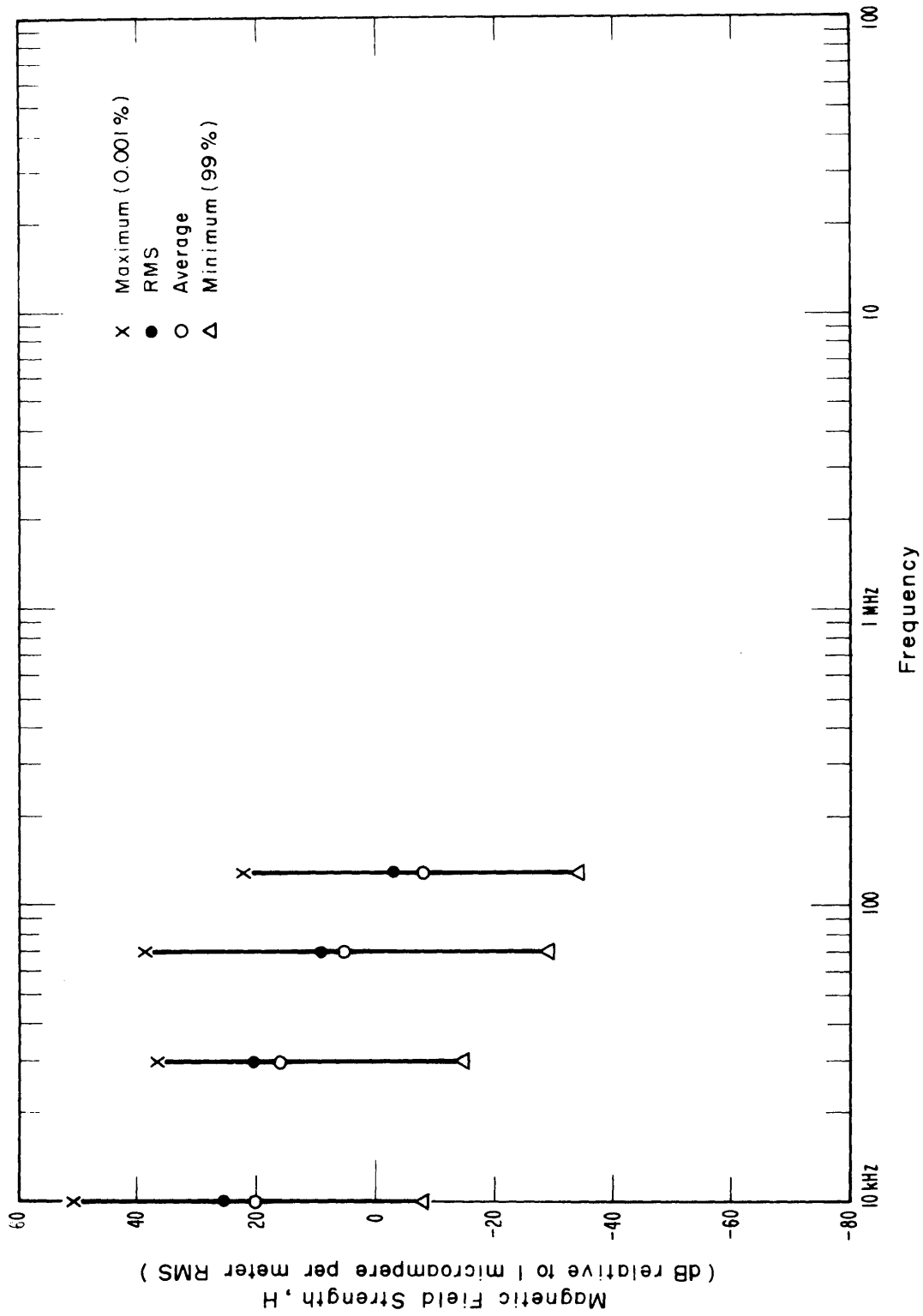


Figure 4-73 Field strength excursions between 0.001% and 99% of the time as a function of frequency, vertical component location B on figure 3-1, 1 kHz predetection bandwidth, April 10, 1973, quiet time measurements, McElroy Mine.

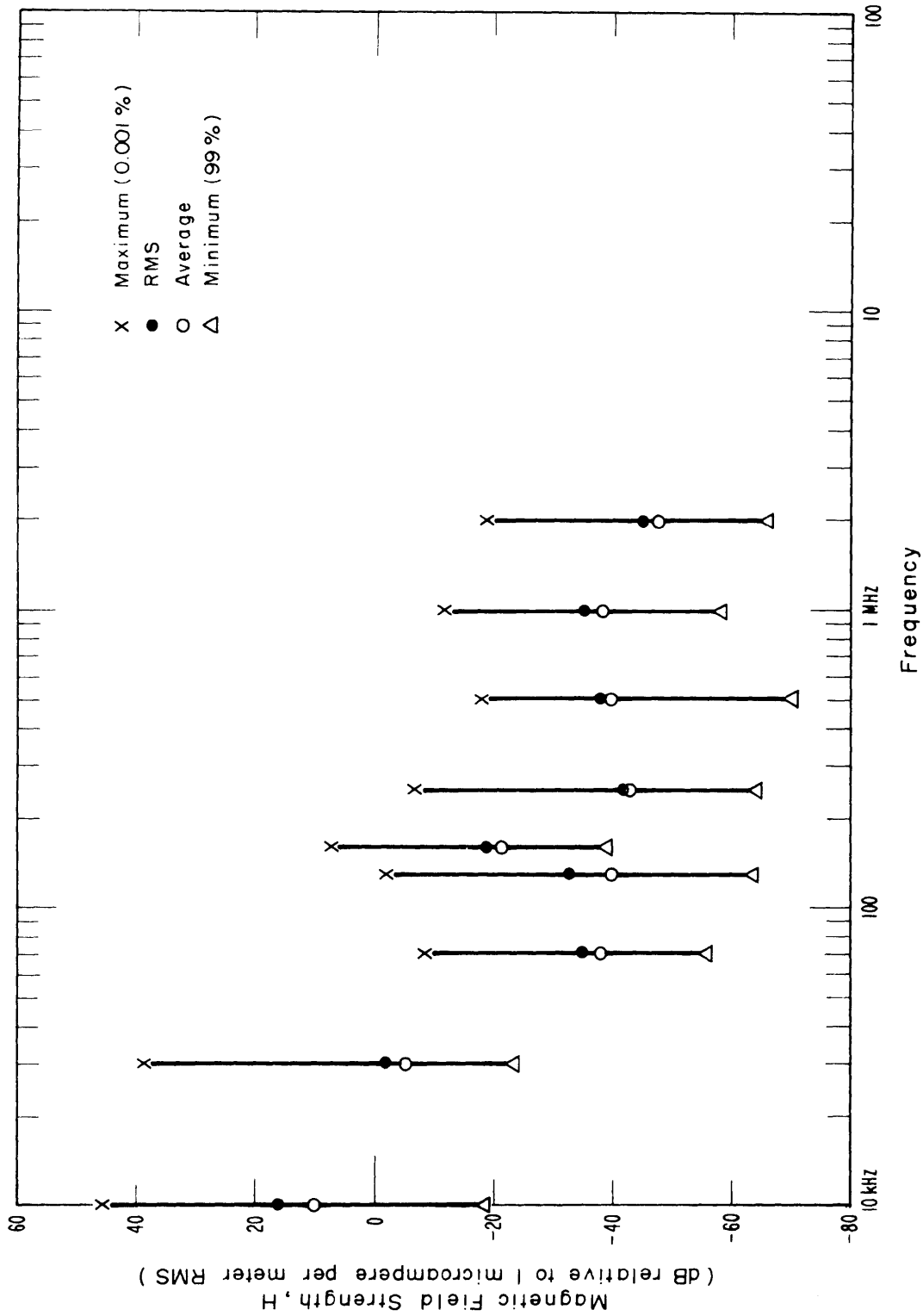


Figure 4-74 Field strength excursions between 0.001% and 99% of the time as a function of frequency, vertical component location A on figure 3-1, 1 kHz predetection bandwidth, April 10, 1973, McElroy Mine.

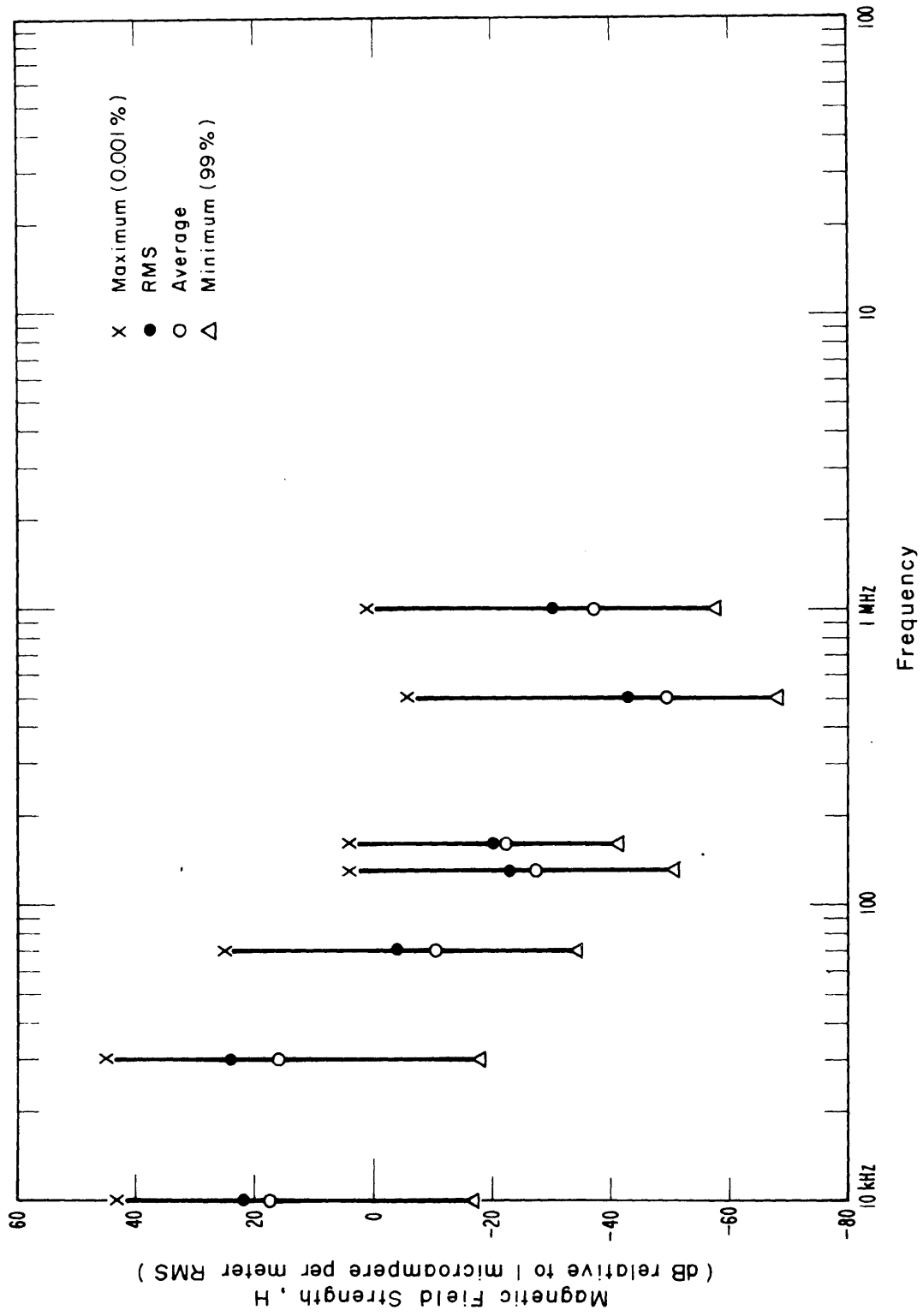


Figure 4-75 Field strength excursions between 0.001% and 99% of the time as a function of frequency, horizontal component, (N-S), location A on figure 3-1, 1 kHz predetection bandwidth, April 10, 1973, McElroy Mine.

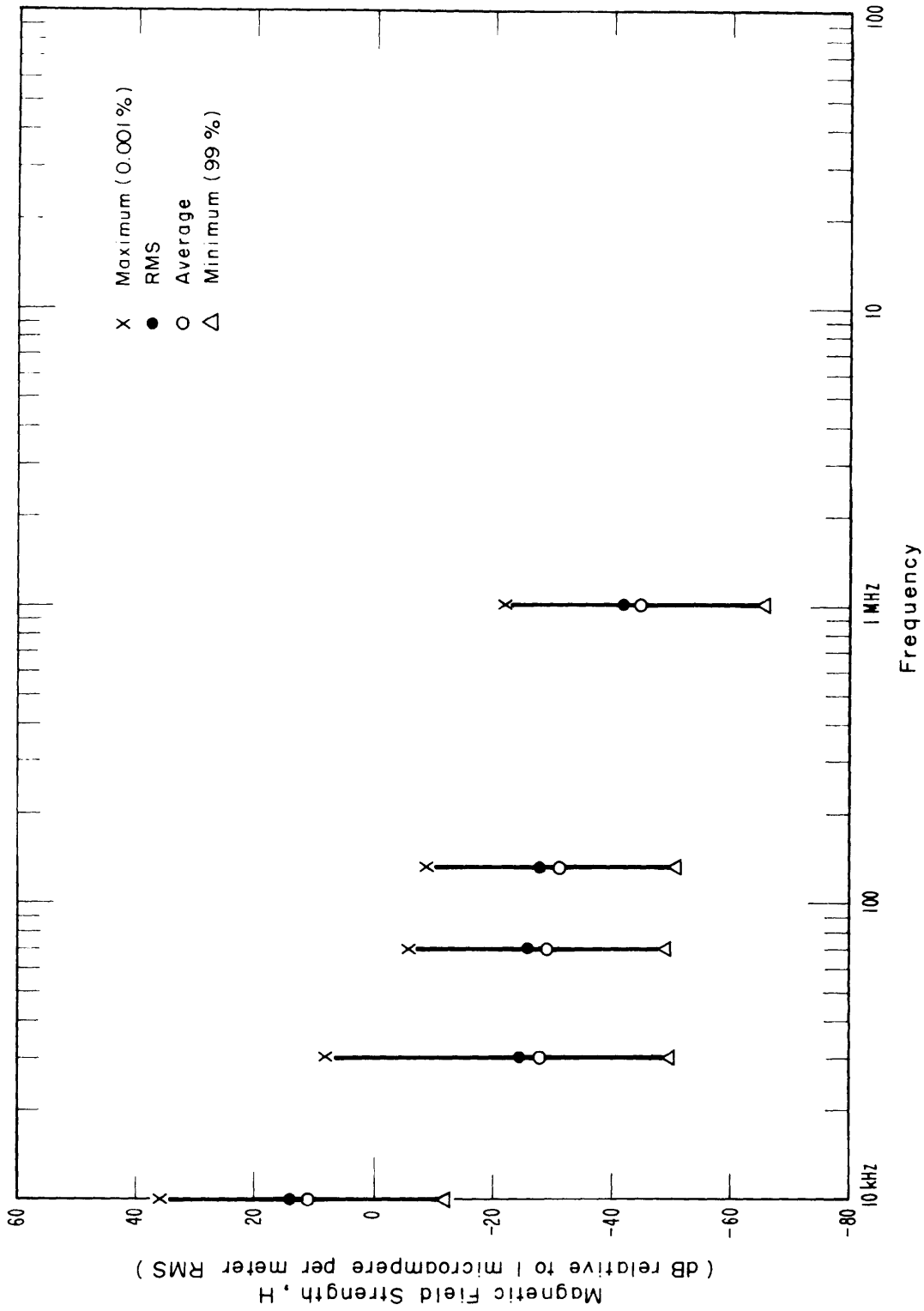


Figure 4-76 Field strength excursions between 0.001% and 99% of the time as a function of frequency, vertical component, location A on figure 3-1, 1 kHz predetection bandwidth, April 10, 1973, quiet time measurements, McElroy Mine.

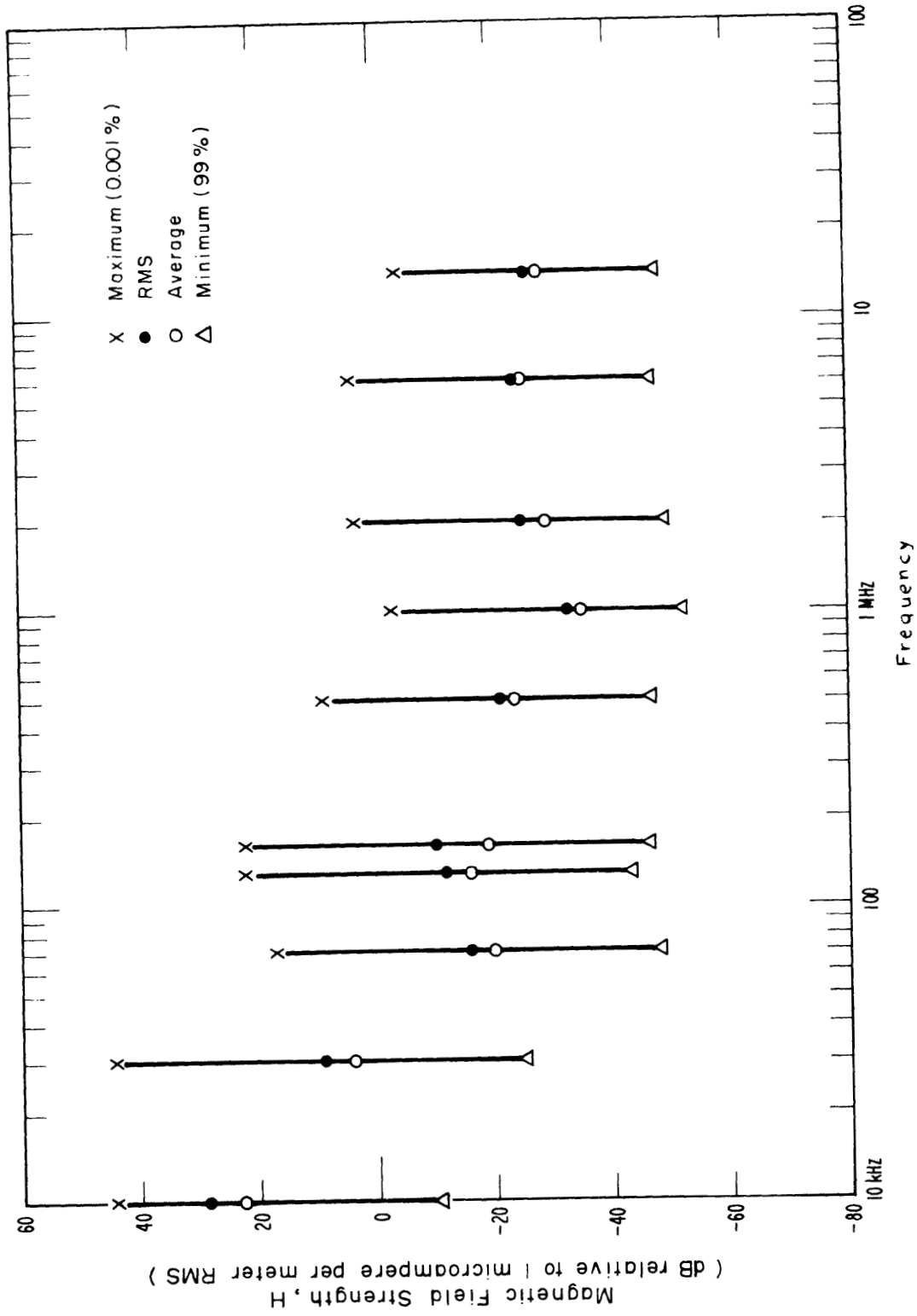


Figure 4-77 Field strength excursions between 0.001% and 99% of the time as a function of frequency, vertical component, location B on figure 3-2, 1 kHz predetection bandwidth, April 12, 1973, McElroy Mine.

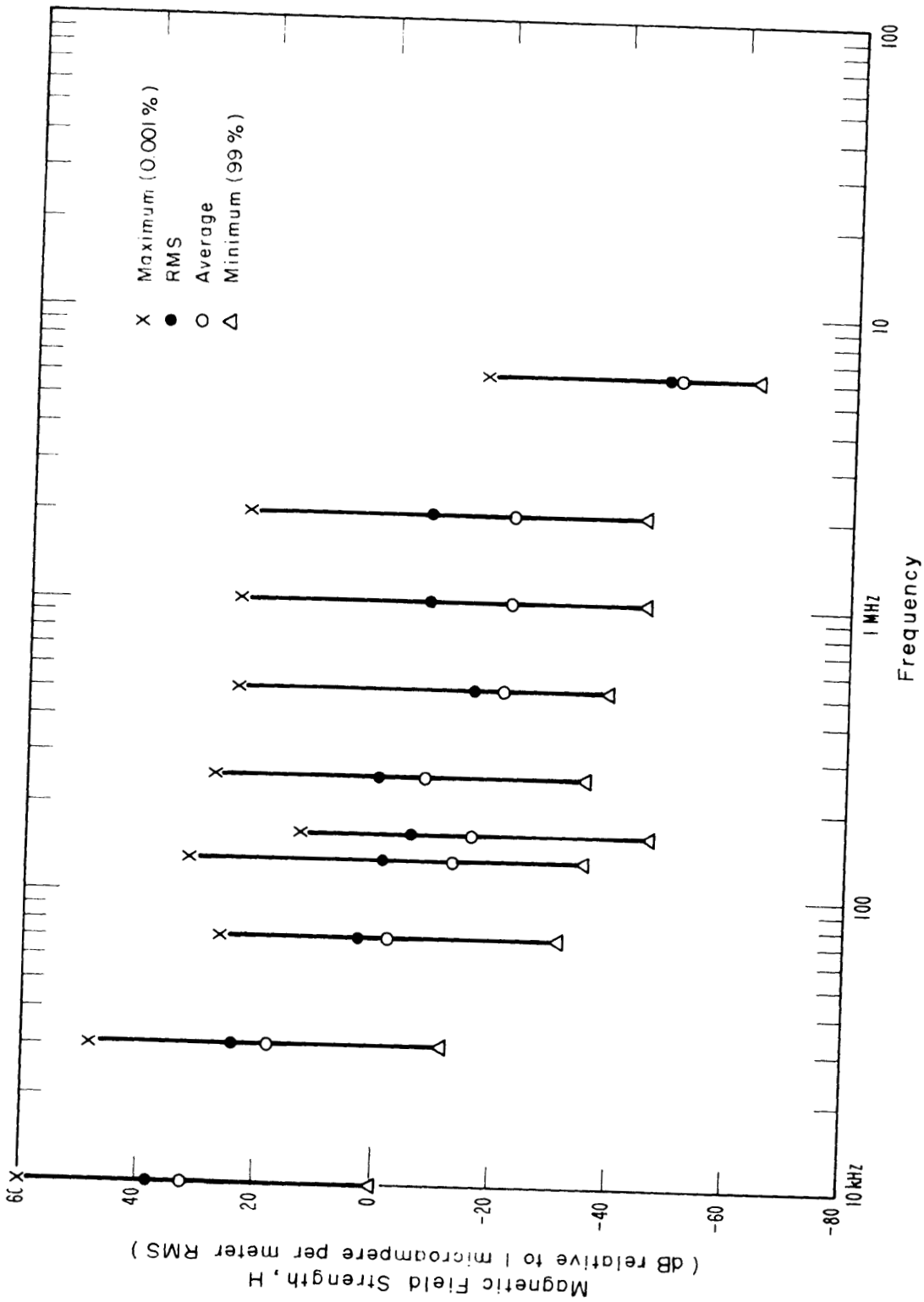


Figure 4-78 Field strength excursions between 0.001% and 99% of the time as a function of frequency, vertical component, location A on figure 3-2, 1 kHz predetection bandwidth, April 12, 1973, McElroy Mine.

5. CONCLUSIONS

The range of magnetic-field noise levels in McElroy is 130 dB, from 90 dB above 1 $\mu\text{V}/\text{m}$ at 60 Hz to 40 dB below 1 $\mu\text{V}/\text{m}$ at 180 kHz. This compares with the 125 dB range in Robena, except that the Robena levels were higher, from +105 dB to -20 dB with respect to 1 $\mu\text{A}/\text{m}$. Grace Mine had a range of 158 dB, from +122 dB to -36 dB. In the lower portion of the spectrum, below 3 kHz, McElroy was approximately 20 dB quieter than Robena in most cases. However, from 3 kHz to 100 kHz the magnetic-field noise levels in Robena and McElroy were both relatively high, 10 to 80 dB above 1 $\mu\text{A}/\text{m}$, near operating equipment, compared to levels in Grace and Itmann mines of -10 to 50 dB above 1 $\mu\text{A}/\text{m}$. From 100 kHz to 200 kHz, McElroy and Itmann had the highest levels, -20 to +15 dB above 1 $\mu\text{A}/\text{m}$. Data from Robena is not available in this frequency range, but levels may well be comparable to those in McElroy and Itmann.

Along haulageways, McElroy was the quietest (by a small margin) of the mines visited. From 30 kHz to 180 kHz, this level was equal to or less than -30 dB above 1 $\mu\text{A}/\text{m}$.

Surface measurements over the underground working section show a number of man-made, cw carriers. If these carriers are omitted, the background, broadband noise is -30 to -40 dB with respect to 1 $\mu\text{A}/\text{m}$. The carriers come up to 0 dB with respect to 1 $\mu\text{A}/\text{m}$. Below 20 kHz, powerline harmonics were the dominant source of noise. The range covers -20 to +60 dB above 1 $\mu\text{A}/\text{m}$.

APD measurements were taken during quiet times as well as during normal operation. The measurements show quiet-time levels at some frequencies at least 60 dB below 1 $\mu\text{A}/\text{m}$, but at most frequencies below 1 MHz, the peak and rms levels did not change significantly from quiet to operating condition. Levels near operating equipment were 30 dB above 1 $\mu\text{A}/\text{m}$

at 30 kHz, and near haulageways, were 10 dB above 1 μ A/m at 30 kHz. The range of these measurements is consistent with the wide range of levels that have been measured in some other mines.

6. RECOMMENDATIONS

Particularly in mines similar to McElroy, but also in most other coal mines as well, the wide ranges of magnetic-field noise levels due to spatial variations should be used to maximum advantage. For example, keep receivers away from noise sources whenever possible. This applies to frequencies below 200 kHz, where interference levels near machinery are extremely severe. Shorter-range, higher-frequency systems could be designed for use near machinery.

Surface noise measurements at McElroy show the need for only one design criterion: avoid powerline harmonics. There are other criteria which show up at other mines, but for low-frequency, through-the-earth communication systems, avoiding use of powerline harmonic frequencies is of primary concern.

7. ACKNOWLEDGMENTS

Those making significant contributions to this program are as follows: laboratory development and field use of measurement equipment, Ed Neisen, Doug Schulze, and Tom Bremer; data processing, Anne Rumfelt, Nancy Tomoeda, Winston Scott, Frank Cowley, and David Stearns. Those making valuable but less time-consuming contributions are Gerry Reeve, Bob Matheson, Don Spaulding, John Chukoski, Lorne Matheson, Dave Lewis, and Sharon Foote.

Winston Scott provided much assistance in proofreading, while Sharon Foote and Janet Becker typed tirelessly through many versions. Jocelyn Spencer and Barbara Bolton provided drafting assistance.

Finally, none of this would have been possible without the excellent cooperation of John Burr of Lee Engineering Company and of Dick Rouse, John Stock, Randy Fizer, and others of Consolidation Coal Company.

8. REFERENCES

- [1] Bensema, W.D., Kanda, M., Adams, J.W., Electromagnetic Noise in Robena No. 4 Coal Mine, NBS Tech. Note 654, April 1974.
- [2] The Institute of Electrical and Electronic Engineers, Inc., IEEE Dictionary of Electrical and Electronic Terms, Std. 100, 1972.
- [3] Taggart, H.E. and Workman, J.L., Calibration Principles and Procedures for Field Strength Meters (30 Hz to 1 GHz), NBS Tech. Note 370, March 1969.
- [4] Adams, J.W., Bensema, W.D., Kanda, M., Electromagnetic Noise in Grace Hardrock Mine, NBSIR 74-388, June 1974.
- [5] Crichlow, W.Q., et al., Amplitude-probability distributions for atmospheric radio noise, NBS Monograph 23 (1960b).
- [6] Thompson, W.I., III, Bibliography of ground vehicle communications and control. AKWIC index, Report No. DOT-TSC-UMTA-71-3, July 1971.
- [7] Spaulding, A.D. and Disney R.T., Man-Made Radio Noise: Part 1: Estimates for Business, Residential, and Rural Areas, Office of Telecommunications OT Report 74-38, June 1974.

9. APPENDIX

Decoding of Spectrum Captions

Spectrum captions are generally organized into the following format:

First line: MP NDT NZS NDA NPO RC DF date, time, frame, serial, where

MP = Two's power of length of Fourier transform, example, 2^{MP} where MP = 12

NDT = Detrending option, example, 0 (dc removed)

NZS = Restart spectral average after output, example, 0 (restarted)

NDA = Data segment advance increment, example, 2048

NPO = Number of spectra averaged between output calls, example, 20

RC = Integration time in seconds per spectra, example, 0.168

DF = Resolution bandwidth, spectral estimate spacing in hertz, example, 62.5

Date = Date of computer processing, example, 03/21/73

Time = Time of computer processing, example, 15:06:34

Frame = Frame set number, example, 10

Serial = Film frame serial number, example, 42.

Second line: DTA DA(1) DA(2) DA(3) NSA NRP NPP, where

DTA = Detrending filter parameter α , example, 0.00195

DA(1) = Detrending filter average, K=1, example, 59.4

DA(2) = Detrending filter average, K=2, example, 0

DA(3) = Detrending filter average, K=3, example, 0

NSA = Number of periodograms averaged, example, 20

NRP = Number of data points processed since spectrum initialization, example, 43008

NPP = Number of data points processed since data initialization, example, 43008.

Third line: RUN, SESSION, DAY, MONTH, YEAR Gain corr., rec. =
tot. constr. =, where

Run and Session = the title of the portrayed frame identifying
the digitizing session and run number,
example, 21 83

Month, Day, Year = date data were recorded in the mine,
example, 8 25 73

Gain corr. rec. = receiver gain correction, example, -6
tot. const. = constant gain correction of entire system,
example, -46.4

Fourth line: C =, RG =, DG =, FG =, AG =, where

C = correction curve used with data, example, 25
RG = receiver gain and accompanying correction in dB added to
the data, example, 200 (-6 dB)
DG = digitizer gain, example, 0
FG = filter gain in dB, often rounded to nearest single digit,
example, 0
AG = absolute gain correction added to data, example, 52

Fifth line: Top of Scale, Standard Error, Spectral Peak, where

Top of Scale = largest scale marking for computer drawn
graph, example, 1.000+004 (1.0×10^4)
Standard Error = standard error of curve, example, 0.3162
Spectral Peak = largest spectral peak observed, example,
4.108+003. (4.108×10^3)

U.S. DEPT. OF COMM. BIBLIOGRAPHIC DATA SHEET	1. PUBLICATION OR REPORT NO. NBSIR 74-389	2. Gov't Accession No.	3. Recipient's Accession No.
4. TITLE AND SUBTITLE Electromagnetic Noise in McElroy Mine		5. Publication Date June 1974	6. Performing Organization Code
7. AUTHOR(S) Motohisa Kanda, John W. Adams, and William D. Bensema		8. Performing Organ. Report No.	
9. PERFORMING ORGANIZATION NAME AND ADDRESS NATIONAL BUREAU OF STANDARDS, Boulder Labs DEPARTMENT OF COMMERCE Washington, D.C. 20234		10. Project/Task/Work Unit No. 2768412	11. Contract/Grant No.
12. Sponsoring Organization Name and Complete Address (Street, City, State, ZIP) U.S. Bureau of Mines 4800 Forbes Avenue Pittsburgh, Pa. 15213		13. Type of Report & Period Covered	
15. SUPPLEMENTARY NOTES		14. Sponsoring Agency Code	
<p>16. ABSTRACT (A 200-word or less factual summary of most significant information. If document includes a significant bibliography or literature survey, mention it here.)</p> <p>Two different techniques were used to make measurements of the absolute value of electromagnetic noise in and above an operating coal mine, McElroy Mine, located near Moundsville, West Virginia. 300-volt-dc and 480-volt-ac machinery was measured to see the electromagnetic environment it created. One technique measures noise over the entire electromagnetic spectrum of interest for brief time periods. It is recorded using broadband analog magnetic tape and the noise data is later transformed to give spectral plots. The other technique records noise amplitudes at several discrete frequencies for a sufficient amount of time to provide amplitude probability distributions.</p> <p>The specific, measured results are given in a number of spectral plots and amplitude probability distribution plots.</p>			
<p>17. KEY WORDS (six to twelve entries; alphabetical order; capitalize only the first letter of the first key word unless a proper name; separated by semicolons) Amplitude probability distribution; coal mine noise; digital data; electromagnetic communications; electromagnetic interference; electromagnetic noise; Fast Fourier Transform; Gaussian distribution; impulsive noise; magnetic field strength; measurement instrumentation; spectral density; time-dependent spectral density.</p>			
<p>18. AVAILABILITY <input checked="" type="checkbox"/> Unlimited</p> <p><input type="checkbox"/> For Official Distribution. Do Not Release to NTIS</p> <p><input type="checkbox"/> Order From Sup. of Doc., U.S. Government Printing Office Washington, D.C. 20402, SD Cat. No. C13</p> <p><input type="checkbox"/> Order From National Technical Information Service (NTIS) Springfield, Virginia 22151</p>		<p>19. SECURITY CLASS (THIS REPORT)</p> <p>UNCLASSIFIED</p>	<p>21. NO. OF PAGES</p>
		<p>20. SECURITY CLASS (THIS PAGE)</p> <p>UNCLASSIFIED</p>	<p>22. Price</p>